2024

Contamination Assessment and Reduction Project – Phase 2 (CARP II)

Appendix A-6. CARP II Models Update Report

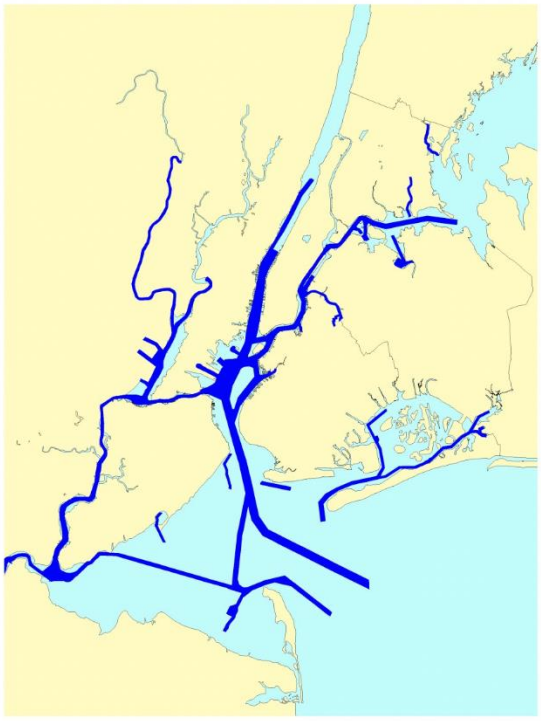

UPDATE OF CARP MODELS

NY/NJ Harbor Contamination Assessment and Reduction Project, CARP II

New Jersey Department of Transportation,

Under Agreement with Monmouth University and the Hudson River Foundation

September 11, 2023

TABLE OF CONTENTS

TABLE OF CONTENTS....1
LIST OF FIGURES....4
PREFACE....8
ABSTRACT....12
1.0 INTRODUCTION....13
2.0 METHODS....14
2.1 Methods for Update of CARP Hydrodynamic Model....14
2.1.1 Methods for CARP Hydrodynamic Model Update, Computational Grid....14
2.1.2 Methods for CARP Hydrodynamic Model Update, Time Varying Bathymetry....15
2.1.3 Methods for CARP Hydrodynamic Model Update, Bottom Friction....16
2.1.4 Methods for CARP Hydrodynamic Model Update, Open Boundary Conditions....17
2.1.5 Methods for CARP Hydrodynamic Model Update, Freshwater Flows and Temperatures....18
2.1.6 Methods for CARP Hydrodynamic Model Update, Wind Conditions and Heat Flux....19
2.2 Methods for Update of CARP Sediment Transport and Organic Carbon Production Model....19
2.2.1 Methods for CARP Sediment Transport and Organic Carbon Production Model Update, Parameters and Constants Controlling Resuspension....19
2.2.2 Methods for CARP Sediment Transport and Organic Carbon Production Model Update, Water Column Vertical Mixing Adjustments....21
2.2.3 Methods for CARP Sediment Transport and Organic Carbon Production Model Update, Sediment Bed Particle Mixing Rate Adjustments....21
2.2.4 Methods for CARP Sediment Transport and Organic Carbon Production Model Update, Initial Bed Thickness....23
2.2.5 Methods for CARP Sediment Transport and Organic Carbon Production Model Update, Base Light Extinction in Lower Hackensack River Marsh Areas....24
2.3 Methods for Update of CARP Contaminant Fate and Transport Model....24
2.3.1 Methods for CARP Contaminant Fate and Transport Model Update, Initial Bed Contaminant Concentrations....25
2.3.2 Methods for CARP Contaminant Fate and Transport Model Update, Di-PCB Phase Partitioning Coefficient....25
2.3.3 Methods for CARP Contaminant Fate and Transport Model Update, Additional Contaminants Robustness Testing....26
3.0 RESULTS....26
3.1 Results for CARP Hydrodynamic Model Update....26
3.1.1 Results for CARP Hydrodynamic Model Update, Model Computational Grid....26

3.1.2 Results for CARP Hydrodynamic Model Update, Tidal Water Elevations 26
3.1.3 Results for CARP Hydrodynamic Model Update, Water Temperature and Salinity 27
3.1.4 Results for CARP Hydrodynamic Model Update, Velocity Currents 29
3.2 Results for CARP Sediment Transport and Organic Carbon Production Model Update 30
3.2.1 Results for CARP Sediment Transport and Organic Carbon Production Model Update, Bed Accumulation 30
3.2.2 Results for CARP Sediment Transport and Organic Carbon Production Model Update, Suspended Sediment Fluxes from the Lower Hudson River to the Harbor 32
3.2.3 Results for CARP Sediment Transport and Organic Carbon Production Model Update, Ambient Suspended Sediment and Organic Carbon Concentrations 32
3.3 Results for CARP Contaminant Fate and Transport Model Update 34
3.3.1 Results for CARP Contaminant Fate and Transport Model Update, Six Contaminants 1998-2016 Calibration 35
3.3.2 Results for CARP Contaminant Fate and Transport Model Update, Twenty-One Additional Contaminants 1998-2016 Validation 38
4.0 DISCUSSION 41
4.1 Discussion of CARP Hydrodynamic Model Update Results 41
4.1.1 Discussion of CARP Hydrodynamic Model Update Results, Model Computational Grid 41
4.1.2 Discussion of CARP Hydrodynamic Model Update Results, Tidal Water Elevations 42
4.1.3 Discussion of CARP Hydrodynamic Model Update Results, Water Temperature and Salinity 43
4.1.4 Discussion of CARP Hydrodynamic Model Update Results, Current Velocity 44
4.2 Discussion of CARP Sediment Transport and Organic Carbon Production Model Update Results 46
4.2.1 Discussion of CARP Sediment Transport and Organic Carbon Production Model Update Results, Bed Accumulation 46
4.2.2 Discussion of CARP Sediment Transport and Organic Carbon Production Model Update Results, Suspended Sediment Fluxes from the Lower Hudson River to the Harbor 48
4.2.3 Discussion of CARP Sediment Transport and Organic Carbon Production Model Update Results, Ambient Suspended Sediment and Organic Carbon Concentrations 48
4.3 Discussion of CARP Contaminant Fate and Transport Model Update Results 50
4.3.1 Discussion of CARP Contaminant Fate and Transport Model Update Results, Six Contaminants 1998-2016 Calibration 50
4.3.2 Discussion of CARP Contaminant Fate and Transport Model Update Results, Twenty-One Additional Contaminants 1998-2016 Validation 53
5.0 CONCLUSION 55

6.0 NEXT STEPS 56
7.0 ACKNOWLEDGMENTS AND DISCLAIMERS 56
8.0 LITERATURE CITED 56
9.0 SECTION 2 FIGURES 59
10.0 SECTION 3 FIGURES 62
APPENDICES 127

LIST OF FIGURES

Figure 2-1. Location of sixty-nine NOAA stations used for the specification of the meteorological inputs 60
Figure 2-2. Contaminant phase partitioning coefficients calculated from CARP 1 water column and CARP 2 sediment bed measurements 61

Figure 3-1. CARP 2 127 x 205 model computational grid, full domain view. 63
Figure 3-2. CARP 2 127 x 205 model computational grid, view of the Harbor portion of the model domain. 64
Figure 3- 3. Newark Bay and the Kill van Kull, including a portion of Upper NY Bay, view of CARP 127 x 205 (top) and 49 x 84 (bottom) model computational grids. 65
Figure 3-4. Lower Passaic and Hackensack Rivers, including a portion of the Hudson River, view of CARP 127 x 205 (top) and 49 x 84 (bottom) model computational grids. 66
Figure 3-5. Kill van Kull and Arthur Kill, including portions of Upper NY and Raritan Bays, view of CARP 127 x 205 (top) and 49 x 84 (bottom) model computational grids. 67
Figure 3-6. Upper NY Bay through Narrows, including the Port Jersey and MOTBY Channels and Gowanus Bay and the mouths of the Hudson and East Rivers and the Kill van Kull, view of CARP 127 x 205 (top) and 49 x 84 (bottom) model computational grids. 68
Figure 3-7. Hudson River, from Troy Dam to the head of Haverstraw Bay, view of CARP 127 x 205 (left) and 49 x 84 (right) model computational grids 69
Figure 3-8. Locations of tidal water elevation model and measurement comparisons. 70
Figure 3-9. Hourly water elevation model and measurement comparisons results. 71
Figure 3-10. Hourly water elevation model and measurement comparisons results. 72
Figure 3-11. Hourly water elevation model and measurement comparisons results. 73
Figure 3-12. Hourly water elevation model and measurement comparisons results. 74
Figure 3-13. Hourly water elevation model and measurement comparisons results. 75
Figure 3-14. Hourly water elevation model and measurement comparisons results. 76
Figure 3-15. Hourly water elevation model and measurement comparisons results. 77
Figure 3-16. Hourly water elevation model and measurement comparisons results after application of a 35-hour low pass filter removing diurnal and semi-diurnal tidal components. 78
Figure 3-17. Locations of salinity model and measurement comparisons shown on Figures 3-18 to 3-21 and in Appendix 5. 79
Figure 3-18. Salinity (psu) model and measurement comparisons results during Harbor deepening projects. Modeled and measured results are presented for the 2001-02 water year at four locations in Newark Bay and the Kill van Kull. 80
Figure 3-19. Salinity (psu) model and measurement comparisons results during Harbor deepening projects. Modeled and measured results are presented for the 2001-02 water year at three locations in the Arthur Kill. 81
Figure 3-20. Salinity (psu) model and measurement comparisons results for the 2009-10 water year at four locations in Newark Bay and the Kill van Kull. 82
Figure 3-21. Salinity (psu) model and measurement comparisons results presented for the 2009-10 water year at two locations in the Kill van Kull and three locations in the Arthur Kill. 83

Figure 3-22. Locations (blue) of velocity currents model and measurement comparisons for 2000-02 water years imposed on 127 x 205 (grey) and 42 x 84 (red) CARP model computational grids. 84
Figure 3-23. Velocity currents model and measurement comparisons for full 2000-02 water years, Station NB-1 longitudinal north/south example. 85
Figure 3- 24. Velocity currents model and measurement comparisons for a portion of the 2000-02 water years, Station NB-1 longitudinal north/south example. 86
Figure 3-25. Locations of velocity currents model and measurement comparisons for 2007-09 water years imposed on 127 x 205 CARP model computational grid. 87
Figure 3-26. Velocity currents model and measurement comparisons for full 2007-09 water years, Station HRF_KVK2, lateral east/west example. 88
Figure 3-27. Velocity currents model and measurement comparisons for a portion of the 2007-09 water years, Station HRF_KVK2 lateral east/west example. 89
Figure 3-28. Regional annual average external solids loadings (gold bars) and bed accumulation results (red bars) for CARP 1 (top) 49 x 84 and CARP 2 (bottom) 127 x 205 sediment transport and organic carbon production models. 90
Figure 3-29. Regional bed accumulation time series results for CARP 127 x 205 sediment transport and organic carbon production model for each water year cumulatively 91
Figure 3-30. Bed accumulation spatial results by model grid cells for CARP 127 x 205 and draft (i.e., under development, not final, subject to change) Newark Bay Superfund sediment transport models .. 92
Figure 3-31. CARP 127 x 205 model computational grid sediment transport model results for bed accumulation. 93
Figure 3-32. CARP 127 x 205 model computational grid sediment transport model results for bed accumulation 94
Figure 3-33. CARP 127 x 205 model computational grid sediment transport model results for bed accumulation in the Hudson River near Manhattan. Between August 19 and September 15, 2011 95
Figure 3-34. CARP 127 x 205 model computational grid sediment transport model results for bed accumulation in the Hudson River near Manhattan for spring and summer conditions. 95
Figure 3-35. Hudson River hydrograph below the confluence with the Mohawk River. 96
Figure 3-36. CARP 127 x 205 model computational grid sediment transport model results for bed accumulation in the Hudson River in Haverstraw Bay. 97
Figure 3- 37. CARP results (green typeface text) for suspended sediment loadings from the Upper Hudson and Mohawk Rivers and the tributaries above Poughkeepsie and the flux of suspended sediment passing downstream of Poughkeepsie. 98
Figure 3-38. Suspended sediment concentrations model and measurement comparison results, Kill van Kull, 2000-01 water year. 99
Figure 3-39. Suspended sediment concentrations model and measurement comparison results, Arthur Kill, 2012-13 water year. 100
Figure 3-40. Suspended sediment concentrations model and measurement comparison results, Newark Bay, 2006-07 water year. 101
Figure 3- 41. Suspended sediment concentrations model and measurement comparison results, Hudson River at Poughkeepsie, 2003. 102
Figure 3-42. Suspended sediment concentrations model and measurement comparison results for six locations in the Hudson River. 103

Figure 3- 43. Suspended sediment concentrations model and measurement comparison results for six locations in Upper NY Bay. 104
Figure 3- 44. Suspended sediment concentrations model and measurement comparison results for six locations in Upper NY Bay, East River, and Jamaica Bay. 105
Figure 3- 45. Particulate organic carbon concentrations model and measurement comparison results for six locations in Upper Newark Bay and the Hackensack River. 106
Figure 3- 46. Particulate organic carbon concentrations model and measurement comparison results for six locations in central Newark Bay. 107
Figure 3- 47. Particulate organic carbon concentrations model and measurement comparison results for six locations in Lower Newark Bay and the Kill van Kull. 108
Figure 3- 48. Dissolved organic carbon concentrations model and measurement comparison results for six locations in Upper Newark Bay and the Hackensack River. 109
Figure 3- 49. Dissolved organic carbon concentrations model and measurement comparison results for six locations in central Newark Bay. 110
Figure 3- 50. Dissolved organic carbon concentrations model and measurement comparison results for six locations in Lower Newark Bay and the Kill van Kull. 111
Figure 3- 51. 2,3,7,8-TCDD solids-normalized sediment bed concentrations model and measurement comparison results for six locations in Lower Newark Bay. 112
Figure 3- 52. Total PCB solids-normalized sediment bed concentrations model and measurement comparison results for six locations in Lower Newark Bay. 113
Figure 3- 53. 2,3,7,8-TCDD solids-normalized sediment bed concentrations model and measurement comparison results for six locations in the Hudson and East Rivers. 114
Figure 3- 54. Total PCB solids-normalized sediment bed concentrations model and measurement comparison results for six locations in the Hudson and East Rivers. 115
Figure 3- 55. 2,3,7,8-TCDD water column concentrations model and measurement comparison results for six locations in upper Newark Bay. 116
Figure 3- 56. Total PCB water column concentrations (estimated as twice the summation of four homologs) model and measurement comparison results for six locations in upper Newark Bay. 117
Figure 3- 57. 2,3,7,8-TCDD water column concentrations model and measurement comparison results for six locations in the Hudson River. 118
Figure 3- 58. Total PCB water column concentrations (estimated as twice the summation of four homologs) model and measurement comparison results for six locations in the Hudson River. 119
Figure 3- 59. Interim (left and middle timeseries) and final (right timeseries) 2,3,7,8-TCDD (ppt) solids-normalized sediment bed concentrations model and measurement comparison results for a single location in the Lower Passaic River. 120
Figure 3- 60. Interim (top and middle timeseries) and final (bottom timeseries) 2,3,7,8-TCDD (ppt) solids-normalized sediment bed concentrations model and measurement comparison results for a single location in Newark Bay. 121
Figure 3- 61. 2,3,7,8-TCDD (top row) and total PCB (bottom row) solids-normalized sediment bed concentrations model and measurement comparison results in the East River on the west side of Riker's Island in South Brother Island Channel, north of Bowery Bay. 122
Figure 3- 62. Di-CB water column concentrations model and measurement comparison results for three locations in the Hudson River before and after adopting a revised phase partitioning coefficient. 123

Figure 3- 63. Di-CB water column concentrations model and measurement comparison results for three locations in Upper NY Bay before and after adopting a revised phase partitioning coefficient. 124
Figure 3- 64. Total PCB solids-normalized sediment bed concentrations model and measurement comparison results for six locations in Lower Newark Bay. 125
Figure 3- 65. Total PCB solids-normalized sediment bed concentrations model and measurement comparison results for six locations in the Hudson and East Rivers. 126

PREFACE

The modeling work reported here is one of several efforts undertaken in connection with the Contamination Assessment and Reduction Project (CARP). The overall purpose of CARP and the context for the CARP modeling work are outlined below.

What is CARP?

CARP is a landmark project bringing together federal, state, and non-government partners in a determined effort to better understand and reduce contamination within the New York/New Jersey Harbor Estuary. This contamination has led to environmental harm and economic hardships. Notably, dredging and disposal activities connected to port activities were severely curtailed in the early 1990's as dredging managers and regulators struggled with finding management options for handling contaminated dredged material. While dredging has since proceeded, the costs have escalated to 10 to 30 times previous levels, largely because of sediment contamination. Other negative impacts continue to plague the system, including fish advisories and substandard water quality, which are impeding the recovery and utilization of many of the estuary's natural resources.

Through workgroup deliberations in connection with the Dredged Material Forum and the NY/NJ Harbor Estuary Program (HEP), a general plan was developed to address the problem of continued contamination of sediments requiring dredging. The operative management questions included: Which sources of contaminants need to be reduced or eliminated to render future dredged material clean? Which actions can yield the greatest benefits? and, which actions are necessary to achieve the 2040 targets recommended in the Dredged Material Management Plan for the Harbor? CARP was initiated to address these questions.

CARP has been implemented in two phases having shared goals and objectives. The second phase of CARP served as a supplement and complement to the first phase. The two phases of CARP are referred to as CARP 1 and CARP 2. The primary funding mechanism for CARP 1 was the 1996 Joint Dredging Plan for the Port of New York and New Jersey, an agreement between the States of New York and New Jersey that was funded by the Port Authority of New York and New Jersey (Port Authority). Additional funds were obtained from the New Jersey Department of Transportation (NJDOT), the Empire State Development Corporation, The U.S. Army Corps of Engineers, the Hudson River Estuary Management Program, the Harbor and Estuary Program (HEP), and the Hudson River Foundation. CARP 2 was made possible by research funding from NJDOT awarded to Monmouth University.

The specific objectives of the CARP are to: 1. Identify and quantify sources of contaminants of concern to the NY/NJ Harbor Estuary from a dredged material standpoint; 2. Establish baseline levels of contaminants of concern in water, sediments, and biota; 3. Determine the relative significance of contaminant inputs in controlling the concentrations of those contaminants in water, sediment and biota: 4. Forecast future conditions in light of various contaminant reduction scenarios; 5. Take action to reduce levels of contaminants of concern in water, sediments, and fish tissue.

CARP is a unique partnership of governmental and non-governmental entities whose activities have been guided by a management committee composed of representatives from the U.S. Environmental Protection Agency, U.S. Army Corps of Engineers, New Jersey Department of Environmental Protection (NJDEP), New York State Department of Environmental Conservation (NYSDEC), New Jersey Department of Transportation (NJDOT), Empire State Development Corporation, Port Authority, Environmental Defense Fund, and the Hudson River Foundation. During CARP 1, NYSDEC and NJDEP completed objectives 1 and 2 above through a comprehensive data collection (sampling and testing) program, which represents about 90% of the $32 million total funding for CARP 1.

It was the consensus of the CARP Management Committee that mathematical modeling tools were needed to help understand the results of the data collection program and the fate and transport of contaminants through the Harbor. These models provide a means for integrating data in a mass balance framework such that relationships between loadings and contaminant concentrations in water, sediment and biota can be evaluated and quantified. Moreover, these models can provide the predictive capacity that managers and scientists need to assess the consequences of existing contaminant loads and potential remedial actions. The CARP 1 modeling work performed by HydroQual, Inc., therefore addressed Objectives 3 and 4 above, and represents about 10% of the total funding for CARP 1.

Utility of CARP to Regional Stakeholders

The major focus of CARP has been on an objective evaluation of the fate and transport of contaminants throughout the entire NY/NJ Harbor Estuary system. The CARP Management Committee guiding CARP 1 and CARP 2 efforts intended for CARP work products to lead to sustained action to reduce both ongoing and historic contamination. The CARP Management Committee includes representatives of federal and state government agencies and is therefore mindful of the various regulatory programs that are in place to address contaminant issues. Consequently, since the inception of CARP, agencies on the Committee have made comments and recommendations to make CARP as relevant as possible to these programs. However, the CARP data collection and modeling efforts were not designed specifically to comply with the requirements of a particular regulatory program. CARP products, especially the modeling results, provide important information for these programs to consider, but further data collection and model refinement may be necessary to suit the scale and requirements of a particular program. And it is only those charged with regulatory responsibilities that can judge whether CARP products comply with their requirements.

CARP Modeling

Given the vast complexities of the entire estuary and the processes that affect contaminant fate and transport, modeling of this system has been a great technical challenge. From the initiation of CARP, it was understood that some aspects of the modeling would be limited because of scientific uncertainties in fully understanding all relevant processes. To ensure that the model components would be state-of-the-science, a Model Evaluation Group (MEG) was established at the outset of the project. Experts in organic and inorganic geochemistry, hydrodynamics, sediment transport and contaminant modeling were solicited to be members of the MEG. The MEG's first responsibility was to be part of the team to select a modeling contractor. It then met repeatedly over five years, to review and comment on the acceptability of modeling concepts and formulations to reproduce estuarine processes, including the review of CARP 1 model validation and hindcast results. The comments and suggestions of the MEG have been addressed by HydroQual, Inc., and a summary of the responses are included in CARP 1 model reports. In addition, the MEG provided comments and guidance on the use and application of the CARP 1 modeling products.

While some CARP model components were verified, refined, and successfully used in other venues prior to CARP, other components were newly designed for CARP 1 or CARP 2. The CARP modeling has elements that could be considered applied science and engineering, while others would be better characterized as research and development. The CARP MEG generally found that the CARP 1 modeling effort has advanced the understanding of contaminant behavior in the estuary and does a very credible job of characterizing the relationships between contaminant loadings and concentrations in the environment.

One of the more challenging issues that the CARP Management Committee addressed was the development of realistic contaminant reduction scenarios to use as an illustration of the CARP modeling framework capability. As the CARP modeling activities progressed, it became increasingly clear that legacy contamination of sediments was a dominant feature in controlling levels of contaminants in the system.

Since two large-scale sediment remediation projects (namely the Hudson River Superfund and Lower Passaic River Superfund projects) were being developed during CARP 1, it made sense to include these projects in the CARP 1 scenario analyses. While neither project was fully defined during CARP 1, the CARP 1 model scenario analyses gave a first glimpse of the potential for these sites (remediated or not) to influence sediment and water quality in the Harbor over the long term. The CARP 1 scenario analyses were refreshed and greatly expanded during CARP 2 with further CARP Management Committee guidance and two Records of Decision for the Lower Passaic River and the completion of remedial dredging on the Upper Hudson River. The analyses of CARP 2 future scenarios also consider the specific long-term future influences of the sites associated with the in-progress Newark Bay and Lower Hackensack River Superfund projects.

CARPs First Phase, CARP 1

More information on CARP 1 is readily available in a CARP 1 project summary report which references numerous CARP 1 reports:

> Lodge, J., Landeck Miller, R.E., Suszkowski, D., Litten, S., Douglas, S. 2015. Contaminant Assessment and Reduction Project Summary Report. Hudson River Foundation, New York, NY. CARP-summary-report-online.pdf (hudsonriver.org).

CARPs Second Phase, CARP 2

The NJDOT commissioned CARP 2 as a research project in response to needs identified by the Harbor's Dredged Material Strategic Planning Group (DMSPG), a task force convened by the U.S. Army Corps of Engineers (USACE). The DMSPG acknowledged that while CARP 1 modeling and the Region's bioaccumulation testing provided evidence that dredged material quality was improving, more information was needed to accurately forecast future HARS suitability for specific channels and berthing areas. Such information is critical for estimating the financial resources needed to maintain the Harbor and/or to determine the impact of planned remediation. The question that CARP 2 answers is the current and future levels (i.e., to 2040, inclusive of the DMSPG's 15-year and 25-year planning horizons) of contaminants within navigation channels of NY/NJ Harbor. The focus of CARP 2 is to demonstrate if the Region is getting closer to HARS suitability. CARP 2 estimation of progress toward HARS suitability in specific reaches of the Harbor at a higher spatial resolution than CARP 1 can guide dredged material managers in selectively pursuing HARS disposal options and spending on dredged material testing.

Other needs and information gaps addressed by CARP 2 include (1) the compilation and assimilation of relevant data collected in the years between CARP 1 and CARP 2; (2) the collection of new field measurements of loading contaminant concentrations and ambient conditions in the Estuary; (3) the evaluation, update, and refinement of models developed and applied during CARP 1; (4) the characterization of sediments in navigation channels and in adjacent off-channel areas; (5) the development of a method for predicting bioaccumulation of sedimentary contaminants in dredged material test organisms; and (6) the evaluation of a passive sampler method for potential prediction of HARS suitability more quickly and at a cost lower than the Region's current laboratory testing.

CARP 2 was initiated in March 2017 and leveraged CARP 1 financial investments by building upon the foundation of CARP 1 measurements and modeling. The CARP 2 principal investigators include Monmouth University, the Hudson River Foundation, HDR, Inc., Manhattan College, NYSDEC (retired personnel), Rutgers University, and the University of Rhode Island. The CARP 2 measurement and modeling work products include a CARP 2 project summary report which references several individual modeling and sampling/measurement-based CARP 2 report deliverables.

The CARP 2 individual report deliverables referenced in the CARP 2 project summary report include:

A. CARP 2 Modeling Report Deliverables:
   1. Evaluation of CARP 1 Models
      a. Task 3.1 Post-Audit Evaluation of the Original CARP Model Projections
   2. Update of the CARP Models
      a. Task 3.2 Update External Forcing Functions for Water Years 2002-2016
      b. Task 3.3 Refine the CARP Models
   3. CARP 2 Future Projections Scenarios
      a. Task 3.4 Projections of Current and Future Levels of Contamination in the Sediments within Navigation Channels of NJ/NY Harbor
B. Other deliverables:
   4. Measurement Summary Reports
      a. Historic Measurement Review
      b. CARP 2 Measurement Collection and Analysis
         i. Loadings Measurements and Ambient Conditions
         ii. Comparison of sediments in navigation channels and off-channel areas
         iii. Data Dictionary
   5. Prediction of Bioaccumulation of Sedimentary Contaminants in Dredged Material Test Organisms

The report included herein is the CARP2 modeling deliverable for Task 3.3, pertaining to refinement of the CARP models, identified as A2b above.

Future Intention

The CARP models should not only be viewed as management tools, but as research tools from which fuller understandings of the fate and transport of contaminants can be gleaned today. In addition, it is the hope of the CARP Management Committee that the CARP modeling work and underlying measurements serve as a foundation for the future from which even more advanced models could be developed and applied, as/if needed, for new management issues as they emerge.

UPDATE OF CARP MODELS

Robin E. Landeck Miller[1*], Kevin J. Farley[2], Laurie De Rosa[1], Nataliya Kogan[1], Ruta Rugabandana[1], and James R. Wands[1]

[1]HDR, Inc., 50 Tice Boulevard, Woodcliff Lake, New Jersey 07677; [2]Manhattan College, Riverdale, New York 10471

ABSTRACT

A CARP 2 task supporting the update of the CARP models has been completed. Update of the CARP models included the development of a higher resolution model computational grid and the sequential application of new model inputs. The higher resolution computational grid leveraged regional model development efforts since CARP 1, results of the CARP 2 post-audit task, and CARP 2 measurement collection efforts. The higher resolution model computational grid incorporates the specification of time-varying bathymetry to represent the progression of Harbor deepening through 2016 and updated bottom roughness. New model inputs for external loading forcing functions for the hydrodynamic, sediment transport/organic carbon production, and contaminant fate and transport models for the period October 1, 1998, through September 30, 2016, developed under a separate CARP 2 task and technical report, were applied first before other model input refinements. The performance of the hydrodynamic, sediment transport/organic carbon production, and contaminant fate and transport models with the updated computational grid and external loading forcing functions was assessed by comparisons to measurements collected by other CARP 2 investigators in 2018, 2019 and 2021 and readily available measurements compiled from a variety of sources for the period 2002 to 2016. In particular, the 2018, 2019, and 2021 measurements collected by other CARP 2 investigators provided additional context for measurements compiled for 2002 to 2016, especially for defining the measured temporal trend where measurements from 2010-2016 were lacking. Based on model performance and the goal of better representing the temporal behavior of contaminants in near-surface sediments, adjustments were judiciously made to other model inputs to achieve model calibration. The other model input refinements include hydrodynamic model temperature, salinity, and elevation open boundary conditions; water temperatures for the freshwater flows associated with external forcing functions; wind conditions; heat flux components; resuspension rates; initial bed thicknesses; water column vertical mixing rates; biological mixing rates in the sediment bed; base light extinction coefficients in the marsh areas of the Hackensack River; initial bed contaminant concentrations; and a revised phase partitioning coefficient for di-PCB. The model refinements developed are necessary for improving the technical defensibility of CARP model calculations for the 1998 to 2016 years during which and since CARP 1 measurements were collected as well as providing a more robust basis for applying the CARP models for projections of future conditions. Together with the outcomes of ongoing CARP 2 bioaccumulation work, the refined CARP models are being applied to assess future contaminant levels in Harbor sediments and organisms of relevance to dredged material testing.

KEY WORDS: CARP, model, HARS suitable, navigation channel, PCB, dioxin, NY/NJ Harbor and Estuary, dredged material testing, contaminant sources

[*] Corresponding author, Email: robin.miller@hdrinc.com

1.0 INTRODUCTION

The Contamination Assessment and Reduction Project (CARP) 1 model was developed as a series of sub-models to provide a detailed representation of the hydrodynamics, sediment transport, organic carbon cycling, and fate and transport of contaminants in the NY/NJ Harbor and Estuary (HydroQual 2007a, 2007b, 2008). The CARP 1 sub-models were calibrated using field measurements that were primarily collected during the 1999-2002 CARP 1 sampling program. The calibrated sub-models were applied in 2002 to project concentrations of PCBs and PCDD/Fs for a 37-year period commencing in October 2002 and ending in September 2039. The projections made in 2002 were necessarily based on information available at that time. Model-projected concentrations were assessed relative to dredged material testing endpoints to estimate the time when Harbor sediments would meet Historic Area Remediation Site (HARS) disposal criteria.

Since the 2002 CARP 1 model projections of time to HARS suitable Harbor sediments were made, the bathymetry of the Harbor has changed significantly. Deepening of navigation channels was accomplished by several projects. In addition, the Harbor has experienced extreme flow events (including Tropical Storms Irene, Lee, and Sandy) that were not simulated in the CARP 1 model projections. Further, measurement collection related to several Superfund projects in the Harbor has been ongoing since 2002. Therefore, to provide NJDOT with a tool for determining the current and future levels of contamination in the sediments within navigation channels of NJ/NY Harbor, refinement of the CARP sub-models was undertaken to account for the deepening of navigation channels, to assess the impacts of extreme flow events on contaminant responses in Harbor sediments, and to consider additional measurements of Harbor contaminant concentrations. The effort to ultimately provide NJDOT with a tool for determining the current and future levels of contamination in the sediments within navigation channels was performed in a series of subtasks which started with a now completed post-audit evaluation of the CARP 1 model (Landeck Miller et al., 2019). The second subtask in the series is the now completed update of model external loading forcing functions (Landeck Miller et al., 2022). The third subtask in the series is the update of the CARP models. The series of subtasks will end with revised projections of PCB and PCDD/Fs contamination in Harbor sediments and dredged-material-test organisms based on new measurements and model refinements.

The completed third subtask, update of the CARP models, is described herein. The ultimate purpose of updating the CARP models is to increase the reliability and technical defensibility of the modeled time responses for Harbor water and sediment concentrations (i.e., biota exposure concentrations) for model projections beyond current conditions, based on extrapolation of available information from recent years rather than only on CARP 1 information from prior to 2002. Measurements collected by other CARP 2 investigators in 2018, 2019 and 2021 along with readily available measurements compiled from a variety of sources for the period 2002 to 2016 were used for assessing model performance and for making decisions for updates to model inputs. In particular, the 2018, 2019, and 2021 measurements collected by other CARP 2 investigators provided additional context for measurements compiled for 2002 to 2016, especially for defining the measured temporal trend where measurements from 2010-2016 were lacking. New model simulations were performed after each refinement to model inputs to assess interim model responses and skill sequentially. Given the relationship between sediment and organic carbon transport and contaminant fate and transport, refinements to the sediment transport/organic carbon production and contaminant fate and transport models were implemented in parallel. Most changes to sediment transport model inputs were tested in both the sediment transport/organic carbon production and contaminant fate and transport models before making an additional change to the sediment transport/organic carbon

production model. The update of model inputs is a necessary precursor to the subsequent planned subtasks focused on model projections.

2.0 METHODS

The methods developed and applied for update of the CARP models are discussed separately in Sections 2.1 to 2.3 for each of the models: hydrodynamic, sediment transport/organic carbon production, and contaminant fate and transport. Although the update methods developed and applied were specific to an input for one of the models, the assessment of the update occurred across models in most cases.

2.1 Methods for Update of CARP Hydrodynamic Model

The update of the CARP hydrodynamic model began with updates to the non-saline flows associated with external forcing functions. The methods for the updates to the non-saline flows associated with external forcing functions were previously reported in a CARP subtask deliverable (Landeck Miller et. al, 2022). These updated flows include tributary heads-of-tide, overland runoff and associated stormwater and combined sewer discharges, outflows from the Meadowlands, and the effluents of water resource recovery facilities and landfill leachates. Additional CARP hydrodynamic model updates include the computational grid, time-varying bathymetry, bottom friction in the model computational grid, open boundary conditions, water temperatures for freshwater flows associated with external forcing functions, wind stress, and heat flux. The methods for these updates are presented below in Sections 2.1.1 to 2.1.6.

2.1.1 Methods for CARP Hydrodynamic Model Update, Computational Grid

The decision to increase the resolution of the CARP model computational grid from 49 x 84 to 127 x 205 longitudinal/lateral elements and to take on the associated additional computational burden was not entered into lightly. As a first step, in-channel and off-channel contaminant concentrations in the bed were considered. In-channel and off-channel contaminant measurements from prior to 2016 available for CARP post-audit purposes were overlapping and post-audit model results were mostly in agreement with the central tendency of the wide-ranging measurements. (Landeck Miller et al., 2019) Proximal CARP 2 in-channel and off-channel contaminant measurements collected in 2019 were generally not appreciably different, especially on an organic carbon normalized basis. Given the post-audit and CARP 2 measurement results, the method followed for updating the CARP model computational grid was not based on representation of in-channel and off-channel areas as first considered.

Increased resolution of the CARP model computational grid was informed by comparing CARP results and results of other modeling efforts completed after CARP 1. HDR work with other models such as for New Jersey Combined Sewer Overflow (CSO) Long Term Control Plan (LTCP) development indicated that the CARP model comparisons to high frequency salinity measurements would be improved with additional model grid resolution, especially in Newark Bay and in the Hudson River. Further, additional grid resolution would correct deficiencies in the representation of Harbor areas noted during the CARP post-audit such as the Shooter's Island vicinity of the Kill van Kull. A synopsis of these observations supporting the decision to increase the resolution of the CARP model computational grid are included in Appendix 1.

The approach for increasing the resolution of the CARP model computational grid centered on leveraging strengths and weaknesses from model computational grids from several previous HDR modeling efforts including the CARP 2010 Hudson River Foundation (HRF) funded research project; the Lower Passaic

River and Newark Bay Superfund Remedial Investigations and Feasibility Studies (RI/FS); and the New Jersey CSO LTCP project. The 49 x 226 element computational grid from the CARP 2010 research project improved CARP model grid resolution only upstream of Haverstraw Bay and was computationally inefficient. The 74 x 268 element computational grid from the Superfund projects improved CARP model grid resolution only in the Newark Bay complex (i.e., Lower Passaic River, Hackensack River, Newark Bay, and Kills) and neglected increased model computational grid resolution increases in other areas. The 125 x 185 element computational grid from the LTCP improved CARP model grid resolution throughout both the Newark Bay complex and the Harbor from the top of Haverstraw Bay. While it was desirable to adopt features from the CARP 2010 and LTCP model computational grids, the two could not be simply combined due to inefficiencies in the CARP 2010 model computational grid. The LTCP model computational grid was used as a starting point and further enhancements to resolution were made in the Hudson River above Haverstraw Bay and in the Upper NY Bay. Draft versions of the CARP model computational grid were tested for stability, run times, and ultimately model and measurement comparisons.

Finalizing the CARP model computational grid resolution involved tuning adjustments to obtain the correct salinity intrusion in the Raritan and Hudson Rivers; to improve tidal dynamics on the Hudson River; and to properly assign bathymetry at the higher longitudinal and lateral resolution systemwide. Specifically for the correct salinity intrusion in the Raritan River, model grid depths were adjusted for in-channel and off-channel areas. For the Hudson River, the typical time for the tidal wave to progress from the Battery to Albany is approximately 8.25 hours. Given the typical 8.25 hours of time lag for the tidal wave to propagate upstream, achieving the timing of tidal phases within 0.5 hours was targeted along with accurate tidal amplitudes and salinity intrusion. For the Hudson River final tweaking adjustments to the model computational grid included addition of grid cells between West Point, NY, and the bottom of Haverstraw Bay and adjustments to model grid cell depths upstream of Piermont Pier near Piermont, NY. Additional depths adjustments consistent with the increased model grid resolution were made along the Ambrose and Anchorage Channels, in the East River from the Battery to western Long Island Sound, and in Jamaica Bay.

2.1.2 Methods for CARP Hydrodynamic Model Update, Time Varying Bathymetry

For the development of time varying bathymetry for CARP October 1, 1998, to September 30, 2016, modeling, a “working backwards” approach was followed to identify various bathymetry epochs. The starting point was the deepened bathymetry representative of conditions for 2010 to 2016 model bathymetry inputs. Shallower bathymetries during earlier time periods were then considered for model bathymetry inputs in prior years. The approach was limited to model grid cells which became deeper rather than shallower due to the dredging efforts for NY/NJ Harbor deepening purposes. Five bathymetry epochs (i.e., four substantial changes in conditions) were identified for representing NY/NJ Harbor deepening in the CARP model bathymetry inputs: 2010 - 2016, 2007 - 2010, 2003 – 2007, 1999 – 2003, and 1998 – 1999.

The October 1, 2010, to September 30, 2016, CARP model bathymetry input epoch represents the completion of 52’ deepening projects in the Port Jersey, Anchorage, and Ambrose Channels and in the navigation channels in Newark Bay and the Kills. The October 1, 2007, to September 30, 2010, CARP model bathymetry input epoch represents interim bathymetry conditions during NY/NJ Harbor deepening projects targeting a depth of 52’ for most navigational areas, especially in Newark Bay and the Kills. The October 1, 2003, to September 30, 2007, CARP model bathymetry input epoch represents the completion of 45’ to 47’ projects in the navigation channels of Newark Bay and the Kill van Kull. The October 1, 1999, to September 30, 2003, CARP model bathymetry input epoch represents interim bathymetry conditions during NY/NJ Harbor deepening projects targeting depths of 45’ to 47’ along the Kill van Kull, channels in Newark Bay and the Port Jersey Channel. The October 1, 1998, to September 30, 1999, CARP model bathymetry input epoch represents pre-deepening conditions, < 40’.

The four water years 1998 - 2002 originally represented by the CARP model with a single bathymetry condition are now represented by two different bathymetry conditions, reflecting the transition from 40' up to 47' navigation channels. Further, the CARP modeling period is expanded to include an additional fourteen water years, 2002 – 2016, and three additional bathymetry conditions associated with the progression of NY/NJ Harbor deepening efforts.

Historic depths conditions were considered along navigation channels from the New York Bight Apex to the Port Jersey Channel in the Upper New York Bay and the Port Elizabeth and Port Newark Channels in Newark Bay and along the Kill van Kull and Arthur Kill. Bathymetry for model grid cells in other locations, although specified for model calibration, was not varied across epochs. NOAA navigation charts published since 1990 were downloaded and reviewed for changes for the targeted Harbor deepening locations. The supplemental information available for assigning CARP model inputs for time varying bathymetry due to NY/NJ Harbor deepening efforts and fixed calibration bathymetry varied across locations.

For the portion of the inner NY/NJ Harbor bounded approximately by the heads-of-tide on the Hackensack, Lower Passaic, and Raritan Rivers, the George Washington Bridge on the Hudson River, Throgs Neck in the East River, and Sandy Hook and the Rockaways in the Bight, CARP model bathymetry was further specified based on bathymetry data compiled by E4 Sciences in 2016 at 18 m to 30 m resolution. Within this area, specifically for Newark Bay and portions of the Arthur Kill and Kill van Kull, CARP model bathymetry was also specified based on survey data collected by the University of Delaware in 2008 in support of USEPA Lower Passaic River and Newark Bay Superfund efforts. Of note, the University of Delaware survey covered both the deep navigation areas and shallow shoal areas in Newark Bay rather than focusing strictly on navigation channels.

For the Hudson River from Albany, New York to Upper NY Bay, CARP model bathymetry was further specified based on 30 m NYSDEC bathymetric survey data from 2007 and the NOAA 30 m digital elevation model published in 2018. The NYSDEC survey covered only deep sections of the Hudson River and omitted many shallow areas. The NOAA digital elevation model filled spatial gaps in the NYSDEC survey. For the New York Bight and Long Island Sound, CARP model bathymetry was specified based on sounding data in NOAA's electronic nautical charts.

For multiple areas within deepening project footprints, numerous USACE NY District tiles of small area bathymetric survey data at different times between 1999 and 2010 when deepening dredging activities were in-progress were reviewed. It was challenging to incorporate these transient data during dredging into synoptic depth conditions for model bathymetry input epochs. There is less confidence in the two bathymetry input epochs representing interim conditions (i.e., 2007 – 2010 dredging for 52' deepening and 1999 – 2003 dredging for 45' to 47' deepening) than in the model bathymetry input epochs representing the completion of the two phases of Harbor deepening (i.e., the 2010 - 2016 completion of 52' deepening projects and the 2003 – 2007 completion of 45' to 47' projects).

2.1.3 Methods for CARP Hydrodynamic Model Update, Bottom Friction

An important calculation performed by the hydrodynamic model is the near bottom shear used to control resuspension in the sediment transport model. The method used for the hydrodynamic model calculation of near bottom shear stress includes the specification of a minimum non-dimensional bottom friction coefficient. The minimum bottom friction coefficient applied in the hydrodynamic model is 0.003 which is used in a model equation for calculation of near bottom shear. A discussion of the model equation for the calculation of the near bottom shear stress and the use of the minimum non-dimensional friction coefficient

in the calculation is presented below in Section 2.2.1. The selection of the minimum non-dimensional friction coefficient of 0.003 has a long history of application dating back to the original System Wide Eutrophication Model (HydroQual, 2001; Blumberg et al., 1999) prior to CARP 1.

While the near bottom shear stress as calculated by the hydrodynamic model is applied directly for most grid cells in the model domain, some spatial adjustments are judiciously made for calibration purposes to reproduce measurements of tidal water elevations, velocity currents, salinity, and temperature, especially in areas of high energy and/or complex geometry. For the original 49 x 84 CARP model computational grid, the spatial adjustments applied to the near bottom shear stress calculated with the hydrodynamic model likely offset deficiencies in lateral grid resolution, including scaling adjustments in the Raritan, Lower Passaic, Hackensack, East, and Harlem Rivers and in portions of Newark Bay. With the spatial resolution improvements of the 127 x 205 model computational grid, spatial adjustments to near bottom shear stress were no longer applied in Newark Bay and the Raritan and Lower Passaic Rivers. Adjustments to near bottom shear stress were still however applied in the Hackensack, East, and Harlem Rivers on the 127 x 205 model computational grid. Also, on the 127 x 205 model computational grid, new adjustments to calculated near bottom shear stress were added in the Peekskill, NY to Cold Spring, NY reach of the Hudson River. The spatial scale factors applied to the near bottom shear stress calculated by the hydrodynamic model on the 127 x 205 model computational grid for calibration purposes include: 5x for the Peekskill, NY to Cold Spring, NY reach of the Hudson River; 10x for most of the Hackensack and East Rivers; 20x for the Harlem River; and 100x for several grid cells in the Lower East River in the vicinity of the eastern shore of Roosevelt Island.

Regarding the adjustments applied for near bottom shear stress on the 127 x 205 model computational grid, there appear to be physical justifications in addition to the calibration improvement needs. The Peekskill, NY to Cold Spring, NY reach of the Hudson River is narrow and tortuous with much broader reaches immediately upstream and downstream and undoubtedly complex transport features. The Hackensack River is surrounded by New Jersey Meadowlands marsh areas, only simplistically represented by the model computational grid. The East River and Harlem Rivers are both energetic tidal straights with strong currents. Further, the East River has numerous islands and irregular shorelines. The Harlem River and the Lower East River channel on the eastern shore of Roosevelt Island are represented laterally only by single model grid cells. Single lateral model grid cells do not resolve small scale physics such as secondary currents and horizontal velocity shear.

2.1.4 Methods for CARP Hydrodynamic Model Update, Open Boundary Conditions

An important element of the CARP hydrodynamic model is the specification of model open boundary conditions for water elevation, temperature, and salinity along the continental shelf break in the New York Bight between Cape May and Nantucket shoals. The same data resources used to specify hydrodynamic model open boundary inputs for the four water years addressed by CARP 1 were, with few exceptions, also available for the fourteen additional water years addressed for CARP 2. The methods for specifying the hydrodynamic model open boundary conditions are described in HydroQual, 2007a. Specific exceptions are noted below.

As described in HydroQual, 2007a, specification of water elevations at the open boundary includes three components, long-term circulation (i.e., geostrophic currents) due to cross-shelf slope; astronomical tidal fluctuations; and subtidal (i.e., meteorological) forcing. Specification of the subtidal forcing component relies on 34-hour low passed measurements of water surface elevations at Sandy Hook. The processing of the measurements for adjustment between Sandy Hook and the location of the model open boundary at the shelf break remain unchanged from the methods in HydroQual, 2007a. Specifically for CARP 2, for

specifying the subtidal component of the water elevation open boundaries of the hydrodynamic model for the period October 29, 2012, to December 7, 2012, when continuous measurements at Sandy Hook were missing, measurements from the Battery were instead used. The measurements from the Battery were handled as though they were collected at Sandy Hook. Measurements from Sandy Hook and the Battery are in close agreement during periods when measurements from both locations are available.

For specifying the CARP hydrodynamic model temperature and salinity open boundaries, the World Ocean Database (WOD) (Boyer, et al., 2018) was used. The WOD was developed to provide reproducibility for the World Ocean Atlas (WOA) series. The WOA series is a continuation of the Climatological Atlas of the World Ocean (Levitus, 1982), a set of global one-degree gridded climatological mean fields of oceanographic variables at standard depth levels in the ocean. The gridded climatological mean fields are useful for, among other things, initial and boundary conditions for coupled climate models. Climatological data, while useful, do not always represent true monthly variations and can often require manual adjustments for use. From the WOD, the 1998 WOA was used to specify the ocean boundary conditions for salinity for both the CARP 1 and CARP 2 hydrodynamic models with a manual adjustment of (-)2 psu. Salinity climatological measurements from the 2013 WOA were considered for use in CARP 2 and were found to be too high and were therefore not used given no clear advantage over continuing to use the manually adjusted 1998 WOA salinity. The 1998 WOA was also used to specify the ocean boundary conditions for temperature for the CARP 1 hydrodynamic model and required manual adjustment. For CARP2, the 2013 WOA was instead used for the ocean boundary conditions for temperature without any manual adjustments. Effectively, the CARP 2 hydrodynamic model uses newer climatological estimates without manual adjustments for temperature ocean boundary conditions and retains the salinity open boundary conditions developed during CARP 1.

2.1.5 Methods for CARP Hydrodynamic Model Update, Freshwater Flows and Temperatures

The freshwater flows included in the CARP hydrodynamic model and described in Landeck Miller et al., 2022, for tributary heads-of-tide, overland runoff and associated stormwater and combined sewer discharges, outflows from the Meadowlands, and the effluents of water resource recovery facilities and landfill leachates, each require temperature specification. There are several measurement sources used for specifying the temperatures associated with the non-saline water entering the CARP hydrodynamic model. For the heads-of-tide for the Hudson River and the tributaries to the Hudson River, daily temperature records from the USGS at Poughkeepsie (https://waterdata.usgs.gov/nwis/uv?site_no=01372058) were applied. For the heads-of-tide for the Hackensack River and the Lower Passaic River and its tributaries, daily temperature records from the USGS on the Passaic River below the Pompton River (https://waterdata.usgs.gov/nwis/uv?site_no=01389005), were applied. For all other head-of-tide locations, daily temperature records from NOAA at the Battery (https://tidesandcurrents.noaa.gov/physocean.html?id=8518750) were applied. Temperature records from NOAA at the Battery were also applied for stormwater and combined sewer discharges outside of New Jersey. Within New Jersey, temperature records from the USGS on the Passaic River below the Pompton River were applied for stormwater, combined sewer discharges, and outflows from the Meadowlands. Temperatures for the treated effluents from water resource recovery facilities and for landfill leachate were based on representative monthly averages from measurements compiled across several facilities as available from the NYCDEP and remain unchanged from CARP 1 (HydroQual, 2007a).

2.1.6 Methods for CARP Hydrodynamic Model Update, Wind Conditions and Heat Flux

Wind stress and heat flux are two major 2-D forcings applied in the hydrodynamic model on the modeled water surface. Wind stress is calculated by the hydrodynamic model from both wind speed and wind direction using X and Y vector components. Heat flux is calculated by the hydrodynamic model from air temperature, relative humidity, barometric (i.e., sea level) pressure, shortwave solar radiation, and cloud cover. For CARP 2, wind speed and wind direction vector components, air temperature, relative humidity, barometric (i.e., sea level) pressure, shortwave solar radiation, and cloud cover were all specified using NOAA Physical Sciences Laboratory (PSL) National Centers for Environmental Prediction (NCEP) North America Regional Reanalysis (NARR) measurements obtained hourly to monthly from sixty-nine stations as shown on Figure 2-1 and downloaded from https://psl.noaa.gov/data/gridded/data.narr.html. The use of the NARR measurements from the sixty-nine stations shown on Figure 2-1 in CARP 2 hydrodynamic model is a big improvement in spatial specificity as compared to the CARP 1 hydrodynamic model. For the CARP 1 hydrodynamic model, the wind stress was based on measurements from Albany, Bridgeport, and John F. Kennedy Airports, and four buoys in the NY Bight and the heat flux was based only on measurements from John F. Kennedy Airport.

2.2 Methods for Update of CARP Sediment Transport and Organic Carbon Production Model

The update of the CARP sediment transport and organic carbon production model began with updates to suspended sediment, organic carbon, and nutrient loading concentrations and/or loadings associated with inputs of non-saline water into the model. The methods for the updates to suspended sediment, organic carbon, and nutrients associated with non-saline inflows were previously reported in a CARP subtask deliverable (Landeck Miller et. al, 2022). These updated sources of suspended sediment, organic carbon, and nutrients include tributary heads-of-tide, overland runoff and associated stormwater and combined sewer discharges, outflows from the Meadowlands, and the effluents of water resource recovery facilities and landfill leachates.

The approach adopted to update the CARP sediment transport and organic carbon production model beyond loadings focused on addressing model input specifications that were related to model grid resolution. Accordingly, the spatially varying CARP sediment transport and organic carbon production model settling and coagulation functions, which are dependent on variations in salinity and fluid shearing rates, and not model grid resolution, were not updated absent other technical justification for doing so and remain consistent with the documentation provided in HydroQual, 2007b. CARP sediment transport and organic carbon production model updates beyond loadings include modifications to several model parameters and constants controlling resuspension, initial bed thickness, water column vertical mixing rates, biological mixing rates in the sediment bed, and base light extinction in the marsh areas along the Hackensack River. The methods for these updates are presented below in Sections 2.2.1 to 2.2.5.

2.2.1 Methods for CARP Sediment Transport and Organic Carbon Production Model Update, Parameters and Constants Controlling Resuspension

For CARP modeling on both the 49 x 84 and 127 x 205 model computational grids, the typical power law function describing the relationship between the resuspension flux rate and near bottom shear stress was applied:

$$Q_s = a_o \left[\frac{\tau_{bottom} - \tau_{critical}}{\tau_{critical}} \right]^n$$

Equation 2.2.1-1

where Q_s is the resuspension flux rate (mg/cm^2/hr), a_o is a fitting coefficient (mg/cm^2-hr), τ_{bottom} is the bottom shear stress (dynes/cm^2), $\tau_{critical}$ is the critical shear stress, which indicates the shear stress required to initiate resuspension of sediment, and n is a unitless fitting coefficient.

For both the 49 x 84 and 127 x 205 model computational grid releases of the CARP model, the fitting coefficients were assigned values of 4 and 1, for a_o and n, respectively. For both the 49 x 84 and 127 x 205 model computational grid releases of the CARP model, $\tau_{critical}$ was assigned 0.5 and 3 dynes/cm^2 for the top 10 cm and deeper bed archive layers, respectively. Literature and site measurements supporting the assigned values for a_o, n, and $\tau_{critical}$ are as described in HydroQual, 2007b.

For both the 49 x 84 and 127 x 205 model computational grid releases of the CARP model, bottom shear stress, τ_{bottom}, is calculated directly from the hydrodynamic model flow field and the bottom roughness as:

$$\tau_{bottom} = \rho u_*^2 \qquad where \qquad u_* = \frac{\kappa u}{ln[z/z_o]}$$

Equation 2.2.1-2

where ρ is the fluid density, u_* is the shear velocity, u is the instantaneous velocity in the bottom water column layer, κ is the von Karmen constant, z is the distance from the bottom to the mid-depth of the bottom water column layer, and z_0 is the roughness height for skin friction. For most of the CARP model domain, model grid cells have both longitudinal (u) and lateral (v) components of instantaneous velocity and the bottom shear stress is calculated as an aerial average as:

$$\tau_{bottom} = \rho \left[\frac{\kappa}{ln[z/z_o]} \right]^2 \iint \left[u^2 + v^2 \right] dy\, dx$$

Equation 2.2.1-3

with the instantaneous velocity components (i.e., both u and v) assumed to vary linearly across the cell.

The von Karmen constant, κ, is set at the canonical value of 0.4 for both the 49 x 84 and 127 x 205 model computational grid releases of the CARP hydrodynamic model. For both the 49 x 84 and the 127 x 205 model computational grid, the hydrodynamic model roughness height for skin friction, z_0, was maintained at 0.001 m throughout the domain.

Equation 2.2.1-3 is a somewhat simplified representation of the equation included in the CARP hydrodynamic model for calculating bottom shear stress, τ_{bottom}. In the hydrodynamic model code, the squared multiplier in Equation 2.2.1-3, including the von Karmen constant, the roughness height for skin friction, and the distance from the bottom to the mid-depth of the bottom water column layer, is replaced by the maximum of the squared multiplier and a minimum non-dimensional bottom friction coefficient specified for the hydrodynamic model. Effectively, the hydrodynamic model code checks for and applies the maximum of the minimum non-dimensional bottom friction coefficient and the squared multiplier in Equation 2.2.1-3. The maximum is further scaled in the hydrodynamic model at some locations for the hydrodynamic model calibration. The minimum non-dimensional bottom friction coefficient in the hydrodynamic model and the location-specific scale factors applied to the maxima in the hydrodynamic model are described in Section 2.1.3.

Within the CARP sediment transport model, there are options for further adjusting the bottom shears stress, τ_{bottom}, developed for the hydrodynamic model calibration. While adjustments to the bottom shears stress, τ_{bottom}, developed for the hydrodynamic model calibration were used in the sediment transport and organic carbon production model for the 49 x 84 model computational grid at several locations to offset wind-driven wave effects and deficiencies in model grid resolution and design (e.g., artificial bends conserving

computational space), further adjustments to bottom shear stresses in the sediment transport model were no longer necessary for the 127 x 205 model computational grid.

Although it was accepted that adjustments to the bottom shears stress, τ_{bottom}, used for the hydrodynamic model calibration were necessary in the sediment transport and organic carbon production model to offset deficiencies in the hydrodynamic transport associated with the 49 x 84 model computational grid, the adjustments were maintained in the early sediment transport and organic carbon production model simulations on the 127 x 205 model computational grid as a first step. Ultimately, after performing numerous model simulations and reviewing model outputs, the spatial adjustments were abandoned as it was determined that the sediment transport and organic carbon production model calculations of net sedimentation and suspended sediment on the 127 x 205 model computational grid were adequate without the spatial adjustments. Thus, transport information passed from the hydrodynamic model on the 127 x 205 model computational grid was used directly in the sediment transport and organic carbon production model, which is a more technically defensible and streamlined approach and a benefit of the higher resolution model computational grid.

2.2.2 Methods for CARP Sediment Transport and Organic Carbon Production Model Update, Water Column Vertical Mixing Adjustments

Within the CARP sediment transport model code, there is capability to adjust the water column vertical mixing rates passed from the hydrodynamic model calibration. While adjustments first developed for the System Wide Eutrophication Model (HydroQual, 2001) to the water column vertical mixing rates calculated by and passed from the hydrodynamic model were used in the CARP sediment transport and organic carbon production model for the 49 x 84 model computational grid at several locations to offset deficiencies in model grid resolution and hydrodynamic transport, adjustments to water column vertical mixing rates were not repeated in the CARP sediment transport and organic carbon production model for the 127 x 205 model computational grid. Transport information passed from the CARP hydrodynamic model on the 127 x 205 model computational grid was used directly in the CARP sediment transport and organic carbon production model, which is a more technically defensible and streamlined approach and a benefit of the higher resolution model computational grid.

2.2.3 Methods for CARP Sediment Transport and Organic Carbon Production Model Update, Sediment Bed Particle Mixing Rate Adjustments

One of the 2D inputs to the sediment transport and organic carbon production model is the sediment bed biological particle mixing rates for the top 10 cm of the bed. In the sediment transport and organic carbon production model, the specified particle mixing rates representing bioturbation by organisms control the depth of aerobic and anerobic zones within the top 10 cm of the sediment bed. The inputted 2D particle biological mixing rates are scaled within the sediment transport model code by model grid cell specific factors including the POC concentration which serves as a surrogate for organism food supply, dissolved oxygen related organism stress, and temperature. Once scaled, the biological particle mixing rates are combined with physical particle mixing rates and are passed forward to the contaminant fate and transport model. The sediment mixing caused by bioturbation impacts the temporal behavior of contaminants in the sediment bed and is a determinant of how rapidly contaminants in the sediment bed exchange with the water column.

During early model calibration for the contaminant fate and transport model for the period October 1, 1998, through September 30, 2016, for the 127 x 205 model computational grid, it was noted that while modeled dioxin and furan concentrations in the Lower Passaic River were within the wide range of available

measurements, they were dropping off rapidly. Given the wide range in available measurements, to better assess if the temporal behavior of the CARP contaminant fate and transport model was realistic, contaminant fate and transport modeling work conducted for the Lower Passaic River and Newark Bay Superfund sites was considered. The Lower Passaic River and Newark Bay Superfund models did not calculate rapidly declining dioxin and furan concentrations. Further inspection of the Lower Passaic River and Newark Bay Superfund modeling work revealed the use of a reduction in particle mixing rates in the Lower Passaic River.

As indicated on Figure 10-2 in USEPA 2016, for purposes of modeling supporting the Record of Decision for the Lower 8.3 miles of the Lower Passaic River, the particle mixing rate in the Lower Passaic River was reduced to 1 cm^2/yr, at the lower end of particle mixing rates reported in the literature (Boudreau, 1994). Boudreau, 1994, shows particle mixing rates varying between 0.2 and 200 cm^2/yr for burial velocities in the 1 to 2 cm/yr range, appropriate for the Lower Passaic River. The reduction of the particle mixing rate to 1 cm^2/yr applied in Superfund modeling was also adopted and applied for the Lower Passaic River for CARP modeling on the 127 x 205 model computational grid for the inputted biological particle mixing rate before adjustments for factors such as food supply, dissolved oxygen stress, and temperature and before combination with the physical mixing term. Sediments in the Lower Passaic River are relatively more highly contaminated than sediments in other Harbor areas and therefore have the potential to adversely impact the activity of organisms achieving sediment mixing via bioturbation. In other areas of the domain of the CARP 127 x 205 model computational grid, the inputted biological particle mixing rate (i.e., before adjustments for factors such as food supply, dissolved oxygen stress, and temperature and before combination with the physical mixing term) remained unchanged from the value applied for the System Wide Eutrophication Model (HydroQual, 2001) and maintained for CARP 1 modeling (HydroQual, 2007b), 438 cm^2/yr. The results for reducing the biological particle mixing rate in the Lower Passaic River in the CARP model are considered in Sections 3.3 and 4.

For further context on the method by which the inputted biological particle mixing rate was adjusted in the Lower Passaic River for CARP modeling using the 127 x 205 model computational grid, Equation 2.2.3-1 is provided. Equation 2.2.3-1 is unchanged from the System Wide Eutrophication Model (HydroQual, 2001) and CARP 1 model (HydroQual, 2007b). Equation 2.2.3-1 shows the inputted biological particle mixing rate, D_P, along with the temperature, food supply, and dissolved oxygen stress adjustment factors and abiotic particle mixing. The biological particle mixing rate, D_P, controls the mixing of the top 10 cm of the sediment bed as follows:

$$\omega_{12} = \frac{D_P \Theta_{D_P}^{(T-20)}}{H_2} \frac{POC_1}{POC_{1,R}} \left(1 - k_S \frac{S_{t-1} + t \frac{K_{M,D_P}}{K_{M,D_P} + DO_0}}{1 + k_S t} \right) + \frac{0.3 \times 10^{-5}}{H_2}$$

Equation 2.2.3-1

where ω_{12} (m/d) is the mixing rate of particles in the sediment bed; D_P (m^2/d) is the biological particle mixing rate; Θ (unitless) is the Arrhenius temperature dependency coefficient for biological particle mixing; T (°C) is the sediment bed temperature; H_2 (m) is the depth of the anaerobic portion of the top 10 cm of the bed over which particle mixing is achieved; POC_1 (ug OC/kg SS) is the concentration of G_1 (i.e., labile, newly deposited) particulate organic carbon representing the food source for benthic organisms mixing sediment particles; $POC_{1,R}$ (ug OC/kg SS, assigned as 10^5 for CARP modeling) is the reference concentration of G_1 (i.e., labile, newly deposited) particulate organic carbon representing no food source limitations for benthic organisms mixing sediment particles; k_S (d^{-1}, assigned as 0.03 for CARP modeling) is the first-order decay coefficient representing the rate at which any accumulated organism oxygen stress is dissipated; S_{t-1} (d) is the accumulated benthic stress time for the previous time interval; t (d) is the time increment (i.e., the

modeled timestep which for CARP 2 is 120 seconds or 0.00138889 days); $K_{M,DP}$ (mg O_2/L, assigned as 4 for CARP modeling) is the particle mixing Michaelis-Menton expression half-saturation constant for dissolved oxygen; DO_0 (mg O_2/L) is the dissolved oxygen in the overlying water column; and finally the abiotic particle mixing rate is specified for CARP 2 modeling at a constant 0.3 x 10^{-5} m^2/d. 438 cm^2/yr, the biological particle mixing rate, D_P, applied for most of the CARP model domain is equivalent to 0.12 x 10^{-3} m^2/d for use in Equation 2.2.3-1. 1 cm^2/yr, the biological particle mixing rate, D_P, applied for the Lower Passaic River portion of the CARP model domain is equivalent to 2.7 x 10^{-7} m^2/d for use in Equation 2.2.3-1.

The theoretical derivation of the biological portion of Equation 2.2.3-1, including supporting literature references, is explained in Chapters 13.2 A and B of DiToro, 2001. It is noted that in DiToro's presentation, the overlying water column dissolved oxygen has a dual role impacting both the food supply factor and the modeled factor for stress to organisms mixing particles. Equation 2.2.3-1 used for System Wide Eutrophication and CARP modeling considers the effect of dissolved oxygen stress to organisms mixing particles with a single factor. Further, DiToro's presentation includes a variable recovery period (i.e., the remainder of a simulation year, potentially ranging from minutes to 365 days but intended for summer to summer) after a low overlying water column dissolved oxygen episode, ignoring factors such as any organism recovery, the duration of the low dissolved oxygen episode, etc. The recovery period included by DiToro is not included for CARP modeling. Rather in System Wide Eutrophication and CARP modeling, recovery is simulated by maintaining the particle mixing Michaelis-Menton expression from Equation 2.2.3-1 at the lowest modeled value for dissolved oxygen in any interval when temperature is sustained above 10°C. At or below 10°C, the particle mixing Michaelis-Menton expression from Equation 2.2.3-1 fluctuates with the modeled dissolved oxygen for each timestep.

2.2.4 Methods for CARP Sediment Transport and Organic Carbon Production Model Update, Initial Bed Thickness

As described in HydroQual, 2007b, the CARP sediment transport and organic carbon production model includes a 10 cm active layer and an archive layer for mass storage. Mass enters the archive layer when deposition is greater than erosion to prevent the volume of the 10 cm active layer from being exceeded. Mass leaves the archive layer to offset depletion of the 10 cm active layer when erosion is greater than deposition. The inputs for the CARP sediment transport and organic carbon production model require the specification of an initial bed thickness (i.e., effectively a solids mass) for the archive layer. As a first step, initial bed thicknesses for the archive layer of the sediment bed for the 127 x 205 model computational grid were assigned using the same assignment developed during CARP 1 for the 49 x 84 model computational grid with each model grid cell from the 49 x 84 model computational grid mapped to numerous model grid cells on the 127 x 205 model computational grid.

Corrections to this initial approach were necessary. In some instances, the hydrodynamic transport on the 127 x 205 model grid changed individual grid cells or groupings of grid cells from depositional to erosional as compared to the 49 x 84 model. Due to such shifts in erosional areas, the initial bed thicknesses first assigned for the 127 x 205 model computational grid were sometimes inappropriate and problematic. In some cases, initial nonzero bed thicknesses were assigned to highly erosional areas and resulted in unrealistic scour of bed solids, if not corrected (i.e., set to zero). Most notably, this problem occurred in the central area of Newark Bay which was too strongly and too broadly depositional in the CARP 1 49 x 84 model. Similarly, for two model grid cells in the East River (between Brother and Rikers Islands), the assigned initial bed thicknesses for the archive layer were also reduced for consistency with strong erosion calculated on the 127 x 205 model grid. In locations such as several model grid cells in the Lower Passaic

River where the CARP 127 x 205 hydrodynamic model results alternate in time between being depositional and erosional rather than strictly erosional as in the CARP 49 x 84 hydrodynamic model, initial bed thicknesses for the archive layer were increased instead of staring with the zero initial bed thicknesses from the 49 x 84 model so that mass suspended in erosion events early in the simulation would not be missed.

2.2.5 Methods for CARP Sediment Transport and Organic Carbon Production Model Update, Base Light Extinction in Lower Hackensack River Marsh Areas

The CARP 127 x 205 model computational grid includes the marsh areas adjacent to the Lower Hackensack River. Since these marsh areas were not included in the CARP 49 x 84 model computational grid, as an initial approach, base light extinction was assigned in the marsh areas based on the base light extinction assigned in the main channel of the Lower Hackensack River in the CARP 49 x 84 model grid. This initial approach resulted in excessive algal growth in the water column as compared to chlorophyll and POC measurements, not only in the marsh areas, but in the Hackensack River as well. The base light extinction coefficients assigned for the marsh areas were increased in a first model simulation by a factor of 3 in the marsh areas and then in a second model simulation were combined with a factor of two increase of the base light extinction coefficients in portions of the Hackensack River mainstem to achieve more reasonable algal growth with the higher 127 x 205 model grid resolution and greater residence time. The increases to the base light extinction coefficients are consistent with the lower end of the central tendency of secchi disk measurements available at two locations within the Hackensack River which served as a guide for the increases to the base light extinction coefficients. The CARP sediment transport and organic carbon production model uses the inputted base light extinction coefficients along with a dynamic calculation of the light extinction due to algal self-shading to determine the total light extinction. The representation of the marsh areas in the CARP 127 x 205 model computational grid is even more extensive than was used for Lower Passaic River and Newark Bay Superfund modeling so in that sense the marsh areas in the CARP 127 x 205 model computational grid represent a newly modeled area.

2.3 Methods for Update of CARP Contaminant Fate and Transport Model

The update of the CARP contaminant fate and transport model began with updates to contaminant concentrations and/or loadings associated with inputs of non-saline water into the model. The methods for the updates to contaminant concentrations associated with non-saline inflows were previously reported in a CARP subtask deliverable (Landeck Miller et. al, 2022). These updated sources of contaminants include tributary heads-of-tide, overland runoff and associated stormwater and combined sewer discharges, outflows from the Meadowlands, and the effluents of water resource recovery facilities, landfill leachates, and atmospheric deposition.

The approach adopted to update the CARP contaminant fate and transport model beyond loadings focused on addressing other model input specifications that were related to having a new computational grid and new hydrodynamic transport and sediment transport. Contaminant fate and transport model simulations were conducted in parallel with the update of the sediment transport and organic carbon production model, especially for updating the sediment transport and organic carbon production model sediment bed particle mixing rates and sediment bed archive layer initial bed thicknesses, both of which are passed from the sediment transport and organic carbon production model to the contaminant fate and transport model. Updates specific to the contaminant fate and transport model include initial bed contaminant concentrations and a revised phase partitioning coefficient for di-PCB. Lastly, the calibration method for the contaminant fate and transport model for six contaminants (2,3,7,8-TCDD, 2,3,4,7,8-PCDF, di-CB, tetra-CB, hexa-CB, and octa-CB) included a robustness challenge or validation in which the calibrated models were applied for six additional PCB homologs and fifteen additional dioxin and furan congeners without adjustments to

methods or the information passed forward from the hydrodynamic transport and sediment transport and organic carbon production models. The methods for these contaminant fate model updates and robustness testing for additional contaminants are presented below in Sections 2.3.1 and 2.3.3.

2.3.1 Methods for CARP Contaminant Fate and Transport Model Update, Initial Bed Contaminant Concentrations

The initial bed contaminant concentrations for the active bed and archive were first assigned for the 127 x 205 model computational grid based on mapping the assignments from the 49 x 84 model computational grid which were based on NYSDEC measurements collected for CARP 1 and USEPA 1998 R-EMAP measurements as described in Section 3.3.3.1 of HydroQual, 2007c. The mapping relied upon the outputs of four-year spin-up simulations on the 49 x 84 model computational grid, a method established during CARP 1. Judicious refinements were required for the calibration on the 127 x 205 model grid, especially in areas where initial bed thicknesses for the archive were adjusted to nonzero as described in Section 2.2.4. Other refinements for the initial bed contaminant concentrations took advantage of using newer measurements as a guide for model grid cells where measurements representative of the 1998 model starting condition were lacking.

2.3.2 Methods for CARP Contaminant Fate and Transport Model Update, Di-PCB Phase Partitioning Coefficient

Contaminant phase partition coefficients for model calibration on the 127 x 205 model computational grid were specified as calculated during CARP 1 (HydroQual, 2007c) for all contaminants except for di-CB. As part of the CARP 2 bioaccumulation effort, measurements were collected which allowed for the calculation of contaminant phase partitioning between bulk sediment and sediment porewater (obtained via passive samplers). The contaminant phase partitioning coefficients calculated with the sediment bed and porewater measurements recently collected during CARP 2 were compared to the phase partitioning coefficients calculated with particulate and dissolved phase water column measurements collected more than twenty years ago during CARP 1. The calculated phase partition coefficients were overall in very good agreement considering the elapsed time and different media sampled. Any disagreements between the CARP 1 water column derived phase partition coefficients and the CARP 2 bed derived phase partition coefficients are likely explained by greater black carbon content and therefore greater binding capacity in the sediment bed particles as compared to the water column particles with dependence on the structure of the contaminant, the potential for incomplete attainment of dissolved phase equilibria during passive sampler deployments, and the difficulties experienced during CARP 1 with obtaining dissolved phase measurement of dioxins and furans in the water column.

Displays of the contaminant phase partitioning coefficients calculated during CARP 2 based on the sediment bed and during CARP 1 based on the water column are provided on Figure 2-2. On the top panel of Figure 2-2 which became available when CARP 2 model calibration was still in progress, it was noted that for the four PCB homologs used for model calibration, di-CB, tetra-CB, hexa-CB and octa-CB, the largest discrepancy between CARP 2 and CARP 1 measurement-based calculations of contaminant phase partitioning coefficients occurred for di-CB. The CARP 1 and CARP 2 log phase partitioning coefficients for POC are 6.04 and 6.92, respectively, almost a full log unit different. A sensitivity simulation was performed in which the contaminant phase partitioning coefficient for di-CB was specified with the higher value, based on CARP 2 rather than CARP 1 measurement-based calculations of contaminant phase partitioning coefficients. The model was relatively insensitive to the tested change in di-CB phase partitioning, with a slight reduction in di-CB water column concentrations for several locations and no adverse effects in the bed. The slight reduction at some locations in di-CB water column concentrations

with the increased phase partitioning coefficient represents slightly more contaminant per particle and slightly more di-CB removal from the water column as particles settle. The di-CB sensitivity simulation, which used the CARP 2 log phase partitioning coefficient for POC in both the water column and the sediment bed, was adopted as the di-CB calibration. Given the relative insensitivity, CARP 1 log phase partitioning coefficients for POC were maintained for contaminants other than di-CB and further sensitivity testing for log phase partitioning coefficients for POC was not undertaken.

2.3.3 Methods for CARP Contaminant Fate and Transport Model Update, Additional Contaminants Robustness Testing

Leveraging the significant effort previously expended to develop updates to contaminant concentrations and/or loadings associated with inputs of non-saline water into the model for ten PCB homologs and seventeen dioxin and furan congeners (Landeck Miller et al., 2022), the 18-year model calibrations for two dibenzo dioxin and furan congeners (i.e., 2,3,7,8-TCDD and 2,3,4,7,8-PCDF) and four PCB homologs (i.e., di-CB, tetra-CB, hexa-CB, and octa-CB) were complemented with 18-year model validation simulations for six additional PCB homologs (i.e., mono-CB, tri-CB, penta-CB, hepta-CB, nona-CB, and deca-CB) and fifteen additional dibenzo dioxin and furan congeners (i.e.,1,2,3,7,8-PCDD; 1,2,3,4,7,8-HxCDD; 1,2,3,6,7,8-HxCDD; 1,2,3,7,8,9-HxCDD; 1,2,3,4,6,7,8-HpCDD; OCDD; 2,3,7,8-TCDF; 1,2,3,7,8-PCDF; 1,2,3,7,8,9-HxCDF; 1,2,3,4,7,8-HxCDF; 1,2,3,6,7,8-HxCDF; 2,3,4,6,7,8-HxCDF; 1,2,3,4,7,8,9-HpCDF; 1,2,3,4,6,7,8-HpCDF; and OCDF). Performing validation simulations for twenty-one additional contaminants further tested the robustness of the results of the hydrodynamic and sediment transport and organic carbon production models that are passed forward to the contaminant fate and transport model for all contaminants and the common methods applied for contaminant-specific update of the contaminant fate and transport model.

3.0 RESULTS

Reported results for the CARP model update are centered around model and measurement comparisons or comparisons between CARP 1 and CARP 2 results for each of the three linked models.

3.1 Results for CARP Hydrodynamic Model Update

Key hydrodynamic model results generated include the final model computational grid, tidal water elevations, temperature, salinity, and velocity currents.

3.1.1 Results for CARP Hydrodynamic Model Update, Model Computational Grid

The result of the methods and considerations described in Section 2.1.1 is the increased resolution CARP model computational grid developed with 127 x 205 model grid elements as shown in Figures 3-1 to 3-7. Figure 3-1 shows the CARP model computational grid over the full model domain. Figures 3-2 shows the portion of the CARP model computational grid in the NY/NJ Harbor and Estuary. Figures 3-3 to 3-7 display zoomed in views of the CARP model computational grid in selected areas of the NY/NJ Harbor and Estuary with comparisons to the original CARP 1 model computational grid which had 49 x 84 model grid elements.

3.1.2 Results for CARP Hydrodynamic Model Update, Tidal Water Elevations

Model and measurement results for tidal water elevations are presented on an hourly basis in Appendix 2 for the 60-day period covering July 27 to September 24 (i.e., for other than leap years, July 26 to September

23 during leap years) and for a twelve-day period covering a portion of January and February for each of the eighteen modeled water years. In addition, in Appendix 3, model and measurement results for tidal water elevations are presented on a thirty-five-hour low pass numerical filter basis (i.e., eliminating variations occurring more frequently than every thirty-five hours highlighting other than diurnal and semi-diurnal tide features such as density-driven estuarine gravitational circulation, local or remote meteorological forcing, and nonlinear tidal dynamics) for each of the full eighteen water years modeled.

The periods presented in Appendix 2 for hourly results (i.e., 1728 hours shown per location per year or 31,104 hours across years per location) were randomly selected as a convenient representation at two temporal resolutions, for sixty days and for twelve days, and a necessary reduction given the eighteen-year length of the calibration period and the large number of potential diagrams (i.e., 157,788 hours per location). The randomly selected periods for hourly results show both winter and summer water elevation conditions. An additional 288 hours of results per location are shown in Appendix 2A for the twelve days October 24 through November 4, 2012, to display model performance during Hurricane Sandy. Each of the presentations of water elevation model and measurement comparisons results in Appendices 2 and 3 includes fifteen to sixteen locations over five to six pages for each of the eighteen water years modeled. Appendix 2A includes six pages for sixteen locations for the period before, during and after Hurricane Sandy. The locations where modeled and measured tidal water elevations are compared on the diagrams in Appendices 2, 2A and 3 and in Figures 3-9 to 3-16 are shown on the map in Figure 3-8.

The tidal water elevation measurements that are compared to the model results at the fifteen to sixteen locations included on the diagrams in Appendices 2 and 3 for each of the eighteen water years modeled were collected mostly by NOAA and as labelled on the diagrams, also by the USGS and the Hudson River Environmental Conditions Observing System (HRECOS, www.hrecos.org). Unless otherwise labelled, NOAA collected the tidal water elevation measurements. No attempt has been made to censor the measurements and there are periods with questionable or missing measurements, especially for the measurements collected by HRECOS. Due to the questionable measurements in some cases, it is important to consider results in Appendices 2 and 3 simultaneously for nearby stations and for January/February, July/September, and annual periods from the same water year.

Selected examples of the water surface elevation model and measurements results comparisons diagrams included in Appendices 2 and 3 are also presented as Figures 3-9 to 3-15 and Figure 3-16. The selected examples presented in Figures 3-9 to 3-15 include periods with perturbations from typical spring and neap tidal conditions which are interesting for assessing model performance. The selected examples presented in Figure 3-16 were chosen for data availability at locations within the Newark Bay complex portion of the model domain.

3.1.3 Results for CARP Hydrodynamic Model Update, Water Temperature and Salinity

Measurements of water temperature and salinity throughout the Harbor and Estuary suitable for comparisons to model results are readily available from ongoing and completed monitoring programs with established collection and quality protocols. The monitoring programs with salinity and temperature measurements for comparisons to model results, in alphabetical order, include: Connecticut Department of Energy and Environmental Protection; Lower Passaic River Superfund Site Cooperating Parties Group (CPG); HDR on behalf of the New Jersey Combined Sewer Overflow (CSO) Long Term Control Plan (LTCP) development project; Hudson River Environmental Conditions Observing System (HRECOS); Meadowlands Environmental Research Institute (MERI); New Jersey Harbor Dischargers Group (NJHDG); New York City Environmental Protection Harbor Survey; and the USGS.

For CARP model calibration, thirty-three pages of model and measurements comparisons diagrams, including ninety-three locations organized into six regional groupings, were created, and considered, for salinity for each of the eighteen years of model calibration. Similarly, for CARP model calibration, thirty-five pages of model and measurements comparisons diagrams, including ninety-nine locations organized into six regional groupings, were created, and considered, for temperature for each of the eighteen years of model calibration. This amounts to 1,224 pages of diagrams with 3,456 parameter/locations/years, too large for inclusion in report appendices. It is noted that not all diagrams had available measurements. For reporting purposes, the single water year 2009-10 was selected for each of the six regional groupings based on measurement richness. This resulted in a selection of thirty-three pages and ninety-three locations for presentation of full 2009-10 water year model and measurement comparisons for salinity and thirty-five pages and ninety-nine locations for presentation of full 2009-10 water year model and measurement comparisons for water temperature. The selected measurements and model results comparisons diagrams for water temperature and salinity are presented in Appendices 4 and 5, respectively. The six regional groupings of water temperature and salinity stations presented in Appendices 4 and 5 include: Lower Passaic River/Newark Bay; Kills/Raritan River and Bay; Hackensack River; Hudson River; East/Harlem Rivers, and Long Island Sound. The individual water temperature and salinity station locations are displayed on several maps included in Appendices 4 and 5.

In addition to the diagrams presented in Appendix 5 for the 2009-10 water year, model and measurement comparison results for salinity are shown for the 2001-02 water year on Figures 3-18 and 3-19 at the seven locations in Newark Bay and the Kills, displayed with other locations on the maps in Figure 3-17. The 2001-02 water year was selected to assess potential results improvements at times/locations of poor CARP 1 model performance (HydroQual, 2007a). Harbor deepening activities during 2001-02 are included as averaged approximations for the first time in the CARP 2 model inputs on the 127 x 205 model computational grid, albeit on a simplified basis as compared to the actual complexities of the evolving conditions. Measurements are displayed on Figures 3-18 and 3-19 for several months in the 2001-02 water year both before and after early March and the model results are displayed for the full year. An archive of salinity measurements from CARP 1 starting from the early March portion of 2002 and continuing through May 2002 could not be retrieved and are absent from Figures 3-18 and 3-19. Specific to the northern Newark Bay location results shown on Figure 3-18, the spring 2002 measurements which could not be retrieved were mostly characterized as unreliable due to a clogged conductivity sensor (Chant, 2006). Related examples for the 2009-10 water year from Appendix 5 at nine measurement-rich locations in Newark Bay and the Kills are shown in Figures 3-20 and 3-21 and illustrate model performance at a later stage of Harbor deepening.

Analogous to the full 2009-10 water year measurements and model results comparisons diagrams for water temperature and salinity presented in Appendices 4 and 5, Appendices 4A and 5A provide measurements and model results comparisons diagrams for water temperature and salinity for the full 2010-11 water year. While 2010-11 lacked continuous measurements at multiple locations as compared to 2009-10, measurement and model comparison results from 2010-11 were selected for additional appendices since 2010-11 includes a large spring freshet as well as two large storms, the Hurricanes Irene and Lee. The full 2009-10 water year measurements and model results comparisons diagrams for water temperature and salinity presented in Appendices 4 and 5 are further supplemented by the results diagrams presented in Appendices 4B and 5B which provide a thirty-day period focus for days 181 to 210 of 2009-10. This February 28 to March 29, 2010, thirty-day period was selected to highlight continuous measurements, expand the x-axis resolution for further clarity and transparency, and show the responses and results of the model during a large springtime freshwater flow event.

3.1.4 Results for CARP Hydrodynamic Model Update, Velocity Currents

Measurements of velocity currents throughout the Harbor and Estuary suitable for comparisons to model results are available for discontinuous portions of the eighteen-year CARP model calibration period from several different sources. The sources of velocity current measurements for comparisons to model results, include: the CARP 1 New Jersey Toxics Reduction Workplan for New York-New Jersey Harbor Study I-E (Chant, 2006); a Hudson River Foundation funded research effort (Sommerfield and Chant, 2010); and various NOAA programs (805 files downloaded from CO-OPS Current Station Data (noaa.gov)). The resolution of the CARP 127 x 205 model computational grid allows for model and measurement comparisons of flooding (+) and ebbing (-) velocity currents in both east/west lateral (u) and north/south longitudinal (v) directions.

The CARP 1 New Jersey Toxics Reduction Workplan for New York-New Jersey Harbor Study I-E (Chant, 2006) includes continuous velocity current measurements for portions of the 2000-01 and 2001-02 water years at two locations in Newark Bay, one location in the Kill van Kull and two locations in the Arthur Kill as shown on Figure 3-22. For each location, measurements were extracted from three fixed-depth bins representing below surface (i.e., within the constraint of the highest reliable measurement bin), middle (i.e., as compared to the average water depth at each location) and bottom (i.e., as defined by the lowest measurement bin) and were aligned with model results extracted for the same depths as the measurement bins rather than from model sigma layers. That is, instead of extracting model results from prescribed sigma layers, layers each 10% of the time-variable depth, model results were selected to align with the fixed depth bins of the extracted measurements which might not always fall within the same sigma layer. For example, a measurement from a foot above bottom was paired with a model result from a foot above bottom overtime regardless of which sigma layer aligned with a foot above bottom at a given time. Measurement and model comparison results for the three depths at each location for the entire two water years and for both the lateral and longitudinal directions are presented on thirty panels on the first ten pages in Appendix 6. Over the next fifty pages of Appendix 6 on one-hundred-fifty panels, the results are repeated for each location/depth/direction with each of the five measurement time intervals within the 2000-02 water years shown separately within sixty-day periods (i.e., blown up x-axes) to allow for closer inspection. Examples of the full-period and single period velocity currents measurement and model comparison results from Appendix 6 are shown for the location in northern Newark Bay on Figures 3-23 and 3-24. It is noted that Harbor Deepening projects were ongoing during the collection of the continuous velocity current measurements for portions of the 2000-01 and 2001-02 water years such that the velocity currents represent water speeds during changing and evolving bathymetry conditions.

The velocity current measurements from the Hudson River Foundation funded research effort (Sommerfield and Chant, 2010) includes continuous velocity current measurements for portions of the 2007-08 and 2008-09 water years at locations in the Lower Passaic River, the Lower Hackensack River, Newark Bay, two locations in the Kill van Kull and one location in the Arthur Kill as shown on Figure 3-25. For each location, measurements were extracted from three fixed-depth bins representing below surface (i.e., within the constraint of the highest reliable measurement bin), middle (i.e., as compared to the average water depth at each location) and bottom (i.e., as defined by the lowest measurement bin) and were aligned with model results extracted for the same depths as the measurement bins rather than from model sigma layers. Measurement and model comparison results for the three depths at each location for the entire two water years and for both the lateral and longitudinal directions are presented on thirty-six panels on the first twelve pages in Appendix 7. Over the next seventy-two pages of Appendix 7 on two-hundred-sixteen panels, the results are repeated for each location/depth/direction with each of the six measurement time intervals within the 2007-09 water years shown separately within sixty-day periods (i.e., blown up x-axes) to allow for closer inspection. Examples of the full-period and single period velocity currents measurement and model

comparison results from Appendix 7 are shown for the western most location in Kill van Kull on Figures 3-26 and 3-27. It is noted that Harbor Deepening projects targeting 52' were ongoing during the collection of the continuous velocity current measurements for portions of the 2007-08 and 2008-09 water years such that the velocity currents represent water speeds during changing and evolving bathymetry conditions.

NOAA (CO-OPS Current Station Data (noaa.gov)) measurements of velocity currents used for comparisons to CARP hydrodynamic model results on the 127 x 205 model computational grid include nineteen locations as displayed on the map in Appendix 8. The available NOAA velocity current measurements, used for comparison to CARP model results, are located at seventeen locations along the Hudson River, at Bergen Point in the Kill van Kull, and in Upper NY Bay at the Gowanus flats, and are available at varying time intervals throughout the eighteen water years of the CARP model calibration for each location, including forty-five locations/intervals. The results for each location/interval include five measurement bin depths on a single page in Appendix 8. The velocity current comparison results in the north/south longitudinal (v) and east/west lateral (u) directions for a location/interval are each presented on a separate page in Appendix 8.

3.2 Results for CARP Sediment Transport and Organic Carbon Production Model Update

Key sediment transport and organic carbon production model results generated include spatial and temporal estimates of bed accumulation, estimates of suspended sediment fluxes from the Lower Hudson River to the Harbor, and ambient suspended sediment and organic carbon concentrations.

3.2.1 Results for CARP Sediment Transport and Organic Carbon Production Model Update, Bed Accumulation

CARP sediment transport and organic carbon production model bed accumulation results on the 127 x 205 model computational grid were examined in three ways: as annual averages by region; as time series by region; and for spatial patterns within Newark Bay, Haverstraw Bay, and the North River.

3.2.1.1 Results for CARP Sediment Transport and Organic Carbon Production Model Update, Bed Accumulation, Regional Annual Averages

The results for regional annual average bed accumulation and external sources of solids are shown on Figure 3-28. The annual averages displayed on Figure 3-28 are based on the CARP 1 (top panel) thirty-seven year hindcast period which selects and artificially sequences hydrographs from the 88-89, 94-95 and 1998-2002 six water years (HydroQual, 2007b) and on the CARP 2 (bottom panel) calibration period for the eighteen water years 1998-2016. As shown in the gold bars on Figure 3-28, there are differences in annual average external solids loadings between CARP 1 and CARP 2. The loading differences are associated with differences in the water years included in the annual average results displayed and differences in the underlying solids loading concentration estimation methods, spatial distribution of loadings, and same-year loadings results as described in Landeck Miller et al., 2022. The external solids loading differences are most apparent in the Hudson River above Wappinger Creek reaches and in the Long Island Sound reach, consistent with Landeck Miller et al., 2022.

Increases in annual average sediment transport model bed accumulation results for CARP 2 as compared to CARP 1 are shown by the red bars on Figure 3-28 for the Hudson River reaches above Wappinger. These increases are most likely caused by model grid resolution and refined hydrodynamic transport rather than revised solids loadings based on early HDR testing of revised solids loadings with the 49 x 84 model

computational grid version of the hydrodynamic and sediment transport and organic carbon production models before moving to the 127 x 205 model computational grid. For Long Island Sound, increases in sediment transport model bed accumulation results for CARP 2 as compared to CARP 1 shown by the red bars on Figure 3-28 are associated with proximal changes to external solids loading results. The red bars on Figure 3-28 also show a slight increase in bed accumulation results for the Hudson above Highlands reach and a slight decrease for the Tappan Zee to Battery reach with less year-to-year variation (shown with black line range bars) for CARP 2 as compared to CARP 1. Overall, the regional annual average bed accumulation results obtained with the CARP 2 and CARP 1 sediment transport and organic carbon production models are very similar, especially given the changes to solids loadings, other hydrodynamic and sediment transport model inputs, and the model grid resolution described in Section 2.

3.2.1.2 Results for CARP Sediment Transport and Organic Carbon Production Model Update, Bed Accumulation, Regional Timeseries

The sediment transport and organic carbon production model bed accumulation time series by region results are shown on Figure 3-29 for the 127 x 205 model computational grid. Sediment transport model bed accumulation results included in the time series on Figure 3-29 are for each of the eighteen water years in the calibration period cumulatively such that sub-yearly variations are not included. For the Lower Hackensack River, Lower Passaic River, Newark Bay, and Kills region, draft (i.e., under development, not final, subject to change) bed accumulation cumulative time series results for the Newark Bay Superfund sediment transport model are also shown for the CARP calibration period on Figure 3-29 for comparison purposes.

3.2.1.3 Results for CARP Sediment Transport and Organic Carbon Production Model Update, Bed Accumulation, Newark Bay Spatial Patterns

Results for spatial patterns of bed accumulation as an accumulated depth for the first fourteen of the eighteen years of the CARP 2 calibration period, October 1, 1998, through September 30, 2012, are shown for individual model computational grid cells in the Lower Passaic and Hackensack Rivers and in Newark Bay on Figure 3-30. For comparison, spatial patterns of bed accumulation results for the draft (i.e., under development, not final, subject to change) Newark Bay Superfund sediment transport model are also shown in Figure 3-30.

3.2.1.4 Results for CARP Sediment Transport and Organic Carbon Production Model Update, Bed Accumulation: North River and Haverstraw Bay Spatial Patterns

Results for spatial patterns of bed accumulation as an accumulated depth in the Hudson River opposite Manhattan (known as the North River) are shown for multiple discrete periods. The discrete periods selected for displaying bed accumulation results in the North River include before, during, and after large upstream flow events to check the ability of the CARP sediment transport model on the 127 x 205 model computational grid to reproduce the occurrence of transient bed accumulation and temporary storage of solids following large flow events. The included periods for displaying spatial patterns of bed accumulation results varying in time are the spring and summer 2001 as analyzed during CARP 1 (HydroQual, 2007b) and shown on Figure 3-31; specific dates in the spring and summer of 1999 as identified by Woodruff et al., 2001, and shown on Figure 3-32; before, during, and after Hurricanes Irene and Lee in 2011 shown on Figure 3-33; and for spring freshet and summer conditions in 2011 shown on Figure 3-34. The flow events associated with these periods are indicated on the hydrograph of the Hudson River shown on Figure 3-35. Results for spatial patterns of bed accumulation as an accumulated depth in Haverstraw Bay are shown on Figure 3-36 for before, during, and after Hurricanes Irene and Lee in 2011.

3.2.2 Results for CARP Sediment Transport and Organic Carbon Production Model Update, Suspended Sediment Fluxes from the Lower Hudson River to the Harbor

CARP sediment transport and organic carbon production model results on the 127 x 205 model computational grid for downstream fluxes of suspended sediment on the Hudson River at Poughkeepsie shown on Figure 3-37 are 4.5 megatonnes (i.e., teragrams) for the portion of the calibration period including October 1, 2004, to August 15, 2011, and 7.2 megatonnes for the portion of the calibration period including October 1, 2004, to September 20, 2015. These periods and the location for results reporting were selected to facilitate comparisons to Ralston and Geyer, 2017. The comparisons to Ralston and Geyer, 2017, are shown on Figure 3-37 and are discussed in Section 4.2.2. The loading and flux results of Ralston and Geyer shown on Figure 3-37 and discussed in Section 4.2.2 are based on various measurements for the full period shown and, in addition, on model results for portions of 2011, 2014, and 2015.

3.2.3 Results for CARP Sediment Transport and Organic Carbon Production Model Update, Ambient Suspended Sediment and Organic Carbon Concentrations

CARP sediment transport and organic carbon production model results on the 127 x 205 model computational grid for ambient suspended sediment concentrations are presented as time series at numerous locations coincident with direct measurements and measured estimates from acoustic backscatter. The model and measurement results for ambient suspended sediment concentrations have been organized into three groupings: Newark Bay and Kills, Hudson River at Poughkeepsie, and throughout NY/NJ Harbor. The throughout NY/NJ Harbor grouping was also used for comparing model results to measurements of particulate and dissolved organic carbon. The results specific to each of the three groupings are identified below.

3.2.3.1 Results for CARP Sediment Transport and Organic Carbon Production Model Update, Ambient Suspended Sediment Concentrations: Newark Bay and Kills

At the five velocity current stations shown on Figure 3-22, measurements of acoustic backscatter were also collected during the 2000-01 and 2001-2 water years and were converted to estimates of suspended sediment concentrations as part of the CARP 1 New Jersey Toxics Reduction Workplan for New York-New Jersey Harbor Study I-E (Chant, 2006). The estimates of suspended sediment concentrations from the acoustic backscatter measurements for the 2000-02 period have been combined with direct measurements of suspended sediment concentrations at similar locations from the New Jersey Harbor Dischargers Group (NJHDG) and the New York City Environmental Protection Harbor Survey (NYCDEP) for comparisons among the three measurement programs and to CARP model results. The comparisons were expanded to include sixteen of the eighteen water years in the CARP model calibration period (i.e., October 2000 to September 2016) and are presented on eighty pages in Appendix 9.

Each page of Appendix 9 displays one of five locations for one of sixteen water years. The CARP model and measurement results are displayed on each page in four panels representing twelve or more meters above bottom, seven to twelve meters above bottom, one to seven meters above bottom, and all depth layers combined. At each depth interval, the suspended sediment concentrations derived from acoustic backscatter measurements are shown as range bars with an average. At each depth interval, the suspended sediment concentration measurements from the New Jersey Harbor Dischargers Group (NJHDG) and the New York City Environmental Protection Harbor Survey (NYCDEP) are shown as grab samples and are accumulated as range bars when all depth layers are combined. The CARP sediment transport model results on the 127 x 205 model computational grid for suspended sediment concentrations in each depth layer are displayed with five lines. Two finely dashed lines represent the instantaneous maxima and minima calculated by the model considering all model layers in the depth interval in each ten-

day period. The purpose of the two finely dashed lines is an attempt to capture the upper and lower bounds of suspended sediment concentrations calculated by the model; however, the attempt is limited by the ten-day output period. A continuous record of instantaneous or even hourly model outputs, precluded by output file size, would be more commensurate to the continuous backscatter and grab sample measurements. The three solid lines represent the highest, average, and lowest 24-hour averages calculated by the model considering all model layers in the depth interval. The purpose of the three solid lines is to capture the central tendency of suspended sediment concentrations calculated by the CARP sediment transport model.

An example of the suspended sediment concentrations model and measurement comparison results presented in Appendix 9 is shown on Figure 3-38 for the Kill van Kull for the 2000-01 water year. Another example for suspended sediment concentration model and measurement comparison results from Appendix 9 is shown on Figure 3-39 for the Arthur Kill for the 2012-13 water year. A third example for suspended sediment concentration model and measurement comparison results from Appendix 9 is shown on Figure 3-40 for Newark Bay for the 2006-07 water year.

3.2.3.2 Results for CARP Sediment Transport and Organic Carbon Production Model Update, Ambient Suspended Sediment Concentrations, Hudson River at Poughkeepsie

The USGS collected suspended sediment concentration measurements on the Hudson River at Poughkeepsie for most years between 2001 and 2016. Measurement richness varies by year with some of the earlier years including measurements at multiple depths. No measurements were collected in 2007, 2010, and 2012. Limited measurements were collected in 2006 and 2011. These measurements along with CARP sediment transport and organic carbon production model results using the 127 x 205 model computational grid for suspended sediment concentrations are present in Appendix 10. In Appendix 10, model and measurement results for each year are presented on a page including time series for three depth intervals and all depth intervals combined. The model results in each depth horizon displayed on the pages of Appendix 10 are shown as three lines representing the instantaneous maximum within each ten-day period, the average over ten days, and the instantaneous minimum within each ten-day period. The time series for 2003 from Appendix 10 are also shown on Figure 3-41 as an example.

3.2.3.3 Results for CARP Sediment Transport and Organic Carbon Production Model Update, Ambient Suspended Sediment and Organic Carbon Concentrations, throughout NY/NJ Harbor

Measurements of suspended sediment are available at eighty-nine locations throughout NY/NJ Harbor. Measurements from eighty-nine locations include a combination of the suspended sediment measurements from the various programs which collected water column measurements of contaminants used for contaminant fate and transport model calibration (i.e., CARP 1 and CARP 2 data collection efforts and the Lower Passaic River and Newark Bay Superfund studies presented in Section 3.3) and from the conventional parameter water quality monitoring programs of the New Jersey Harbor Dischargers Group (NJHDG) and the New York City Department of Environmental Protection (NYCDEP). The NJHDG and NYCDEP stations for suspended sediment extend beyond the Newark Bay and Kills locations identified in Section 3.2.3.1. The eighty-nine suspended sediment measurement stations have been organized into fifteen reach groups of five or six stations each for purposes of time series model and measurement comparisons. The same eighty-nine stations and the organization into fifteen reach groups has also been used for organic carbon model and measurement comparisons. The model and measurement comparison results for suspended sediment and organic carbon concentrations throughout the Harbor are included in Appendix 11.

Each page in Appendix 11 includes a map showing the locations for the five or six timeseries of model and measurement comparison results included on the page. The time series presented span the eighteen water years used for CARP sediment transport and organic carbon production model calibration on the 127 x 205 model computational grid. The model results are presented on a ten-day basis. The ten-day model results are presented as depth averages over ten model water column sigma layers (royal blue lines) and as instantaneous maxima and minima within each ten-day interval over ten model water column depth layers (pale blue lines). Examples of the model and measurement results presented in Appendix 11 are also presented on the nine Figures 3-42 to 3-50.

Figures 3-42 to 3-44 show the CARP sediment transport and organic carbon production model results using the 127 x 205 model computational grid for suspended sediment concentrations in the Hudson River, Upper NY Bay, East River, and Jamaica Bay reaches of the Harbor. These example locations were selected from others throughout the Harbor included in Appendix 11 because suspended sediment concentration timeseries results at these locations were not previously displayed on diagrams associated with Sections 3.2.3.1 and 3.2.3.2. Figures 3-45 to 3-50 show the CARP sediment transport and organic carbon production model results using the 127 x 205 model computational grid for particulate organic carbon (POC) and dissolved organic carbon (DOC) in the Upper Newark Bay, Middle Newark Bay, and Lower Newark Bay/Kills reaches of the Harbor. These example locations were selected from others throughout the Harbor included in Appendix 11 to highlight model timeseries results for organic carbon concentrations in a critical area for maintenance dredging and dredged material management.

A cursory check of CARP sediment transport and organic carbon production model results using the 127 x 205 model computational grid for concentrations of additional water quality parameters that are related to suspended sediment and organic carbon, including chlorophyll, dissolved oxygen, ammonia nitrogen, phosphate phosphorus, and secchi depth/light extinction, is included in Appendix 12. The time series presented in Appendix 12 for chlorophyll, dissolved oxygen, ammonia nitrogen, phosphate phosphorus, and secchi depth/light extinction are as described for Appendix 11 suspended sediment, particulate organic carbon and dissolved organic carbon in terms of period, model output frequency, depth averaging, and time averaging.

3.3 Results for CARP Contaminant Fate and Transport Model Update

Key contaminant fate and transport model results generated include the final model calibrations for eighteen water years (i.e., 1998-2016) for six contaminants, 2,3,7,8-TCDD, 2,3,4,7,8-PCDF, di-CB, tetra-CB, hexa-CB, and octa-CB as well as methods validation testing for twenty-one additional contaminants (i.e., mono-CB, tri-CB, penta-CB, hepta-CB, nona-CB, and deca-CB) and fifteen additional dibenzo dioxin and furan congeners (i.e.,1,2,3,7,8-PCDD; 1,2,3,4,7,8-HxCDD; 1,2,3,6,7,8-HxCDD; 1,2,3,7,8,9-HxCDD; 1,2,3,4,6,7,8-HpCDD; OCDD; 2,3,7,8-TCDF; 1,2,3,7,8-PCDF; 1,2,3,7,8,9-HxCDF; 1,2,3,4,7,8-HxCDF; 1,2,3,6,7,8-HxCDF; 2,3,4,6,7,8-HxCDF; 1,2,3,4,7,8,9-HpCDF; 1,2,3,4,6,7,8-HpCDF; and OCDF) using the 127 x 205 CARP model computational grid. The calibration and validation results are presented in Sections 3.3.1 and 3.3.2. Interim contaminant fate and transport model results are also presented within Section 3.3.1 supporting the methods and decisions utilized to arrive at the final eighteen-year contaminant fate and transport model calibrations for the 127 x 205 CARP model computational grid. Additional contaminant fate and transport model results will be generated in subsequent tasks when the final eighteen-year model calibration for six contaminants will be applied for future projections as indicated in Section 6.

3.3.1 Results for CARP Contaminant Fate and Transport Model Update, Six Contaminants 1998-2016 Calibration

Results for the CARP contaminant fate and transport model are presented in Appendices 13 and 14. The results in Appendices 13 and 14 use the 127 x 205 model computational grid and the other input modifications described in Section 2. The results in Appendices 13 and 14 are for the eighteen water years 1998-2016 for the six contaminants 2,3,7,8-TCDD, 2,3,4,7,8-PCDF, di-CB, tetra-CB, hexa-CB, and octa-CB. The results in Appendices 13 and 14 are presented as model and measurement comparisons timeseries for sediment bed and water column contaminant concentrations, respectively.

3.3.1.1 Results for CARP Contaminant Fate and Transport Model Update, Six Contaminants 1998-2016 Calibration, Sediment Bed

The model and measurement comparison results in Appendix 13 for sediment bed contaminant concentrations include sixteen pages for each contaminant/summation and for each normalization with each page representing results for a reach containing five or six discrete locations. In total, model and measurement comparison results for sediment bed contaminants are presented for ninety-five discrete locations. The model and measurement comparison results for sediment bed contaminant concentrations are presented on two hundred twenty-four pages in Appendix 13 for six contaminants and a PCB summation, ninety-five locations, and solids and organic carbon normalizations.

Each reach page, in Appendix 13 and on Figures 3-51 to 3-54, includes a location map with the 127 x 205 model computational grid shown. On the map, the model computational grid cells for the five or six discrete locations for which the time series of model results are presented are colored in bright green. Pastel colors are used on the map to indicate the surrounding model computational grid cells from which measurements have been aggregated for the comparisons and from which ranges of model results are derived. The pastel colors on the map correspond to the original 49 x 84 model computational grid considered during the post-audit (Landeck Miller et al., 2019) and used previously for CARP (HydroQual, 2007a, 2007b, 2007c).

At each location shown in Appendix 13 and on Figures 3-51 to 3-54, measurements representing up to the top 15 cm of the sediment bed are presented. Measurements from various sources as compiled and described for the CARP post-audit (Landeck Miller et al., 2019) are shown with blue and red circles for in-channel and off-channel samples, respectively, in Appendix 13 and on Figures 3-51 to 3-54. Additional measurements have been added since the completion of the post-audit (Landeck Miller, et al., 2019) and are shown with various symbols and colors as identified in the legend on the diagrams in Appendix 13 and on Figures 3-51 to 3-54. The additional measurements are derived from sampling conducted in support of contemporary navigational maintenance dredging projects (shown with brown triangles, labelled “Dredge data”) and from the work of other CARP investigators (shown with pink and green squares, labelled “CARP2”). A listing of the contemporary navigational maintenance dredging projects from which measurements were obtained is provided in Appendix 15. Reporting for CARP 2 data collection is in preparation.

Various model timeseries results for sediment bed contaminant concentrations are displayed in Appendix 13 and on Figures 3-51 to 3-54 with several different lines and shading. A lime green line is used to show the timeseries of ten-day-average contaminant concentrations calculated by the model for the top 10 cm of the bed in a single model grid cell (identified in bright green on the maps). A lime green shade is used to show the range in the top 10 cm calculated by the model for each ten-day interval for the single model grid cell. A grey shade is used to show the range of contaminant concentrations for the top 10 cm of the bed calculated by the model for the several surrounding model grid cells from which measurements were aggregated (identified with pastel colors on the maps). A pale blue line is used for reference to show the

contaminant concentrations calculated by the model for the sediment bed archive layer for the same single model grid cell as was shown in lime for the model calculated concentrations in the top 10 cm. The sediment bed archive layer of variable depth is used by the model to store and track mass specified through initial bed thickness or whenever appreciable deposition exceeding resuspension is calculated and to provide the inventory of mass available for subsequent resuspension.

Although not specifically discussed, solids and organic carbon normalized bed contaminant concentration results presented in Appendix 13 are similar. There are only a few instances, such as several locations in Upper and Lower New York Bays shown in Appendix 13, with discernible differences in solids and organic carbon normalized bed concentrations of 2,3,7,8-TCDD and total PCB.

Figures 3-51 and 3-54 are examples of the model and measurement comparison results, from the CARP contaminant fate and transport model using the 127 x 205 model computational grid, included in Appendix 13. On Figure 3-51 and 3-52, results are shown for the sediment bed at six locations in Lower Newark Bay. On Figure 3-53 and 3-54, results are shown for the sediment bed at six locations in the Hudson and East Rivers. Figures 3-51 and 3-53 show results for 2,3,7,8-TCDD solids-normalized concentrations in the bed. Figures 3-52 and 3-54 show results for total PCB solids-normalized concentrations in the bed. On Figures 3-52 and 3-54, the measurements represent ten PCB homologs, and the model results are based on twice the summation of the four PCB homologs modeled for calibration and future projection purposes. The application of the factor of two to the summation of four PCB homologs (i.e., di-CB, tetra-CB, hexa-CB, and octa-CB) to approximate total PCB was established during CARP 1 (HydroQual, 2007c) and can be further verified during method validation efforts which include model simulations for the remaining six homologs as described in Section 3.3.2.

3.3.1.2 Results for CARP Contaminant Fate and Transport Model Update, Six Contaminants 1998-2016 Calibration, Water Column

The model and measurement comparison results in Appendix 14 for water column contaminant concentrations include twelve pages for each contaminant/summation with each page representing results for a reach containing three to six discrete locations. In total, model and measurement comparison results for water column contaminants are presented for sixty-one discrete locations. The model and measurement comparison results for water column contaminant concentrations are presented on eighty-four pages in Appendix 14 for six contaminants and a PCB summation at sixty-one locations.

Each reach page, in Appendix 14 and on Figures 3-55 to 3-58, includes a location map with the 127 x 205 model computational grid shown. On the map, the model computational grid cells for three to six discrete locations for which the time series of model results are presented are shown. At each location shown in Appendix 14 and on Figures 3-55 to 3-58, measurements representing the water column are presented. Measurements from various sources as compiled and described for the CARP post-audit (Landeck Miller et al., 2019) are shown with red squares in Appendix 14 and on Figures 3-55 to 3-58. Many of the compiled measurements are reported and displayed at detection limits as shown with pale pink squares in Appendix 14 and on Figures 3-55 to 3-58, especially for concentrations of 2,3,4,7,8-PCDF in Appendix 14. Measurements shown at detection limit are an important consideration for the evaluation of model and measurement comparisons. Additional measurements have been added since the completion of the post-audit (Landeck Miller, et al., 2019) and are shown with bright pink circles as identified in the legend on the diagrams in Appendix 14 and on Figures 3-55 to 3-58. The additional measurements are derived from the recent work of other CARP investigators. Reporting for CARP 2 data collection is in preparation.

Various model timeseries results for water column contaminant concentrations are displayed in Appendix 14 and on Figures 3-55 to 3-58 with several different lines and shading. A blue line is used to show the timeseries of ten-day-average contaminant concentrations calculated by the model over depth. A blue shade is used to show the contaminant concentration range over depth in the water column calculated by the model for each ten-day interval. For reference, a gray line is used to show the timeseries of ten-day-average contaminant concentrations in the particulate phase calculated by the model over depth in the water column. For reference, a gray shade is used to show the particulate phase contaminant concentration range over depth in the water column calculated by the model for each ten-day interval.

Figures 3-55 and 3-56 are examples of the model and measurement comparison results, from the CARP contaminant fate and transport model using the 127 x 205 model computational grid, included in Appendix 14. On Figure 3-55 and 3-56, results are shown for the water column at six locations in Upper Newark Bay. On Figure 3-57 and 3-58, results are shown for the water column at five locations in the Hudson River. Figures 3-55 and 3-57 show results for 2,3,7,8-TCDD concentrations in the water column. Figures 3-56 and 3-58 show results for total PCB concentrations in the water column. On Figures 3-56 and 3-58, the measurements and the model results are based on twice the summation of the four PCB homologs modeled for calibration and future projection purposes. The application of the factor of two to the summation of four PCB homologs (i.e., di-CB, tetra-CB, hexa-CB, and octa-CB) to approximate total PCB was established during CARP 1 (HydroQual, 2007c) and can be further verified during method validation efforts which include model simulations for the remaining six homologs as described in Section 3.3.2.2.

3.3.1.3 Results for CARP Contaminant Fate and Transport Model Update, Six Contaminants 1998-2016 Calibration, Sediment Bed Particle Mixing Rates

As described in Section 2.2.3, reductions to biological particle mixing rates in the sediment bed of the Lower Passaic River that were applied for purposes of Superfund modeling were also applied in the CARP sediment transport and organic carbon production model on the 127 x 205 model computational grid. Interim and final CARP contaminant fate and transport model and measurement timeseries comparison results have been developed to understand the impact (i.e., model sensitivity) of the specified reduced biological particle mixing rates in the sediment transport model for the sediment bed of the Lower Passaic River. Results presented on Figures 3-59 and 3-60 show CARP contaminant fate and transport model calculations of 2,3,7,8-TCDD concentrations for single example locations in the sediment bed of the Lower Passaic River and Newark Bay for before and after the application of reduced particle mixing rates in the Lower Passaic River. In addition, results presented on Figures 3-59 and 3-60 show CARP contaminant fate and transport model calculations of 2,3,7,8-TCDD concentrations for single example locations in the sediment bed of the Lower Passaic River and Newark Bay for before and after the application of adjustments to specified sediment bed initial bed thicknesses and contaminant concentration conditions. The final 2,3,7,8-TCDD bed concentrations model and measurement comparison results shown on Figures 3-59 and 3-60 are examples taken from Appendix 13. The interim (i.e., before the input adjustments) results shown on Figures 3-59 and 3-60 do not appear elsewhere is this report. Both the interim and final model 2,3,7,8-TCDD bed concentrations results, shown on Figures 3-59 and 3-60, follow the plotting conventions described for Appendix 13 in Section 3.3.1.1.

3.3.1.4 Results for CARP Contaminant Fate and Transport Model Update, Six Contaminants 1998-2016 Calibration, Sediment Bed Initial Conditions

As described in Sections 2.3.1, adjustments to sediment bed initial conditions for contaminant concentrations and in some cases bed archive layer initial thicknesses were needed for the transition between the 49 x 84 and 127 x 205 CARP model computational grids. In addition to results for the Lower

Passaic River and Newark Bay presented on Figures 3-59 and 3-60, interim and final calibration sediment bed contaminant concentration timeseries model and measurement comparison results are presented on Figure 3-61 for the East River on the west side of Riker's Island in South Brother Island Channel, north of Bowery Bay, to provide another example of the impact of sediment bed initial conditions adjustments on contaminant concentration results. The final contaminant concentration calibration results shown on Figure 3-61 are examples taken from Appendix 13 for 2,3,7,8-TCDD (top row) and total PCB (bottom row). The interim (i.e., before) calibration results shown on Figure 3-61 do not appear elsewhere is this report. Both the interim and final calibration results, shown on Figure 3-61 and labelled as ''Before" and "After", respectively, follow the plotting conventions described for Appendix 13 in Section 3.3.1.1.

3.3.1.5 Results for CARP Contaminant Fate and Transport Model Update, Six Contaminants 1998-2016 Calibration, di-PCB Phase Partitioning

Interim and final calibration water column time series model and measurement comparison results are presented on Figures 3-62 and 3-63 to show the impact on results associated with adopting the new contaminant phase partitioning coefficient for di-CB described in Section 2.3.2. The final calibration results shown on Figures 3-62 and 3-63 are examples taken from Appendix 14 for locations in the Hudson River and Upper NY Bay. The interim calibration results shown on Figures 3-62 and 3-63 do not appear elsewhere is this report. Both the interim and final calibration results, shown on Figures 3-62 and 3-63 and labelled as ''Before" and "After", respectively, follow the plotting conventions described for Appendix 14 in Section 3.3.1.2. On Figures 3-62 and 3-63 and in Appendix 14, blue lines are used to show the model results for the timeseries of water column di-CB concentrations. The gray lines on Figures 3-62 and 3-63 and in Appendix 14 are informational and display the model results for the times series of water column di-CB concentrations in the particulate phase.

3.3.2 Results for CARP Contaminant Fate and Transport Model Update, Twenty-One Additional Contaminants 1998-2016 Validation

Validation results for the CARP contaminant fate and transport model are presented in Appendices 16 and 17. The results in Appendices 16 and 17 use the 127 x 205 model computational grid and the other input modifications described in Section 2. The results in Appendices 16 and 17 are for the eighteen water years 1998-2016 for the twenty-one validation contaminants mono-CB; tri-CB; penta-CB; hepta-CB; nona-CB; deca-CB; 1,2,3,7,8-PCDD; 1,2,3,4,7,8-HxCDD; 1,2,3,6,7,8-HxCDD; 1,2,3,7,8,9-HxCDD; 1,2,3,4,6,7,8-HpCDD; OCDD; 2,3,7,8-TCDF; 1,2,3,7,8-PCDF; 1,2,3,7,8,9-HxCDF; 1,2,3,4,7,8-HxCDF; 1,2,3,6,7,8-HxCDF; 2,3,4,6,7,8-HxCDF; 1,2,3,4,7,8,9-HpCDF; 1,2,3,4,6,7,8-HpCDF; and OCDF). The results in Appendices 16 and 17 are presented as model and measurement comparisons timeseries for sediment bed and water column contaminant concentrations on an "as is" basis for purposes of further validating the methods applied for the six calibration contaminants. For the twenty-one validation contaminants, single simulations only were performed to provide a screening. The validation contaminants did not receive the same level of attention as the calibration contaminants.

3.3.2.1 Results for CARP Contaminant Fate and Transport Model Update, Twenty-One Contaminants 1998-2016 Validation, Sediment Bed

Like the calibration results in Appendix 13, the validation model and measurement comparison results in Appendix 16 for sediment bed contaminant concentrations include sixteen pages for each contaminant/summation and normalization with each page representing results for a reach containing five or six discrete locations. In total, validation model and measurement comparison results for sediment bed contaminants are presented for ninety-five discrete locations. The validation model and measurement

comparison results for sediment bed contaminant concentrations are presented on seven hundred four pages in Appendix 16 for twenty-one contaminants and a ten-homolog PCB summation, ninety-five locations, and solids and organic carbon normalizations.

Like Appendix 13 and the Figures 3-51 to 3-54, each reach page, in Appendix 16 and on Figures 3-64 to 3-65, includes a location map with the 127 x 205 model computational grid shown. On the map, the model computational grid cells for the five or six discrete locations for which the time series of model results are presented are colored in bright green. Pastel colors are used on the map to indicate the surrounding model computational grid cells from which measurements have been aggregated for the comparisons and from which ranges of model results are derived. The pastel colors on the map correspond to the original 49 x 84 model computational grid considered during the post-audit (Landeck Miller et al., 2019) and used previously for CARP (HydroQual, 2007a, 2007b, 2007c).

At each location shown in Appendix 16 and on Figures 3-64 to 3-65, measurements representing up to the top 15 cm of the sediment bed are presented. Measurements from various sources as compiled and described during the CARP post-audit (Landeck Miller et al., 2019) are shown with blue and red circles for in-channel and off-channel samples, respectively, in Appendix 16 and on Figures 3-64 to 3-65. Additional measurements have been added since the completion of the post-audit (Landeck Miller, et al., 2019) and are shown with various symbols and colors as identified in the legend on the diagrams in Appendix 16 and on Figures 3-64 to 3-65. The additional measurements are derived from sampling conducted in support of contemporary navigational maintenance dredging projects (shown with brown triangles, labelled “Dredge data”) and from the work of other CARP investigators (shown with pink and green squares, labelled “CARP2”). A listing of the contemporary navigational maintenance dredging projects from which measurements were obtained is provided in Appendix 15. Reporting for CARP 2 data collection is in preparation.

Various model timeseries results for sediment bed contaminant concentrations are displayed in Appendix 16 and on Figures 3-64 to 3-65 with several different lines and shading. A lime green line is used to show the timeseries of ten-day-average contaminant concentrations calculated by the model for the top 10 cm of the bed in a single model grid cell (identified in bright green on the maps). A lime green shade is used to show the range in the top 10 cm calculated by the model for each ten-day interval for the single model grid cell. A grey shade is used to show the range of contaminant concentrations for the top 10 cm of the bed calculated by the model for the several surrounding model grid cells from which measurements were aggregated (identified with pastel colors on the maps). A pale blue line is used for reference to show the contaminant concentrations calculated by the model for the sediment bed archive layer for the same single model grid cell as was shown in lime for the model calculated concentrations in the top 10 cm. The sediment bed archive layer of variable depth is used by the model to store and track mass specified through initial bed thickness or whenever appreciable deposition exceeding resuspension is calculated and to provide the inventory of mass available for subsequent resuspension.

Figures 3-64 and 3-65 are examples of the validation model and measurement comparison results, from the CARP contaminant fate and transport model using the 127 x 205 model computational grid, included in Appendix 16. On Figure 3-59, results are shown for the sediment bed at six locations in Lower Newark Bay. On Figure 3-60, results are shown for the sediment bed at six locations in the Hudson and East Rivers. Figures 3-59 and 3-60 show results for total PCB solids-normalized concentrations in the bed. Different from Figures 3-52 and Figures 3-54, both the measurements and the model results on Figures 3-64 and 3-65 are based on the summation of ten PCB homologs. The model results are a combination of the calibration results for four PCB homologs and the validation results for the remaining six PCB homologs.

The validation summation of ten homolog sediment bed concentrations results provides the opportunity to assess the application of the factor of two to the summation of four PCB homologs (i.e., di-CB, tetra-CB, hexa-CB, and octa-CB) to approximate total PCB established during CARP 1 (HydroQual, 2007c) and used for CARP 2 calibration (Appendices 13 and 14) and eventually future projections (Section 6). The water year 2003-04 was randomly selected along with four model grid cells to test the validity of twice the sum of four PCB homologs as an approximation for the summation of ten PCB homologs. The solids normalized sediment bed concentrations resulting from the two types of summations were each averaged over the 2003-04 water year for testing purposes. The results of the testing are as follows. For model grid cell 20,153, in the Lower Passaic River, approximately five miles downstream of head-of-tide, the 2003-04 averages are 404.3 ppb from twice the sum of four homologs and 384.3 ppb from the sum of ten homologs with twice the sum of four homologs having +5.2% error. For model grid cell 31,103, at the mouth of the Hackensack River, the 2003-04 averages are 420.1 ppb from twice the sum of four homologs and 420.2 ppb from the sum of ten homologs with twice the sum of four homologs having -0.014% error. For model grid cell 25,101, in the northwest reach of Newark Bay below the mouth of the Lower Passaic River, the 2003-04 averages are 489.9 ppb from twice the sum of four homologs and 457.6 ppb from the sum of ten homologs with twice the sum of four homologs having +7.1% error. For model grid cell 15,83, in the pierhead reach of the Port Newark Channel, between the branch reaches of the Port Newark and Port Elizabeth Channels, 2003-04 averages are 413 ppb from twice the sum of four homologs and 399.2 ppb from the sum of ten homologs with twice the sum of four homologs having +3.5% error. The four model grid cell locations are displayed repeatedly on various maps found in Appendices 13 and 14. Specific examples of these maps displaying the four model grid cell locations are found in Appendix 13 on pages 98 (at position 5), 100 (at position 6), 101 (at position 3), and 103 (at position 1).

3.3.3.2 Results for CARP Contaminant Fate and Transport Model Update, Twenty-One Contaminants 1998-2016 Validation, Water Column

Like the calibration results in Appendix 14, the validation model and measurement comparison results in Appendix 17 for water column contaminant concentrations include twelve pages for each contaminant/summation with each page representing results for a reach containing three to six discrete locations. In total, model and measurement comparison results for water column contaminants are presented for sixty-one discrete locations. The model and measurement comparison results for water column contaminant concentrations are presented on two hundred sixty-four pages in Appendix 17 for twenty-one contaminants and a ten-homolog PCB summation at sixty-one locations.

Each reach page, in Appendix 17 and on Figures 3-66 to 3-67, includes a location map with the 127 x 205 model computational grid shown. On the map, the model computational grid cells for three to six discrete locations for which the time series of model results are presented are shown. At each location shown in Appendix 17 and on Figures 3-66 to 3-67, measurements representing the water column are presented. Measurements from various sources as compiled and described for the CARP post-audit (Landeck Miller et al., 2019) are shown with red squares in Appendix 17 and on Figures 3-66 to 3-67. Non-detect measurements plotted at detection limits are shown with pink squares. The non-detect measurements are important for the interpretation of model results, especially for several dioxin and furan congeners. Additional measurements have been added since the completion of the post-audit (Landeck Miller, et al., 2019) and are shown with bright pink circles as identified in the legend on the diagrams in Appendix 17 and on Figures 3-66 to 3-67. The additional measurements are derived from the recent work of other CARP investigators. Reporting for CARP 2 data collection is in preparation.

Various model timeseries results for water column contaminant concentrations are displayed in Appendix 17 and on Figures 3-66 to 3-67 with several different lines and shading. A blue line is used to show the

timeseries of ten-day-average contaminant concentrations calculated by the model over depth. A blue shade is used to show the contaminant concentration range over depth in the water column calculated by the model for each ten-day interval. For reference, a gray line is used to show the timeseries of ten-day-average contaminant concentrations in the particulate phase calculated by the model over depth in the water column. For reference, a gray shade is used to show the particulate phase contaminant concentration range over depth in the water column calculated by the model for each ten-day interval.

Figures 3-66 and 3-67 are examples of the model and measurement comparison results, from the CARP contaminant fate and transport model using the 127 x 205 model computational grid, included in Appendix 17. On Figure 3-66 results are shown for the water column at six locations in Upper Newark Bay. On Figure 3-67 results are shown for the water column at five locations in the Hudson River. On Figures 3-66 and 3-67, the measurements and the model results are based on the summation of the ten PCB homologs modeled. Figures 3-66 and 3-67 therefore show both calibration and validation results for total PCB concentrations in the water column. The model results on Figures 3-66 and 3-67 are a combination of the calibration results for four PCB homologs (Figures 3-56 and 3-58 and Appendix 14) and the validation results for the remaining six PCB homologs (Appendix 17).

4.0 DISCUSSION

Like the reporting of the results for the CARP model update, the discussion of the results is centered around model and measurement comparisons or comparisons between CARP 1 and CARP 2 results for each of the models. In some cases, the discussion is expanded to include comparisons to literature or independent models. The discussion also attempts to highlight implications for dredged material management and model limitations where applicable.

4.1 Discussion of CARP Hydrodynamic Model Update Results

Key CARP hydrodynamic model results that are discussed include the final model computational grid, tidal water elevations, water temperature, salinity, and velocity currents.

4.1.1 Discussion of CARP Hydrodynamic Model Update Results, Model Computational Grid

The vast improvement of the CARP 127 x 205 model computational grid over the 49 x 84 model computational grid to resolve features of local waterways, evidenced in Figures 3-3 to 3-7, is possible due to advances in computational power. To a certain extent, the CARP 127 x 205 model computational grid resolution remains limited by the size of the model domain and the length of the simulation periods, eighteen water years for model calibration simulations and an additional twenty-three water years for projections to the end of September 2039 for 2040 dredged material management planning. The numbers of contaminants considered for calibration and projections (i.e., six) and validation (i.e., twenty-one) purposes also limit the resolution of the CARP 127 x 205 model computational grid. The CARP 127 x 205 provides greater resolution than contemporary efforts such as the New Jersey Combined Sewer Overflow (CSO) Long Term Control Plan (LTCP) development which considers fewer pollutants, simpler kinetics, and shorter simulation periods. The CARP 127 x 205 model computational grid has some advantages over Superfund efforts by providing greater resolution in the Lower Hackensack River and in all areas beyond the Newark Bay complex. For the level of complexity of the CARP models, the CARP 127 x 205 model computational grid represents a practical maximum for model grid resolution.

4.1.2 Discussion of CARP Hydrodynamic Model Update Results, Tidal Water Elevations

The model and measurement comparison results presented for tidal water elevations in Appendices 2 and 2A and on the Figures 3-9 to 3-15 examples collectively show that the measured tidal amplitudes, ranges between spring and neap tidal cycles, timing of high and low waters, and amplification of the tidal range between locations are generally well reproduced by the CARP hydrodynamic model.

As presented in Figures 3 -9 to 3-15, the CARP hourly water elevation model results do a particularly good job of representing rapid increases and declines in water elevation occurring in September 1999 during Hurricane Floyd (around water year 1998-99 modeled days 350 to 352), in September 2006 during Hurricanes Ernesto/Florence (around water year 2005-06 modeled days 336 to 338), and in late August and early September of 2011 during Hurricanes Irene and Lee (around water year 2010-11 modeled days 330-334 and 340-344). As shown on Figures 3-9 through 3-15, the modeled and measured increased water elevations and rapid declines in water elevation associated with the Hurricanes include the Battery at the tip of Manhattan in NY, on the Raritan Bay side of the Sandy Hook peninsula in NJ, at Kings Point, NY near the confluence of the Upper East River and western Long Island Sound, (see results on the three Figures 3-9, 3-11, and 3-14 during Hurricanes Floyd, Ernesto/Florence, and Irene, respectively) at Bergen Point on the north side of the Kill van Kull at Newark Bay in Bayonne, NJ (see results in the two Figures 3-10 and 3-15 during Hurricanes Floyd and Irene, respectively), in the Hackensack River in northern NJ and in the New York Bight near Atlantic City in southern NJ (see results in Figure 3-12 during Hurricane Ernesto/Florence), and in the Upper Hudson River between Albany, NY and Norrie Point, NY (see results in Figure 3-13 during both Hurricanes Irene and Lee).

The model also performed very well under the challenging conditions of Hurricane Sandy in late October 2012, capturing the rapid increase and recovery set-down at sixteen locations as displayed in Appendix 2A. The model slightly missed the magnitude of the highest measured hourly elevations at the Battery in Upper New York Bay and at Bergen Point in Newark Bay occurring on October 29, 2012. Approximately simultaneously, instruments at Sandy Hook in Raritan Bay and at Poughkeepsie in the Hudson River stopped recording. Prior to instruments shutting down, the model was accurately representing the measured rising elevations.

Hurricane Floyd which occurred in September 1999 included 10 to 15 inches of rain in the NY metropolitan area over a 24-hour period. According to NOAA National Weather Service (NWS) records (NOAA, 2023), September 1999 was the wettest September in the Albany area since 1826 and September 16, 1999, is the wettest single day recorded for Albany by the NWS since 1874. During Hurricane Irene in August 2011, the NOAA NWS (NOAA, 2023) recorded the second wettest August for Albany since 1826 and the second wettest day on August 28, 2011, since 1874. On the basis of these remarkable infrequencies of occurrence (going back to the 1800's), the CARP model's eighteen year calibration period for the 127 x 205 model computational grid incorporates water volumes/tidal elevations from several extreme flow events for the Hudson River and most likely numerous other local tributaries (e.g., Lower Passaic, Raritan, and Connecticut Rivers) and therefore conditions of a large delivery of solids and associated contaminants from the various watersheds to the navigational channels of the Harbor.

Hurricane Sandy was unremarkable in terms of the Hudson River hydrograph, as evidenced on Figure 3-35, and presumably was unremarkable for the hydrographs of other headwaters. However, the 3.4 m storm tide measured by NOAA at the Battery during Hurricane Sandy has an estimated return period of 1570 years (Brandon et al., 2014). Further, simulated hurricane climatology results rank Hurricane Sandy as a once in 900 years event (Brandon et al., 2014).

The full set of hourly model and measurement comparison diagrams for tidal water elevations in Appendix 2 demonstrate good model performance but do not show perfect agreement at every time and location; however, the sporadic disagreements between measured and modeled in most cases are readily explained and are typically a consequence of working with unaudited and uncensored measurements. For example, for the Schodack station on the Hudson, the higher than modeled measurements for July/September of 2010 are not credible relative to the measurements upstream at Albany and downstream at Norrie Point for the same period and the good model and measurement agreement earlier in January/February 2010 (i.e., from the same 2009-10 water year) at the Schodack station. Similarly, at the Bergen Point station in July/September 2015, the higher than modeled measurements are inconsistent with the strong model and measurement elevation agreements during January/February 2015.

A representative example of acceptable model performance for reproducing features of the measured water elevations after applying a thirty-five-hour low pass filter as presented in Appendix 3 is shown on Figure 3-16 for the 2004-05 water year for the Hackensack River, Lower Passaic River, and in the Kill van Kull near Newark Bay (i.e., Bergen Point). The model reproduces tidal features with lower frequencies than diurnal and semi-diurnal dynamics.

The overall strong agreement with few exceptions between model and measurement results for tidal water elevations show that the model properly accounts for the propagation of energy originating in the ocean throughout the model domain under a wide range of typical and atypical conditions.

4.1.3 Discussion of CARP Hydrodynamic Model Update Results, Water Temperature and Salinity

For the 2002 portion of the 2001-02 water year, the CARP 1 hydrodynamic model on the 49 x 84 model computational grid was characterized by bottom salinity underprediction throughout the Kills and Newark Bay (HydroQual, 2007a). The underprediction was attributed to dredging activity in the Kills for the 41' deepening projects and the CARP 1 hydrodynamic model having water depths in the Kills of only 24' to 30' for most of 1998-2002 (HydroQual, 2007a). In at least once instance (i.e., northern Newark Bay between mid-March and early May), the CARP 1 model was unknowingly compared to erroneously high salinity associated with a clogged conductivity sensor (Chant, 2006). These salinity measurements should not have been considered in characterizing the CARP 1 hydrodynamic model performance and are not considered for CARP 2 hydrodynamic model assessments. The locally higher salinity reported due to the clogged sensors in northern Newark Bay is inconsistent with the higher-than-average Lower Passaic River freshwater flows which occurred at the time of March 2002 instrument deployment. Early March 2002 included above average flow on the Lower Passaic River in a water year of near drought conditions (Chant, 2006).

The CARP 2 hydrodynamic model on the 127 x 205 model computational grid not only has higher resolution, but also water depths of less than 40' for the 1998-99 water year and greater than 40' for the three water years 1999-2003, attempting to represent interim conditions for the 45' to 47' deepening projects. The four water years 1998 - 2002 originally represented by the CARP 1 model with a single bathymetry condition are now represented by two different bathymetry conditions, reflecting the transition from less than 40' up to 47' navigation channels. Given the improvements in time-varying model bathymetry inputs and model computational grid resolution since CARP 1, the hydrodynamic model and measurement results for salinity on the 127 x 205 model computational grid were checked for the ability to successfully reproduce 2001-02 water year salinity measurements in Newark Bay and the Kills as shown on the Figures 3-18 to 3-19. The CARP 2 model is performing well in Newark Bay and the Kill van Kull as compared to the 2001-02 measurements, an improvement over CARP 1 results. CARP model underprediction of salinity at the end

of 2002 in the Arthur Kill was improved but not entirely alleviated by the approximated varying bathymetry inputs and 127 x 205 model computational grid resolution.

Further, as compared to CARP 1, the CARP modeling calibration period is expanded to include an additional fourteen water years, 2002 – 2016, and three additional bathymetry conditions associated with the progression of NY/NJ Harbor deepening efforts, supporting the model performance exemplified in the 2009-10 and 2010-11 water years model and measurement comparison results for temperature and salinity presented in Appendices 4 and 5 and in Appendices 4A and 5A. Figures 3-20 to 3-21 show that by the 2009-10 water year when water depths are more well-known and established in the Newark Bay complex (close to completion of 52' deepening projects), the CARP hydrodynamic model on the 127 x 205 model computational grid represents salinity well in Newark Bay and throughout the Kill van Kull and the Arthur Kill underscoring the importance of the hydrodynamic model bathymetry inputs and the challenges of hydrodynamic modeling during periods of transient and evolving bathymetry such as 2001-02 and 2007-09. Additional displays of 2009-10 water year model and measurement comparison results for temperature and salinity presented in Appendices 4B and 5B highlight model performance during a springtime freshet. Salinity results in Appendix 5B from 2009-10 for Newark Bay and the Kills indicate that the measured timing of diurnal fluctuations is reproduced by the model and that the development and collapse of vertical stratification associated with a spring freshet is well represented despite some model over-prediction of measured stratification around day 190.

Of specific additional interest is the ability of the CARP hydrodynamic model to reproduce salinity measurements collected on the Hudson, Raritan, and Lower Passaic Rivers. Other HDR hydrodynamic modeling efforts since the completion of CARP 1 using the 49 x 84 model computational grid struggled to achieve the HRECOS measurements of salinity on the Hudson at Piermont Pier and Yonkers and on the Lower Passaic River near the physical location of the PVSC WWTP dock as described in Appendix 1. HDR also found the salinity intrusion on the Raritan River to be sensitive to model grid resolution. The success of the CARP hydrodynamic model with the 127 x 205 model computational grid on the Hudson, Raritan, and Lower Passaic Rivers for reproducing temperature and salinity measurements is shown in Appendices 4 and 5 for the 2009-10 water year. For the 2009-10 water year the model and measured propagation of the salt front is shown in Appendix 5 along the Hudson River at nine locations between Battery Park and West Point; along the Raritan River at four locations between Raritan Bay near the mouth of the Raritan River and the I-95 crossing at Edgebrook, NJ; and along the Lower Passaic River at nine locations between the Kearny Point Reach and river mile 13.5. Appendix 5 also displays the modeled salt front propagation along these rivers for numerous additional locations which were not sampled in 2009-10. The model has similar success with capturing measured salinity features for additional water years, including years with hurricanes, such as 2010-11 displayed in Appendix 5A. Salinity results in Appendix 5B from 2009-10 for the Lower Passaic and Hudson Rivers indicate that the measured timing of diurnal fluctuations is reproduced by the model and the development and collapse of vertical stratification associated with a spring freshet is well represented albeit with some overprediction of the measured near-surface amplitude.

Although not highlighted with specific additional figures or discussion, the modeled and measured comparisons of water temperature results throughout the model domain for 2009-10 shown in Appendices 4 and 4B and for 2010-11 shown in Appendix 4A are strong and underscore the representativeness of the hydrodynamic model input updates described in Section 2.1.

4.1.4 Discussion of CARP Hydrodynamic Model Update Results, Current Velocity

The examples of the full-period and single-period current velocity measurement and hydrodynamic model comparison results from Appendix 6 shown for the location in northern Newark Bay on Figures 3-23 to 3-

24 for the CARP 127 x 205 model computational grid as well as other diagrams in Appendix 6, do not show the large underprediction of measured north/south longitudinal current velocity (v direction) that was evident for the CARP 1 hydrodynamic model on the 49 x 84 model computational grid (HydroQual, 2007a) during the 2000-02 water years, a benefit of having increased model computational grid resolution in Newark Bay. Performance of the CARP hydrodynamic model on the 127 x 205 model computational grid for reproducing measured north/south longitudinal current velocity remains favorable in the Arthur Kill at two locations. Model underestimation of the highest magnitude flooding (+) and ebbing (-) current velocity, u direction (i.e., lateral) in the Kill van Kull for earlier surveys in 2000-02 and v direction (i.e., longitudinal) in southern Newark Bay for all surveys in 2000-02, especially near surface, occurs despite the improved model computational grid resolution. The underestimation is likely related to deepening activities during measurement collections in the 2000 to 2002 water years, underscoring the importance of considering measurements from periods after deepening projects.

The examples of the full-period and single-period current velocity measurement and hydrodynamic model comparison results from Appendix 7 shown for the location in the Kill van Kull on Figures 3-26 and 3-27 as well as other diagrams in Appendix 7 for the 2007-09 water years, show an improvement in model performance in the Kill van Kull as compared to 2000-02 results in Appendix 6 for model estimation of the highest magnitude flooding (+) and ebbing (-) current velocity in the east/west u direction (i.e., lateral). The improvement in the Kill van Kull current velocity model and measurement comparison results for 2007-09 as compared to 2000-01 was achieved even with 52' deepening activities and evolving bathymetries during 2007-09.

The current velocity model and measurement results shown in Appendix 7 for the 2007-09 water years are generally good in the Lower Passaic River and Newark Bay in both the u and v directions. For the Hackensack River, the results in Appendix 7 are better for the v direction than the u direction. It is noted that the ADCP deployed at the mouth of the Hackensack River was close to the interface of the narrower Hackensack River with the wider Newark Bay. The model results were extracted from the wider Newark Bay as shown on Figure 3–25. A check of the model results for one model computational grid cell north of the ADCP location showed a dramatic reduction, smaller than measured, in the modeled amplitude of the u direction (i.e., east/west lateral) current velocity within the Hackensack River. An averaging of the model results for current velocity for the two model computational grid cells proximal to the ADCP location is likely to compare most favorably to the u direction ADCP measurements of current velocity near the mouth of the Hackensack River.

For the Arthur Kill, as shown in Appendix 7 for 2007-09, the hydrodynamic model results overpredict the measured current velocity in the u direction and underpredict the current velocity the v direction. It is noted that the ADCP deployed in the Arthur Kill corresponds to a model computational grid cell that is in a corner and is oriented almost diagonal to flow coming from the Kill van Kull as shown on Figure 3–25. A check of the model results for one model computational grid cell south of the ADCP location where the model computational grid geometry is less complex did not show much change in the model results for current velocity.

Although not highlighted with specific additional figures or discussion, the modeled and measured comparisons of current velocity results for various periods shown in Appendix 8, mostly for the Hudson River, are largely favorable and underscore the representativeness of the model input updates described in Section 2.1. The CARP hydrodynamic model comparison results for the NOAA velocity current measurements are strongest for reproducing the amplification between locations and the phase timing, typical magnitude, amplification over depth, and change of direction at a location, with some discrepancies occurring between the measured and modeled magnitude extremes at a location.

4.2 Discussion of CARP Sediment Transport and Organic Carbon Production Model Update Results

Key CARP sediment transport and organic carbon production model results that are discussed include spatial/temporal estimates of bed accumulation, estimates of suspended sediment fluxes from the Lower Hudson River to the Harbor, and ambient suspended sediment and organic carbon concentrations.

4.2.1 Discussion of CARP Sediment Transport and Organic Carbon Production Model Update Results, Bed Accumulation

The spatial/temporal estimates of bed accumulation results have been considered as annual averages by reach; as cumulative time series by reach; for spatial patterns in the Newark Bay complex and as spatial patterns in the North River (i.e., opposite Manhattan) and Haverstraw Bay portions of the Hudson River.

4.2.1.1 Discussion of CARP Sediment Transport and Organic Carbon Production Model Update Results, Bed Accumulation, Regional Annual Averages

Broadly, the overall similarity of sediment transport model results on the 127 x 205 and 49 x 84 model computational grids for regional annual average bed accumulation shown with the red bars on Figure 3-28 is a significant finding. The similarity of bed accumulation results attained supports several CARP 2 sediment transport methods decisions in addition to updated solids loadings, including successfully applying bottom shear stresses for sediment transport as calibrated for hydrodynamics without any further adjustments for sediment transport (see Section 2.2.1). This clean application of bottom shear stresses for sediment transport achieved with the 127 x 205 model computational grid was not possible with the 49 x 84 model computational grid.

On a more focused basis, another significant finding is that the greater annual average bed accumulation achieved with the sediment transport model on the 127 x 205 model computational grid as compared to the 49 x 84 model computational grid for the Hudson River above Hudson Highlands, as shown by the red bars on Figure 3-28, is consistent with the work of other investigators occurring after CARP 1 completion. Ralston et al., 2013, reached the conclusion that much of the new material introduced into the Hudson River by large storms is retained in the tidal freshwater River without significant seaward transport. Further, Ralston and Geyer, 2017, report that a measurement-based sediment budget for the tidal Hudson over the period 2004-2015 includes trapping in the tidal freshwater region of the Hudson River of about 40% of the input. Unlike the CARP sediment transport model bed accumulation results for the 49 x 84 model computational grid, the CARP sediment transport model bed accumulation results for the 127 x 205 model computational grid include trapping in the tidal freshwater region of the Hudson River, consistent with the recent literature and updated understanding of solids trapping in the Hudson River. A related results discussion, the flux of solids leaving the tidal freshwater region of the Hudson River, is provided in Section 4.2.2.

CARP 2 average annual accumulation results for eight reaches within the Hudson River are shown on Figure 3-28 with the highest accumulations occurring in three reaches, the Moordener Kill and above reach, in the Catskill Creek and above to Moordener Kill reach, and in the Hudson Highlands to Tappan Zee reach. These three relative highest accumulations for the Hudson River calculated with the CARP 127 x 205 model computational grid over an eighteen-year calibration period align well with the longitudinal locations of accumulation maxima model results that Ralston and Geyer, 2017, report for an eighty-five-day period in

2014 at Hudson River km 225, km 175, and km 55 on their Figure 5C. It is noted that the modeled accumulation maxima modeled locations results from Ralston and Geyer, 2017, that are compared to CARP model results, are produced from a more complex model. Ralston and Geyer model five classes of solids over a range of settling speeds rather than the single aggregated solids class modeled for CARP.

4.2.1.2 Discussion of CARP Sediment Transport and Organic Carbon Production Model Update Results, Bed Accumulation, Regional Timeseries

The presentation of the cumulative time series of CARP sediment transport and organic carbon production model regional bed accumulation results as shown on Figure 3-29 was conceptualized during CARP 1 sediment transport modeling on the 49 x 84 model computational grid (HydroQual, 2007b). The displays of cumulative time series by region model bed accumulation results were first used as a tool for assessing movement of bed accumulation between regions for different input assumptions tested during CARP 1 thirty-seven year hindcast simulations as the CARP 1 model calibration simulations were only four years. The original tool for the smaller grid displayed sub-yearly results. For the 127 x 205 model computational grid sediment transport and organic carbon production model, the display of cumulative time series results shown on Figure 3-29 facilitated checking for any anomalous results which might have been missed by the annual average bar diagrams shown on Figure 3-28. Annual average results (Figure 3-28) and the time series results (Figure 3-29) for bed accumulation on the 127 x 205 model computational grid are consistent.

Figures 3-28 and 3-29 suggest that CARP bed accumulation results in the Newark Bay complex are somewhat less than those calculated with the draft (i.e., under development, not final, subject to change) Newark Bay Superfund sediment transport model. The Superfund model has higher model grid resolution in Newark Bay and the Lower Passaic River than the CARP 127 x 205 model computational grid. The Superfund model also has a more sophisticated sediment transport model as compared to the basic equations applied for sediment transport in the CARP sediment transport and organic carbon production model. Despite these differences in resolution, computational complexity, and cumulative magnitude, within the Lower Passaic and Hackensack Rivers and in Newark Bay, on an individual grid cell basis, the results in Figure 3-30 show that spatial patterns and relative magnitudes of bed accumulation and erosion are relatively consistent between CARP and draft Superfund results.

4.2.1.3 Discussion of CARP Sediment Transport and Organic Carbon Production Model Update Results, Bed Accumulation, Newark Bay Spatial Patterns

The CARP sediment transport model results for bed accumulation shown in Figure 3-30 from the 127 x 205 model computational are much different than preliminary results which used initial sediment bed archive layer thicknesses mapped from the CARP sediment transport model on the 49 x 84 model computational grid. The initial sediment bed archive layer thicknesses used as starting values on the 127 x 205 model computational grid inappropriately had large sediment bed archive layer thicknesses in highly erosional model grid cells and resulted in the calculation of unrealistic erosion rates. The correction of the initial sediment bed archive layer thicknesses as described in Section 2.2.4 was instrumental in achieving the bed accumulation results shown on Figure 3-30 which are in reasonable agreement with draft Superfund model results.

4.2.1.4 Discussion of CARP Sediment Transport and Organic Carbon Production Model Update Results, Bed Accumulation: North River and Haverstraw Bay

The reach-scale results on Figures 3-28 and 3-29 suggest minimal cumulative bed accumulation in the Tappan Zee to Battery portion of the Hudson River with relatively more cumulative bed accumulation in the

Haverstraw Bay to Tappan Zee reach, consistent with published literature. Ralston and Geyer, 2017, found from their modeling of an 85-day period in 2014 that less than 15% of total sediment input to the Hudson River moves downstream of the limit of the salinity intrusion and noted trapping of a portion of the 15% within Haverstraw Bay. Features in common as well as differences between CARP sediment transport and organic carbon production model bed accumulation results and literature (Woodruff et al., 2001; Ralston and Geyer, 2017) are further demonstrated by examining CARP model outputs on a sub-yearly and model grid cell basis for several flow conditions including spring freshets and summer storms (Figures 3-31 to 3-36).

Bed accumulation results shown on Figures 3-31 to 3-34 demonstrate that the CARP sediment transport and organic carbon production model on the 127 x 205 model computational grid exhibits sub-yearly bed accumulation and temporary storage in the North River portion of the Hudson River as described in the literature (e.g., Woodruff et al., 2001). The bed accumulation results shown on Figures 3-31 to 3-34 demonstrate that the CARP model calculates the occurrence of temporary storage zones in the North River portion of the Hudson River for various flow conditions (Figure 3-35) at spatial scales ranging from bank-to-bank to the individual model grid cells along shorelines.

Bed accumulation results shown on Figures 3-28, 3-29 and 3-36 demonstrate that the CARP sediment transport and organic carbon production model on the 127 x 205 model computational grid captures cumulative and sub-yearly changes in bed accumulation and storage within Haverstraw Bay, consistent with the estuarine turbidity maximum at Hudson River kilometer 55 (Haverstraw Bay) described by others (Ralston and Geyer, 2017).

4.2.2 Discussion of CARP Sediment Transport and Organic Carbon Production Model Update Results, Suspended Sediment Fluxes from the Lower Hudson River to the Harbor

The CARP sediment transport and organic carbon production model results on the 127 x 205 model computational grid for downstream fluxes of suspended sediment on the Hudson River at Poughkeepsie shown on Figure 3-37 are in excellent agreement with the results of Ralston and Geyer, 2017, for before, during, and after Hurricanes Irene and Lee. The CARP result of 4.5 megatonnes (i.e., teragrams) for the portion of the calibration period including October 1, 2004, to August 15, 2011, before Hurricanes Irene and Lee, compares well with Ralston and Geyer's estimate of 5 megatonnes (i.e., a percent difference of 10.5%). The CARP result of 7.2 megatonnes for the portion of the calibration period including October 1, 2004, to September 20, 2015, before, during, and after Hurricanes Irene and Lee, compares well with Ralston and Geyer's estimate of 7.5 megatonnes (i.e., a percent difference of 4.1%). These favorable comparisons for CARP downstream fluxes of suspended sediment results further validate the CARP bed accumulation results reported for the Hudson River in Section 3.2.1 and discussed in Section 4.2.1. The flux of solids past Poughkeepsie from the Upper Hudson River is of interest for bistate dredged material management given that the solids passing Poughkeepsie will ultimately reach the Harbor, including portions of Newark Bay, as was shown during CARP 1 loading source component projection work (HydroQual, 2007c).

4.2.3 Discussion of CARP Sediment Transport and Organic Carbon Production Model Update Results, Ambient Suspended Sediment and Organic Carbon Concentrations

Like the presentation of CARP sediment transport and organic carbon production model update results for ambient suspended sediment and organic carbon concentrations in Section 3.2.3, the results are discussed as three groupings: Newark Bay and Kills, Hudson River at Poughkeepsie, and throughout NY/NJ Harbor.

4.2.3.1 Discussion of CARP Sediment Transport and Organic Carbon Production Model Update Results, Ambient Suspended Sediment Concentrations: Newark Bay and Kills

The suspended sediment concentration results for five locations in Newark Bay and the Kills for sixteen water years shown in Appendix 9 and repeated for three example locations/water years in Figures 3-38, 3-39, and 3-40 highlight that the measured suspended sediment concentrations collected by different programs provide different and conflicting targets for assessing model skill. The collocated measurements are most often not in agreement with each other and may have resulted from differing analytical methods. It is not clear cut that the measurements from any one of the programs should be summarily discarded. Further, it is highly likely that resuspension introduced by vessel traffic and in some cases in-progress Harbor deepening activities are reflected in the measurements, but not in the model results. Despite discrepancies between measurements and between measurement and model results and anthropogenic influences on the measurements, the model calculations reflect the general magnitude of the measurements and capture reasonable depth variation. The model and measurement comparisons are more favorable on a full depth rather than a depth interval basis which in the case of the comparisons to estimates from acoustic backscatter measurements may be an artifact of the pairing of model results from sigma layers to measurements from fixed depth bins.

4.2.3.2 Discussion of CARP Sediment Transport and Organic Carbon Production Model Update Results, Ambient Suspended Sediment Concentrations, Hudson River at Poughkeepsie

The measured and modeled suspended sediment concentration results for the Hudson River at Poughkeepsie for the sixteen calendar years shown in Appendix 10 and repeated for the 2003 calendar year in Figure 3-41 show that the CARP suspended sediment and organic carbon production model on the 127 x 205 model computational grid can reproduce most but not all the measured instantaneous variation in suspended sediment concentrations. A results line of evidence related to model performance for suspended sediment concentrations on the Hudson River at Poughkeepsie is the excellent agreement between CARP model results and independent literature estimates of suspended sediment fluxes past Poughkeepsie presented in Section 3.2.2 and discussed in Section 4.2.2. The 4.1% difference result for suspended sediment fluxes past Poughkeepsie indicates that the CARP model is properly representing suspended sediment mass transport and therefore suspended sediment concentrations on the Hudson River near Poughkeepsie.

4.2.3.3 Discussion of CARP Sediment Transport and Organic Carbon Production Model Update Results, Ambient Suspended Sediment and Organic Carbon Concentrations, throughout NY/NJ Harbor

The timeseries results included in Appendix 11, comparing modeled suspended sediment concentrations to suspended measurements collected coincident with water column contaminant sampling by CARP 1 in 1998-2002, Lower Passaic River and Newark Bay Superfund efforts in 2005 and 2011/12, CARP 2 in 2019, and the NYCDEP Harbor survey in all years, are generally good to slightly low throughout the Harbor. While there are some large discrepancies between the range of the model results and the measurements collected by the NJHDG, the NJHDG measurements are suspect in some reaches relative to other measurements such as in the Middle Newark Bay, Lower Newark Bay/Kill van Kull, and Arthur Kill reaches shown on pages 3, 4, and 11 of Appendix 11. The model and measurement timeseries comparison results for suspended sediment concentrations in Appendix 11 and on the Figures 3-42 to 3-44 for the Hudson River, Upper New York Bay, East River, and Jamaica Bay indicate good model performance with CARP 1 (1998-2002), CARP 2 (2019), and NYCDEP Harbor survey (all years) measurements and some underpredictions compared to NJHDG measurements which may not be correct.

The model and measurement timeseries comparison results for particulate organic carbon concentrations throughout Newark Bay and the Kill van Kull included in Appendix 11 and on the Figures 3-45 to 3-47 indicate the CARP sediment transport and organic carbon production model on the 127 x 205 model computational grid captures the particulate organic carbon measurements collected coincident with water column contaminant sampling for 1998-2002 CARP 1, 2005 and 2011/12 Lower Passaic River and Newark Bay Superfund, and 2019 CARP 2. For seventy-one other locations displayed in Appendix 11 having less data richness, the water column particulate organic carbon concentrations model and measurement comparison results are also favorable.

The model and measurement timeseries comparison results for dissolved organic carbon concentrations throughout Newark Bay and the Kill van Kull included in Appendix 11 and on the Figures 3-48 to 3-50 indicate the CARP sediment transport and organic carbon production model on the 127 x 205 model computational grid captures the dissolved organic carbon measurements collected coincident with water column contaminant sampling for 1998-2002 CARP 1, 2005 and 2011/12 Lower Passaic River and Newark Bay Superfund, and 2019 CARP 2. The model results for dissolved organic carbon concentrations in Newark Bay and the Kill van Kull also capture the central tendency, but not the full range, of NJHDG measurements. Similar model and measurement comparison results for water column dissolved organic carbon concentrations are presented in Appendix 11 for twelve addition reaches and seventy-one additional model computational grid cell locations.

A cursory check of CARP sediment transport and organic carbon production model results using the 127 x 205 model computational grid for concentrations of additional water quality parameters that are related to suspended sediment and organic carbon, including chlorophyll, dissolved oxygen, ammonia nitrogen, phosphate phosphorus, and secchi depth/light extinction is included in Appendix 12 for Harbor locations. Although not the focus for contamination concentration prediction in dredged material, the time series displays of the related water quality parameters illustrate that the model generally represents the central tendency and much of the range of measurements at individual locations and captures measured spatial gradients across locations. These results were also monitored periodically as the CARP hydrodynamic and sediment transport models were migrated to the 127 x 205 model computational grid and the CARP hydrodynamic and sediment transport and organic carbon production models were progressively updated. The results for the related water quality parameters remained very consistent and without adverse impact from hydrodynamic and sediment transport model update.

4.3 Discussion of CARP Contaminant Fate and Transport Model Update Results

Discussion is provided for the contaminant fate and transport calibration and validation results in Sections 4.3.1 and 4.3.2.

4.3.1 Discussion of CARP Contaminant Fate and Transport Model Update Results, Six Contaminants 1998-2016 Calibration

Discussion of the results in Appendices 13 and 14 and on the associated Figures 3-51 to 3-58, for model and measurement comparisons timeseries for concentrations of 2,3,7,8-TCDD, 2,3,4,7,8-PCDF, di-CB, tetra-CB, hexa-CB, and octa-CB for the eighteen water years 1998-2016, is included in Section 4.3.1.1 for the sediment bed and in Section 4.3.1.2 for the water column.

4.3.1.1 Discussion of CARP Contaminant Fate and Transport Model Update, Six Contaminants 1998-2016 Calibration, Sediment Bed

Positions 1, 2, and 3 displayed on Figures 3-51 and 3-52 show important measurement results for solids-normalized 2,3,7,8-TCDD and total PCB concentrations in the sediment bed of Lower Newark Bay. The measurement results which span 1996 through 2019 are critical for establishing a target for the temporal behavior of the model. Further there is excellent consistency between the measurements compiled for the post-audit from numerous sources (Landeck Miller et al., 2019, red and blue circles), contemporary dredging projects (listing provided in Appendix 15, brown triangles), and measurements collected in 2019 by CARP investigators (report in preparation, pink and green squares). Especially for the solids-normalized total PCB concentrations in Lower Newark Bay as shown on Figure 3-52, the measurements from the dredging projects and CARP investigators fill a very important temporal gap in measurements critical for model calibration. Similar measurement results for establishing a robust temporal target for model calibration and for consistency among measurements from numerous collectors are apparent for additional locations, congeners, and homologs on the diagrams included in Appendix 13 and on Figures 3-53 and 3-54.

The model results (green lines and green and gray shades) shown on Figure 3-53 for 2,3,7,8-TCDD solids-normalized sediment bed concentrations for six locations in the Hudson and East Rivers compare reasonably well to the limited measurements collected for multiple programs. Location 5 includes a non-detect measurement at detection limit (open symbol). Stronger model and measurement comparison results at Hudson River locations 3 and 5 on Figure 3-53 may offset the importance of the potential underprediction based on one measurement further upstream at location 1. The model results (green lines and green and gray shades, twice the sum of four homologs) shown on Figure 3-54 for total PCB solids-normalized sediment bed concentrations for six locations in the Hudson and East Rivers compare well to limited measurements collected for multiple programs. Like the 2,3,7,8-TCDD results on Figure 3-53, the stronger model and measurement comparison results for total PCB at Hudson River locations 3 and 5 shown on Figure 3-54 may offset the importance of the potential underprediction further upstream at location 1.

The model and measurement comparison results shown on Figures 3-51 and 3-52 for 2,3,7,8-TCDD and total PCB solids-normalized concentrations in the sediment bed of Lower Newark Bay, on Figures 3-53 and 3-54 for 2,3,7,8-TCDD and total PCB solids-normalized concentrations in the sediment bed of the Hudson and East Rivers, and in Appendix 13 for other locations, congeners, and homologs, indicate that the model agrees well with the central tendency of the measurements and reflects some of the variation in the measurements. Most significantly, the measurement and model results, for contaminant concentrations in the sediment bed for ninety-five locations, both demonstrate relatively flat temporal behavior.

A comparison of the model and measurement bed concentration results presented on Figures 3-51 and 3-53 demonstrates that the model captures a spatial gradient of approximately an order of magnitude in the measured solids-normalized concentrations of 2,3,7,8-TCDD between the Lower Newark Bay reach shown on Figure 3-51 (~10^1 to 10^2 ppt range) and the Hudson and East River reaches shown on Figure 3-53 (~10^0 to 10^1 ppt range). A comparison of the model and measurement bed concentration results presented on Figures 3-52 and 3-54 demonstrates that the model also captures the absence of a pronounced spatial gradient in the measured solids-normalized concentrations of total PCB between the Lower Newark Bay reach shown on Figure 3-52 and the Hudson and East River reaches shown on Figure 3-54 (~10^2 to 10^3 ppb range for the three reaches).

4.3.1.2 Discussion of CARP Contaminant Fate and Transport Model Update, Six Contaminants 1998-2016 Calibration, Water Column

The model and measurement comparison results shown on Figures 3-55 and 3-56 for 2,3,7,8-TCDD and total PCB concentrations in the water column of upper Newark Bay, on Figures 3-57 and 3-58 for 2,3,7,8-TCDD and total PCB concentrations in the water column of the Hudson River, and in Appendix 14 for other locations, congeners, and homologs, indicate that the model agrees reasonably well with the central tendency of the temporally-limited measurements and reflects some of the variation in the measurements. The temporal limitations of the water column contaminant concentration measurements underscore the importance of the temporal expanse of the sediment bed contaminant concentration measurements for establishing model calibration targets.

A comparison of the model and measurement water column concentration results presented on Figures 3-55 and 3-57 demonstrates that the model captures a spatial gradient in the measured water column concentrations of 2,3,7,8-TCDD between the Upper Newark Bay reach shown on Figure 3-55 ($>10^{-3}$ ng/L) and the Hudson River reach shown on Figure 3-57 ($< 2 \times 10^{-4}$ ng/L). A comparison of the model concentration results presented on Figures 3-56 and 3-58 demonstrates that the model calculates a slight spatial gradient in water column concentrations of total PCB between the Upper Newark Bay reach shown on Figure 3-56 and the Hudson River reach shown on Figure 3-58. The model water column concentrations of total PCB in Newark Bay are somewhat higher than in the Hudson River, likely associated with different homolog distributions. For a homolog such as di-CB (in Appendix 14), which is associated with an Upper Hudson River source, the opposite water column concentration gradient is true. The model calculates higher di-PCB water column concentrations for the Hudson River reach shown as compared to Upper Newark Bay. In general, PCB homolog spatial distribution results are relatively flat throughout the Harbor.

4.3.1.3 Discussion of CARP Contaminant Fate and Transport Model Update Results, Six Contaminants 1998-2016 Calibration, Sediment Bed Particle Mixing Rates

The decision to adopt a reduction to the specified sediment bed particle mixing rate for the Lower Passaic River from Superfund modeling efforts was consequential for determining the time behavior of the CARP 127 x 205 model computational grid contaminant fate and transport model results for 2,3,7,8-TCDD concentrations in the bed of the Lower Passaic River and Newark Bay. Results shown on Figure 3-59 indicate that without the reduction to particle mixing rates, 2,3,7,8-TCDD bed concentrations at the example location in the Lower Passaic River would decrease by ~980 ppt over the 13 water years between October 1998 and September 2011, a half-life of only 2.3 years. Results shown on Figure 3-59 also indicate that with the reduction to particle mixing rates, 2,3,7,8-TCDD bed concentrations at the example location in the Lower Passaic River would instead decrease by ~800 ppt over the 13 water years between October 1998 and September 2011, a half-life of 5.6 years. Of similar consequence as also shown on Figures 3-59 and 3-60 was the correction of bed initial conditions for archive layer thickness and contaminant concentrations in the Lower Passaic River and Newark Bay which alleviated unrealistic excessive scour. Final calibration results shown on Figure 3-59 indicate that with the reduction to particle mixing rates and the correction of bed initial conditions, 2,3,7,8-TCDD bed concentrations at the example location in the Lower Passaic River would instead decrease by ~100 ppt over the 13 water years between October 1998 and September 2011, a half-life of 17.6 years.

The reduced sediment bed particle mixing rates that have been assigned for the Lower Passaic River in the CARP sediment transport and organic carbon production model will not be maintained for future projection scenarios (see Section 6) that include implementation of Lower Passaic River remediation. It is expected that the organisms responsible for particle mixing within the sediment bed would achieve similar particle mixing rates as in other Harbor areas once the Lower Passaic River is remediated.

4.3.1.4 Discussion of CARP Contaminant Fate and Transport Model Update Results, Six Contaminants 1998-2016 Calibration, Sediment Bed Initial Conditions

The model results for sediment transport using the 125 x 207 model computational grid include a patchwork of erosional and depositional areas in the East River on the west side of Riker's Island in South Brother Island Channel, north of Bowery Bay. The CARP sediment transport model on the 49 x 84 model computational grid did not capture such detail and represented the area more simply as depositional. Accordingly, when initial bed thickness information for the sediment archive layer was passed from the 49 x 84 to the 125 x 207 model computational grid versions of the CARP sediment transport model, erosional model grid cells in the 125 x 207 model computational grid were assigned an archive layer thickness which resulted in scour and redeposition which artificially elevated contaminant concentrations in near surface sediments above measured concentrations. Such elevated contaminant concentrations are displayed in the left column of Figure 3-61. Once the mapping of initial bed thicknesses for the sediment archive layer were adjusted in the sediment transport and organic carbon production model and the contaminant fate and transport model was run using the updated outputs of the sediment transport model, contaminant concentrations in near surface sediment bed concentrations aligned better with measured concentrations as shown in the right column of Figure 3-61. Similar adjustments to sediment bed initial conditions were also made at other locations and are ultimately reflected in the final contaminant fate and transport model calibration results for sediment bed contaminant concentrations presented in Appendix 13.

4.3.1.5 Discussion of CARP Contaminant Fate and Transport Model Update Results, Six Contaminants 1998-2016 Calibration, di-PCB Phase Partitioning

As identified in Section 2.3.2, the disparity in phase partitioning coefficients for di-CB calculated with CARP 1 water column and CARP 2 sediment bed measurements was used as an opportunity to perform sensitivity testing with the CARP contaminant fate and transport model on the 127 x 205 model computational grid. The contaminant fate and transport model on the 127 x 205 model computational grid was relatively insensitive to the testing of the di-CB phase partitioning coefficient. Although the model was not very sensitive to the change in the di-CB phase partitioning coefficient tested, there was some improvement in model and measurement comparisons at several locations in the water column. The largest improvements are shown on Figures 3-62 and 3-63 for locations in the Hudson River and Upper NY Bay. Given the improvements in model and measurement comparisons shown on Figures 3-62 and 3-63, the tested value of the di-CB phase partitioning coefficient based on sediment measurements was maintained for the final calibration.

4.3.2 Discussion of CARP Contaminant Fate and Transport Model Update Results, Twenty-One Additional Contaminants 1998-2016 Validation

The validation results for the CARP contaminant fate and transport model presented in Appendices 16 and 17 and Figures 3-64 through 3-65 which screen model performance for twenty-one additional contaminants are generally reasonable with model performance varying by contaminant and location. The overall reasonableness of the results demonstrates that the methods applied for the update of the CARP models for six contaminants as presented in Section 2 were also applicable to twenty-one additional contaminants, a very important and favorable outcome. The reasonable performance of the contaminant fate and transport model both temporally and spatially for twenty-seven contaminants is also a positive indicator of the representativeness of the hydrodynamic, sediment transport and organic carbon production models. There are obvious imperfections in the model validation single-simulation results, such as model overprediction of limited mono-CB measurements in the water column, which have not been addressed.

Discussion of the model and measurements comparisons timeseries validation results presented in Appendices 16 and 17 and on Figures 3-4 through 3-65 is limited to highlighting a few features specific to the additional twenty-one validation contaminants. The limited discussion is provided for the PCB summation of ten homologs and for pointing out an apparent elevation of modeled nona-CB concentrations in the sediment bed and water column of portions of the Harbor during remedial dredging on the Upper Hudson River. The apparent elevation of modeled nona-CB concentrations in the sediment bed and water column of portions of the Harbor during remedial dredging on the Upper Hudson River was an unexpected result. Lower chlorinated homologs, not nona-CB, are associated with historic General Electric, Inc. operations and releases and the sediment bed of the Upper Hudson River prior to remedial dredging completion.

4.3.2.1 Discussion of CARP Contaminant Fate and Transport Model Update Results, Twenty-One Additional Contaminants 1998-2016 Validation, PCB summation of Ten Homologs

The testing of the application of the factor of two to the summation of four PCB homologs (i.e., di-CB, tetra-CB, hexa-CB, and octa-CB) to approximate total PCB established during CARP 1 (HydroQual, 2007c) and used for CARP 2 calibration and projections had incredible method validation results. The percentage errors calculated in comparisons to summations of model results from ten homologs were very small, ranging from -0.014% to +7.1% for four randomly selected sediment bed locations for time averages from a randomly selected water year. More extensively and equally reassuring, for eighteen water years, for ninety-five sediment bed locations, and for sixty-one water column locations, total PCB concentration time series model results are almost indistinguishable as evidenced by comparing the model results on the sediment bed total PCB diagrams in Appendices 13 (twice the sum of four homologs) and 16 (sum of ten homologs) and the water column total PCB diagrams in Appendices 14 (twice the sum of four homologs) and 17 (sum of ten homologs).

4.3.2.2 Discussion of CARP Contaminant Fate and Transport Model Update Results, Twenty-One Additional Contaminants 1998-2016 Validation, Nona-CB Concentrations During Remedial Dredging

For the period of remedial dredging on the Hudson River starting in 2009, all PCB homologs were modeled with higher loading concentrations from the Hudson River above Mohawk River than for either pre- or post-dredging as presented in Landeck Miller et al., 2022. Despite these increased loading concentrations from the Upper Hudson River associated with remedial dredging, elevated PCB homolog concentrations in the Harbor sediment bed and water column are only apparent in the modeled results presented in Appendices 13, 14, 16 and 17 for nona-CB, not for other homologs. Specifically on the reach pages for the Hudson and East Rivers and the Upper NY Bay 1, 2, and 3 pages in Appendix 16 for the sediment bed, and the reach page for the Hudson River in Appendix 17 for the water column, there are noticeable increases of modeled nona-CB concentrations starting in 2009 (i.e., during remedial dredging) at several individual locations. The explanation for this behavior is that the modeled increase in loading from the Hudson River above Mohawk due to remedial dredging that is transported to the Harbor in the model for nona-CB is larger relative to modeled local Harbor sources for nona-CB than for other homologs. As for the magnitude of the modeled nona-CB loading from the Hudson River above Mohawk, the regression equation used for estimating the nona-CB loading during remedial dredging (see Landeck Miller et al., 2022) was based on three measurements, 31.4 ng/L at 10,800 cfs; 0.109 ng/L at 11,100 cfs; and 1.146 ng/L at 18,900 cfs and was strongly driven by the first measurement which is likely an outlier. Nona-CB loading from the Hudson River above Mohawk due to remedial dredging was likely lower than modeled.

5.0 CONCLUSION

The CARP hydrodynamic transport, sediment transport and organic carbon production, and contaminant fate and transport models have been successfully migrated from a 49 x 84 model computational grid to a 127 x 205 model computational grid. The migration of the CARP models to the larger computational grid provides vastly enhanced spatial resolution, especially in areas of importance to dredged material management such as Upper NY Bay and Newark Bay. The calibration of the CARP models on the 127 x 205 model computational grid includes the expansion of the calibration period from four water years to eighteen water years. The expanded calibration period includes the large storm events Hurricanes Irene, Lee, and Sandy, in addition to Hurricane Floyd, and addresses concerns that the prior CARP model calibration was conducted primarily for low flow conditions. The expanded calibration period allows for the consideration of solids transport from the watershed to the Harbor during a wide range of conditions, including major storm events.

The ability of the CARP sediment transport model on the 127 x 205 model computational grid to utilize the outputs of the CARP hydrodynamic transport model directly without modification improves the technical defensibility of the CARP models. Sediment accumulation and storage on the Hudson River and the flux of solids from the Hudson to the Harbor calculated with the CARP models on the 127 x 205 model computational grid differ from calculations with the 49 x 84 model computational grid (HydroQual, 2007b) and are more consistent with published literature (Ralston, et al. 2013; Ralston and Geyer, 2017; Woodruff et al., 2001). CARP model calculations of sediment accumulation and erosion within Newark Bay improved tremendously with the use of the sediment transport model on the 127 x 205 model computational grid and are much more consistent with draft results from elaborate and sophisticated sediment transport modeling efforts ongoing for Superfund. The success of the CARP sediment transport model calibration for eighteen water years validates new methods developed and implemented for estimation of CARP model solids loadings (Landeck Miller et al., 2022).

CARP contaminant phase partitioning coefficients for PCB homologs and dioxin and furan congeners developed previously based on water column measurements and used in the CARP contaminant fate and transport model were confirmed by new contaminant phase partitioning coefficients calculated with sediment measurements collected by CARP investigators conducting bioaccumulation studies (report in preparation). Testing of a discrepancy between the estimates of the phase partitioning coefficient specifically for di-CB showed the CARP contaminant fate and transport model to be relatively insensitive to the level of discrepancy observed for the two estimates of contaminant phase partitioning coefficients.

Contemporary measurements of contaminants in the sediment bed and water column throughout the Harbor collected by CARP investigators (report in preparation) and from navigational maintenance dredging projects (Appendix 15) were critical for establishing the time behavior of contaminants during the eighteen-year CARP model calibration period, especially given high variability and/or sparseness in measurements from earlier periods for some of the locations considered for the CARP post-audit (Landeck Miller et al, 2019).

The CARP contaminant fate and transport model on the 127 x 205 model computational grid captures measured temporal trends at specific Harbor locations as well as spatial gradients across various Harbor reaches for 2,3,7,8-TCDD and total PCB. The CARP models on the 127 x 205 computational grid as calibrated are appropriate to use for developing 2040 projections of the HARS suitability of future dredged material. CARP contaminant fate and transport model calibration results on the 127 x 205 model computational grid confirm that twice the summation, of the four PCB homologs, di-CB, tetra-CB, hexa-CB, and octa-CB, that will be simulated in CARP 2040 projections, is a good surrogate for total PCB.

6.0 NEXT STEPS

The update, of the CARP hydrodynamic transport, sediment transport and organic carbon production, and contaminant fate and transport models, represents the next to last deliverable in a series of CARP model-related deliverables and takes advantage of previous deliverables such as the post-audit and loadings development. The purpose, for the update of the CARP hydrodynamic transport, sediment transport and organic carbon production, and contaminant fate and transport models, is to refine CARP 1 projections of the HARS suitability of future dredged material. Accordingly, the updated CARP models will be applied for 2040 projections of contaminant levels in Harbor sediments and, by using Biota-Sediment-Accumulation-Factors (BSAFs), 2040 projections of contaminant body burdens in dredged material test organisms. Reporting on the 2040 projections will be provided as a separate deliverable.

7.0 ACKNOWLEDGMENTS AND DISCLAIMERS

The update of the CARP models was funded by basic agreement number 2016-MU-1 between the New Jersey Department of Transportation (NJDOT) and Monmouth University. The content of this report is solely the positions of the authors and not the positions of NJDOT and therefore does not constitute a standard, specification, or regulation.

The development and update of the CARP model computational grid, time-varying bathymetry, hydrodynamic model inputs, and hydrodynamic model and measurement comparisons reflect the significant efforts of Nicholas Kim who retired from HDR in 2021 prior to the drafting of this report. The measurements of contaminants in the sediment bed from contemporary maintenance dredging projects listed in Appendix 15 and used for model and measurement comparisons in Appendix 13 and various report figures were provided by Mark Reiss of USEPA Region 2. The measurements of suspended sediment in the Hudson River near Poughkeepsie were provided by Gary Wall of the USGS.

8.0 LITERATURE CITED

Blumberg, A.F., L.A. Khan, J.P. St. John. 1999. Three-Dimensional Hydrodynamic Model of New York Harbor Region. *J. Hydr. Engrg., ASCE*. 125(8): 799-816.

Boudreau, B.P. 1994. Is burial velocity a master parameter for bioturbation? *Geochim. Cosmochim. Acta*. 59: 1243-1249.

Boyer, T.P., O.K. Baranova, C. Coleman, H.E. Garcia, A. Grodsky, R.A. Locarnini, A.V. Mishonov, C.R. Paver, J.R. Reagan, D. Seidov, I.V. Smolyar, K.W. Weathers, M.M. Zweng. 2018. World Ocean Database 2018. A. V. Mishonov, Technical Editor, NOAA Atlas NESDIS 87. wod_intro_0.pdf (noaa.gov)

Brandon, C., Woodruff, J., Donnelly, J. *et al.* 2014. How Unique was Hurricane Sandy? Sedimentary Reconstructions of Extreme Flooding from New York Harbor. *Sci Rep* **4**, 7366 (2014). https://doi.org/10.1038/srep07366.

Chant, R.J. 2006. *Hydrodynamics of the Newark Bay/Kills System, The New Jersey Toxics Reduction Workplan for New York-New Jersey Harbor Study I-E*. Institute of Marine and Coastal Studies, Rutgers University New Brunswick, New Jersey 08904. Prepared for New Jersey Department of Environmental Protection Division of Science, Research and Technology. 90p. (Appendix A-2 at https://www.hudsonriver.org/article/carp-appendices)

DiToro, D.M. 2001. *Sediment Flux Modeling*. New York: John Wiley & Sons, Inc. ISBN 0-471-13535-6. 624p.

HydroQual, Inc., 2001. Newtown Creek WPCP Project East River Water Quality Plan, Task 10.0 - System-wide Eutrophication Model (SWEM), Sub-task 10.4 Calibrate SWEM for Water Quality, Sub-task 10.6, Validate SWEM for Water Quality, report and appendices prepared under contract to Greeley and Hansen for the City of New York Department of Environmental Protection.

HydroQual, Inc., 2007a. A Model for the Evaluation and Management of Contaminants of Concern in Water, Sediment, and Biota in the NY/NJ Harbor Estuary: Hydrodynamic Transport Sub-model, Final Report, Submitted to the Hudson River Foundation, New York, NY. (Appendix A-5 at https://www.hudsonriver.org/article/carp-appendices)

HydroQual, Inc., 2007b. A Model for the Evaluation and Management of Contaminants of Concern in Water, Sediment, and Biota in the NY/NJ Harbor Estuary: Sediment Transport/Organic Carbon Production Sub-model, Final Report, Submitted to the Hudson River Foundation, New York, NY. (Appendix A-6 at https://www.hudsonriver.org/article/carp-appendices)

HydroQual, Inc., 2007c. A Model for the Evaluation and Management of Contaminants of Concern in Water, Sediment, and Biota in the NY/NJ Harbor Estuary: Contaminant Fate and Transport and Bioaccumulation Sub-models, Final Report, Submitted to the Hudson River Foundation, New York, NY. (Appendix A-7 at https://www.hudsonriver.org/article/carp-appendices)

Landeck Miller, R.E., K.J. Farley, J.R. Wands, B. Yadav, and N. Kogan. 2019. *Post-Audit Evaluation of the CARP 1 Model 2040 Projections*, HDR report for NY/NJ Harbor Contamination Assessment and Reduction Project, CARP II, New Jersey Department of Transportation, Under Agreement with Monmouth University and the Hudson River Foundation.

Landeck Miller, R.E., K.J. Farley, L. De Rosa, N. Kogan, R. Rugabandana, and J.R. Wands. 2022. Update of CARP Model External Loading Forcing Functions, HDR report for NY/NJ Harbor Contamination Assessment and Reduction Project, CARP II, New Jersey Department of Transportation, Under Agreement with Monmouth University and the Hudson River Foundation.

Levitus, S. 1982. *Climatological Atlas of the World Ocean*, U.S. Gov. Printing Office, Wash., D.C., 173 pp., cited in Boyer et al., 2018.

Maa, J.P-Y, L.P. Sanford, J.P. Halka, 1998. Sediment Resuspension Characteristics in Baltimore Harbor, Maryland. *Marine Geology*, 146(1-4): 137-145.

NOAA. 2023. *National Weather Service Albany, NY Precipitation – Extremes and Records*. Wettest months and dates diagrams accessed during January 2023 from https://www.weather.gov/aly/recordpcpn.

Ralston, D. K., J. C. Warner, W. R. Geyer, and G. R. Wall. 2013. Sediment transport due to extreme events: The Hudson River estuary after tropical storms Irene and Lee. *Geophys. Res. Lett.*, 40, 5451–5455, doi:10.1002/2013GL057906.

Ralston D. K. Ralston and W. Rockwell Geyer. 2017. *Sediment Delivery, Trapping, and Storage during Extreme Flow Events*. Final Report, Hudson River Foundation Grant No. 004/13A. Woods Hole Oceanographic Institution Woods Hole, MA 02543

Sommerfield, C.K. and R.J. Chant. 2010. *Mechanisms of Sediment Trapping and Accumulation in Newark Bay, New Jersey: An Engineered Estuarine Basin*. Final report to the Hudson River Foundation, (HRF 008/07A). 40p. (Microsoft Word - HRF008_07A_finaltechnical report_072210.doc (epa.gov))

USEPA. 2016. Record of Decision – *Responsiveness Summary Attachment E – Updated Mechanistic Model – Part 1 of 6 for the Lower Eight Miles of the Lower Passaic River*. Document ID 377122, 532 pp. (https://semspub.epa.gov/work/02/377122.pdf).

Woodruff, J.D., W.R. Geyer, C.K. Sommerfield, and N.W. Driscoll. 2001. Seasonal variation of sediment deposition in the Hudson River estuary. *Marine Geology* 179(2001): 105-119.

9.0 SECTION 2 FIGURES

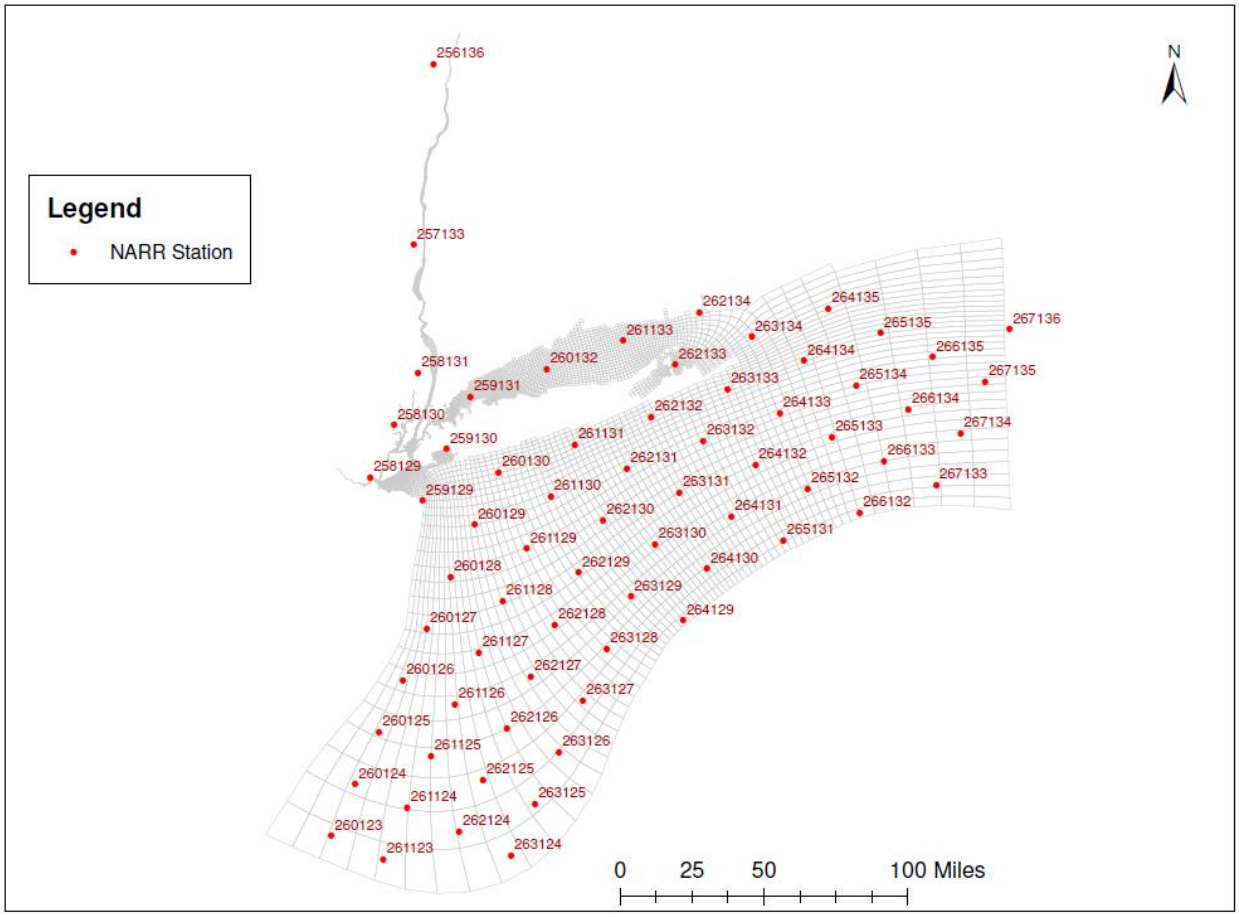

Figure 2-1. Location of sixty-nine NOAA stations used for the specification of the meteorological inputs needed for hydrodynamic model calculations of 2D wind stresses and heat fluxes.

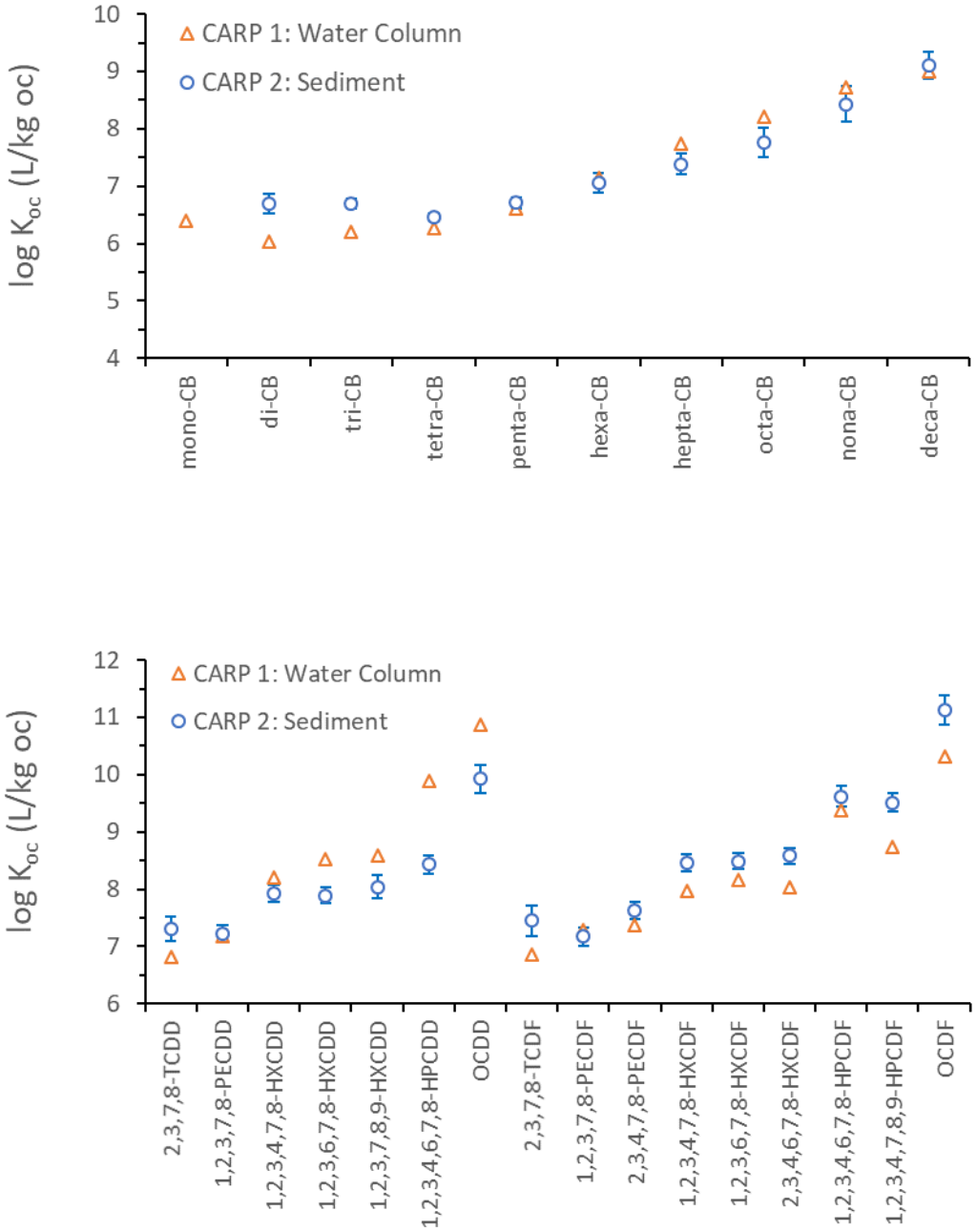

Figure 2-2. Contaminant phase partitioning coefficients calculated from CARP 1 water column and CARP 2 sediment bed measurements are in reasonable agreement for PCB homologs (top panel) and dioxin and furan congeners (bottom panel) and for the six CARP 2 calibration contaminants di-CB, tetra-CB. hexa-CB, octa-CB, 2,3,7,8-TCDD, and 2,3,4,7,8-PCDF.

10.0 SECTION 3 FIGURES

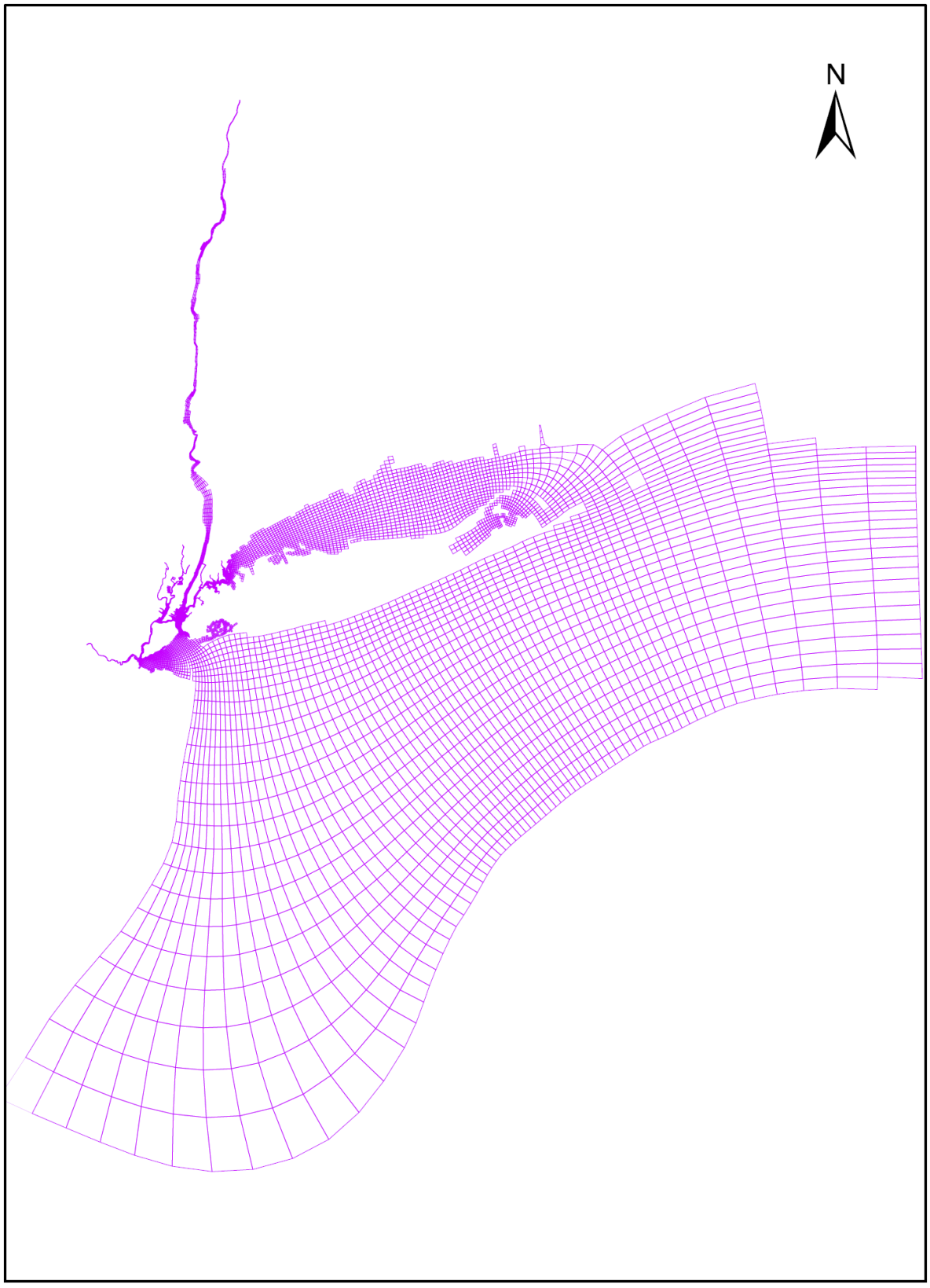

Figure 3-1. CARP 2 127 x 205 model computational grid, full domain view.

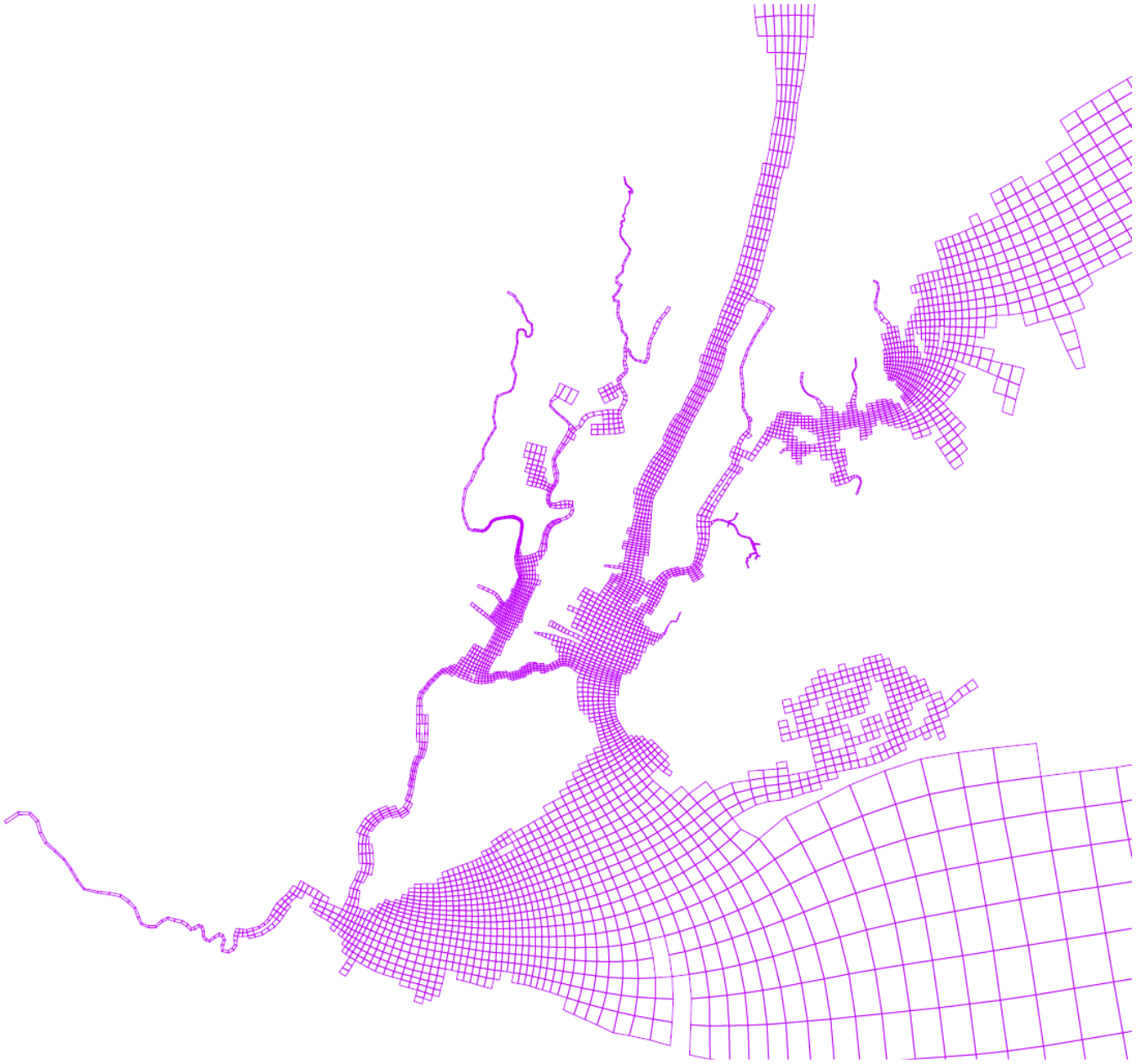

Figure 3-2. CARP 2 127 x 205 model computational grid, view of the Harbor portion of the model domain.

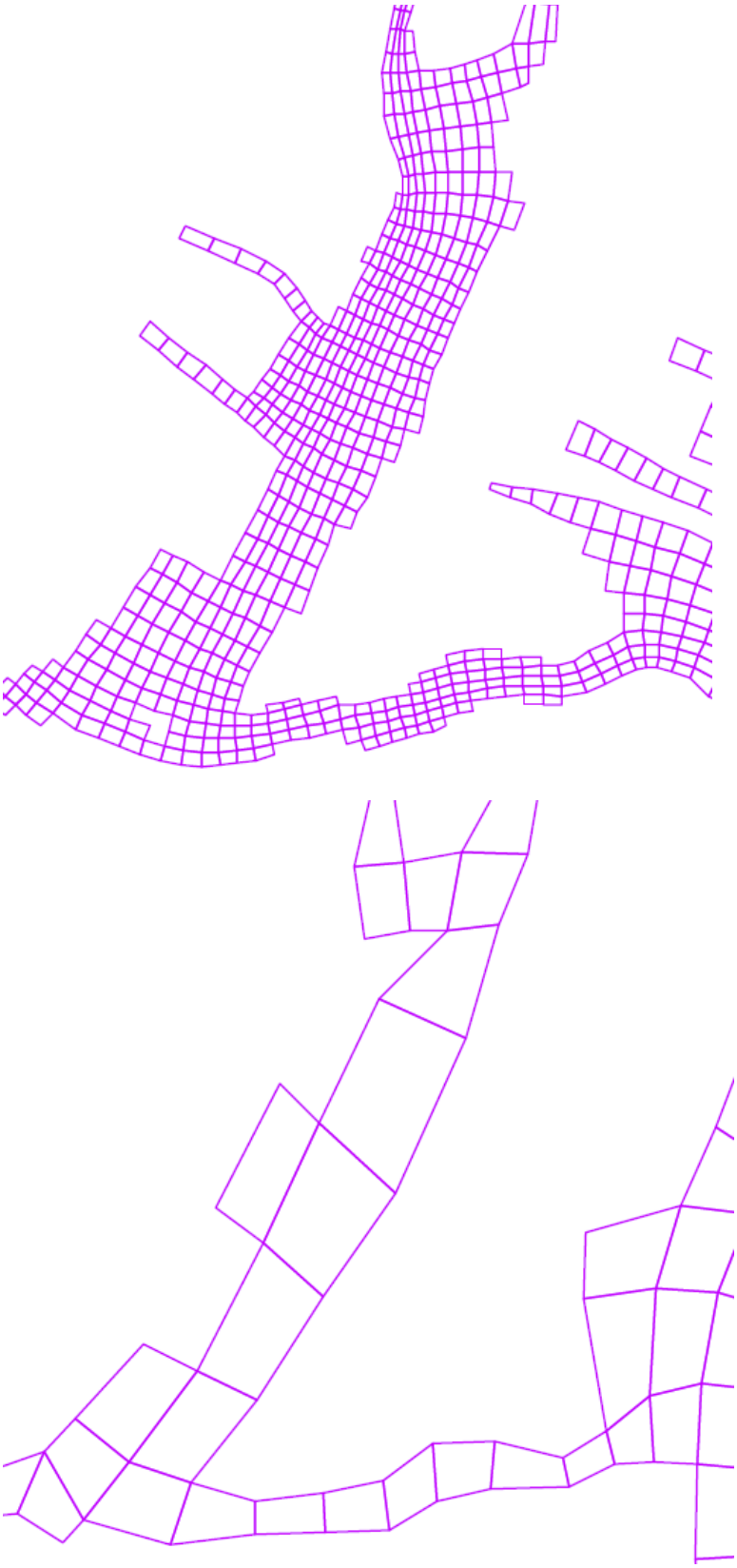

Figure 3- 3. Newark Bay and the Kill van Kull, including a portion of Upper NY Bay, view of CARP 127 x 205 (top) and 49 x 84 (bottom) model computational grids.

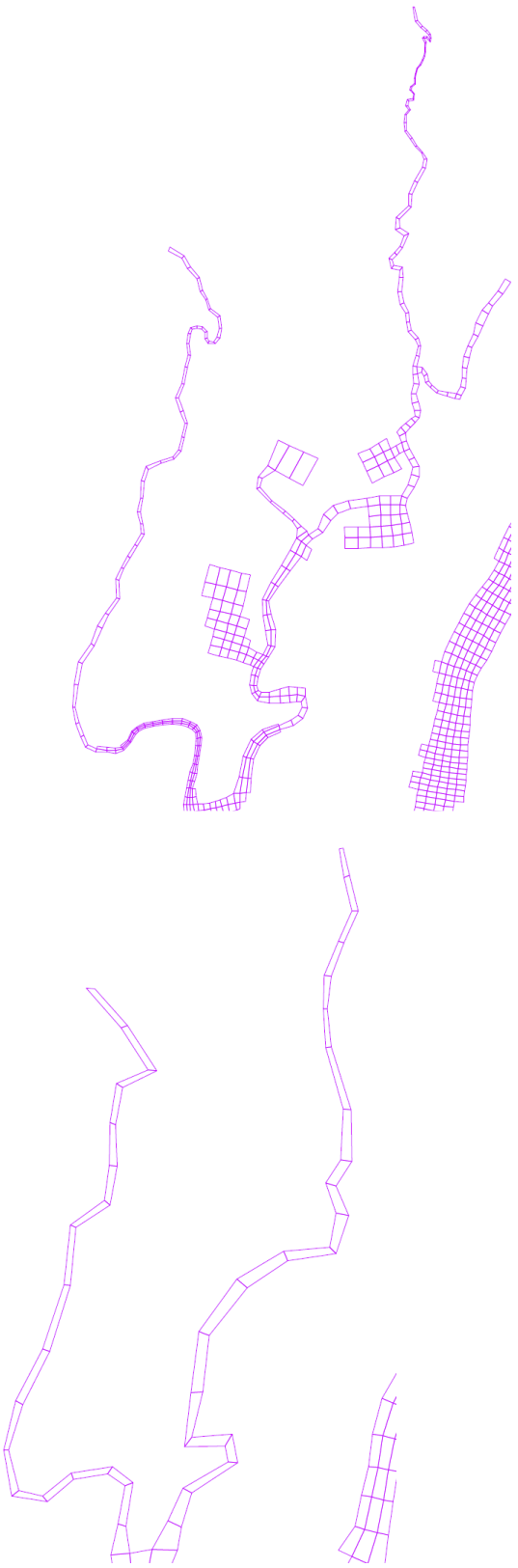

Figure 3-4. Lower Passaic and Hackensack Rivers, including a portion of the Hudson River, view of CARP 127 x 205 (top) and 49 x 84 (bottom) model computational grids.

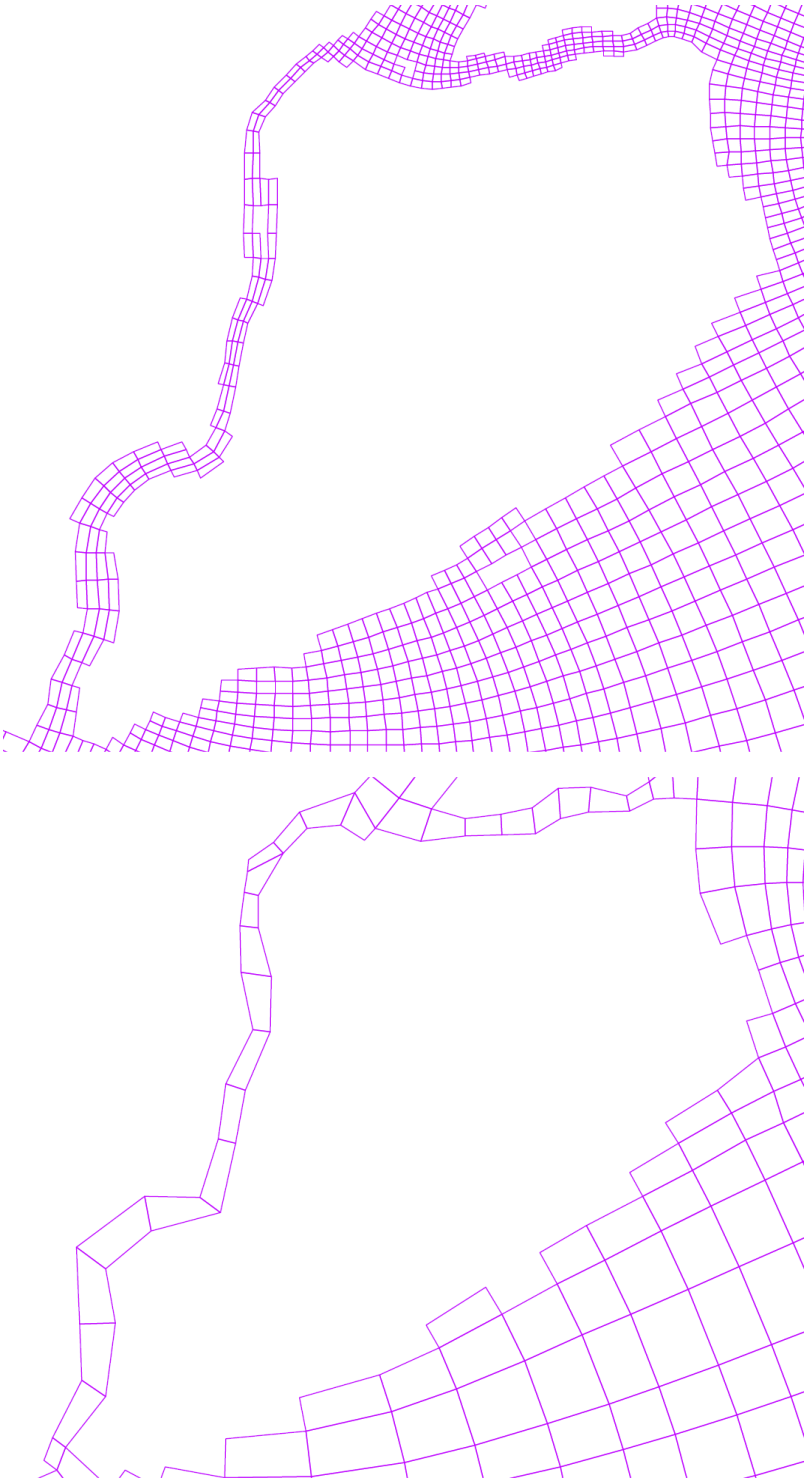

Figure 3-5. Kill van Kull and Arthur Kill, including portions of Upper NY and Raritan Bays, view of CARP 127 x 205 (top) and 49 x 84 (bottom) model computational grids.

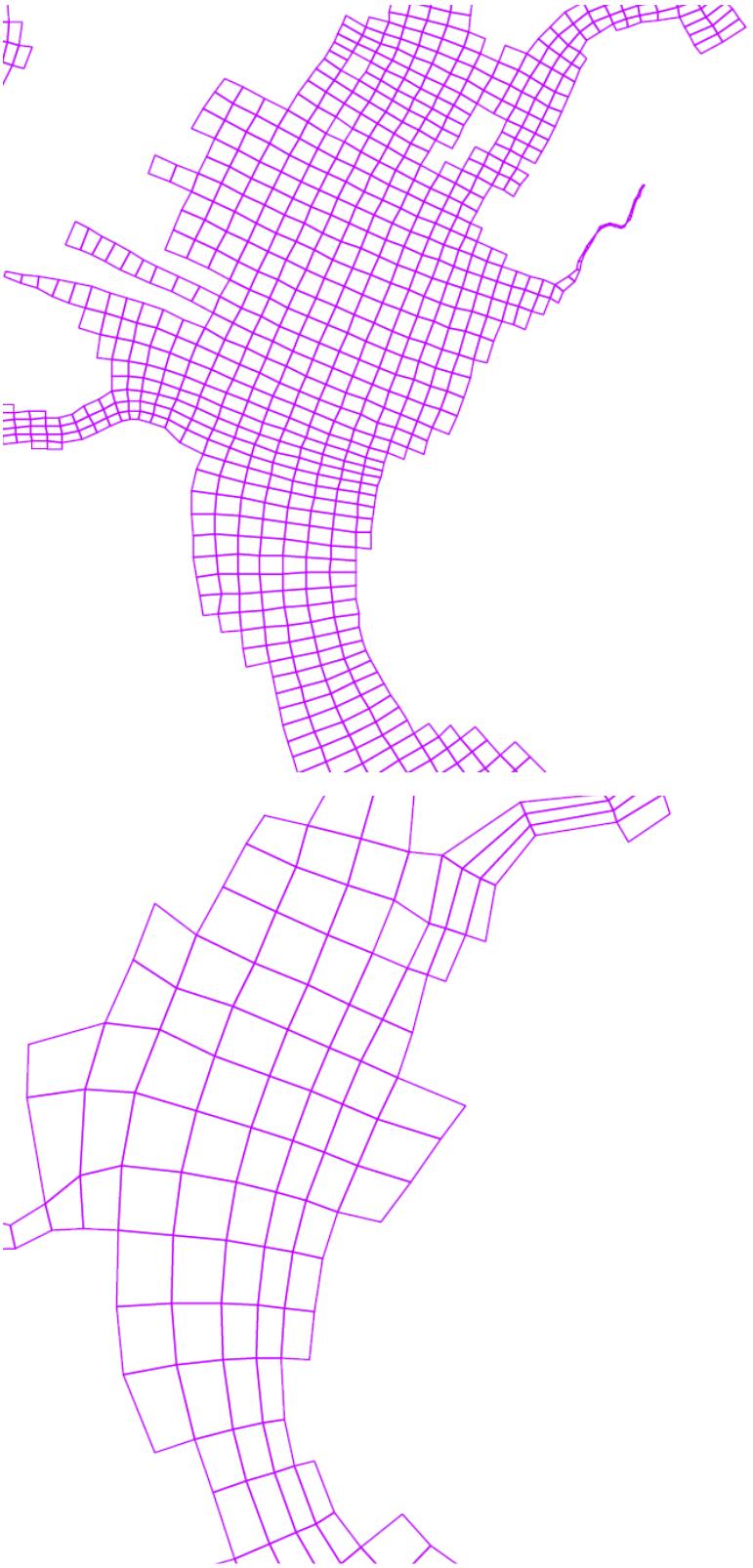

Figure 3-6. Upper NY Bay through Narrows, including the Port Jersey and MOTBY Channels and Gowanus Bay and the mouths of the Hudson and East Rivers and the Kill van Kull, view of CARP 127 x 205 (top) and 49 x 84 (bottom) model computational grids.

Figure 3-7. Hudson River, from Troy Dam to the head of Haverstraw Bay, view of CARP 127 x 205 (left) and 49 x 84 (right) model computational grids.

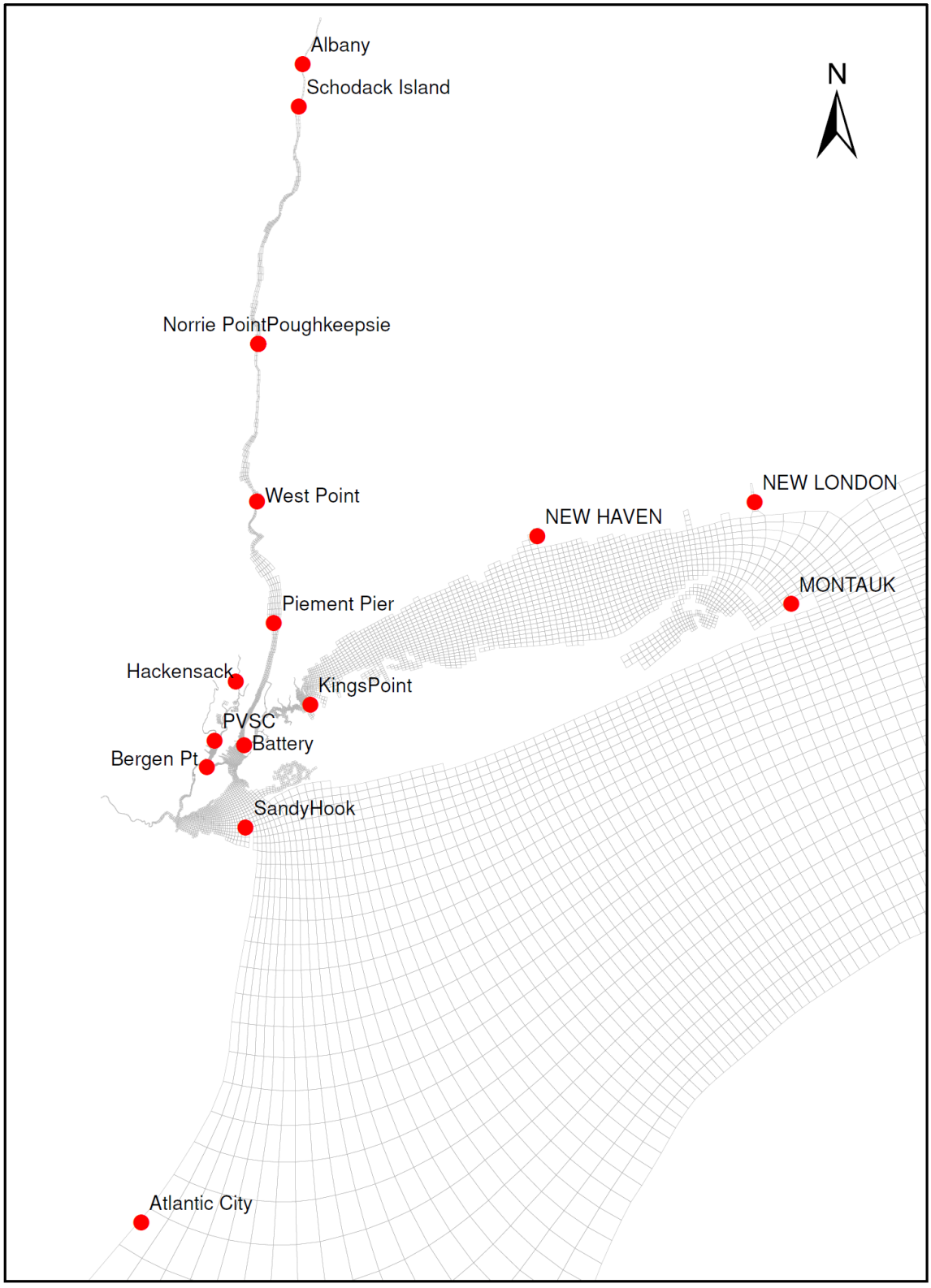

Figure 3-8. Locations of tidal water elevation model and measurement comparisons.

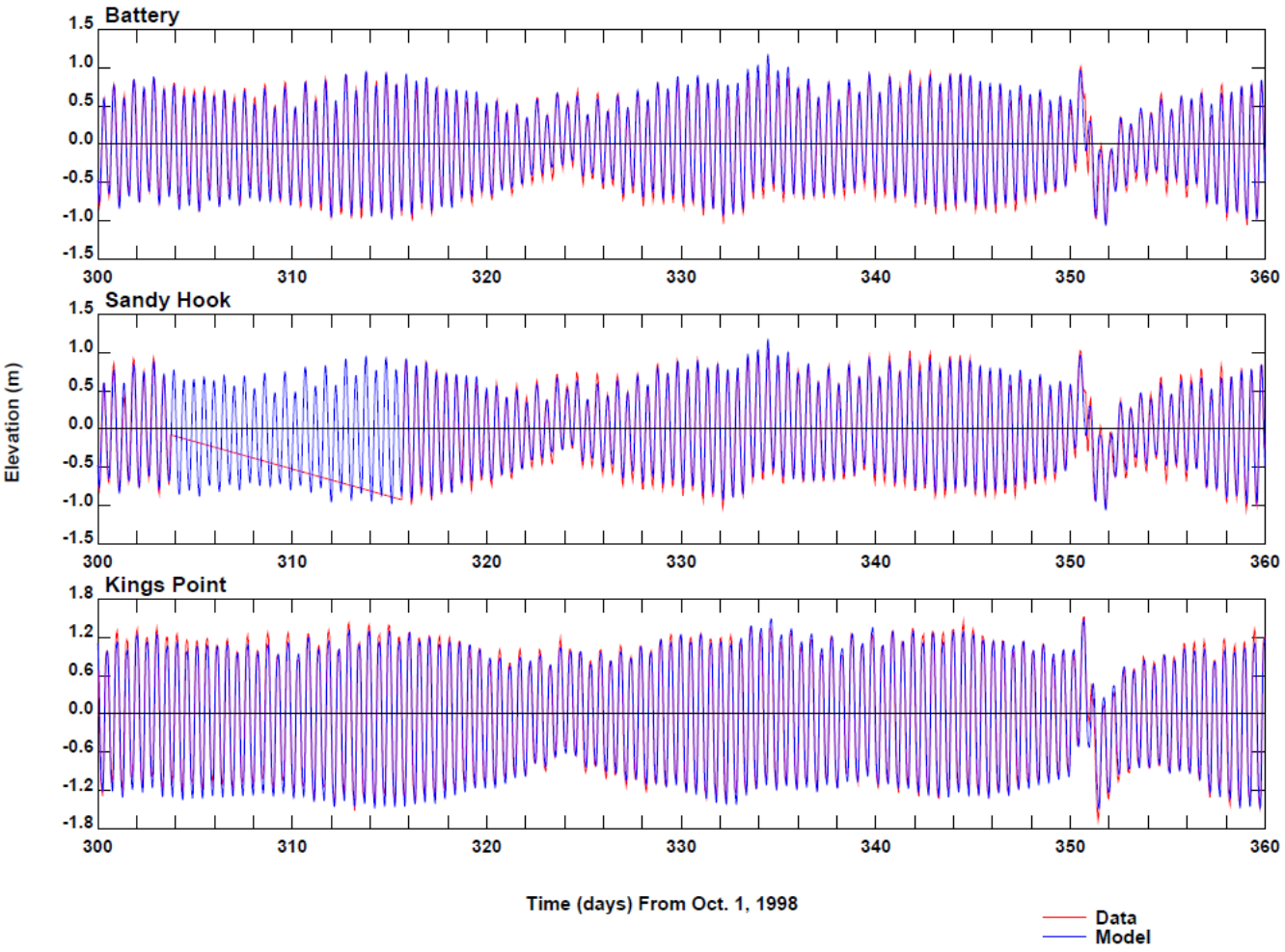

Figure 3-9. Hourly water elevation model and measurement comparisons results. Modeled and measured results presented between days 350 and 352 show relatively higher water elevations during Hurricane Floyd and the sharp gradient rapid decline.

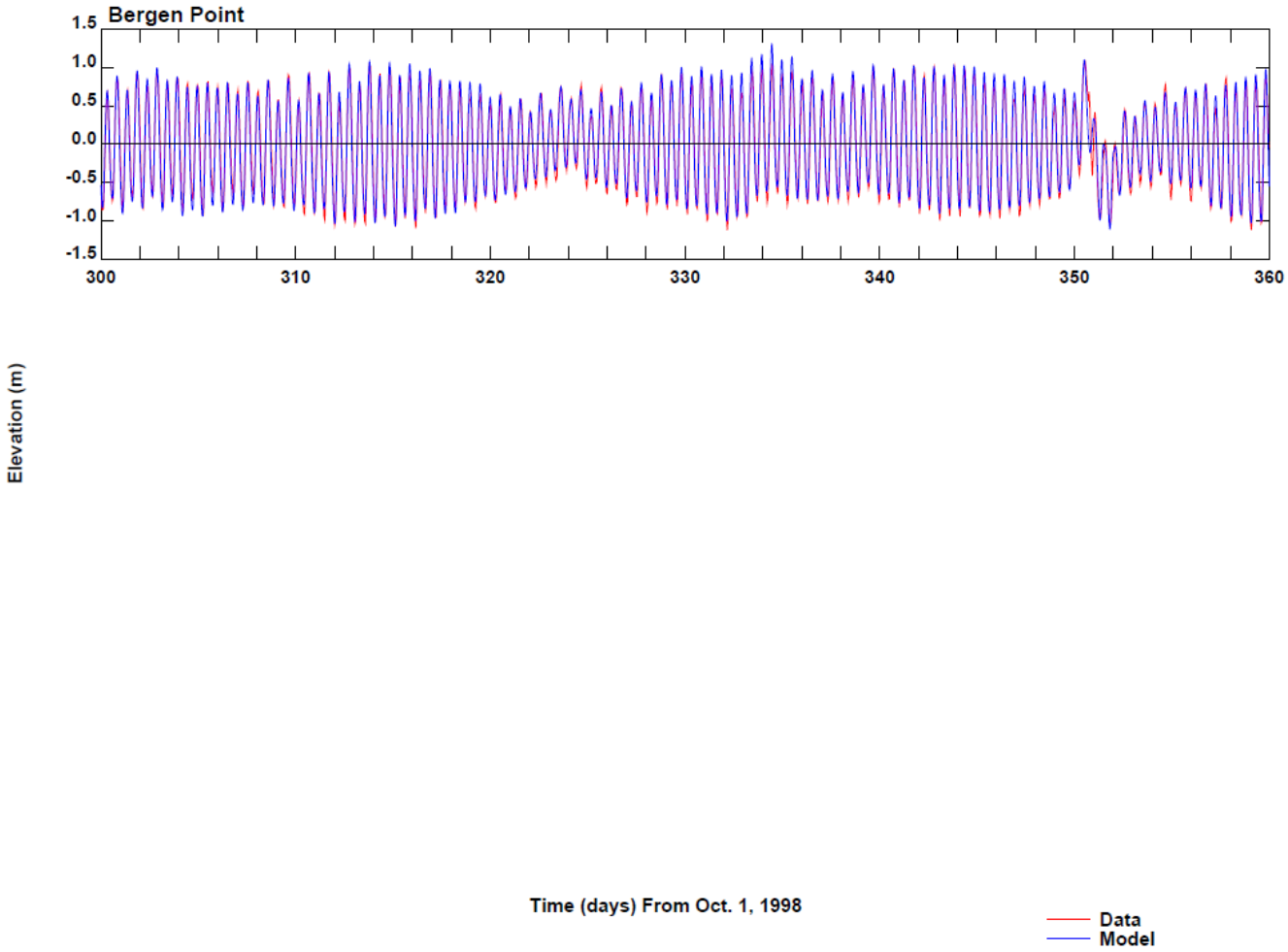

Figure 3-10. Hourly water elevation model and measurement comparisons results. Modeled and measured results presented between days 350 and 352 show relatively higher water elevations in the northern Kill van Kull near Newark Bay during Hurricane Floyd and the sharp gradient rapid decline.

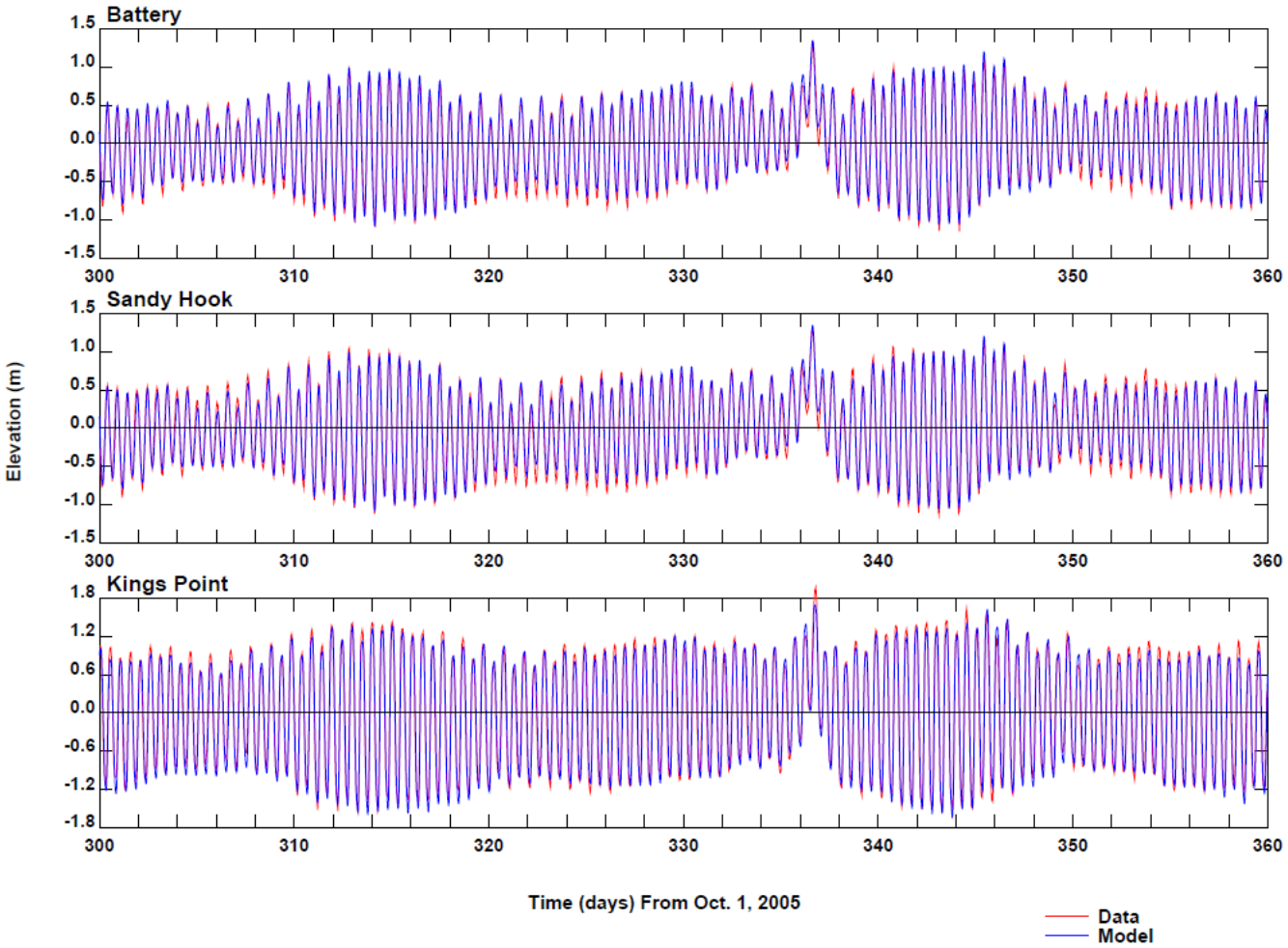

Figure 3-11. Hourly water elevation model and measurement comparisons results. Modeled and measured results presented between days 336 and 338 show relatively higher water elevations during Hurricane Ernesto/Florence and the sharp gradient rapid decline.

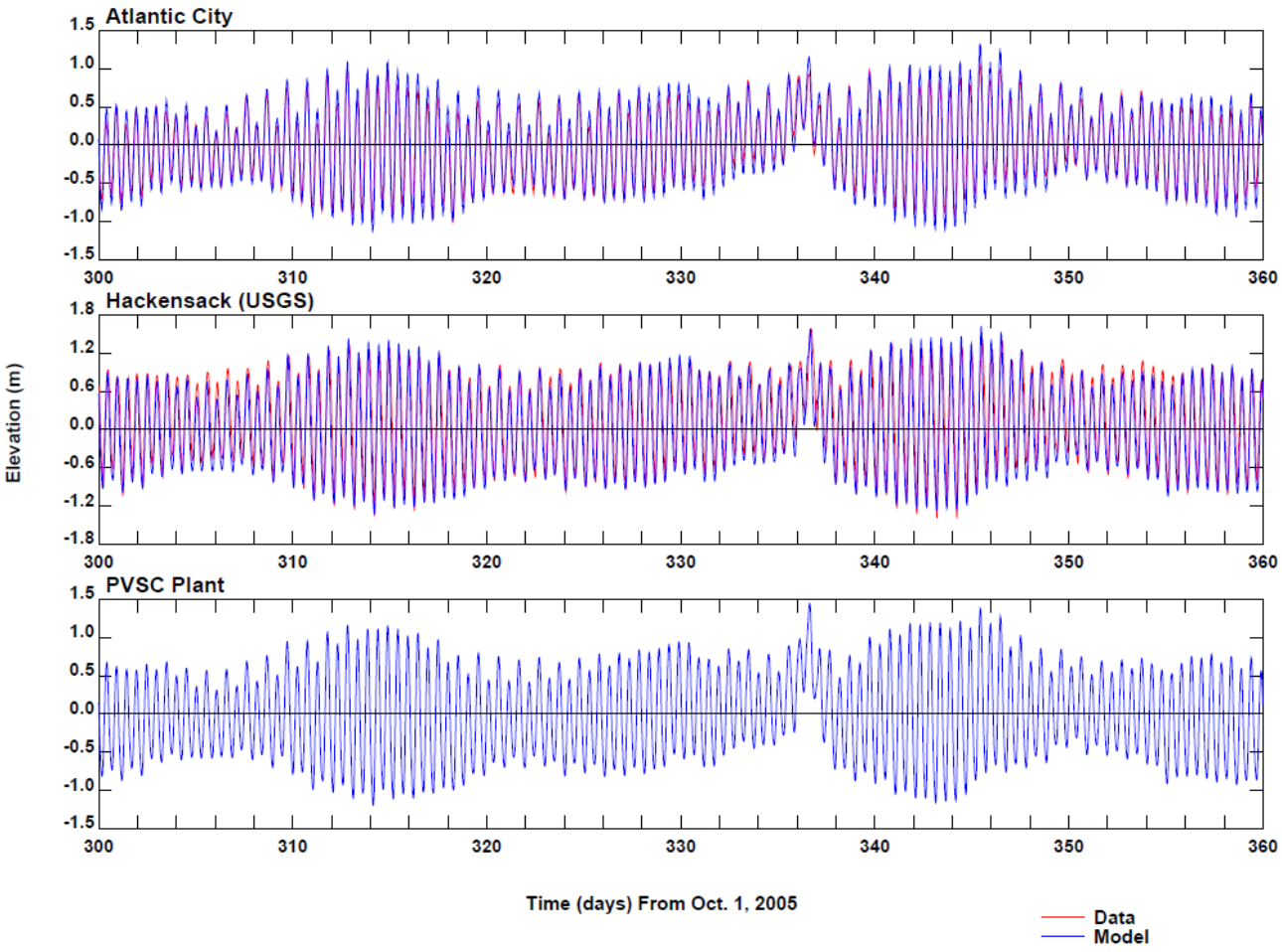

Figure 3-12. Hourly water elevation model and measurement comparisons results. Modeled and measured results presented between days 336 and 338 show relatively higher water elevations during Hurricane Ernesto/Florence and the sharp gradient rapid decline.

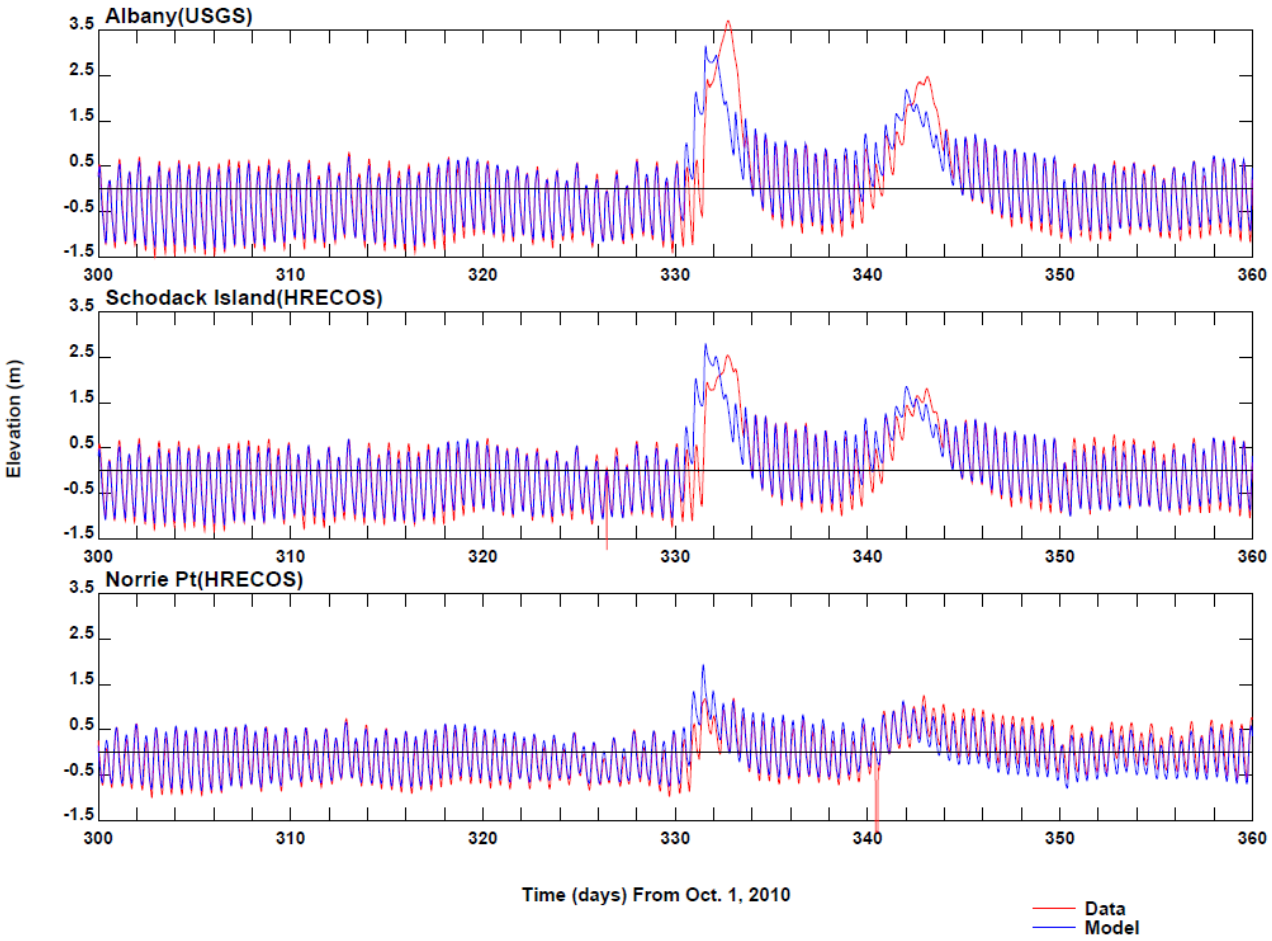

Figure 3-13. Hourly water elevation model and measurement comparisons results. Modeled and measured results presented between days 330 and 334 and between days 340 and 344 show relatively higher water elevations during Hurricanes Irene and Lee and the sharp gradient rapid decline. The modeled peak hourly water elevations for these events occurs slightly sooner than measured at the two most upstream measurement locations on the Hudson River.

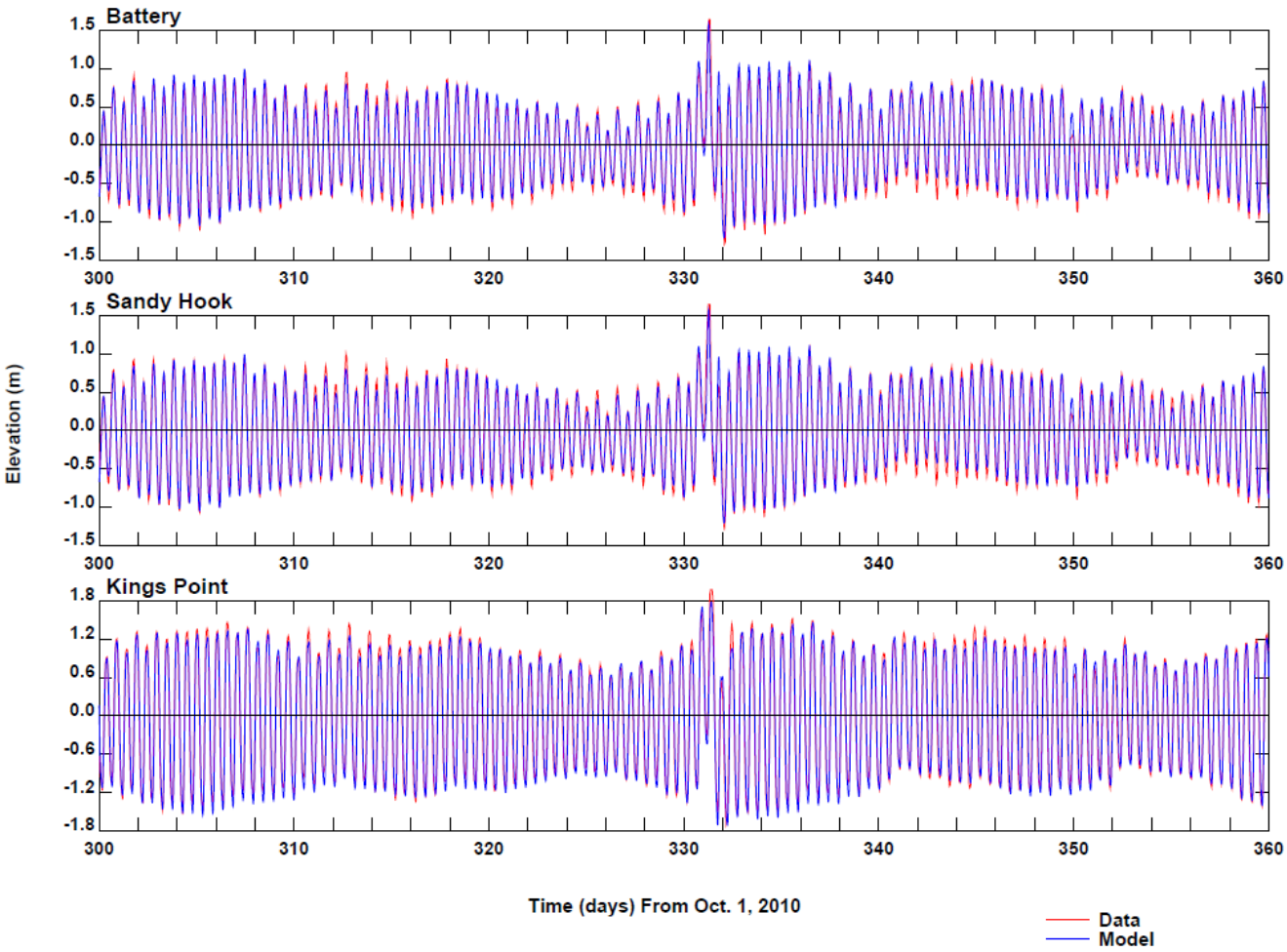

Figure 3-14. Hourly water elevation model and measurement comparisons results. Modeled and measured results presented between days 330 and 334 show relatively higher water elevations during Hurricane Irene and the sharp gradient rapid decline.

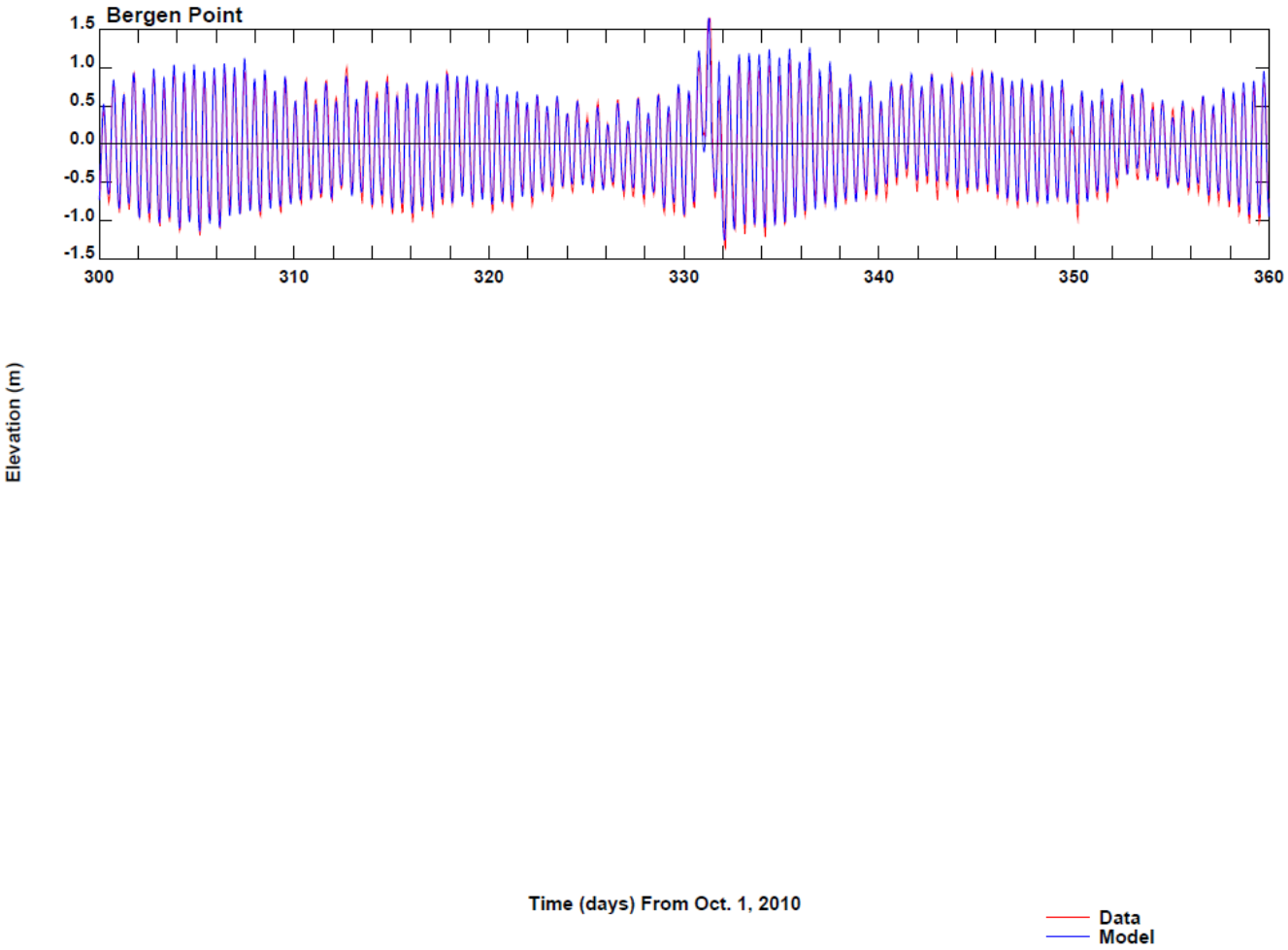

Figure 3-15. Hourly water elevation model and measurement comparisons results. Modeled and measured results presented between days 330 and 334 show relatively higher water elevations during Hurricane Irene and the sharp gradient rapid decline.

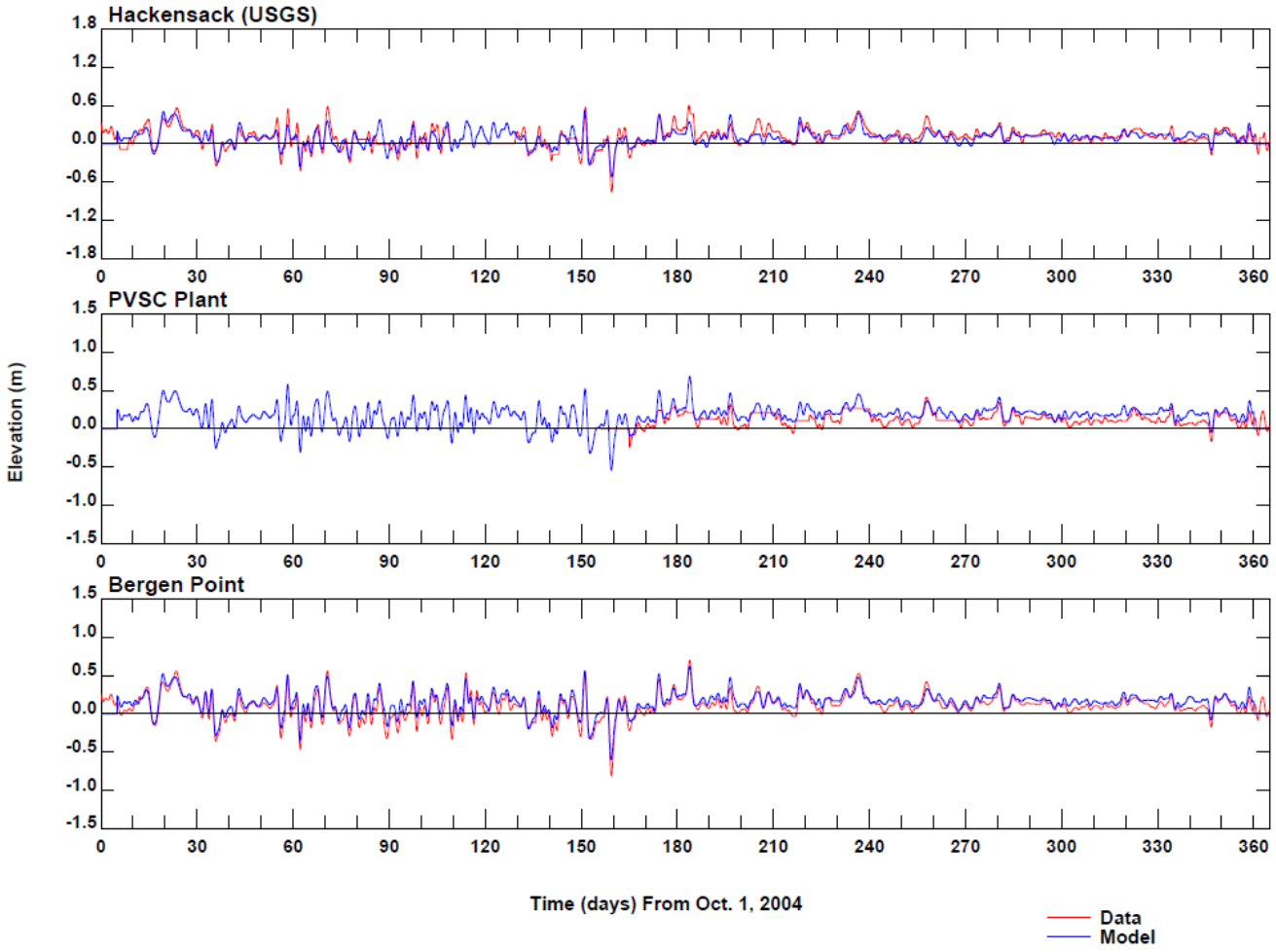

Figure 3-16. Hourly water elevation model and measurement comparisons results after application of a 35-hour low pass filter removing diurnal and semi-diurnal tidal components. Modeled and measured results are presented for the 2004-05 water year at three locations in the Newark Bay complex.

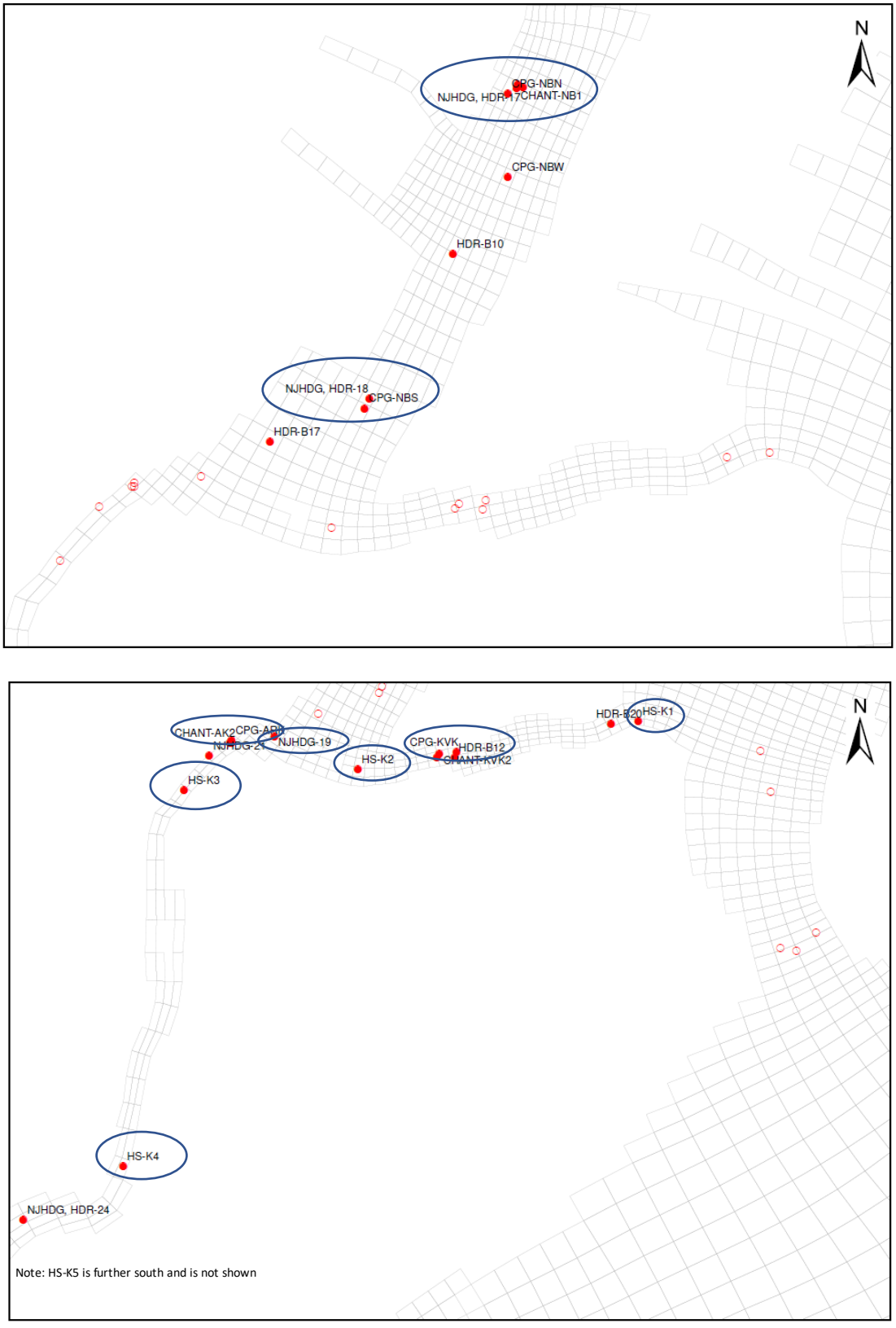

Figure 3-17. Locations of salinity model and measurement comparisons shown on Figures 3-18 to 3-21 and in Appendix 5.

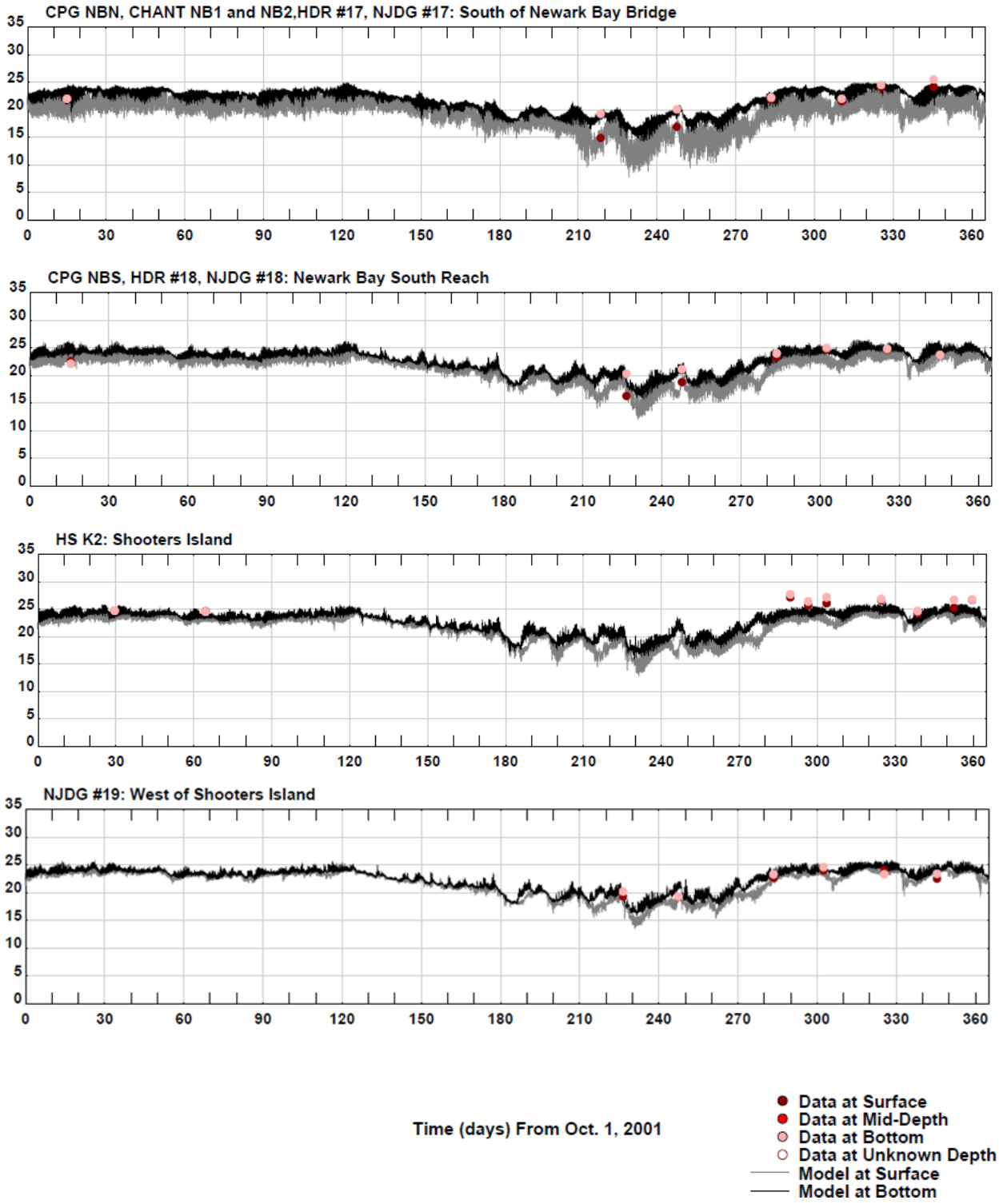

Figure 3-18. Salinity (psu) model and measurement comparisons results during Harbor deepening projects. Modeled and measured results are presented for the 2001-02 water year at four locations in Newark Bay and the Kill van Kull.

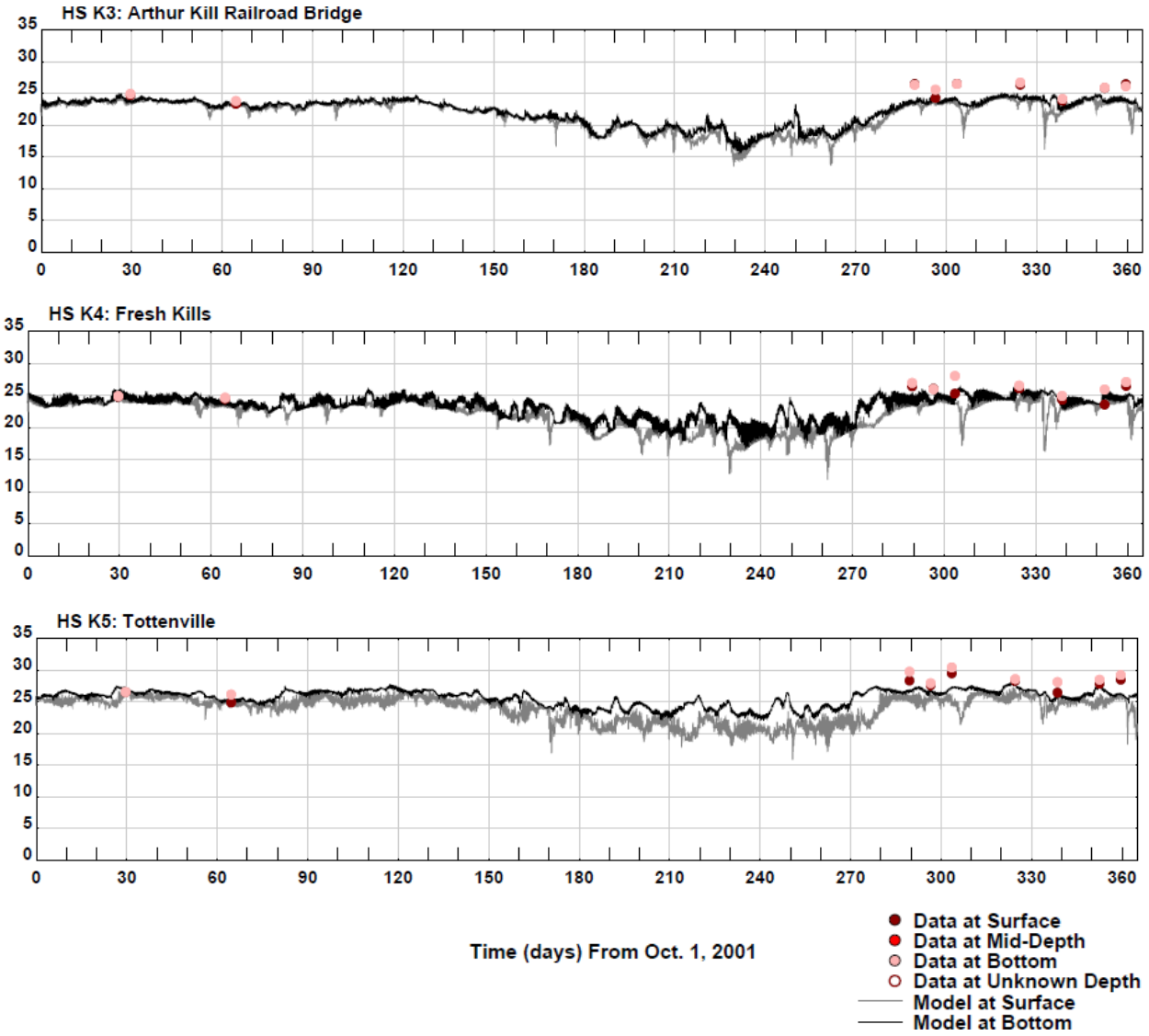

Figure 3-19. Salinity (psu) model and measurement comparisons results during Harbor deepening projects. Modeled and measured results are presented for the 2001-02 water year at three locations in the Arthur Kill.

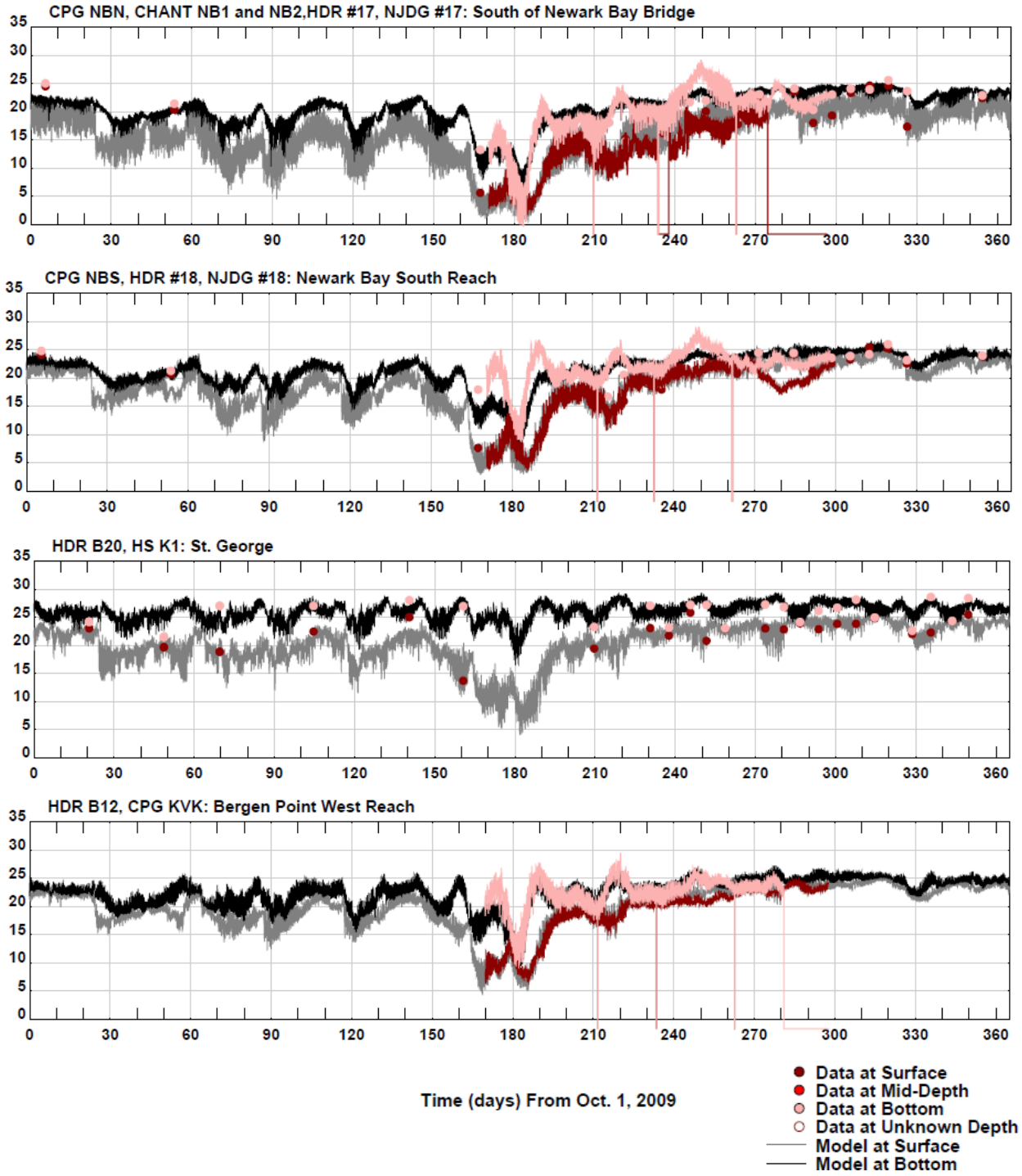

Figure 3-20. Salinity (psu) model and measurement comparisons results for the 2009-10 water year at four locations in Newark Bay and the Kill van Kull.

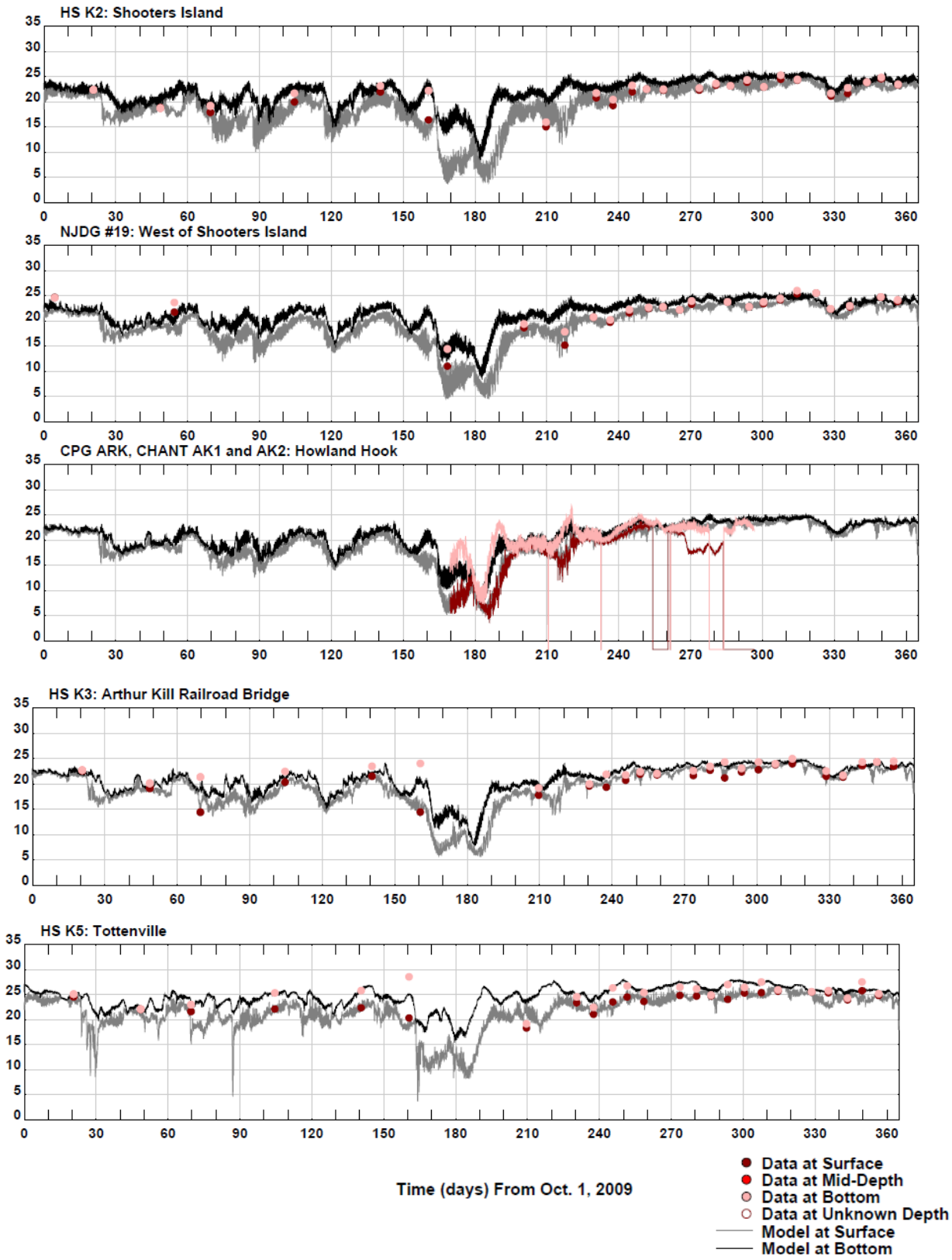

Figure 3-21. Salinity (psu) model and measurement comparisons results presented for the 2009-10 water year at two locations in the Kill van Kull and three locations in the Arthur Kill.

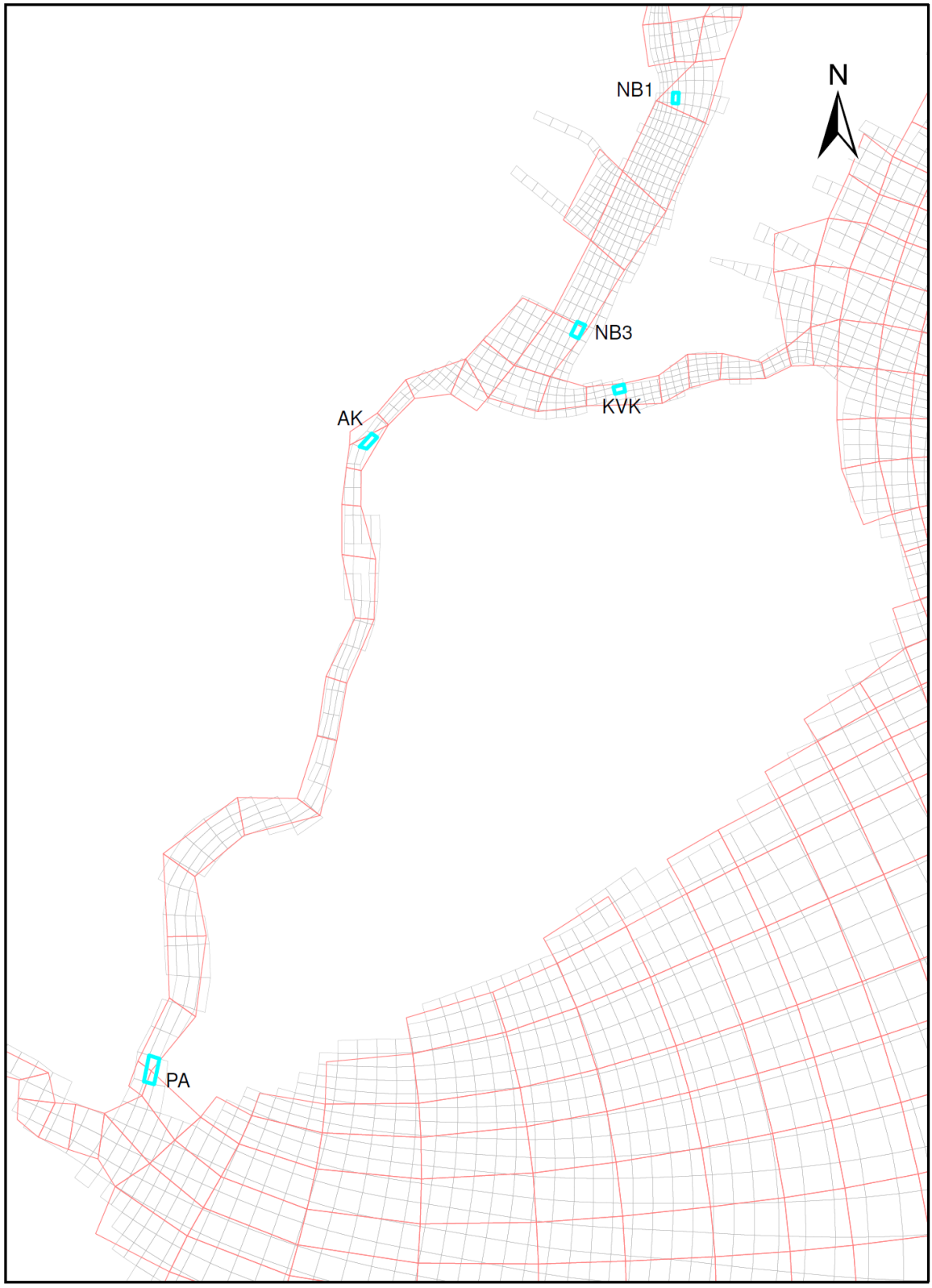

Figure 3-22. Locations (blue) of velocity currents model and measurement comparisons for 2000-02 water years imposed on 127 x 205 (grey) and 42 x 84 (red) CARP model computational grids.

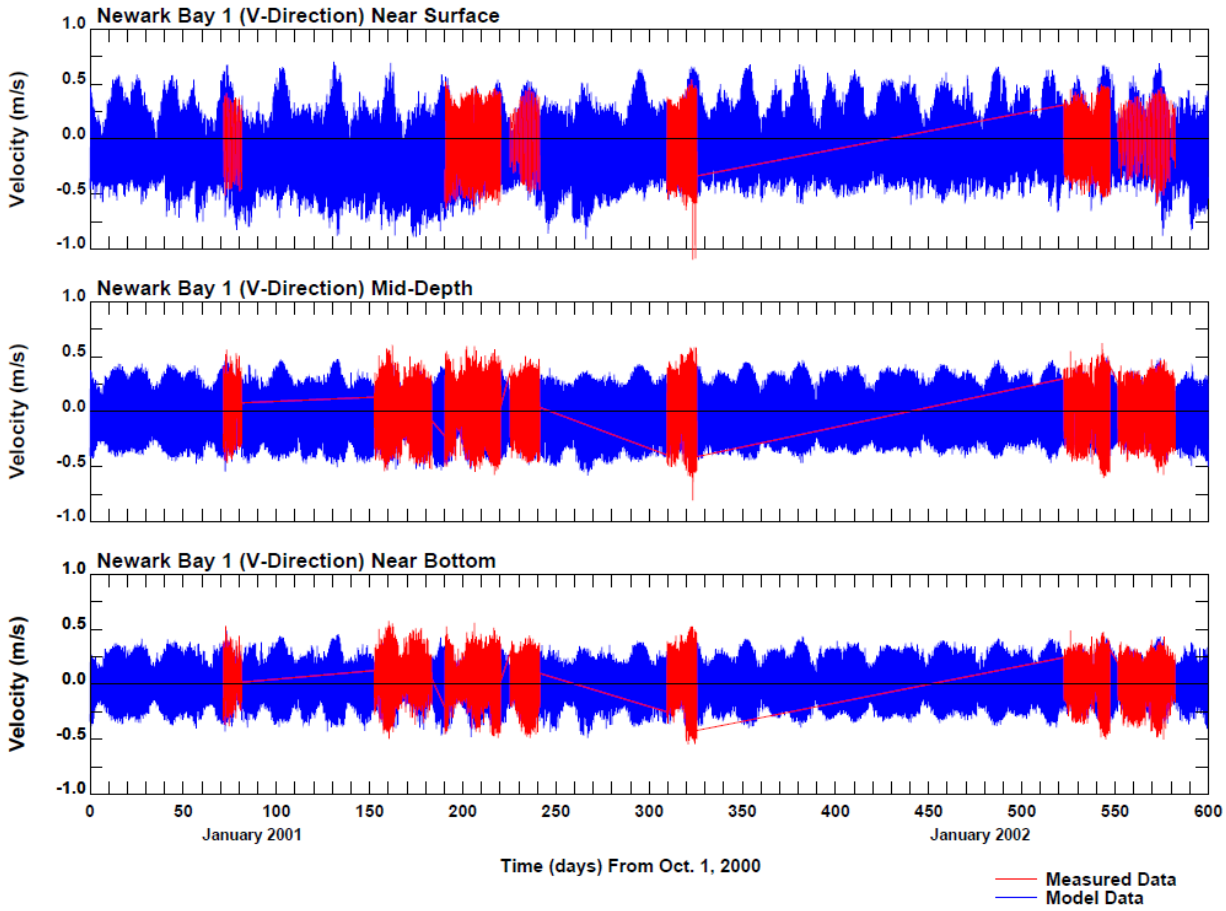

Figure 3-23. Velocity currents model and measurement comparisons for full 2000-02 water years, Station NB-1 longitudinal north/south example.

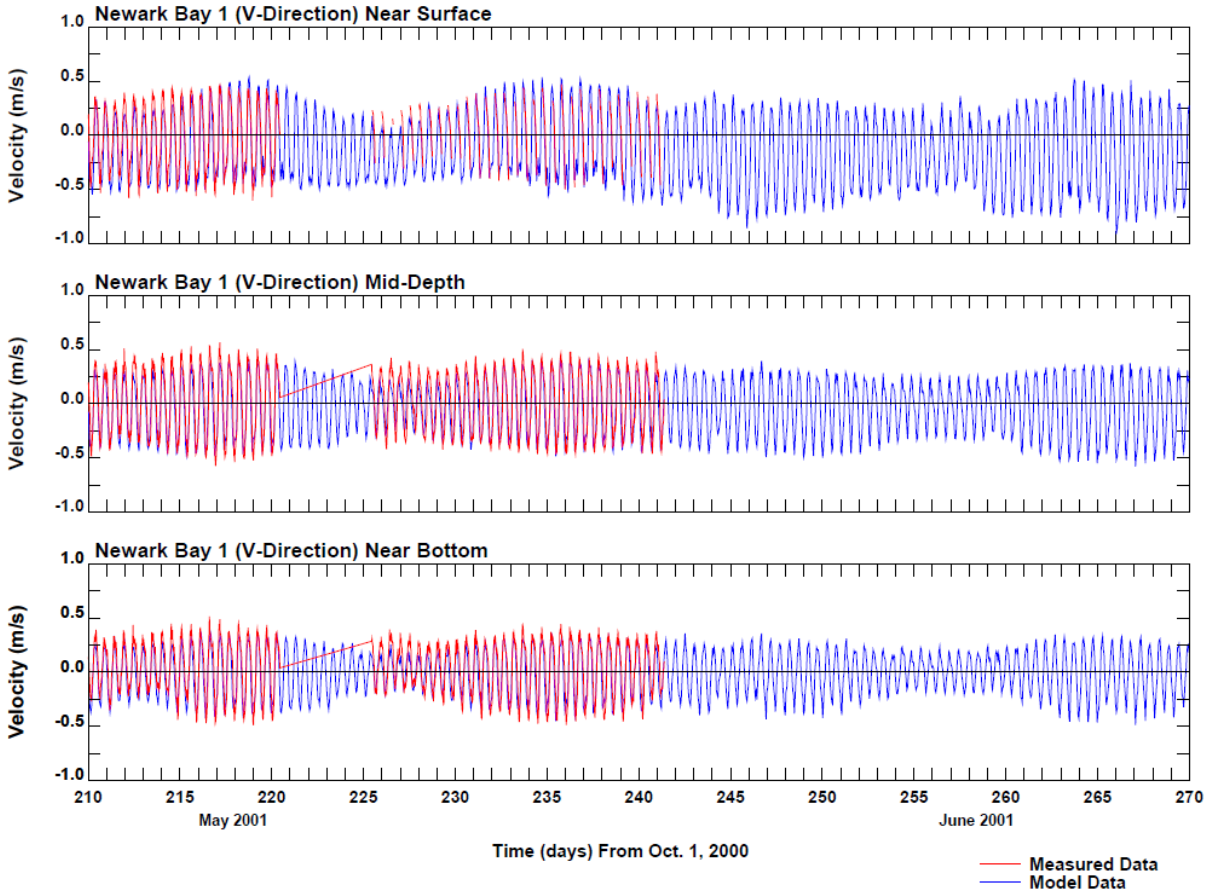

Figure 3- 24. Velocity currents model and measurement comparisons for a portion of the 2000-02 water years, Station NB-1 longitudinal north/south example.

Figure 3-25. Locations of velocity currents model and measurement comparisons for 2007-09 water years imposed on 127 x 205 CARP model computational grid.

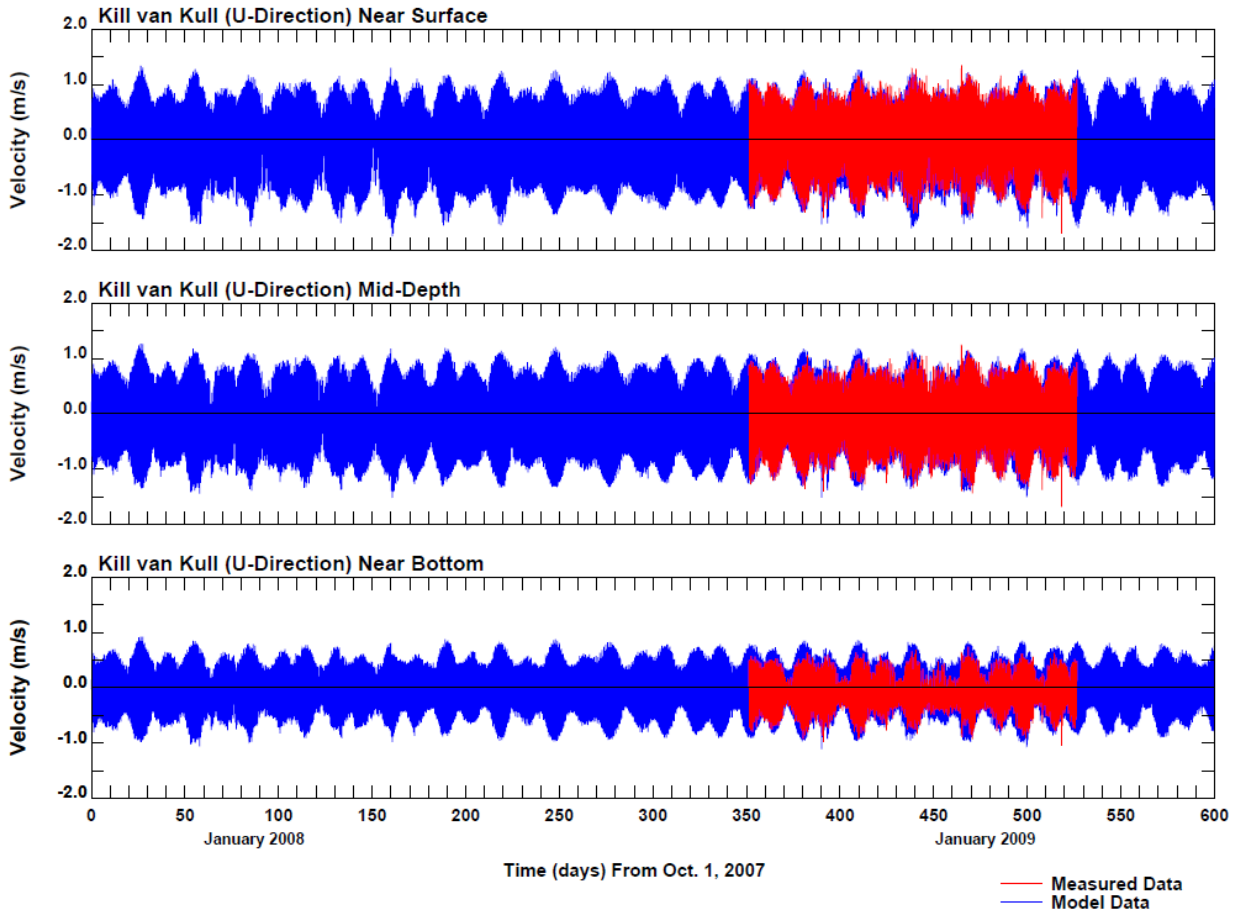

Figure 3-26. Velocity currents model and measurement comparisons for full 2007-09 water years, Station HRF_KVK2, lateral east/west example.

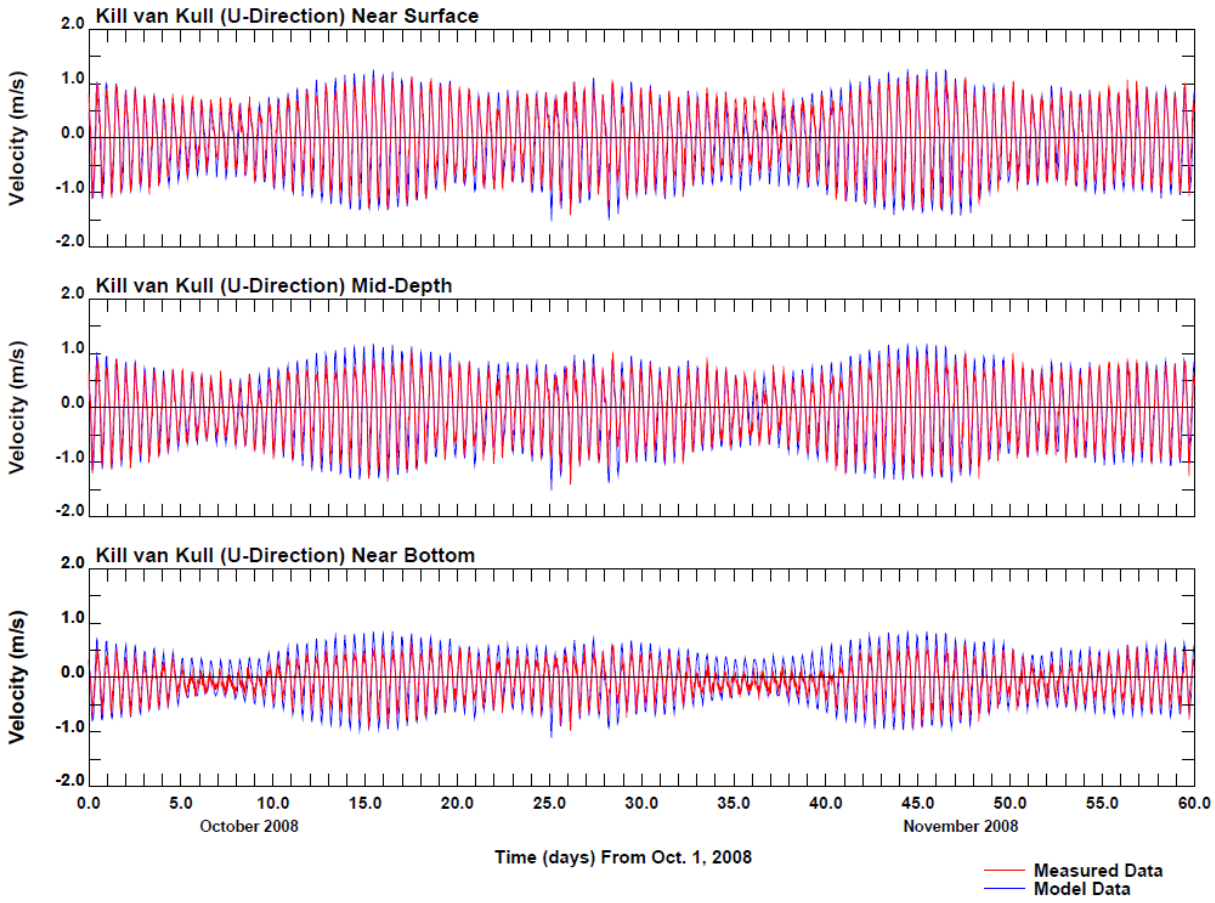

Figure 3-27. Velocity currents model and measurement comparisons for a portion of the 2007-09 water years, Station HRF_KVK2 lateral east/west example.

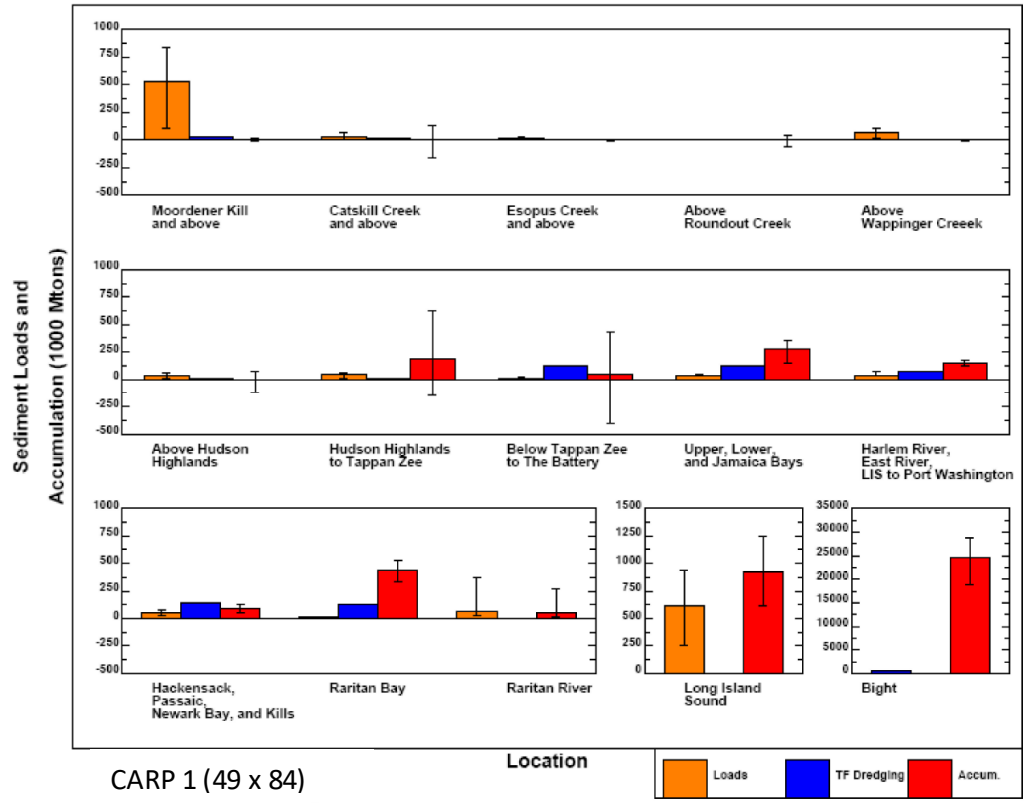

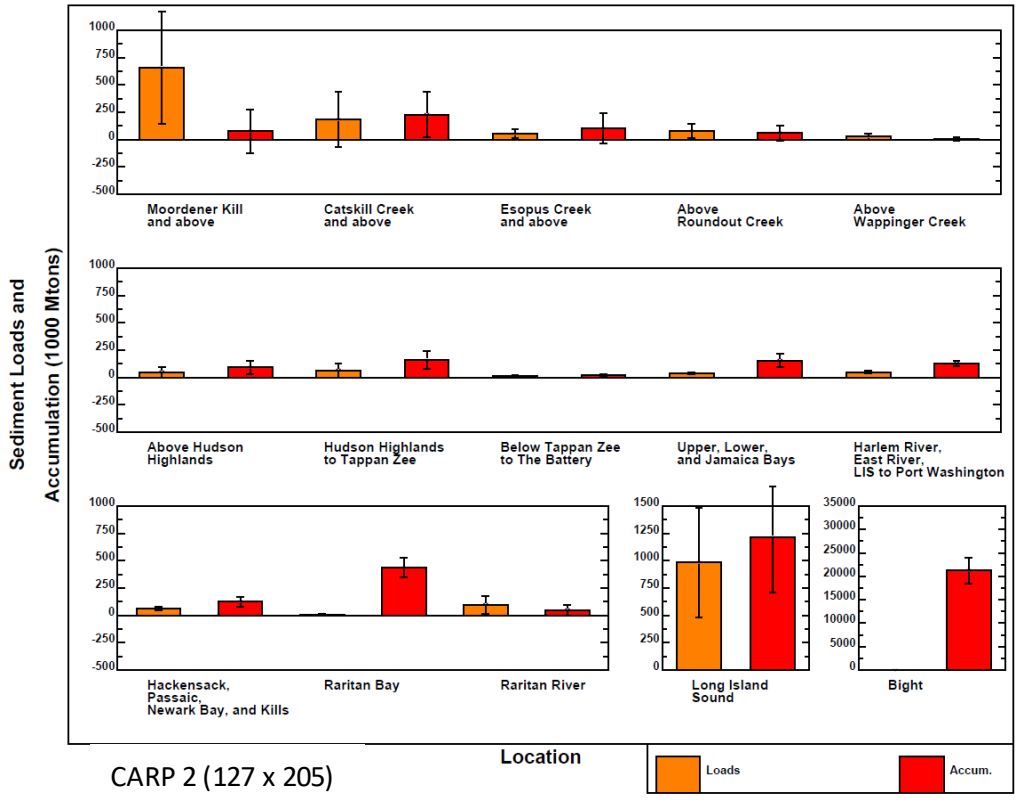

Figure 3-28. Regional annual average external solids loadings (gold bars) and bed accumulation results (red bars) for CARP 1 (top) 49 x 84 and CARP 2 (bottom) 127 x 205 sediment transport and organic carbon production models.

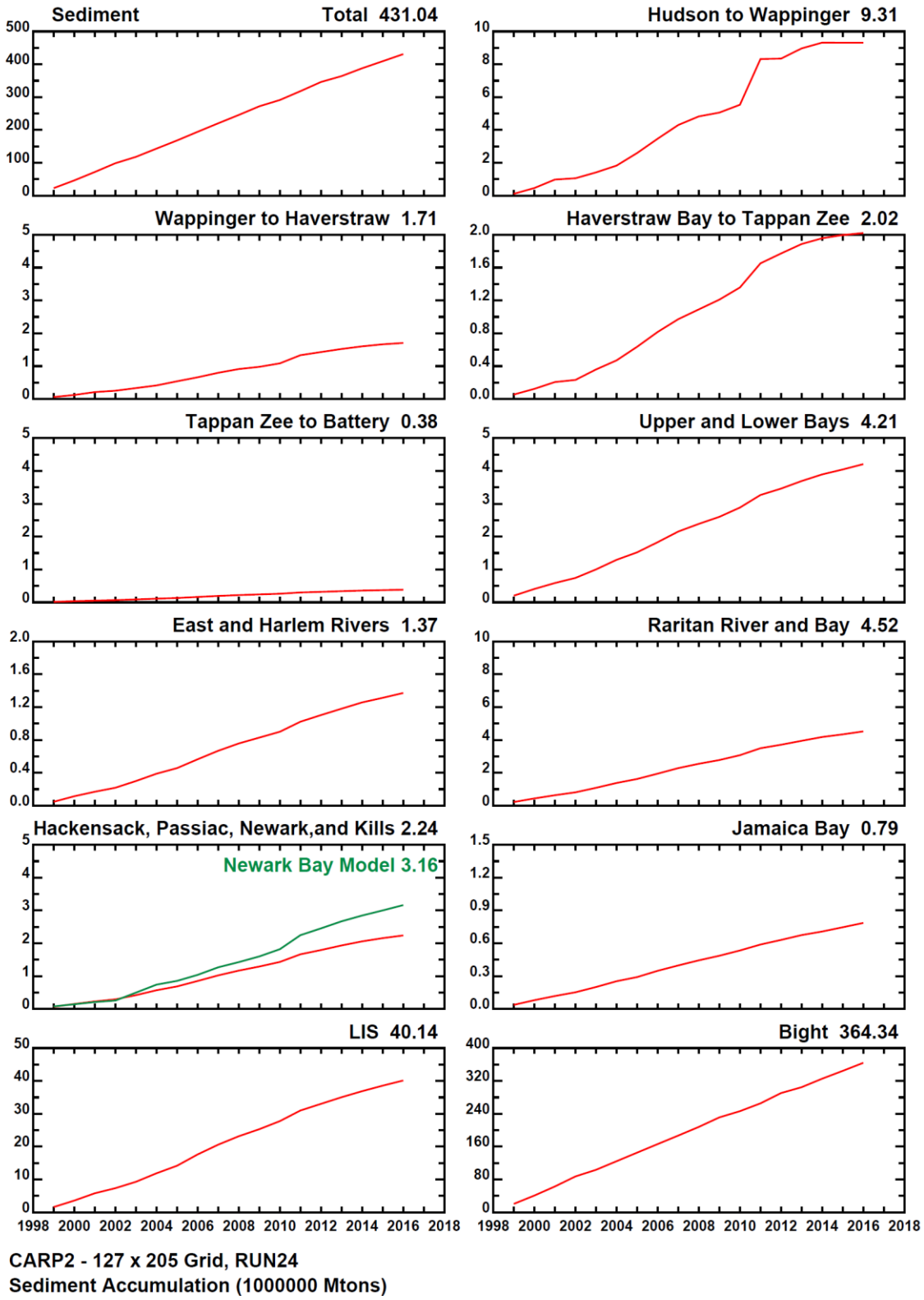

Figure 3-29. Regional bed accumulation time series results for CARP 127 x 205 sediment transport and organic carbon production model for each water year cumulatively with comparison to draft (i.e., under development, not final, subject to change) Newark Bay Superfund sediment transport model results.

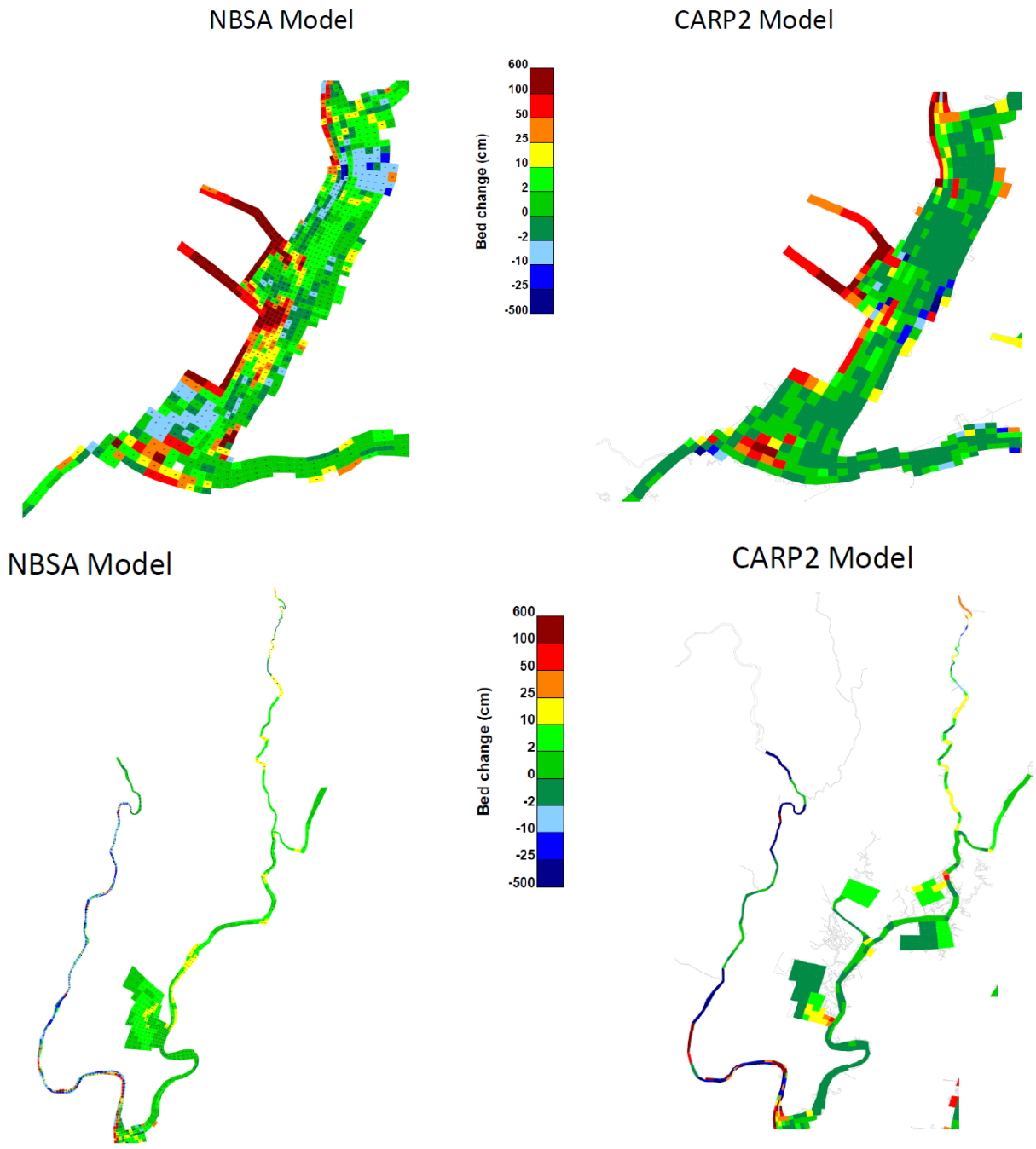

Figure 3-30. Bed accumulation spatial results by model grid cells for CARP 127 x 205 and draft (i.e., under development, not final, subject to change) Newark Bay Superfund sediment transport models for Newark Bay (top row) and the Lower Passaic and Hackensack Rivers (bottom row). Results are cumulative for the fourteen waters years October 1, 1998, to September 30, 2012.

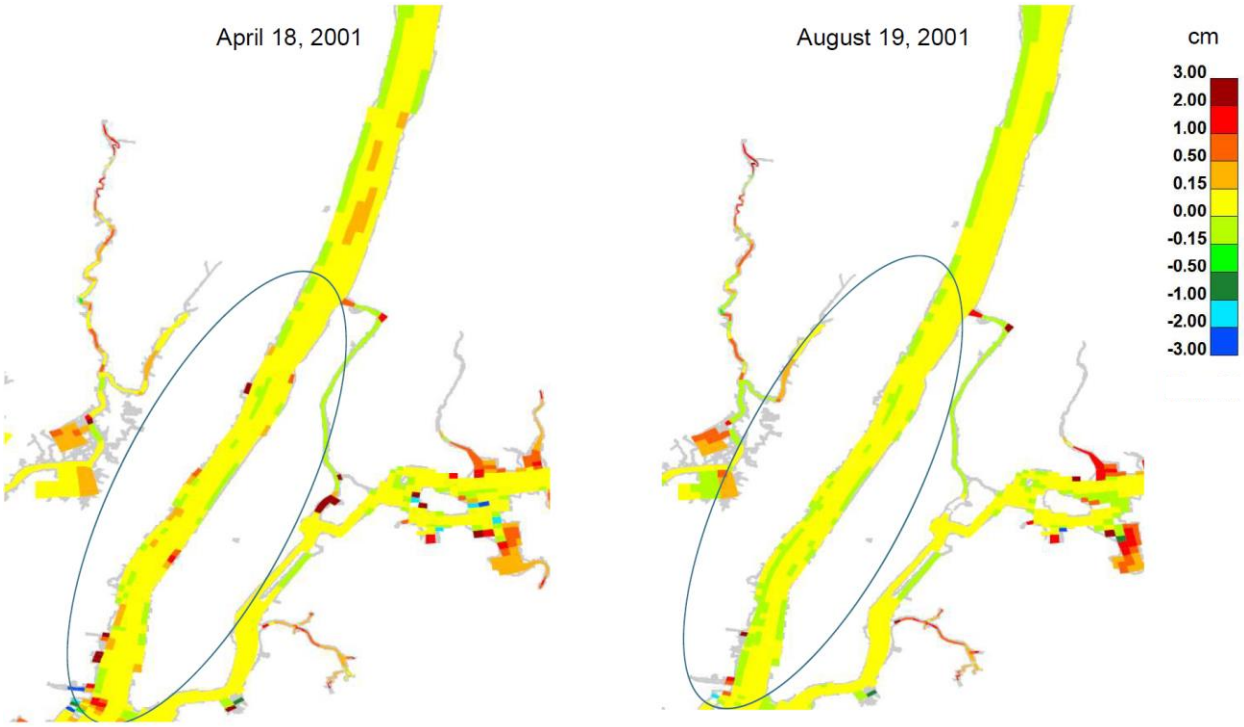

Figure 3-31. CARP 127 x 205 model computational grid sediment transport model results for bed accumulation. Elevated bed accumulation results are shown in shades of orange and red along shorelines opposite Manhattan (i.e., circled area) for April 2001 in the left image. Bed accumulation results for August 2001 shown in the right image were not similarly elevated. The CARP sediment transport model results for bed accumulation are indicative of temporary storage of solids in April 2001 that are no longer present in August 2001.

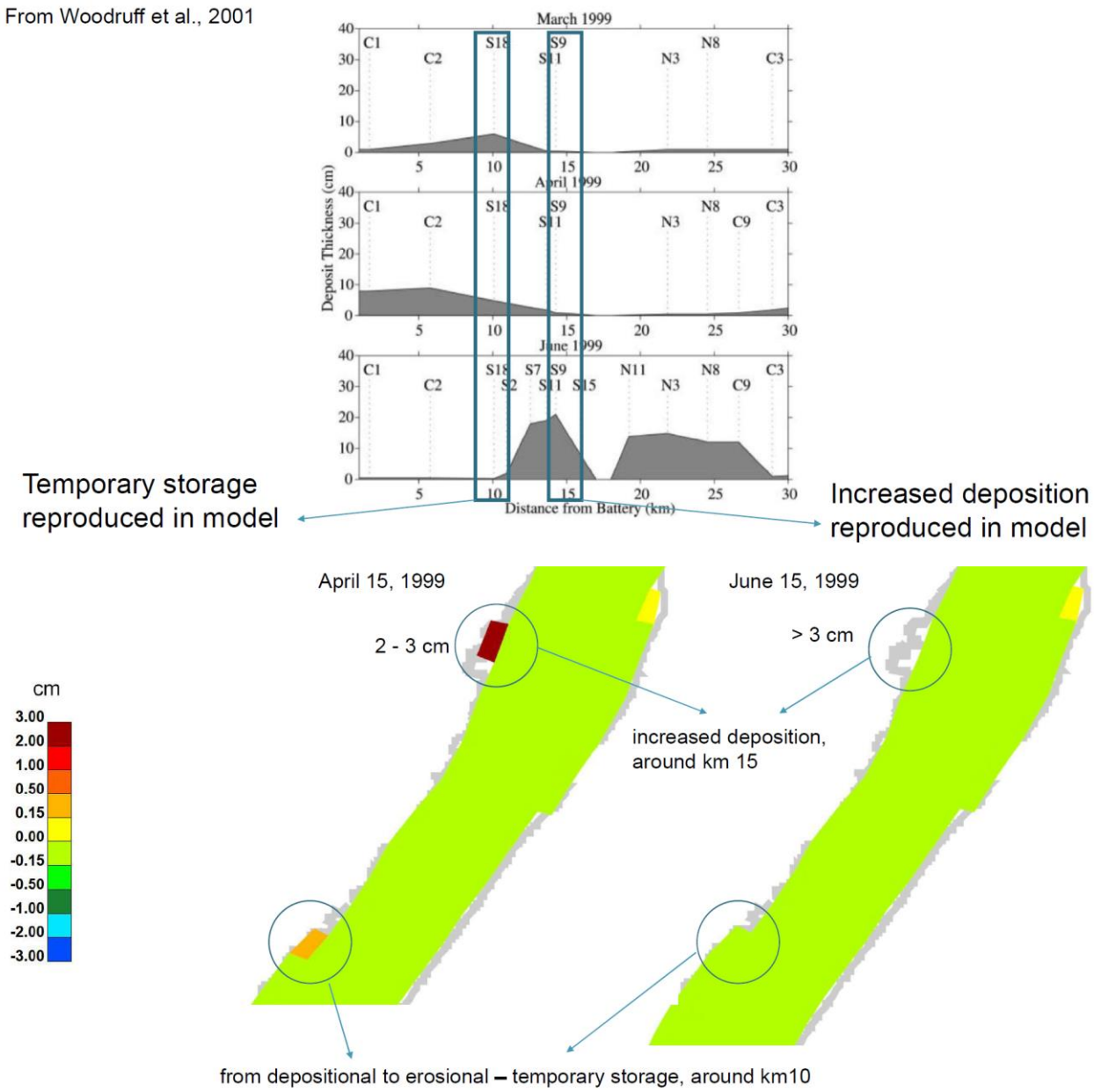

Figure 3-32. CARP 127 x 205 model computational grid sediment transport model results for bed accumulation (bottom panel). Between April 15 and June 15, 1999, the model calculates a transition from depositional to erosional near Hudson River km 10 shoreline (gold to lime) and an increase in deposition around km 15 shoreline (brick to clear), a trend consistent with the observations of Woodruff et al., 2001 (top panel). Note that the CARP 127 x 205 model is not producing the same magnitude of accumulation or spatial extent in the western channel as estimated in Woodruff et al., 2001 from visual inspections of depth of olive brown sediments in three 11-cm-wide cores, S18, S9, and S11, in the vicinity of km 10 and km 14.

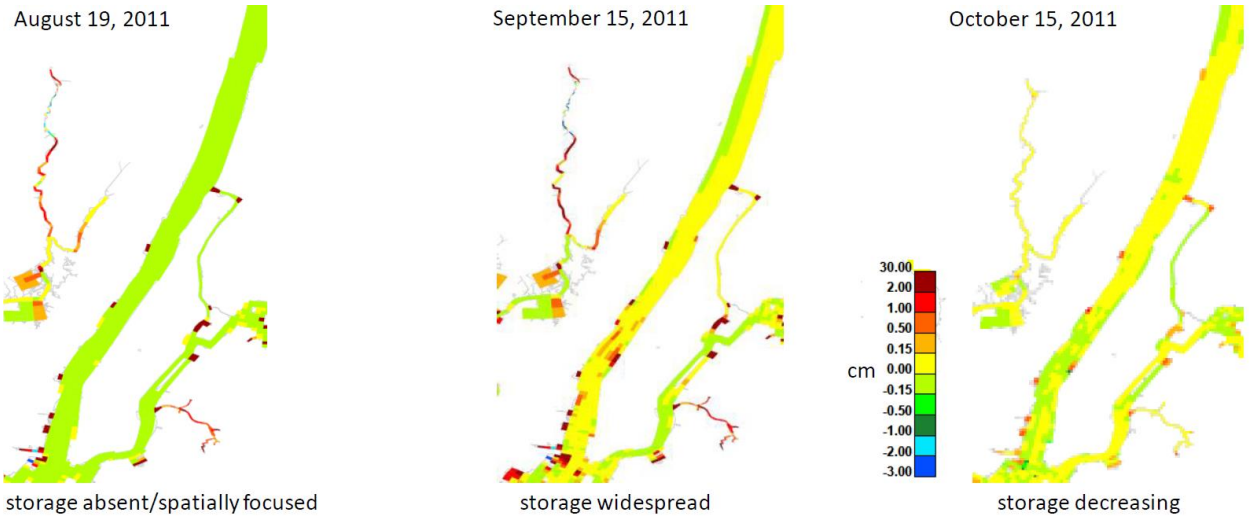

Figure 3-33. CARP 127 x 205 model computational grid sediment transport model results for bed accumulation in the Hudson River near Manhattan. Between August 19 and September 15, 2011, the model calculates a transition from slight erosion (light green) in broad areas to deposition (yellow to red) in response to Hurricanes Irene and Lee. By October 15, 2011, the model calculates less bed accumulation as temporary storage erodes.

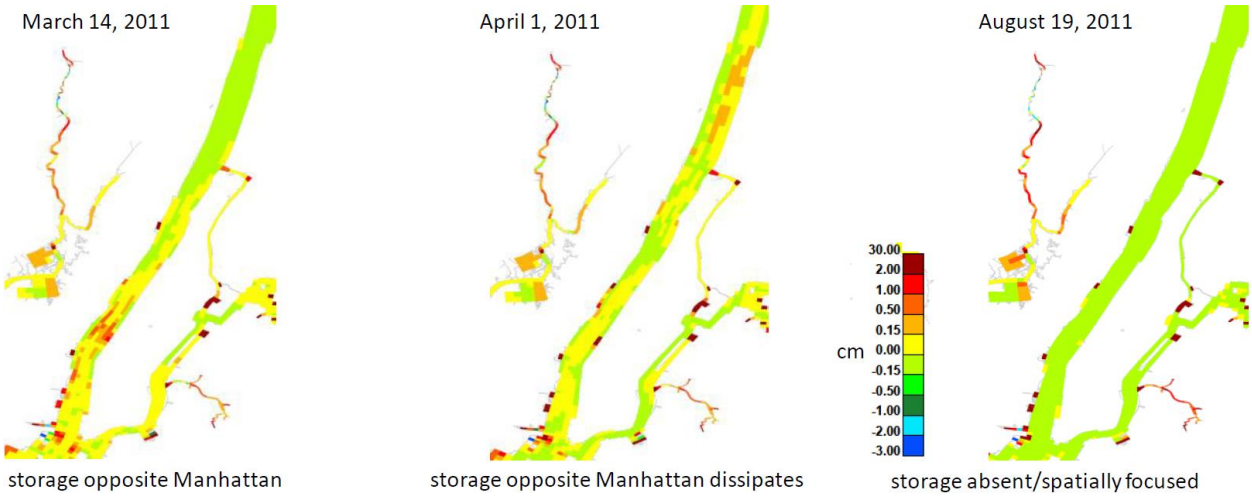

Figure 3-34. CARP 127 x 205 model computational grid sediment transport model results for bed accumulation in the Hudson River near Manhattan for spring and summer conditions. For March 14, 2011, the model calculates bed accumulation opposite Manhattan (yellow, orange, red). For April 1, 2011, the calculated bed accumulation is reduced in the main channel opposite Manhattan, intensifies along shorelines opposite Manhattan, and increases further upstream in the Hudson River. By August 19, 2011, the model calculates widespread erosion and bed accumulation only in shoreline areas opposite Manhattan.

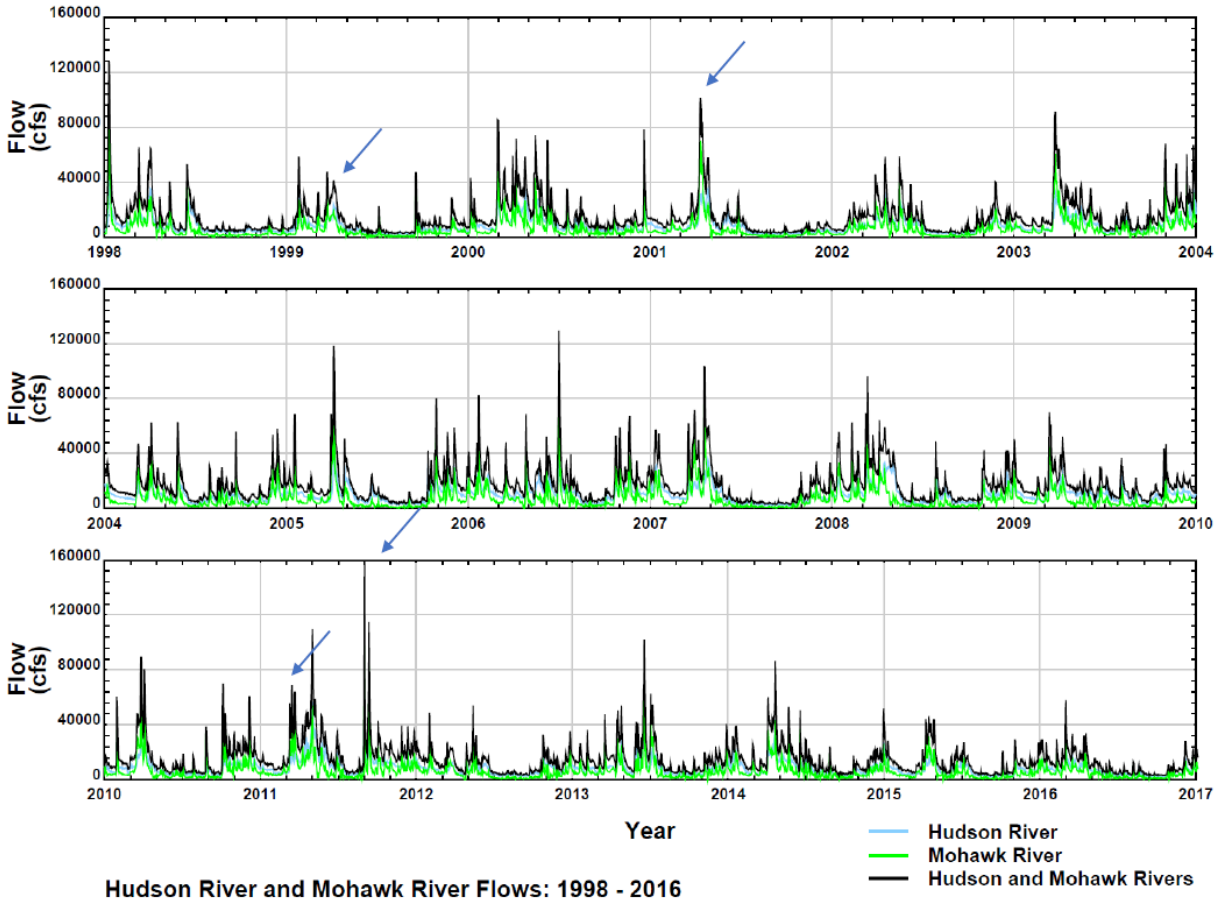

Figure 3-35. Hudson River hydrograph below the confluence with the Mohawk River. Blue arrows indicate the April 18, 2001, event analyzed for CARP 1; the March/April 1999 events considered by Woodruff et al., 2001; Hurricanes Irene and Lee in late summer 2011; and a spring storm in March 2011.

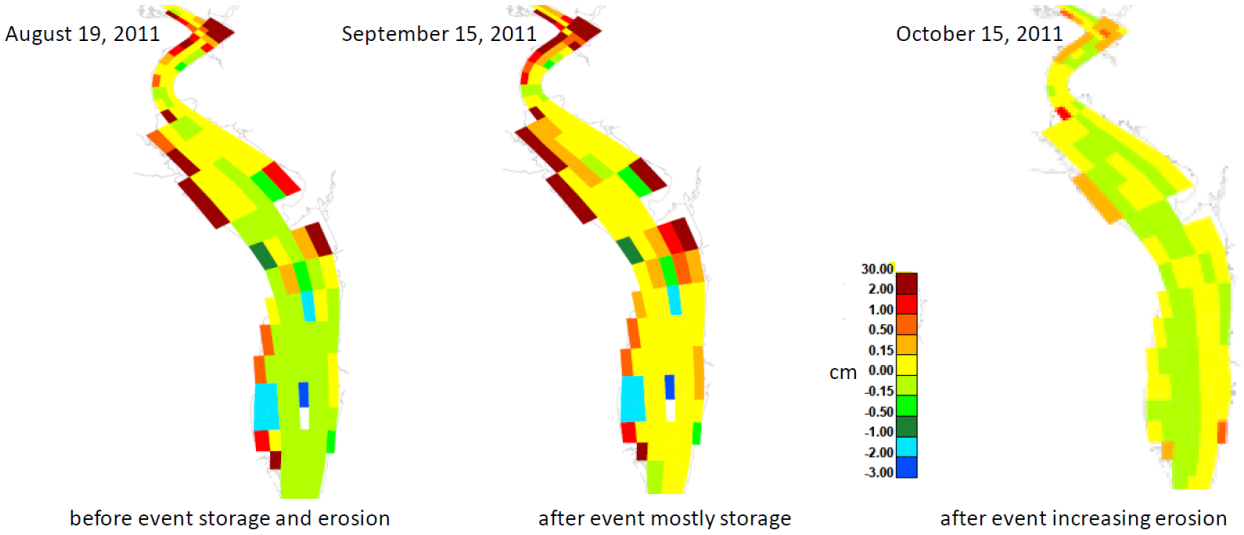

Figure 3-36. CARP 127 x 205 model computational grid sediment transport model results for bed accumulation in the Hudson River in Haverstraw Bay. Between August 19 and September 15, 2011, the model calculates a transition to greater accumulation and temporary storage in response to Hurricanes Irene and Lee. By October 15, 2011, the model calculates less bed accumulation as much of the storm-associated temporary storage has eroded.

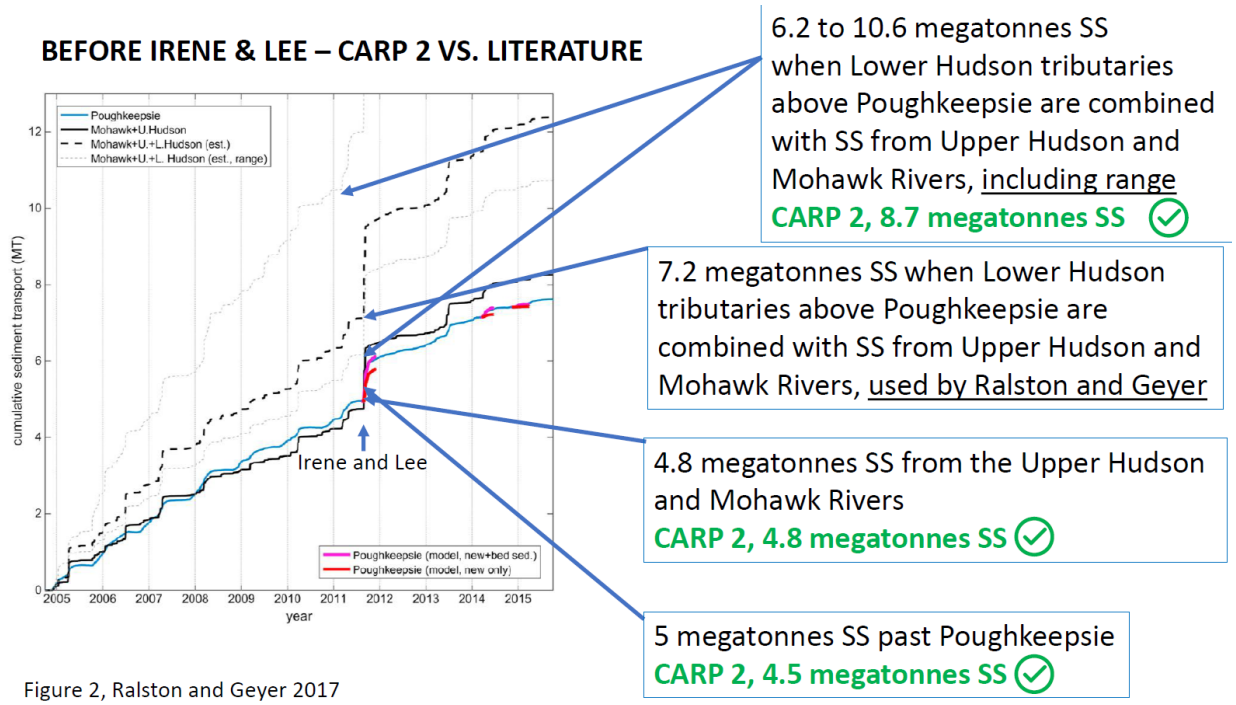

Figure 2, Ralston and Geyer 2017

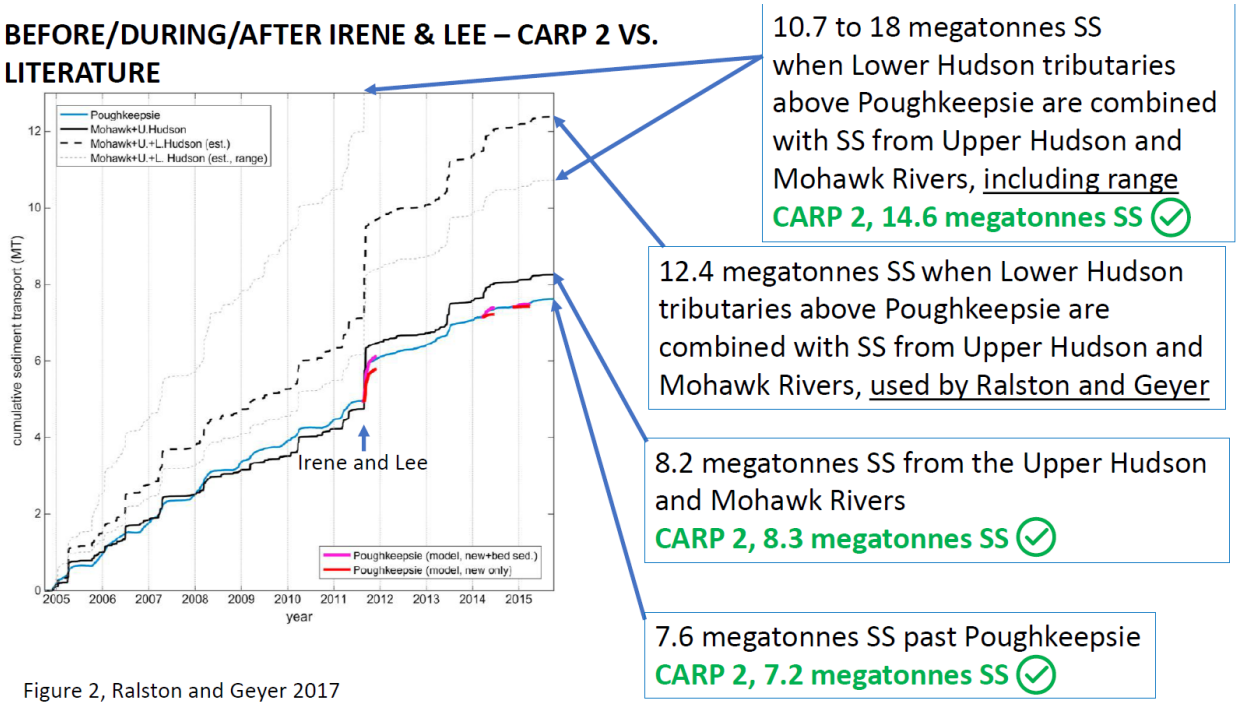

Figure 2, Ralston and Geyer 2017

Figure 3- 37. CARP results (green typeface text) for suspended sediment loadings from the Upper Hudson and Mohawk Rivers and the tributaries above Poughkeepsie and the flux of suspended sediment passing downstream of Poughkeepsie. The CARP results are compared to the results of Ralston and Geyer, 2017 (black typeface text and diagrams). The two sets of results are for before (upper panel) and for before, during, and after (lower panel) Hurricanes Irene and Lee.

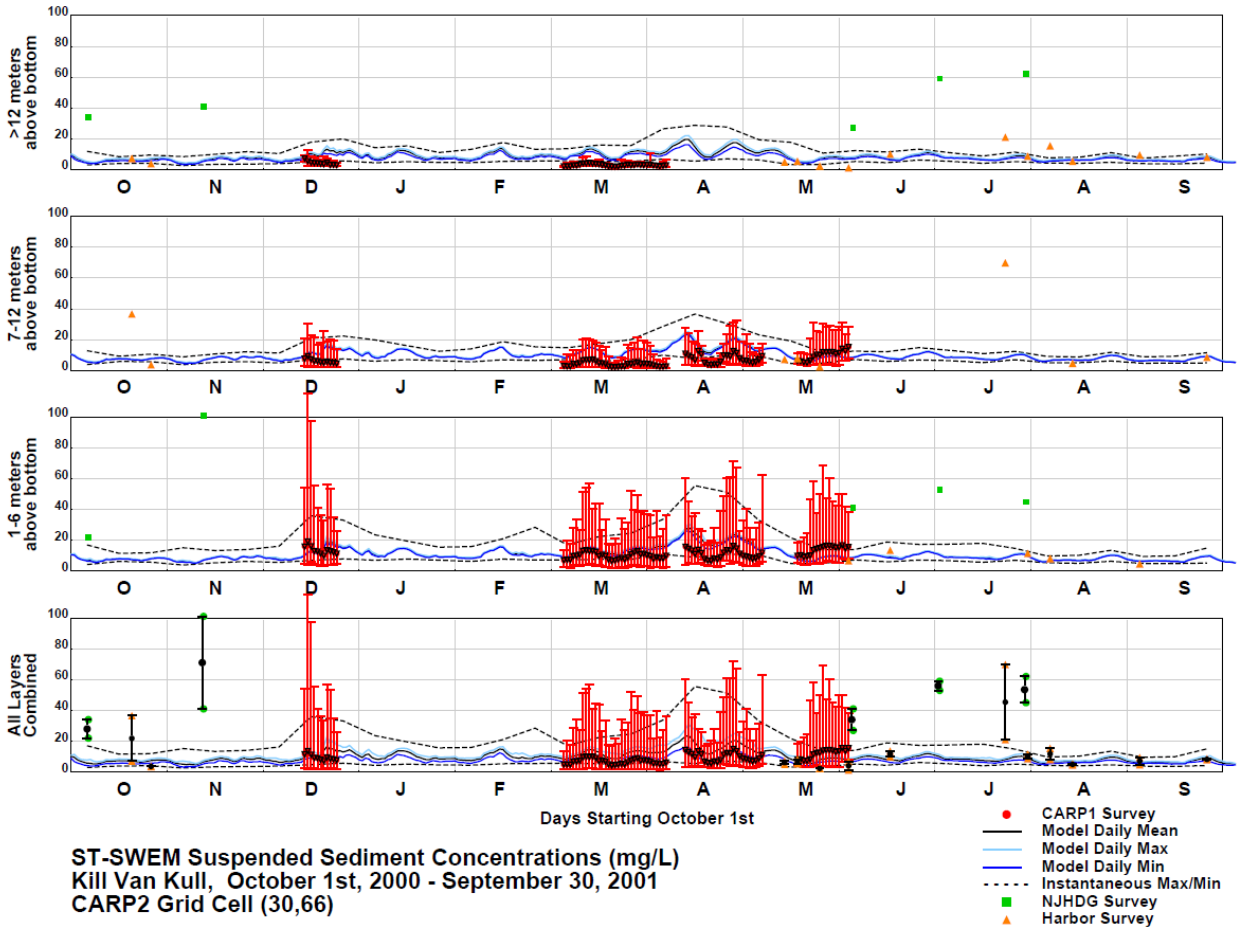

Figure 3-38. Suspended sediment concentrations model and measurement comparison results, Kill van Kull, 2000-01 water year. Estimates of suspended sediment concentrations from acoustic backscatter (red bars) generally agree with model results (solid and dashed lines) magnitude but have a larger range and somewhat lower central tendency. The Harbor Survey (orange triangles) and NJHDG measurements (green squares) do not agree with each other and were mostly not collected at the same time as acoustic backscatter measurements. The model results agree better with the Harbor Survey measurements than the NJHDG measurements for this location/water year.

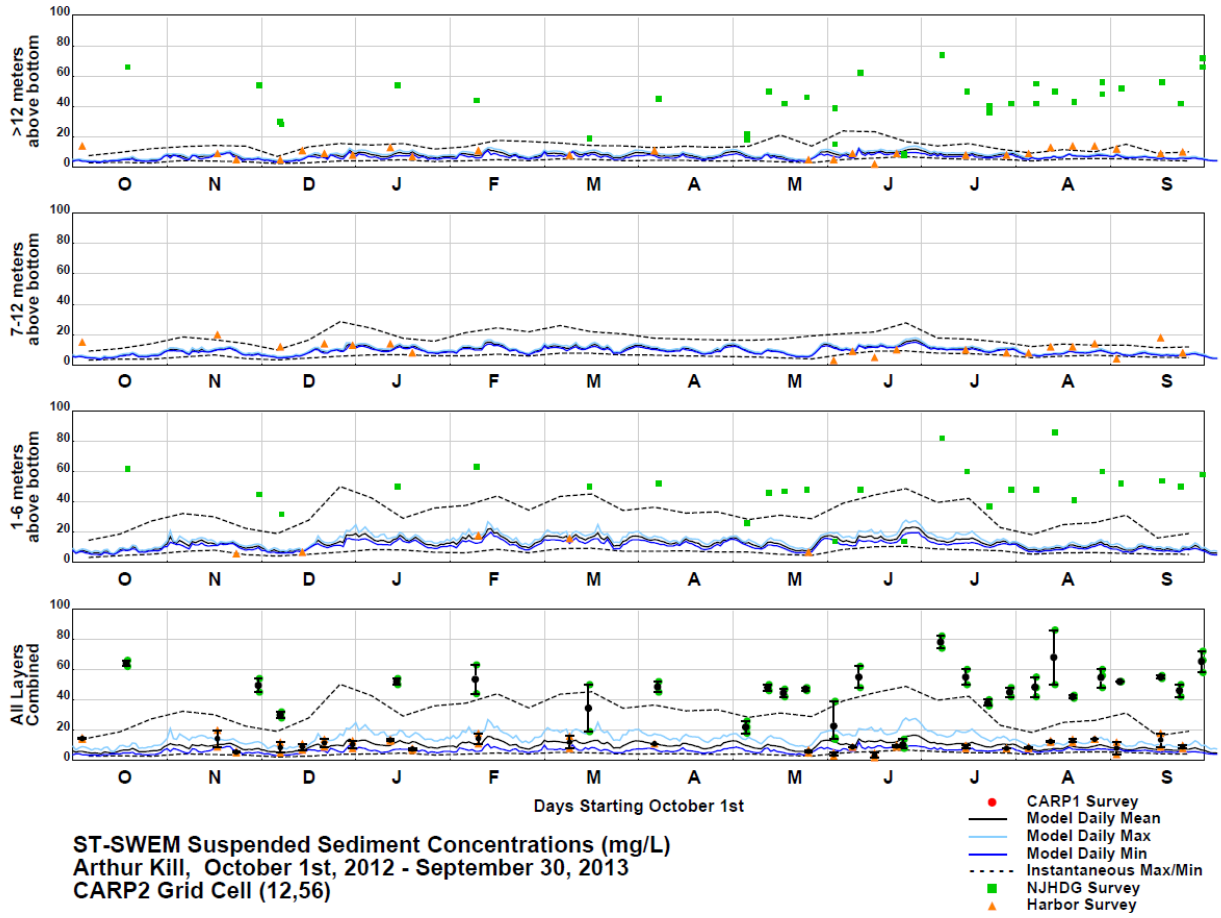

Figure 3-39. Suspended sediment concentrations model and measurement comparison results, Arthur Kill, 2012-13 water year. The Harbor Survey (orange triangles) and NJHDG measurements (green squares) do not agree. The model results (solid and dashed lines) agree with the Harbor Survey measurements for this location/water year.

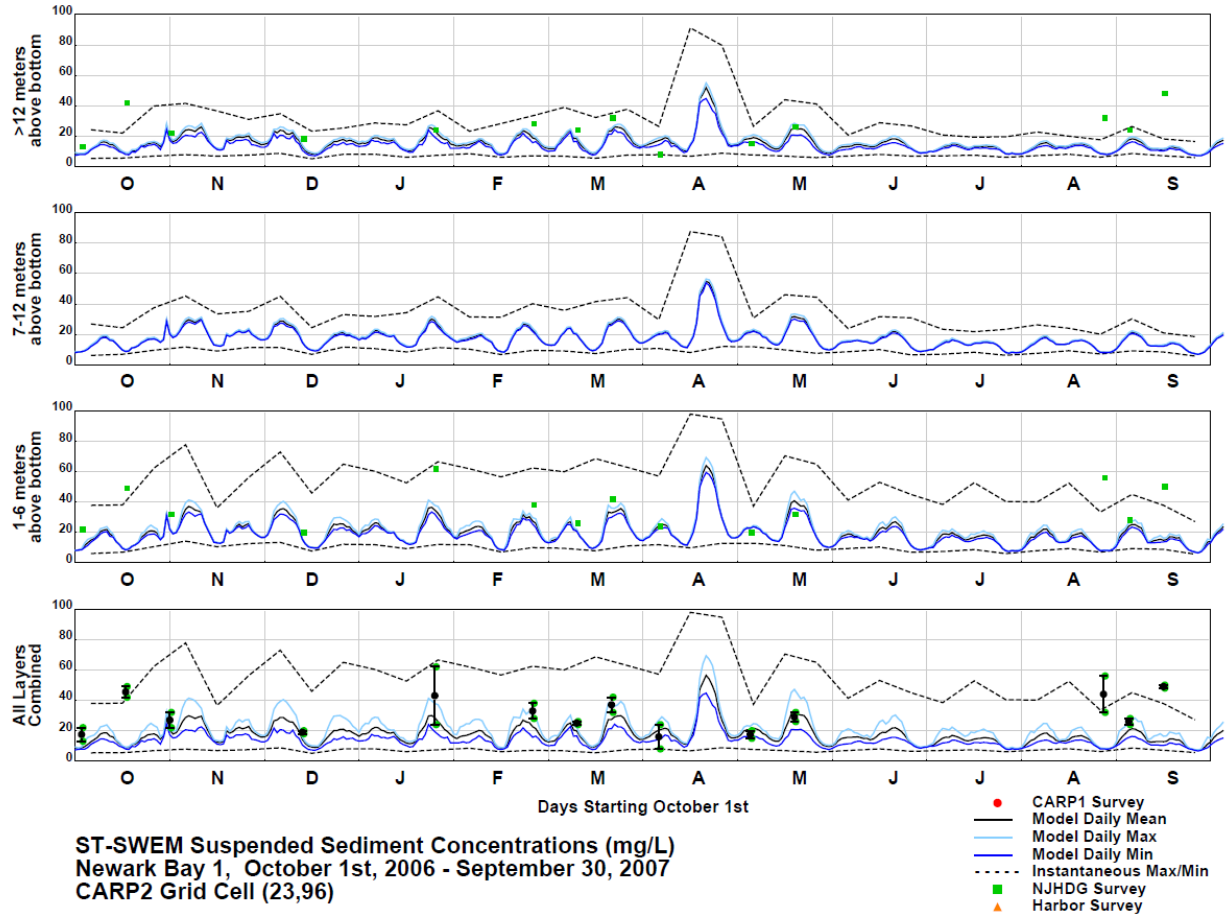

Figure 3-40. Suspended sediment concentrations model and measurement comparison results, Newark Bay, 2006-07 water year. The range of model results (dashed lines) capture the NJHDG grab sample measurements (green squares) very well near surface and near bottom for this location/water year and the model central tendency (solid lines) tracks the central tendency of the measurements over depth (bottom panel).

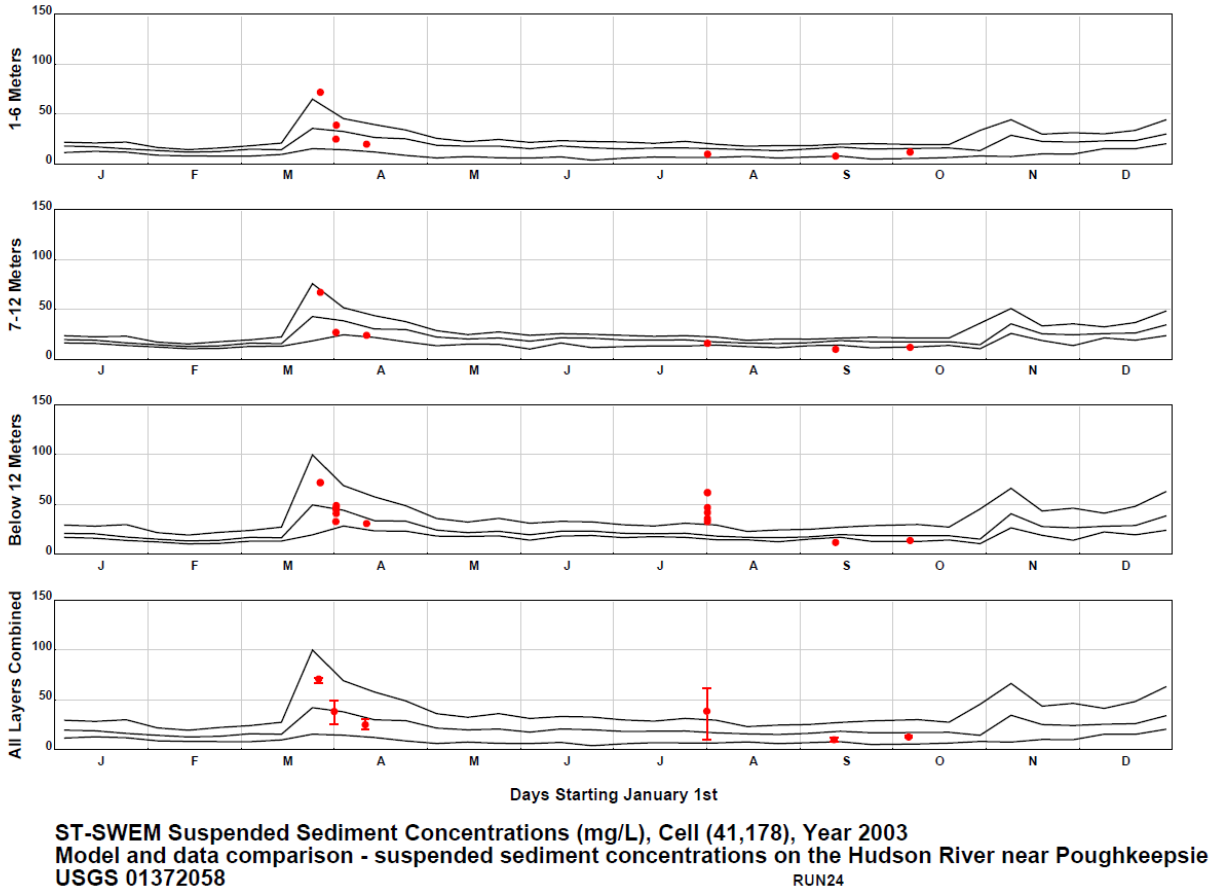

Figure 3- 41. Suspended sediment concentrations model and measurement comparison results, Hudson River at Poughkeepsie, 2003. The range of model results (instantaneous maxima and minima every 10 days and 10-day averages) generally captures the range in USGS grab sample measurements (red circles) especially when all depth layers are combined, including elevated concentrations in March 2003.

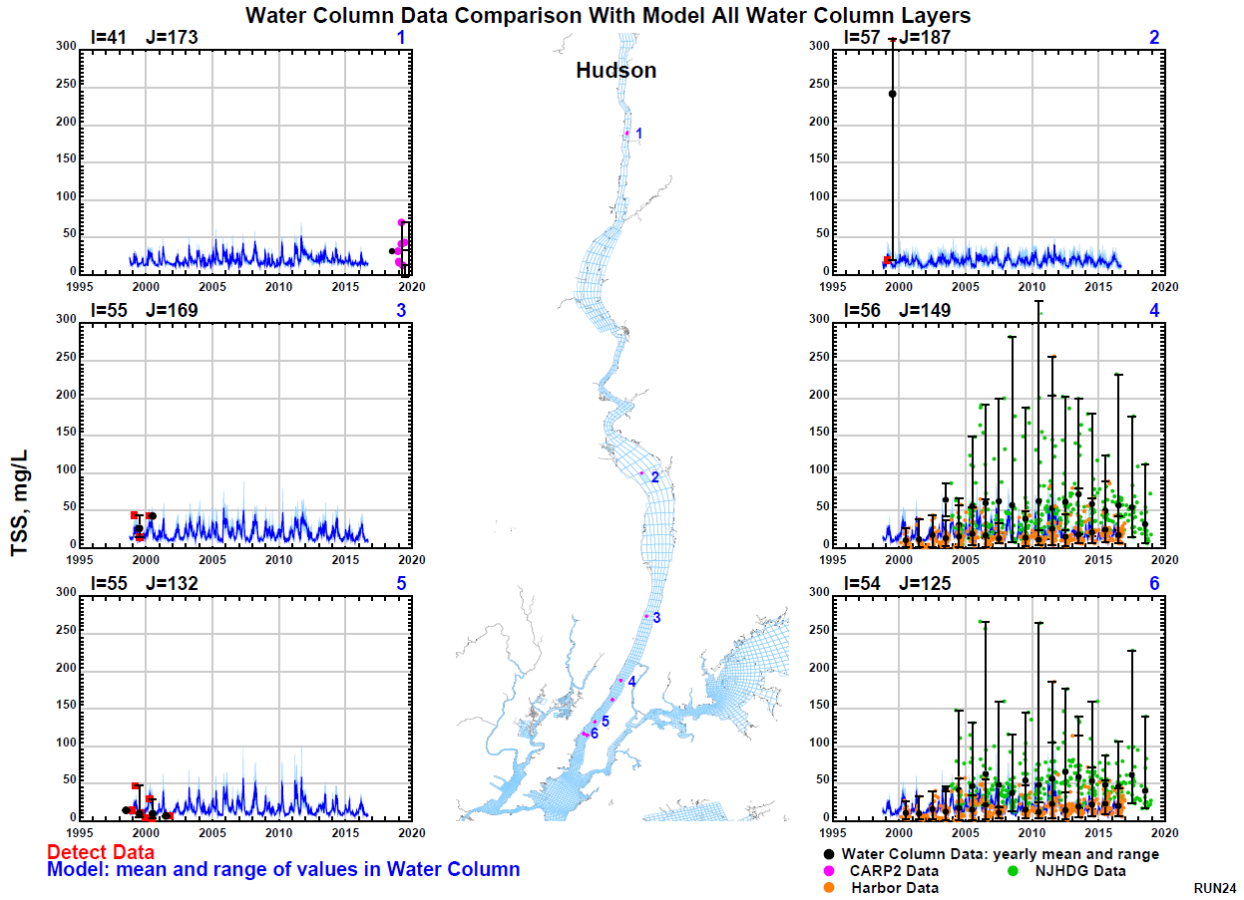

Figure 3-42. Suspended sediment concentrations model and measurement comparison results for six locations in the Hudson River. The model results (blue lines) compare well to CARP 1 (1998-2001, red squares), CARP 2 (2019, pink circles), and NYCDEP Harbor survey (multiple years, orange circles) measurements with underpredictions compared to NJHDG measurements (multiple years, green circles) which may not be correct.

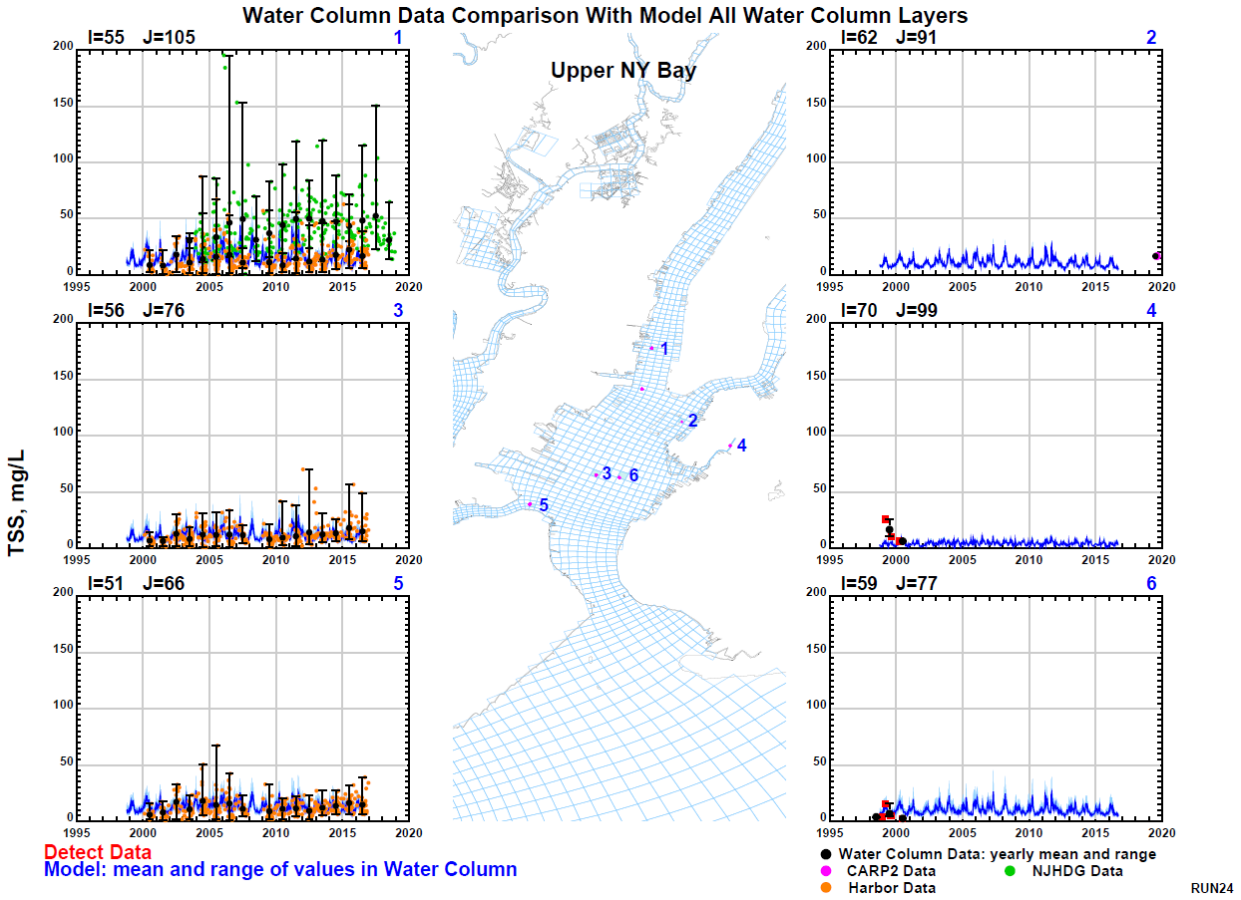

Figure 3- 43. Suspended sediment concentrations model and measurement comparison results for six locations in Upper NY Bay. The model results (blue lines) compare well to CARP 1 (1998-2000, red squares), CARP 2 (2019, pink circles), and NYCDEP Harbor Survey (multiple years, orange circles) measurements with underpredictions compared to NJHDG measurements (multiple years, green circles) which may not be correct.

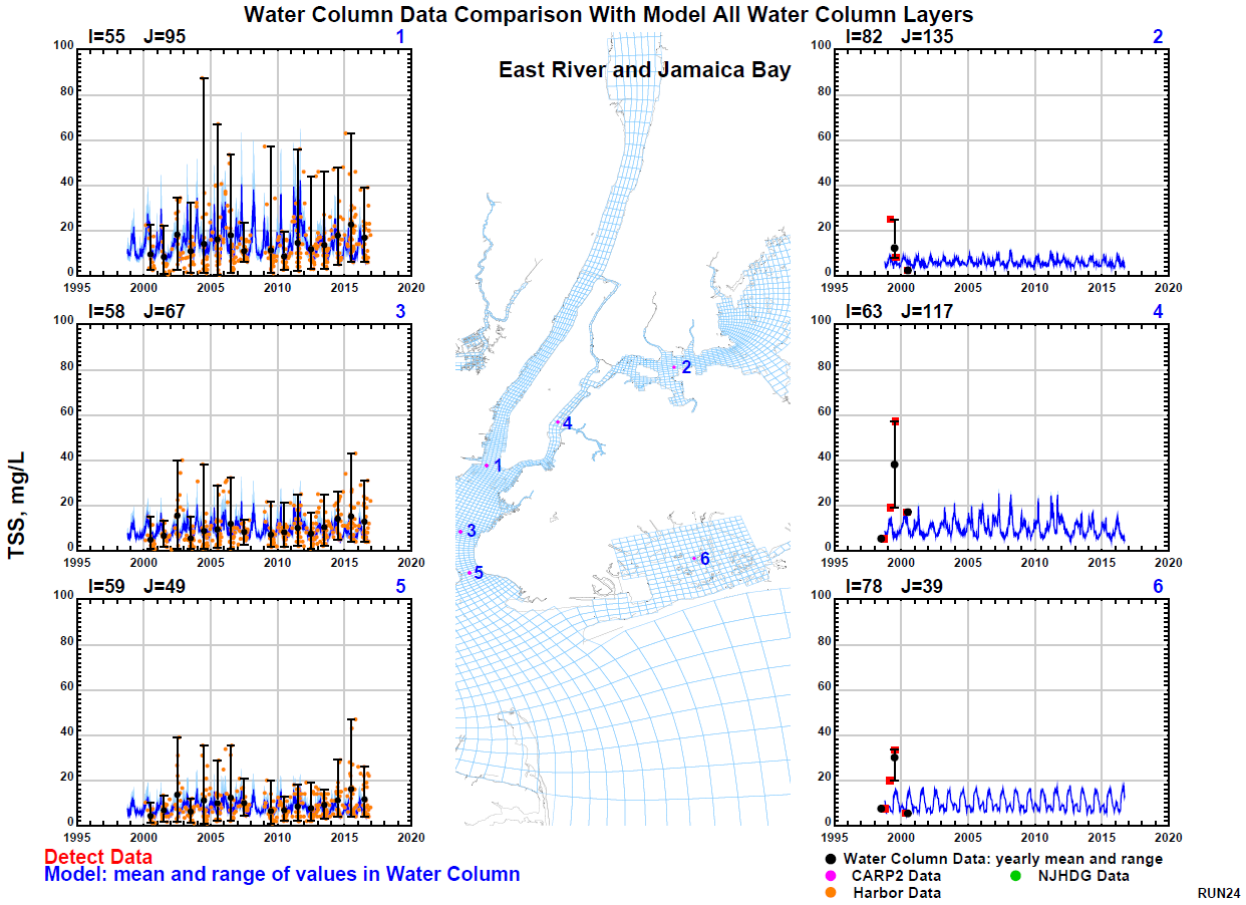

Figure 3- 44. Suspended sediment concentrations model and measurement comparison results for six locations in Upper NY Bay, East River, and Jamaica Bay. The model results (blue lines) compare well to NYCDEP Harbor survey (multiple years, orange circles) measurements and select years of CARP 1 (1998-2000, red squares) measurements. The model results miss much of the elevated 1999 range in CARP 1 measurements (1998-2000, red squares) at the East River and Jamaica Bay locations shown in the right-side panels.

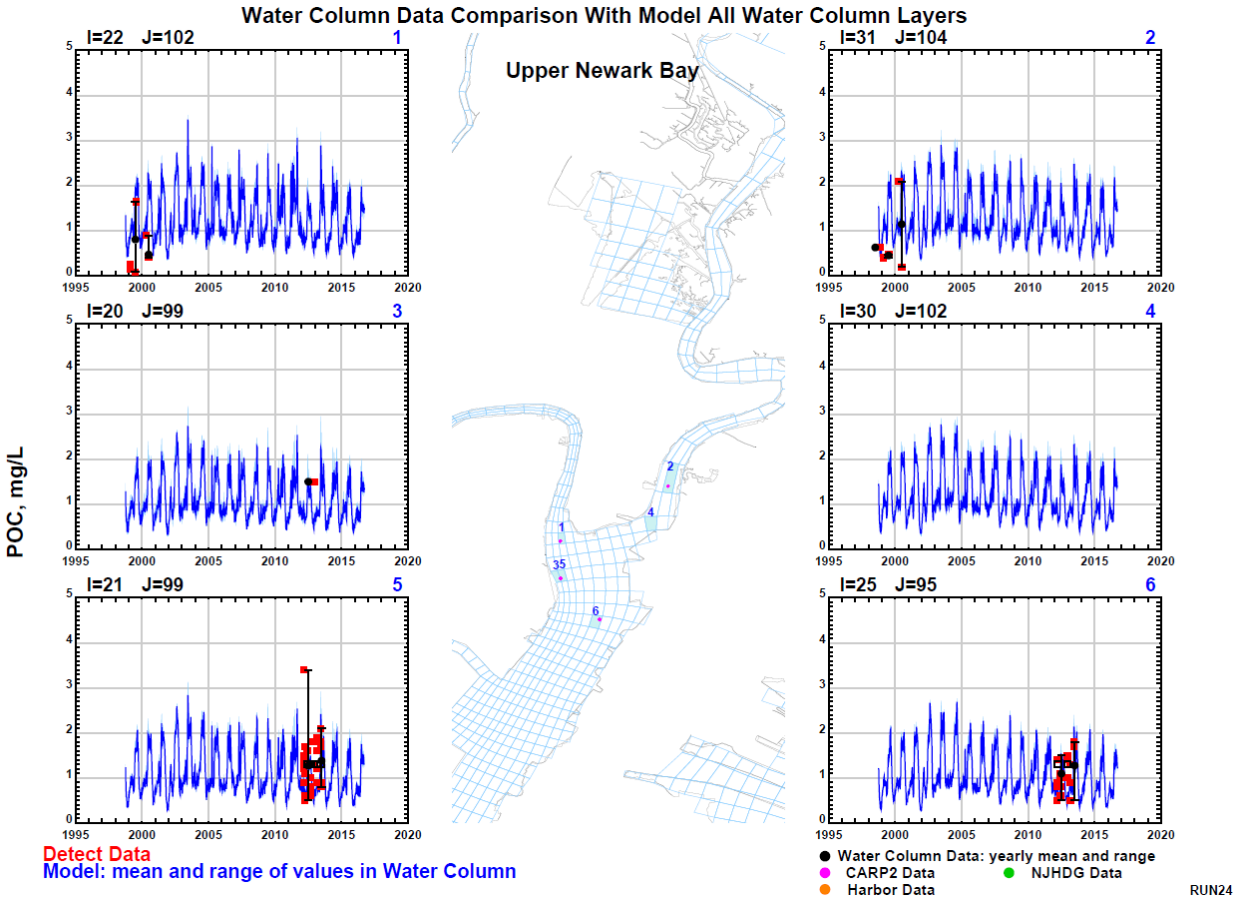

Figure 3- 45. Particulate organic carbon concentrations model and measurement comparison results for six locations in Upper Newark Bay and the Hackensack River. The model results (blue lines) compare well to CARP 1 (1998-2000, red squares) and Superfund Study (2012-13, red squares) measurements.

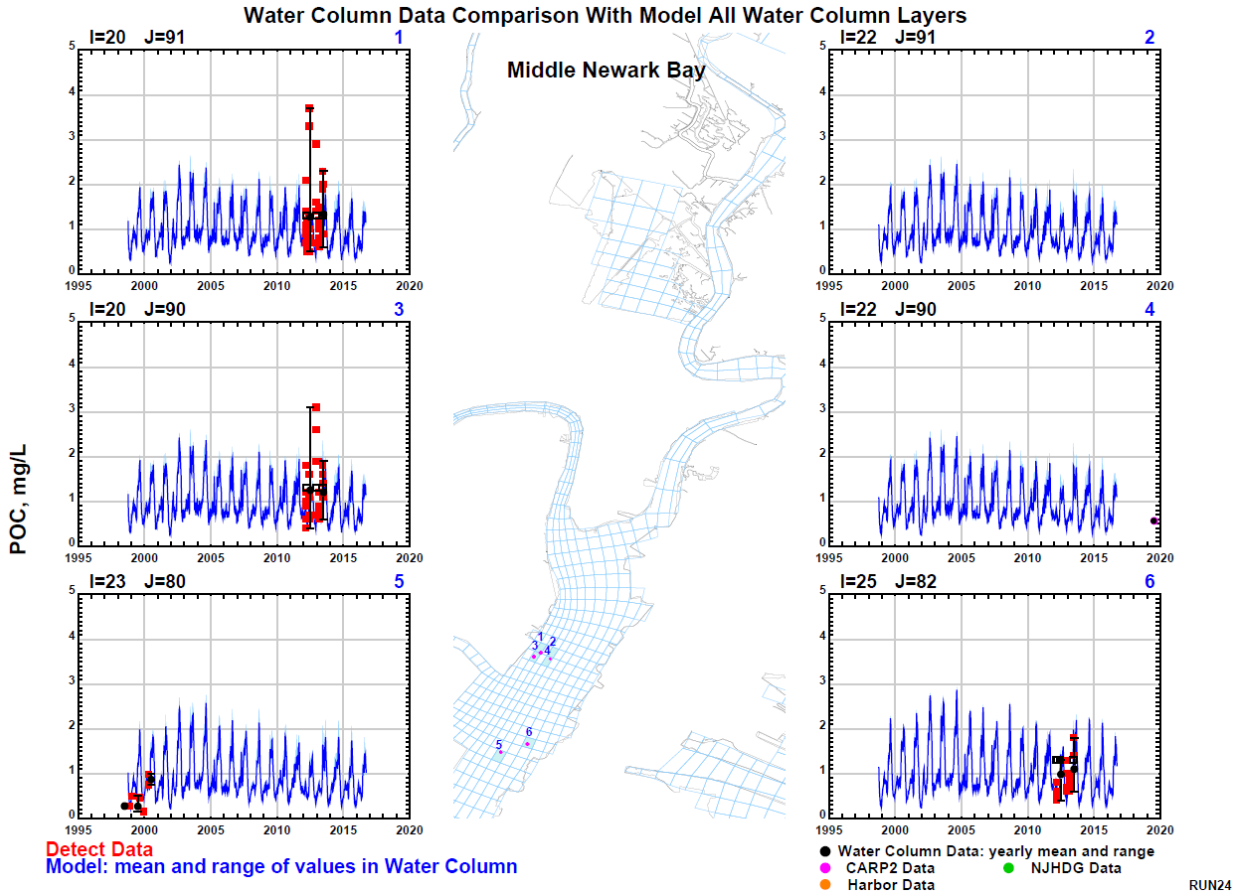

Figure 3- 46. Particulate organic carbon concentrations model and measurement comparison results for six locations in central Newark Bay. The model results (blue lines) compare well to measurements collected for CARP 1 (1998-2000, red squares), Superfund (2012-13, red squares), and CARP 2 (2019, pink circles).

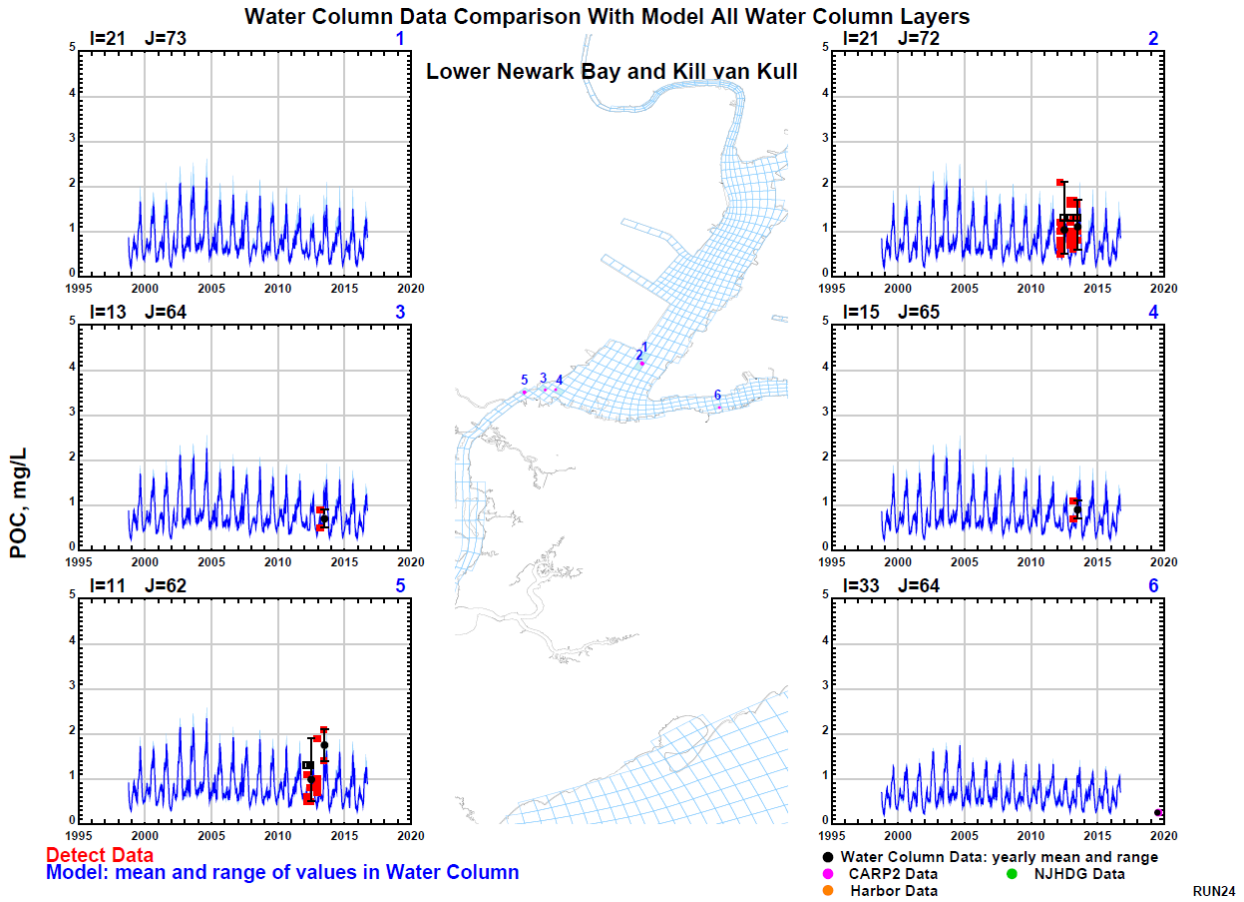

Figure 3- 47. Particulate organic carbon concentrations model and measurement comparison results for six locations in Lower Newark Bay and the Kill van Kull. The model results (blue lines) compare well to measurements collected for Superfund (2012-13, red squares) and CARP 2 (2019, pink circles).

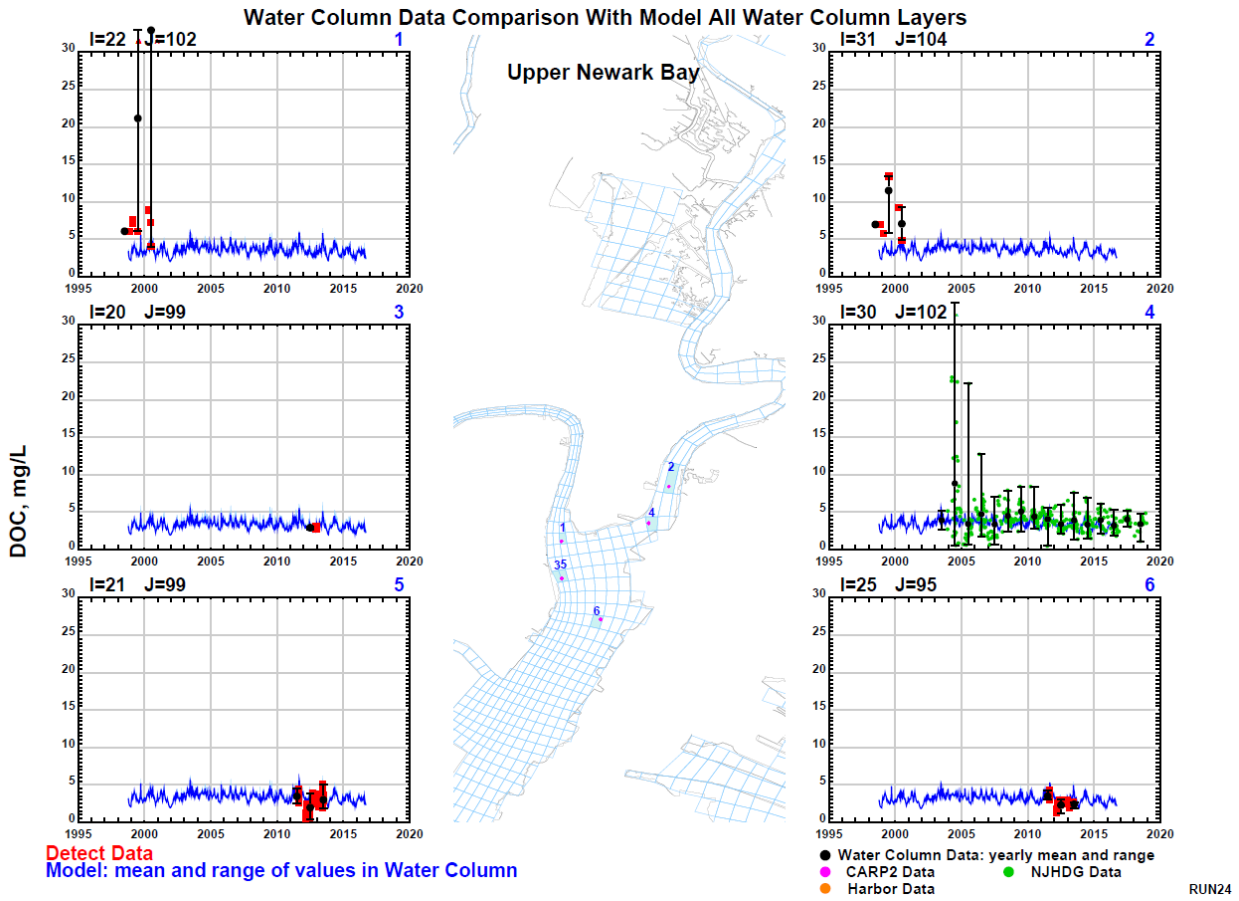

Figure 3- 48. Dissolved organic carbon concentrations model and measurement comparison results for six locations in Upper Newark Bay and the Hackensack River. The model results (blue lines) underestimate CARP 1 (1998-2000, red squares) measurements at two locations but agree well with Superfund Study (2011-13, red squares) measurements and to the central tendency of NJHDG (multiple years, green circles) measurements.

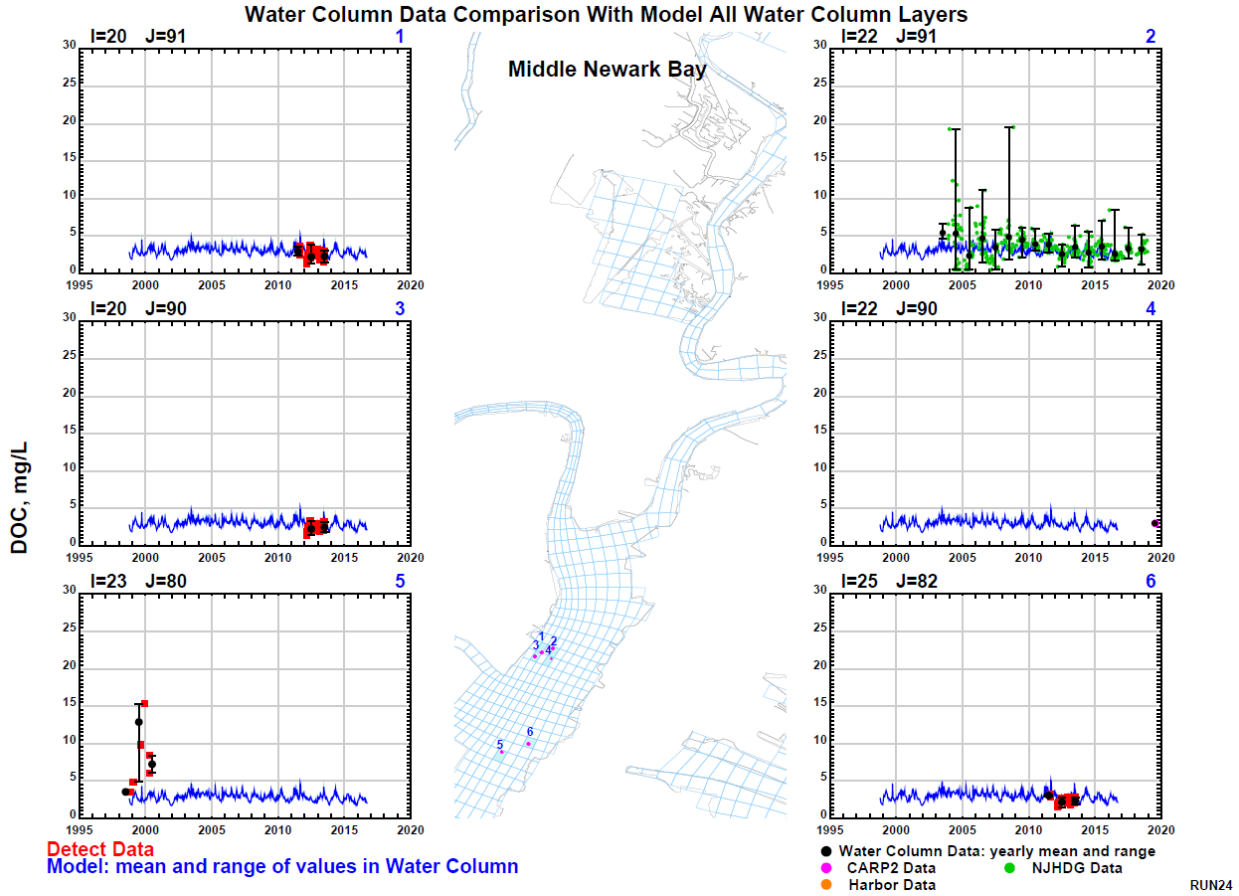

Figure 3- 49. Dissolved organic carbon concentrations model and measurement comparison results for six locations in central Newark Bay. The model results (blue lines) compare underpredict measurements collected for CARP 1 (1998-2000, red squares) at one location. The model results (blue lines) compare well to measurements collected for Superfund (2011-13, red squares) and CARP 2 (2019, pink circles) and to the central tendency of NJHDG (multiple years, green circles) measurements.

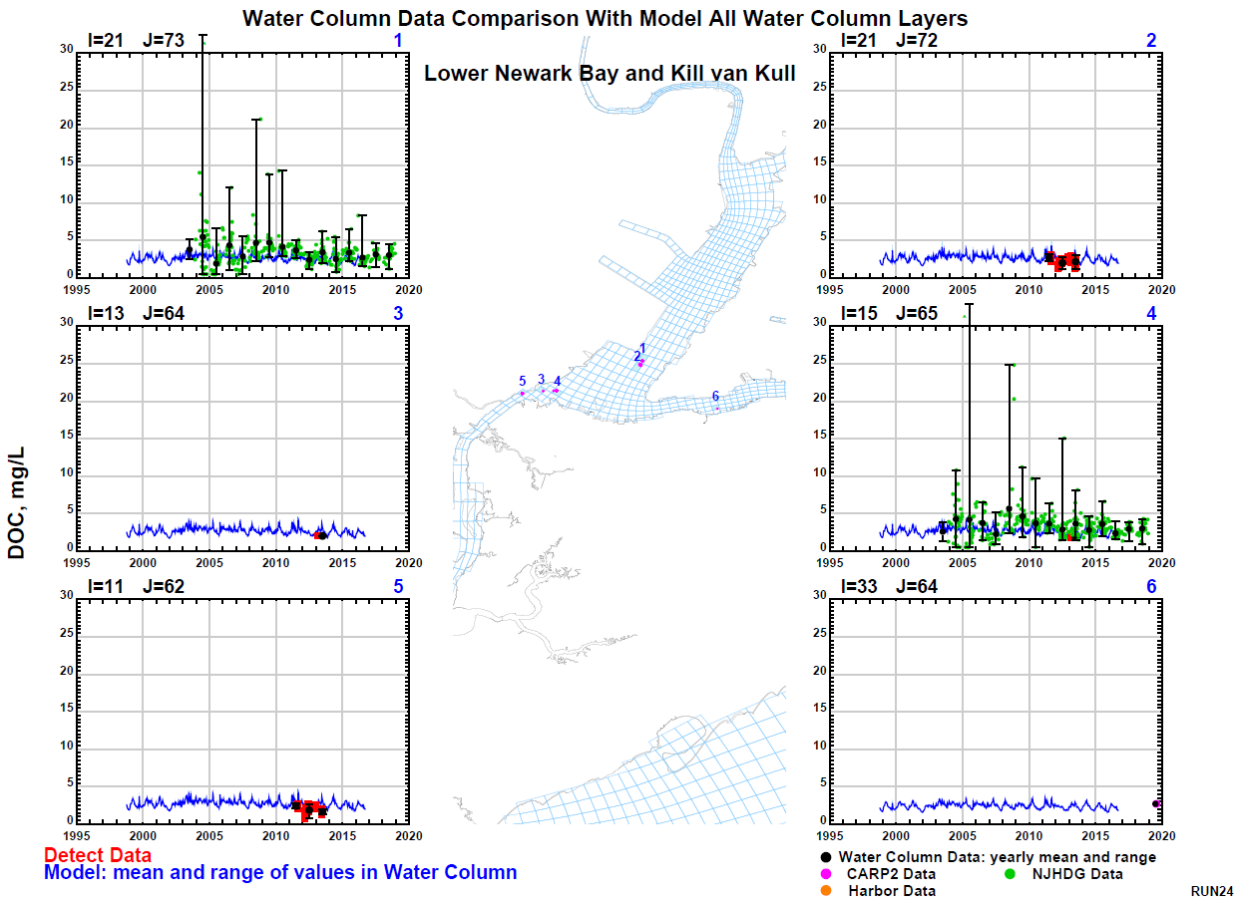

Figure 3- 50. Dissolved organic carbon concentrations model and measurement comparison results for six locations in Lower Newark Bay and the Kill van Kull. The model results (blue lines) compare well to measurements collected for Superfund (2011-13, red squares) and CARP 2 (2019, pink circles) and to the central tendency of NJHDG (multiple years, green circles) measurements.

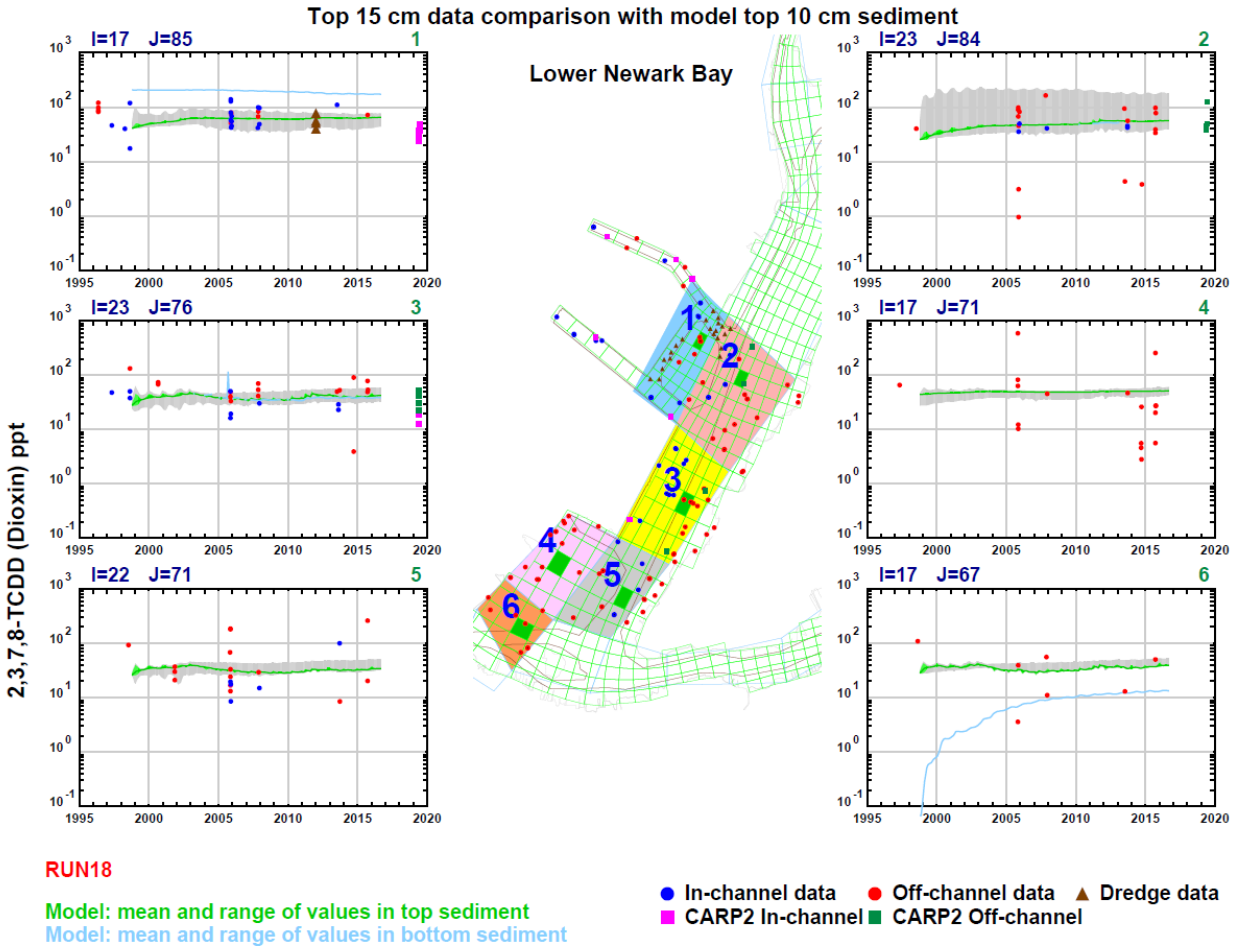

Figure 3- 51. 2,3,7,8-TCDD solids-normalized sediment bed concentrations model and measurement comparison results for six locations in Lower Newark Bay. Measurement results are very consistent across programs. The model results (green lines and green and gray shades) compare well to measurements collected for multiple programs. Model and measurement results suggest relatively flat temporal gradients.

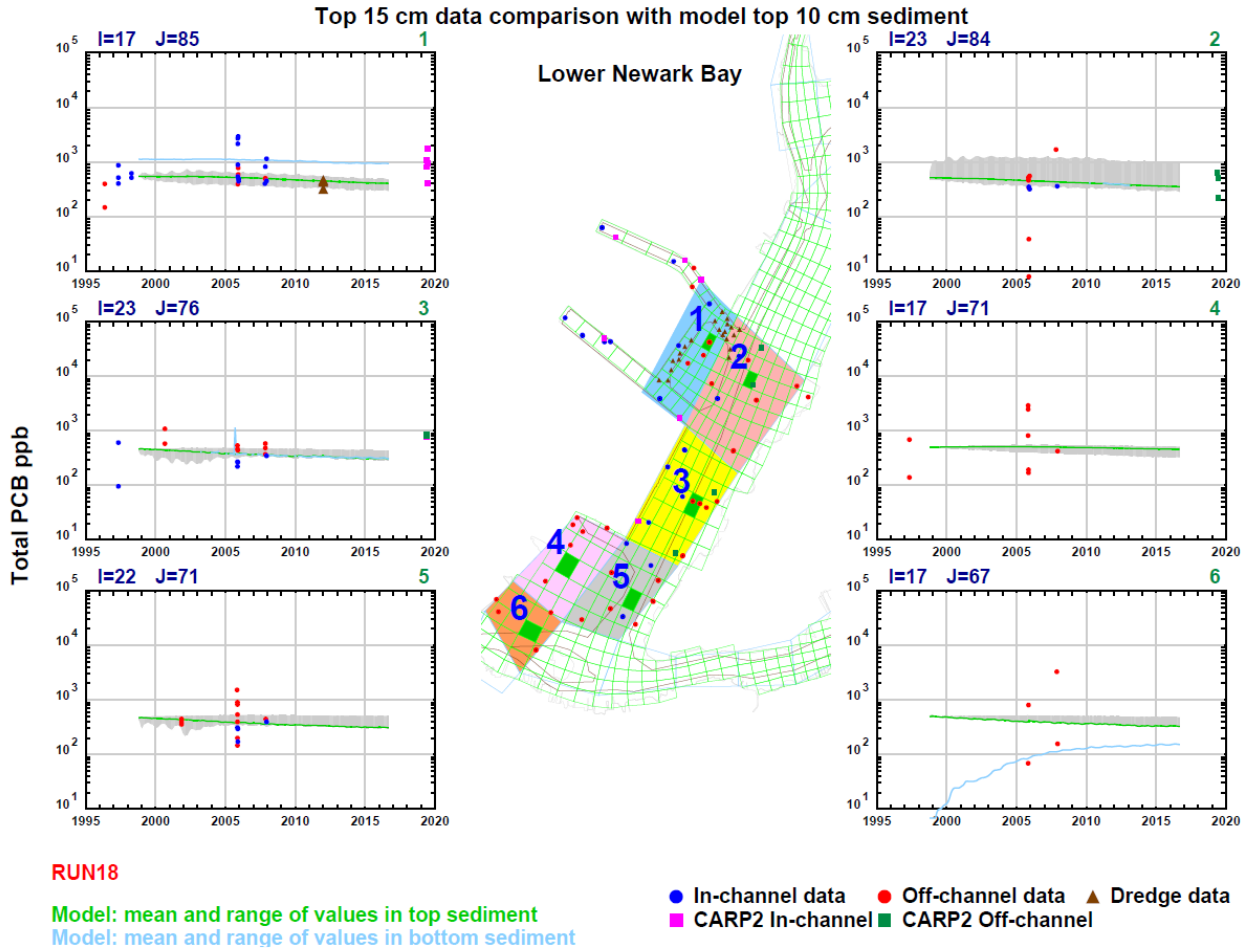

Figure 3- 52. Total PCB solids-normalized sediment bed concentrations model and measurement comparison results for six locations in Lower Newark Bay. Measurement results (sum of ten homologs) are very consistent across programs. The model results (green lines and green and gray shades, twice the sum of four homologs) compare well to measurements collected for multiple programs. Model and measurement results suggest relatively flat temporal gradients.

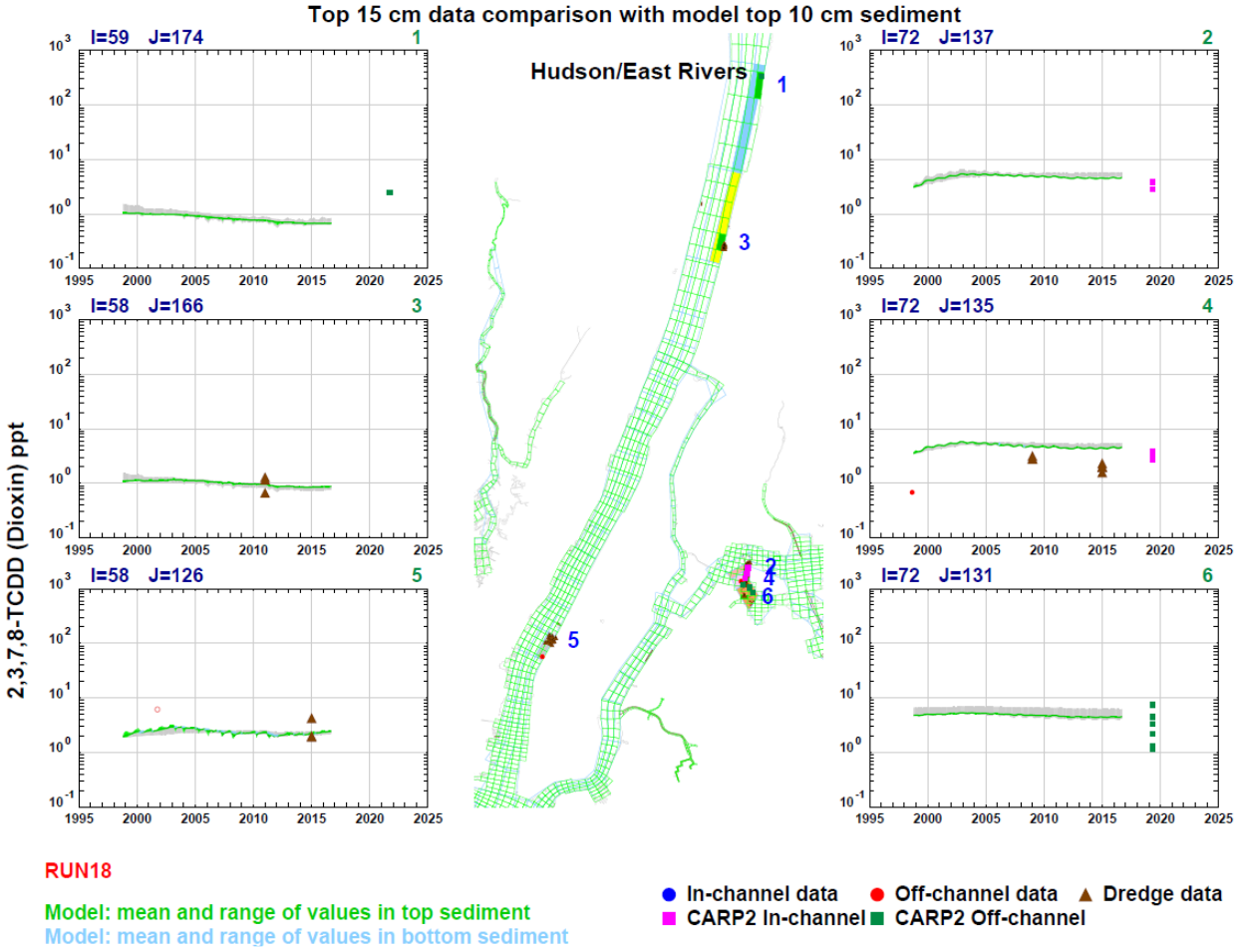

Figure 3- 53. 2,3,7,8-TCDD solids-normalized sediment bed concentrations model and measurement comparison results for six locations in the Hudson and East Rivers. The model results (green lines and green and gray shades) compare reasonably well to limited measurements collected for multiple programs. Location 5 includes a non-detect at detection limit (open symbol). Stronger model and measurement comparisons at locations 3 and 5 may offset the importance of the potential underprediction further upstream at location 1.

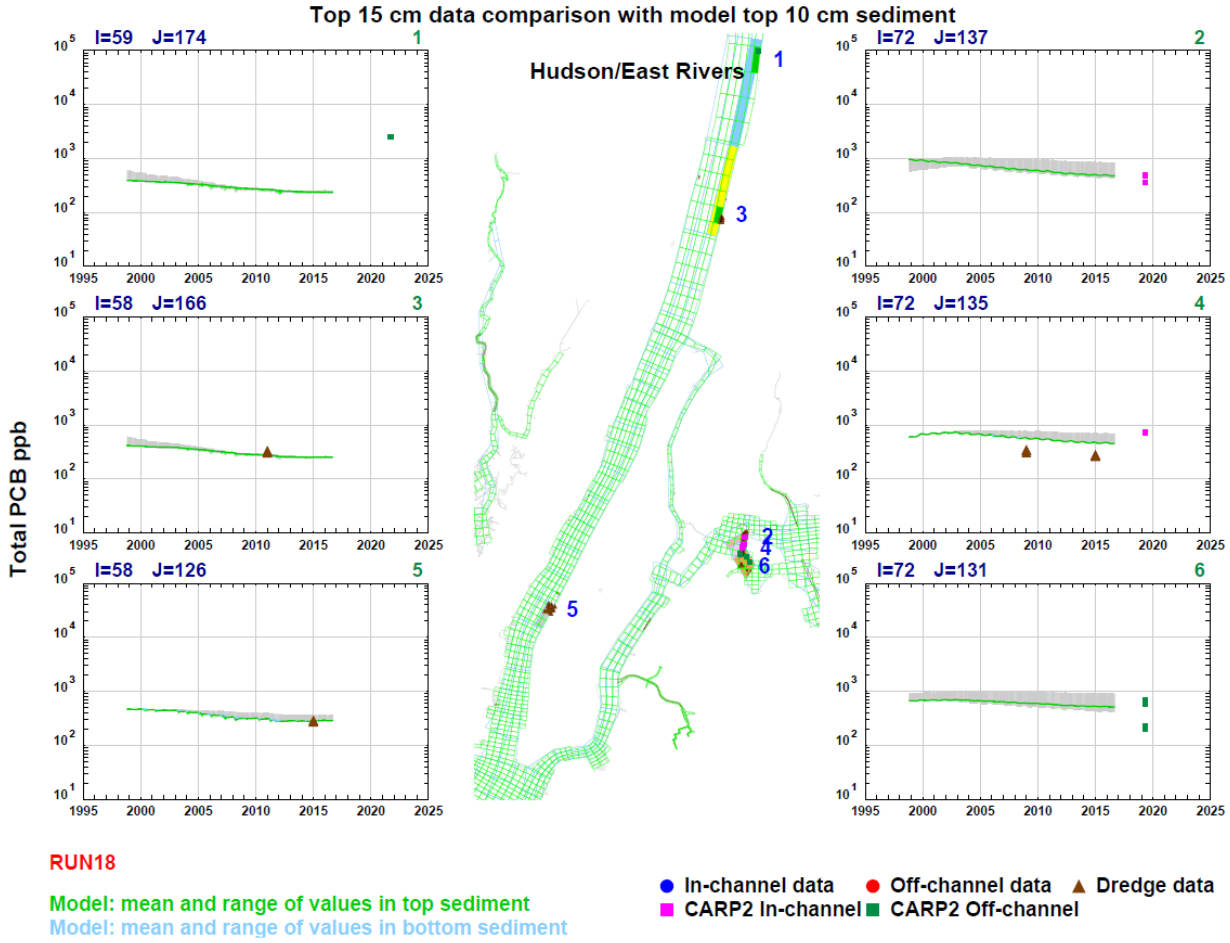

Figure 3- 54. Total PCB solids-normalized sediment bed concentrations model and measurement comparison results for six locations in the Hudson and East Rivers. The model results (green lines and green and gray shades, twice the sum of four homologs) compare well to limited measurements collected for multiple programs. Stronger model and measurement comparisons at locations 3 and 5 may offset the importance of the potential underprediction further upstream at location 1.

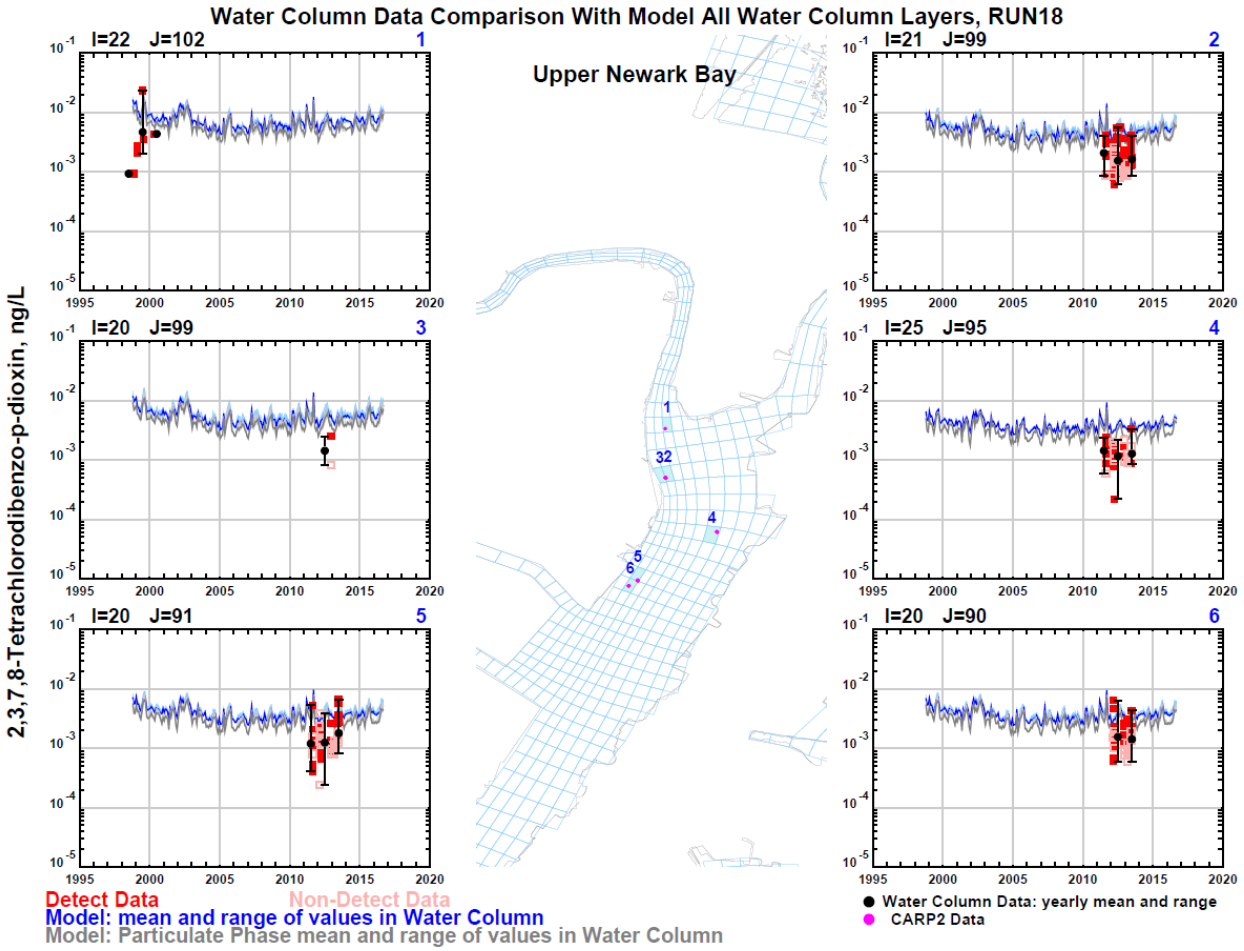

Figure 3- 55. 2,3,7,8-TCDD water column concentrations model and measurement comparison results for six locations in upper Newark Bay. Measurement results (red squares) also include non-detects at detection limit (pale pink squares). The model results (blue lines and shades) are within the range of or higher than measurements collected for multiple programs compiled for post-audit. For reference, model results for particulate phase concentrations of 2,3,7,8-TCDD are shown in gray. Model results suggest relatively flat temporal gradients.

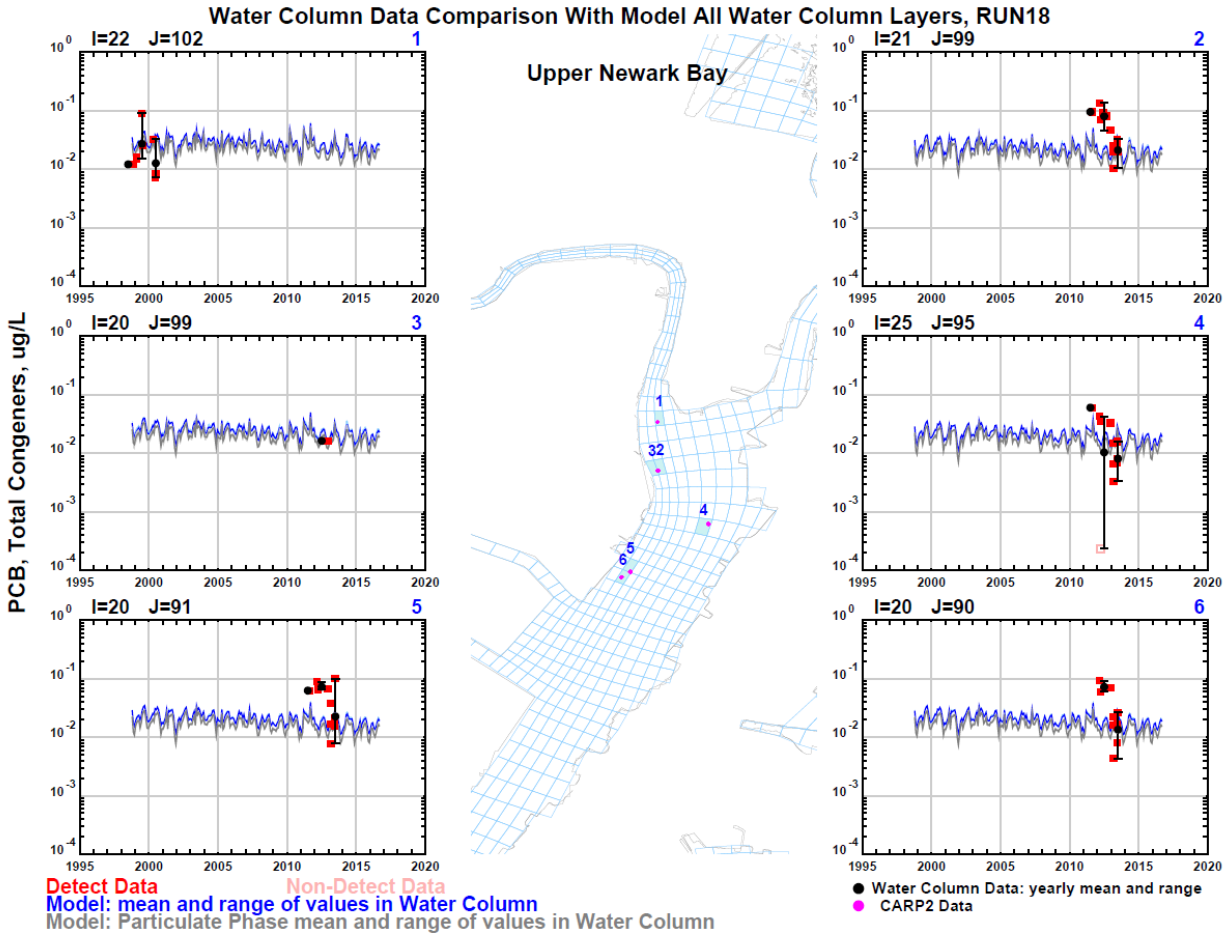

Figure 3- 56. Total PCB water column concentrations (estimated as twice the summation of four homologs) model and measurement comparison results for six locations in upper Newark Bay. Measurement results (red squares) also include non-detects at detection limit (pale pink squares). The model results (blue lines and shades) capture most of the measurements collected for multiple programs compiled for post-audit. For reference, model results for particulate phase concentrations of total PCB are shown in gray. Model results suggest relatively flat temporal gradients.

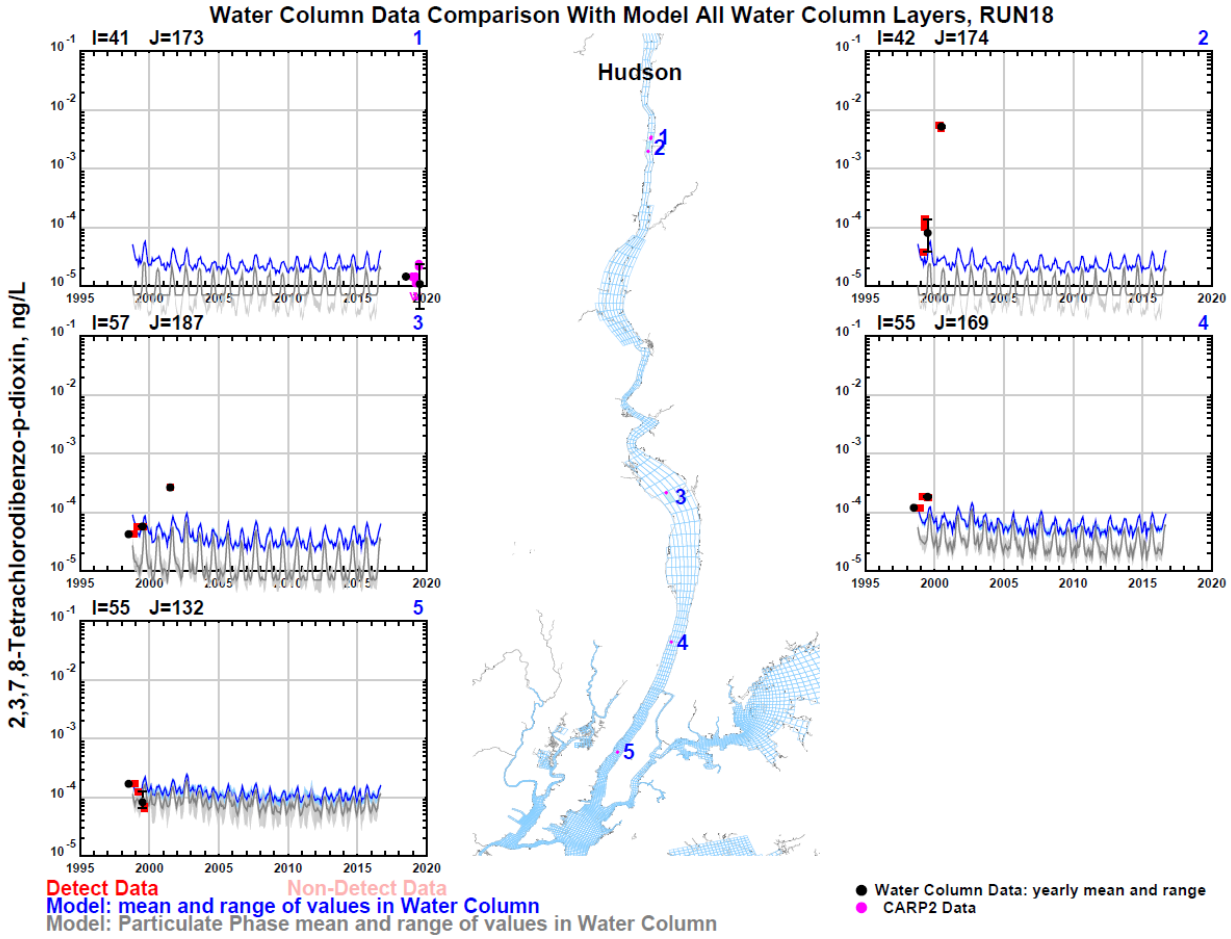

Figure 3- 57. 2,3,7,8-TCDD water column concentrations model and measurement comparison results for six locations in the Hudson River. The model results (blue lines and shades) agree with the measurements collected for multiple programs compiled for post-audit (red square) and by CARP 2 investigators (bright pink circles). For reference, model results for particulate phase concentrations of 2,3,7,8-TCDD are shown in gray. Model and measurement (when locations 1 and 2 are combined) results suggest relatively flat temporal gradients.

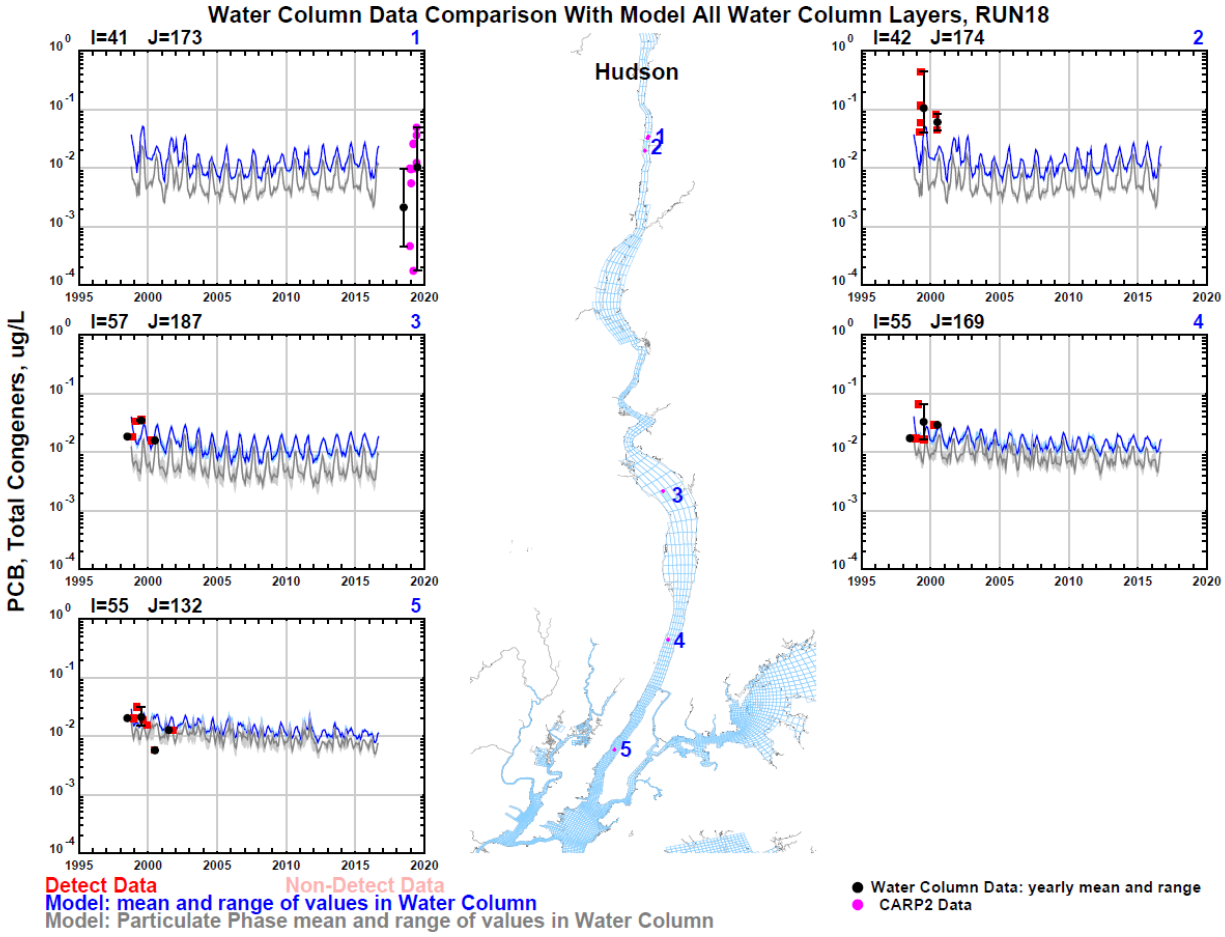

Figure 3- 58. Total PCB water column concentrations (estimated as twice the summation of four homologs) model and measurement comparison results for six locations in the Hudson River. The model results (blue lines and shades) agree with most of the measurements collected for multiple programs compiled for post-audit (red squares) and by CARP 2 investigators (bright pink circles). For reference, model results for particulate phase concentrations of total PCB are shown in gray. Model results suggest relatively flat to slightly declining temporal gradients. Measurement results (when locations 1 and 2 are combined) suggest the potential for a temporal gradient. 2019 measurements available at one location unfortunately span three orders of magnitude and are therefore somewhat inconclusive for this location and contaminant.

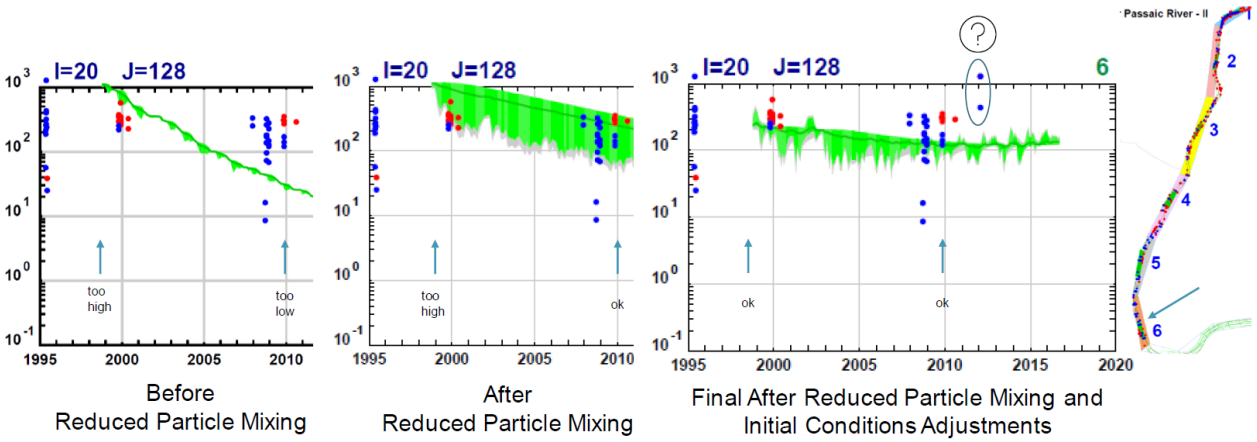

Reduced particle mixing in the Lower Passaic River helped with temporal decline, but not enough. Correction of initial conditions also needed.
Unlike Superfund, CARP does not manually reset the model to capture elevated measurements in 2012.

2,3,7,8-TCDD ppt – CARP 2 Calibration Progression Top 10 cm, Lower Passaic

Figure 3- 59. Interim (left and middle timeseries) and final (right timeseries) 2,3,7,8-TCDD (ppt) solids-normalized sediment bed concentrations model and measurement comparison results for a single location in the Lower Passaic River. The temporal trend of the model results (green lines and green and gray shades) is highly sensitive to adjustments to particle mixing rates in the bed of the Lower Passaic River (left to middle timeseries) and to adjustments to bed initial archive layer thicknesses and contaminant concentrations conditions (middle to right timeseries). The final model result (right times series) captures some of the scatter in the measurements (red and blue circles) and have a relative flat temporal gradient. No attempt was made to manually adjust model results to capture elevated measurements from 2012 occurring at several Lower Passaic River locations.

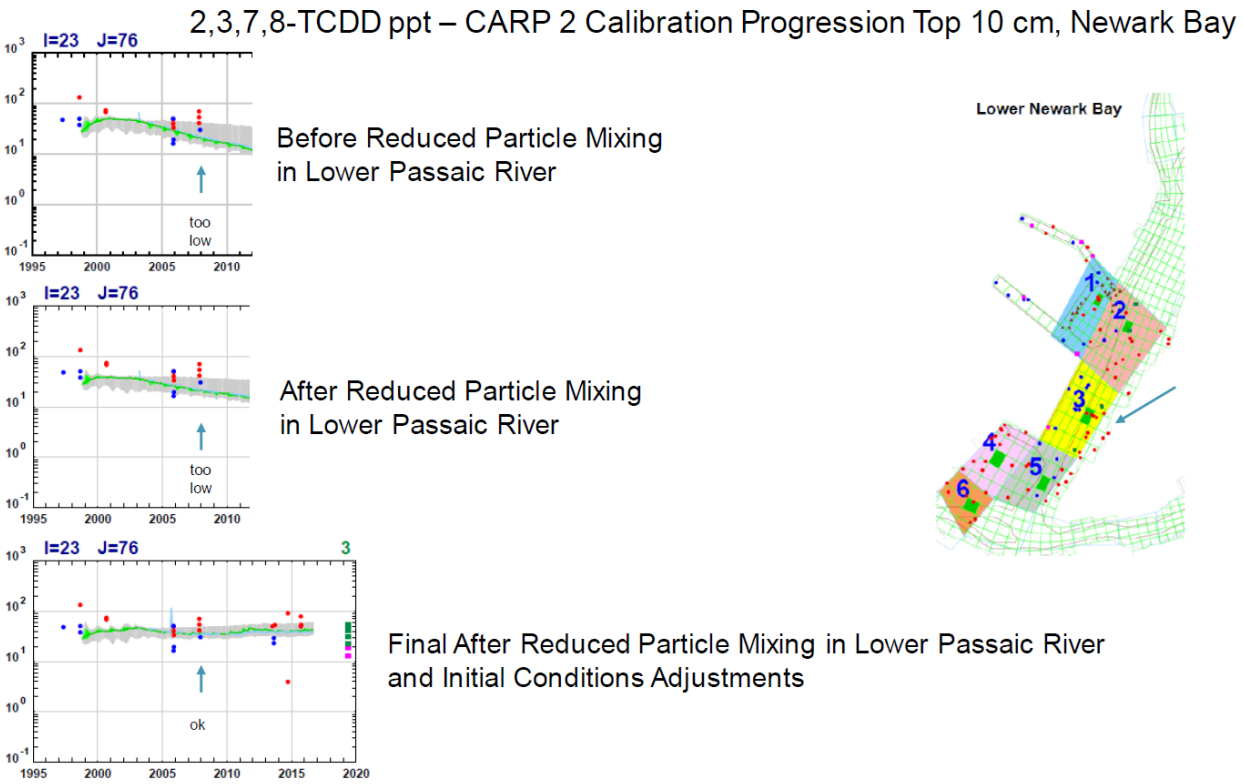

Figure 3- 60. Interim (top and middle timeseries) and final (bottom timeseries) 2,3,7,8-TCDD (ppt) solids-normalized sediment bed concentrations model and measurement comparison results for a single location in Newark Bay. The temporal trend and magnitude of the model results (green lines and green and gray shades) are sensitive to adjustments to particle mixing rates in the bed of the Lower Passaic River (top to middle timeseries) and to adjustments to bed initial archive layer thicknesses and contaminant concentrations conditions (middle to bottom timeseries). The measurements (red and blue circles, pink and green squares) suggest the temporal behavior of the final model calibration (bottom timeseries) is correct.

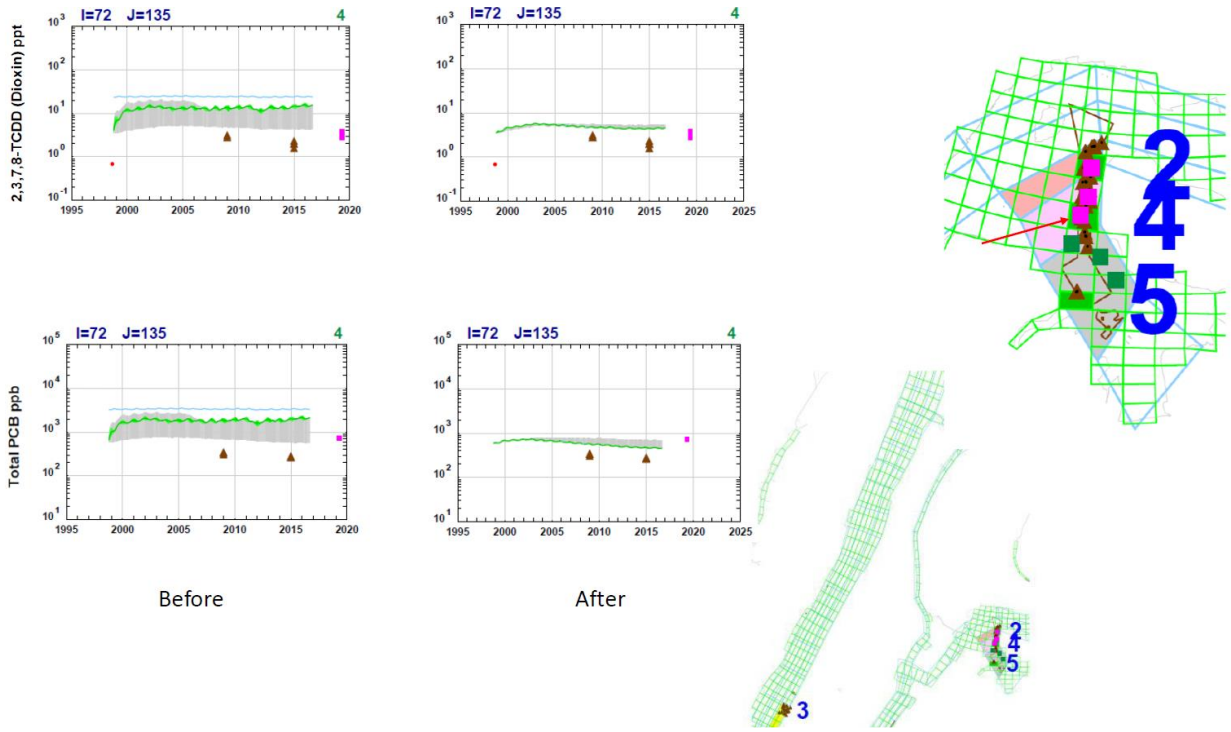

Figure 3- 61. 2,3,7,8-TCDD (top row) and total PCB (bottom row) solids-normalized sediment bed concentrations model and measurement comparison results in the East River on the west side of Riker's Island in South Brother Island Channel, north of Bowery Bay. The model results (green lines and green and gray shades) compare more favorably to measurements after more accurate discretization of initial bed archive layer thicknesses passed from the 49 x 84 model computational grid to the 127 x 205 model computational grid. With revised archive layer thicknesses, the model results for solids-normalized bed contaminant concentrations in the single grid cell (green lines) are closer to measurements and there is less contaminant concentration variation across model results for immediately adjacent grid cells (gray shades). The single cell model results are shown for location 4 indicated on the map with an arrow. The model grid cells used for adjacent cells model results are colored in pale pink on the map.

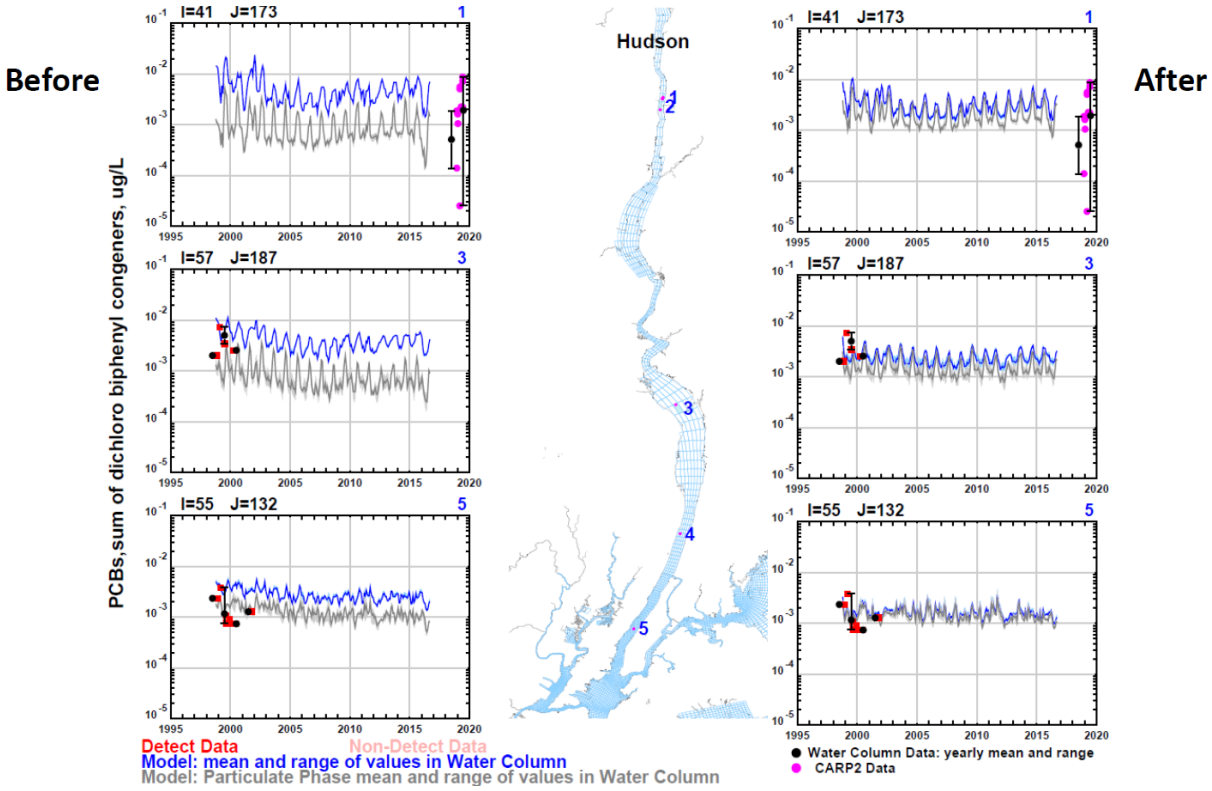

Figure 3- 62. Di-CB water column concentrations model and measurement comparison results for three locations in the Hudson River before and after adopting a revised phase partitioning coefficient. The model results (blue lines and shades) agree better with the measurements collected for multiple programs compiled for post-audit (red squares) and by CARP 2 investigators (bright pink circles) after applying the new phase partitioning coefficient. For reference, model results for particulate phase concentrations of total PCB are shown in gray. The new di-CB phase partitioning coefficient increases the modeled fraction particulate in the water column (i.e., closeness of gray and blue lines from "before" to "after") and reduces modeled total di-CB in the water column (i.e, drop in blue lines from "before" to "after").

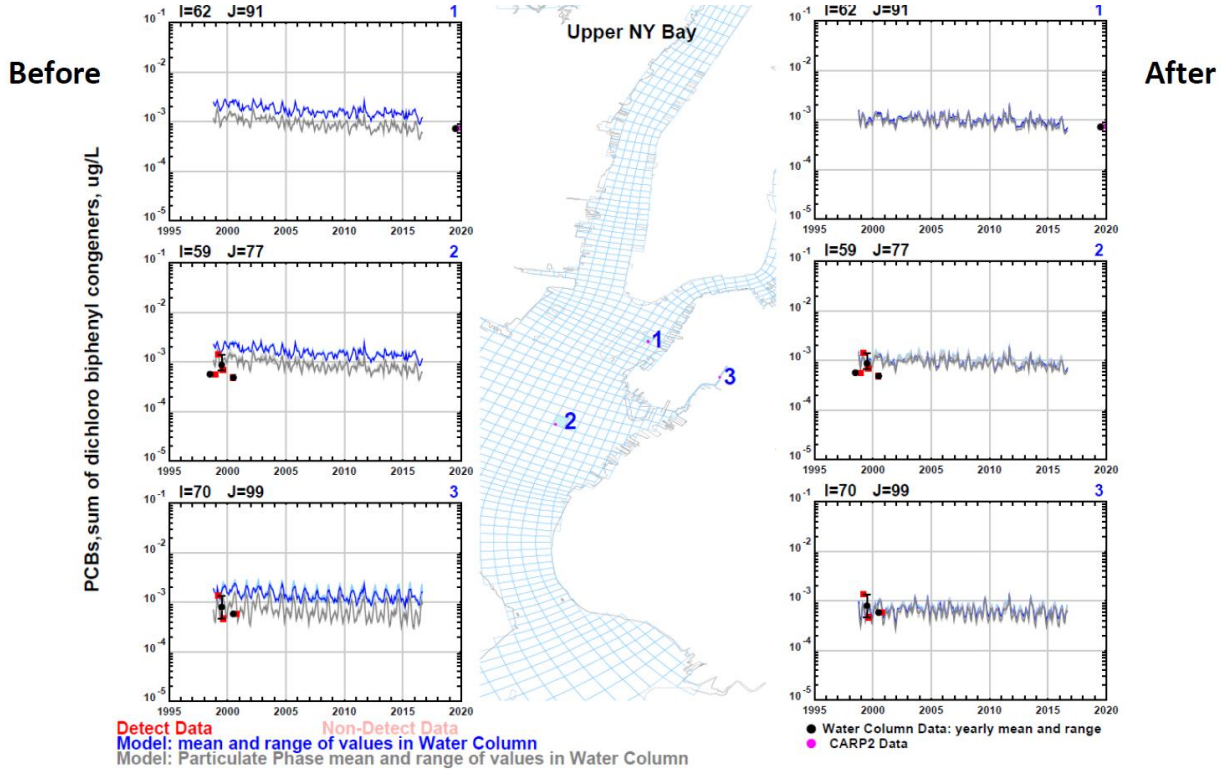

Figure 3- 63. Di-CB water column concentrations model and measurement comparison results for three locations in Upper NY Bay before and after adopting a revised phase partitioning coefficient. The model results (blue lines and shades) agree better with the measurements collected for multiple programs compiled for post-audit (red squares) and by CARP 2 investigators (bright pink circles) after applying the new phase partitioning coefficient. For reference, model results for particulate phase concentrations of total PCB are shown in gray. The new di-CB phase partitioning coefficient increases the modeled fraction particulate in the water column (i.e., closeness of gray and blue lines from "before" to "after") and reduces the modeled total di-CB in the water column (i.e., drop in blue lines from "before" to "after").

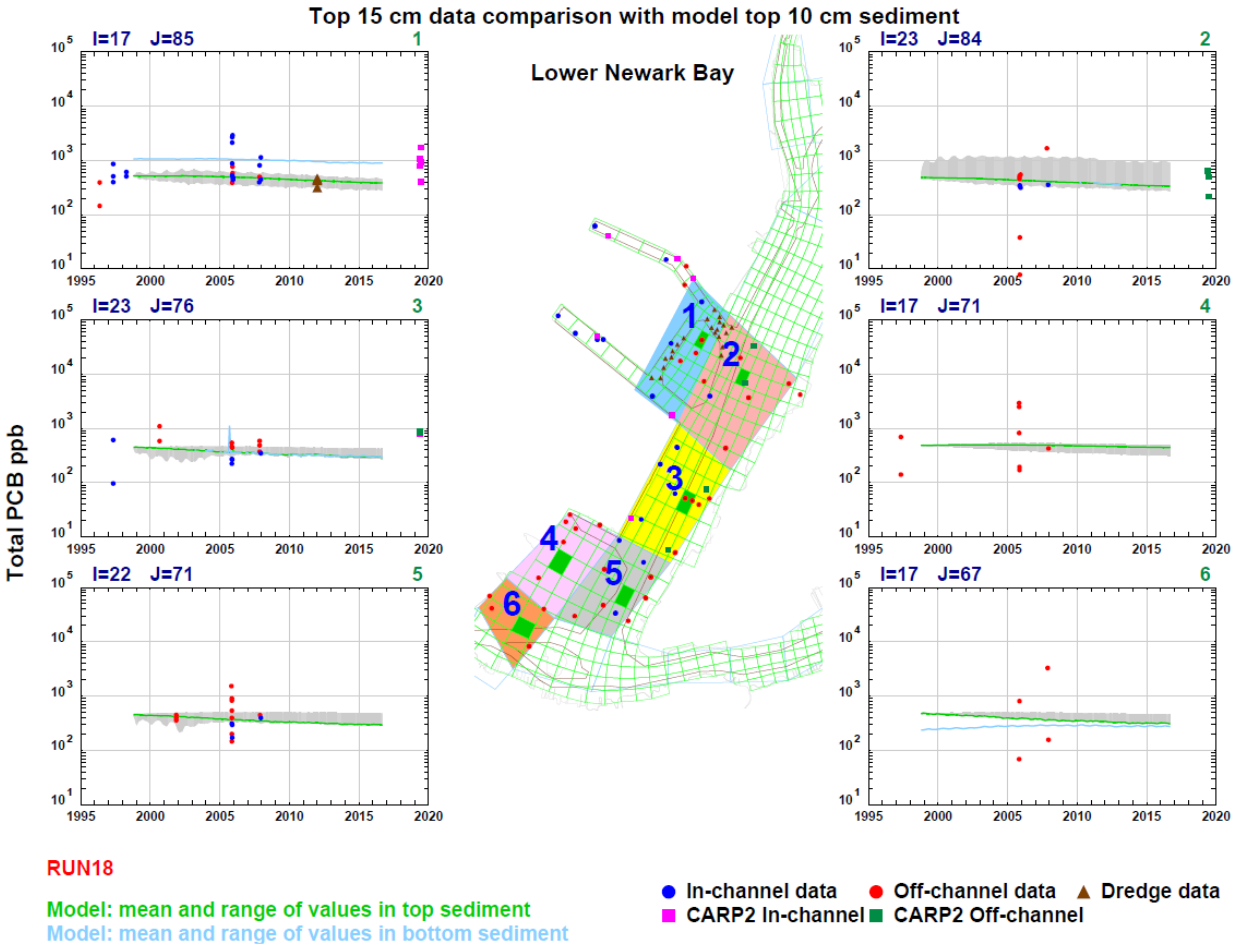

Figure 3- 64. Total PCB solids-normalized sediment bed concentrations model and measurement comparison results for six locations in Lower Newark Bay. Measurement results (sum of ten homologs) are very consistent across programs. The model results (green lines and green and gray shades, ten homologs sum) compare well to measurements collected for multiple programs. Model and measurement results suggest relatively flat temporal gradients. Model results are close to the approximated results from four homologs presented in Figure 3-52.

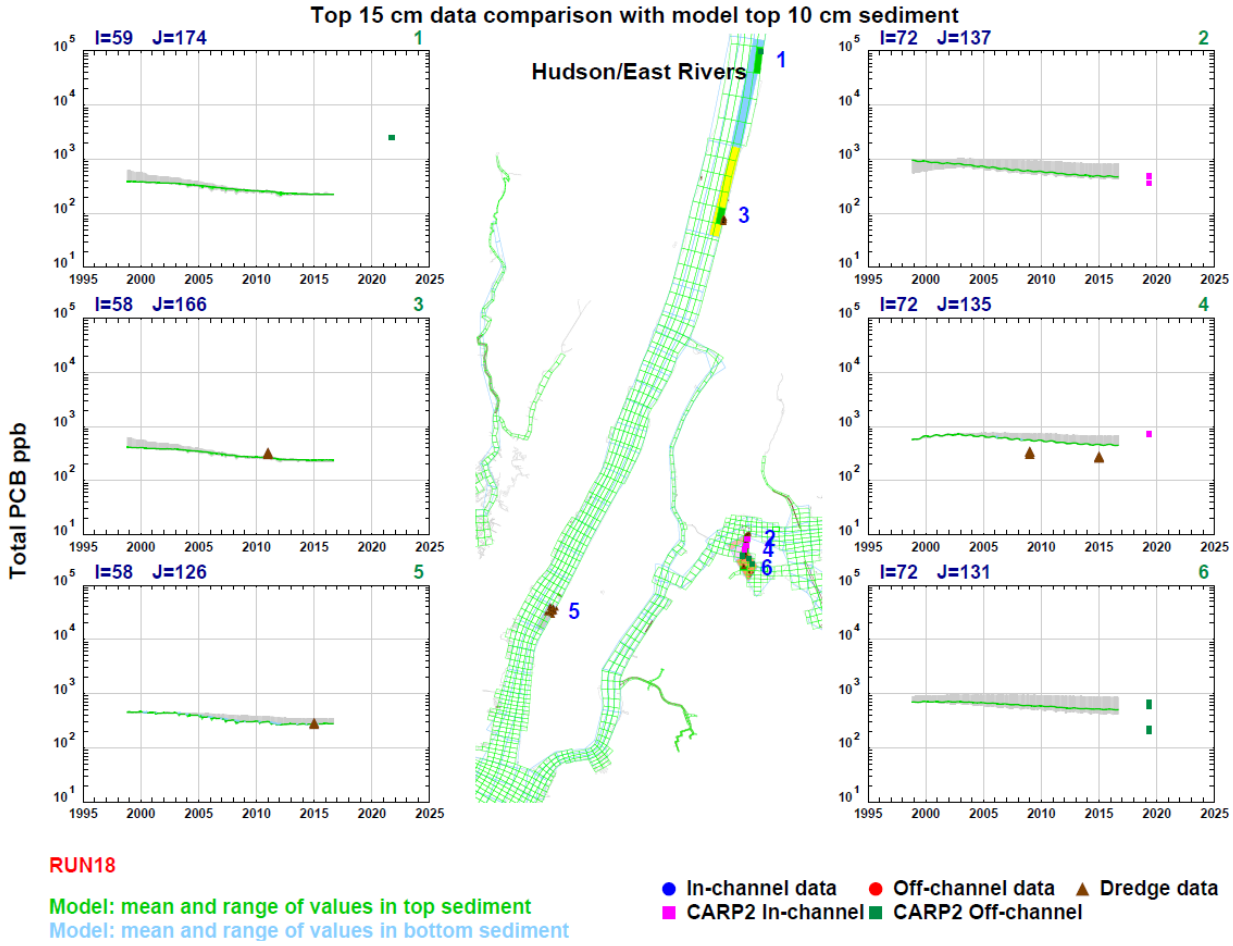

Figure 3- 65. Total PCB solids-normalized sediment bed concentrations model and measurement comparison results for six locations in the Hudson and East Rivers. The model results (green lines and green and gray shades, ten homologs sum) compare well to limited measurements collected for multiple programs. Stronger model and measurement comparisons at locations 3 and 5 may offset the importance of the potential underprediction further upstream at location 1. Model results are close to the approximated results from four homologs presented in Figure 3-54.

APPENDICES

LIST OF APPENDICES (Appendices are provided separately.)

APPENDIX 1 – Information Supporting Decision to Increase CARP Model Computational Grid Resolution

APPENDIX 2 – Hourly Surface Water Elevations Model and Measurement Comparisons Results Diagrams

APPENDIX 2A – Hourly Surface Water Elevations Model and Measurement Comparisons Results Diagrams during Hurricane Sandy

APPENDIX 3 – Low Pass Numerical Filter Surface Water Tidal Elevations Model and Measurement Comparisons Results Diagrams

APPENDIX 4 – Water Temperature Model and Measurement Comparisons Results Diagrams, 2009-10 Water Year

APPENDIX 4A – Water Temperature Model and Measurement Comparisons Results Diagrams, 2010-11 Water Year

APPENDIX 4B – Water Temperature Model and Measurement Comparisons Results Diagrams, 2009-10 Water Year, 30-Day Focus

APPENDIX 5 – Salinity Model and Measurement Comparisons Results Diagrams, 2009-10 Water Year

APPENDIX 5A – Salinity Model and Measurement Comparisons Results Diagrams, 2010-11 Water Year

APPENDIX 5B – Salinity Model and Measurement Comparisons Results Diagrams, 2009-10 Water Year, 30-Day Focus

APPENDIX 6 – Velocity Currents Model and Measurement Comparisons Results Diagrams, CARP 1 New Jersey Toxics Reduction Workplan for New York-New Jersey Harbor Study I-E Stations, 2000-02 Water Years

APPENDIX 7 – Velocity Currents Model and Measurement Comparisons Results Diagrams, Sommerfield and Chant, 2010, 2007-09 Water Years

APPENDIX 8 – Velocity Currents Model and Measurement Comparisons Results Diagrams, NOAA stations, various periods

APPENDIX 9 – Suspended Sediment Concentrations Model and Measurement Comparisons Results Diagrams, CARP 1 New Jersey Toxics Reduction Workplan for New York-New Jersey Harbor Study I-E Stations, 2000-02 Water Years and Proximal New Jersey Harbor Dischargers Group (NJHDG) and New York City Environmental Protection Harbor Survey Stations, 2000-16 Water Years

APPENDIX 10 – Suspended Sediment Concentrations Model and Measurement Comparisons Results Diagrams, USGS Measurements, Hudson River at Poughkeepsie, 2001-16 Calendar Years

APPENDIX 11 – Suspended Sediment and Organic Carbon Concentrations Model and Measurement Comparisons Results Diagrams, Various Measurement Programs, Eighty-Nine Locations throughout NY/NJ Harbor, 1998-2016 Water Years

APPENDIX 12 - Additional Parameters Related to Suspended Sediment and Organic Carbon Concentrations Model and Measurement Comparisons Results Cursory Check Diagrams, Various Measurement Programs, Eighty-Nine Locations throughout NY/NJ Harbor, 1998-2016 Water Years

APPENDIX 13 - Contaminant Concentrations in the Sediment Bed Model and Measurement Comparisons Results Diagrams, Calibration, Various Measurement Programs, Ninety-Five Locations throughout NY/NJ Harbor, 1998-2016 Water Years

APPENDIX 14 - Contaminant Concentrations in the Water Column Model and Measurement Comparisons Results Diagrams, Calibration, Various Measurement Programs, Sixty-One Locations throughout NY/NJ Harbor, 1998-2016 Water Years

APPENDIX 15 - Contemporary Dredging Projects Data, Project Listing and Application Notes

APPENDIX 16 - Contaminant Concentrations in the Sediment Bed Model and Measurement Comparisons Results Diagrams, Validation, Various Measurement Programs, Ninety-Five Locations throughout NY/NJ Harbor, 1998-2016 Water Years

APPENDIX 17 - Contaminant Concentrations in the Water Column Model and Measurement Comparisons Results Diagrams, Validation, Various Measurement Programs, Sixty-One Locations throughout NY/NJ Harbor, 1998-2016 Water Years